

Mechanism of iodine-catalyzed multicomponent cyclocondensation reactions: Synthesis of  
polysubstituted quinoline "archipelago" asphaltene mimics

by

David E. Scott

A thesis submitted in partial fulfillment of the requirements for the degree of

Doctor of Philosophy

Department of Chemistry  
University of Alberta

© David E. Scott, 2019

# Abstract

Asphaltenes constitute the heaviest and least understood sub-class of bitumen. The degree of difficulty regarding upgrading arises from the diverse and complex mixture of organic and organometallic molecules characteristic of heavy petroleum. It is hypothesized that these molecular constituents are entwined and tightly aggregated to form complex suprastructures. The numerous structural properties of asphaltenes (vast polycyclic aromatics, heteroatoms, polar functional groups, aliphatic segments and substituents, etc.) instigate inter- and intramolecular interactions causing irreversible aggregation. To increase the value and/or use of this material, efficient new upgrading procedures are required in order to address global, ever-expanding, energy needs.

Significant achievements in analytical technology has surpassed the basic understanding of the bulk properties of bitumen. Analytical methods such as ICP-MS, VPO, SANS, ITC, and AFM/STM have begun to intimately define the structural make-up of complex asphaltene molecules. Initial modeling of asphaltene components was limited to commercial aromatic compounds; however, rational molecular design and modern organic synthesis have begun to build a library of structural candidates, to accurately represent the supramolecular behaviour of native asphaltenes.

This dissertation describes a new catalytic cyclocondensation procedure, allowing us to prepare a range of quinoline-core asphaltene model compounds. The concise synthetic methodology utilizes a multicomponent reaction (MCR) to build compounds that incorporate a basic nitrogen entity. As a result of low yields and irreproducible results, substantial effort was applied to improve the reaction. Extensive optimizations were conducted to generalize and control the MCR. New mechanistic detail was obtained by our in-depth analysis and we identified the true role of the

catalyst, the necessary requirement of added oxygen, and the need for other additives. Effectively, once optimized, a wide range of quinoline-core compounds were synthesized in high purity and yield. These quinoline-based compounds have tremendous value in assessing the behaviour of authentic asphaltene samples. As a result of the complex solubility characteristics of asphaltenes, model compounds have been used to study the difference in solubility and chemical structure using Hansen solubility parameters. Though early work using quinoline-based model compounds has shown that solubility of model compounds is complex due to slight changes in structure, the need for further investigation requires a diverse library of models. Furthermore, the model compounds will be needed to test aggregation, which is expected to differentiate when one or a mixture of compounds are studied (ITC, NMR, IR, etc.). Overall, the key to this methodology is the simplicity to modulate the individual components and increase the complexity required for the types of compounds required.

# Preface

The various first generation of pyrene archipelago model compounds described in Chapter 1, was accomplished by my former colleague, Colin Diner. During this work, I collaborated along side him synthesizing “island” tethers on large scale. This work resulted in a publication, Diner, C.; Scott, D. E.; Tykwinski, R. R.; Gray, M. R.; Stryker, J. M. “Scalable, Chromatography-Free Synthesis of Alkyl-Tethered Pyrene-Based Materials. Application to First Generation “Archipelago Model” Asphaltene Compounds”, *J. Org. Chem.* **2015**, *80*, 1719-1726. As well, segments of this asphaltene review were expanded into a comprehensive review of model compounds, which includes an in-depth analysis of aggregation, analysis of porphyrinic model compounds, and a prognosis for the field. I am first author of the review, submitted as Scott, D. E.; Schulze, M.; Stryker, J. M.; Tykwinski, R. R.; “Deciphering the Asphaltenes: Hypothesis-driven Design and Synthesis of Model Compounds”.

Chapter 2 defines heterocycles and nomenclature, traditional quinoline synthesis, and our first I<sub>2</sub>-catalyzed multicomponent reactions. In this chapter I discuss the collaboration with a former colleague, Matthias Schulze. Herein, I determined the precise water percentage and optimal catalyst/catalyst loading required to optimize MCR conditions. This work resulted in a publication, Schulze, M.; Scott, D. E.; Scherer, A.; Hampel, F.; Hamilton, R. J.; Gray, M. R.; Tykwinski, R. R.; Stryker, J. M. “Steroid-Derived Naphthoquinoline Asphaltene Model Compounds: Hydriodic Acid Is the Active Catalyst in I<sub>2</sub>-Promoted Multicomponent Cyclocondensation Reactions”, *Org. Lett.* **2015**, *17*, 23, 5930-5933.

Chapter 3 of this thesis describes the synthetic sequence used to prepare the components for the MCR. In addition, this chapter reports our initial optimization and the synthesis of a range of

substituted benzoquinoline archipelago model asphaltene compounds. I was assisted in the scale-up of this procedure by two undergraduate research assistants, Jose F. Rodriguez and Mark Aloisio. Furthermore, I had the pleasure collaborating with a visiting scientist from AIST (The National Institute of Advanced Industrial Science and Technology) in Japan, Dr. Masato Morimoto, who separated and identified the side-products from one non-selective reaction. The manuscript for publication is in progress: Scott, D. E.; Aloisio, M. D.; Morimoto, M.; Rodriguez, J. F.; Hamilton, R. J.; Tykwinski, R. R.; Stryker, J. M. Dual “Single-atom” Catalysts for Oxidative Multicomponent Reactions. In addition, select compounds synthesized in this chapter were used to study Hansen solubility parameters which resulted in a publication, Morimoto, M.; Fukatsu, N.; Tanaka, R.; Takanohashi, T.; Kumagai, H.; Morita, T.; Tykwinski, R. R.; Scott, D. E.; Stryker, J. M.; Gray, M. R.; Sato, T.; Yamamoto, H. “Determination of Hansen Solubility Parameters of Asphaltene Model Compounds”, *Energy Fuels* **2018**, 32, 11296–11303.

*“Success consists of going from failure to failure without loss of enthusiasm.”*

*-Sir Winston Churchill*

*For Paul, Linda, Matthew, and Katie*

# Acknowledgements

I would like to begin by thanking my supervisor, Prof. Jeffrey M. Stryker. As my supervisor, he has been a supportive, enthusiastic, and patient influence. Jeff has continuously encouraged me to undertake various opportunities, and none more important than a research internship to Japan, for which I am so grateful. I have been extremely fortunate to have Jeff's untiring support from when I was an undergraduate student. His willingness to afford me the freedom to make mistakes and learn from them has proven to be invaluable. However, when I did struggle, I could always rely on him for several solutions. Eventually, I would learn, and he trusted me to discover the right answer for myself. This has been fundamental over the years and as my Ph.D. program comes to an end, Jeff's influence to constantly improve has been extremely important.

I am very appreciative of my host in Osaka Japan, Prof. Sensuke Ogoshi. He is a marvelous individual and made my time in his group very beneficial. The hospitality of his group was exceptional and extremely welcoming. I developed new skills while experiencing new and unfamiliar chemistry. I also had the pleasure of seeing and experiencing an amazing country. I look forward to visiting again!

I will always be thankful to Prof. Derrick Clive. He provided me my first research opportunity where I discovered my passion for synthetic chemistry. His initial influence, when I was still an undergraduate, was instrumental to discovering a future in chemistry.

I thank my committee for reading my thesis and attending my defense. I am very appreciative of Profs. Hall, Bergens, Lowary, and McCaffrey for their input during my candidacy exam. I would like to extend my thanks to Prof. Lundgren for attending my Ph.D. defense. I also thank Prof. Dmitrii Perepichka for his participation as my Ph.D. external examiner. Lastly, I am thankful for

the discussions and advice from Prof. Rik Tykwinski, who I have had the pleasure to collaborate with over my tenure as a graduate student.

My graduate research has greatly benefitted from analytical facilities and staff in the Department of Chemistry. Thank you to Ryan McKay, Mark Miskolzie, and Nupur Dabral from NMR services. Thank you to Wayne Moffat, and Jennifer Jones for elemental analyses and infrared spectroscopy. Thank you to the mass spectrometry group, specifically, Drs. Randy Whittal and Angie Morales. I also thank Andrew Yeung, Bernie Hippel, Matthew Kingston and Michael Barteski from Chemistry Stores, Jason Dibbs from the Glass Shop, Ryan Lewis from Shipping and Receiving, as well as our administrative help, Anita Weiler, Lynne Lechelt, Lin Ferguson, and Laura Pham.

A portion of my Ph.D. experience was spent as a Teaching Assistant. I was fortunate to work alongside Prof. Vederas, Prof. Stryker, and Dr. Hayley Wan who provided an enlightening and enjoyable experience in an otherwise chaotic environment. Also, I have benefited from the help of many individuals, but the assistance from Dr. Robin Hamilton, Dr. Orain Brown, Dr. Asama Vorapattanapong, Dr. Masato Morimoto, and Mark Aloisio has been the most significant. I would also like to thank all the past and present members of the Stryker group. The graduate experience would not have been as enjoyable if it wasn't for my friends in the department. Thank you to Tom Scully, Tom Warner, Sean Larade, Samantha Kwok, Ryan Sweeny, Randy Sanichar, Helen Clement, Patrick Moon, Sarah Parke, and Hannah Hackney.

Finally, I thank my parents for their encouragement throughout my education. I would not have been able to achieve this without them. I thank my Grandmother for her unwavering support, and I extend my thanks to my brother Matthew and his wife Katie for their support and constant encouragement the last number of years. Lastly, thank you to Bryce Manchak, Brent Kugyelka, and Dan Townes for their friendship during my time as a graduate student.

# Table of Contents

<b>1. History of Asphaltene Model Compound Synthesis .....</b>	<b>1</b>
Fossil Fuels– The Composition of Bitumen.....	1
1.1. Advances in asphaltene analytical science .....	3
1.2. Chemical composition of asphaltenes .....	4
1.3. Asphaltene structural models.....	7
Asphaltene Model Compounds .....	10
1.4. Synthetic continental model compounds.....	11
1.5. Unorthodox continental model compounds.....	16
1.6. Early synthetic methods for preparing archipelago model compounds.....	17
1.7. Advanced synthetic methodology for archipelago model compounds.....	20
Limitations to Model Compound Synthesis .....	26
Research Objectives .....	27
Experimental Section.....	28
<b>2. Synthetic Approaches to Quinoline Derivatives .....</b>	<b>30</b>
General Introduction to Nitrogen Heterocycles.....	30
2.1. Substituted quinoline heterocycles: a little nomenclature .....	32
2.2. Classical strategies for quinoline synthesis .....	33
Multicomponent Reactions – A General Introduction .....	38
2.3. MCR synthesis of tetrahydroquinolines by iodine catalysis .....	40
2.4. Condensed quinolines – extended quinoline-core compounds.....	44
Summary.....	52
Experimental Section.....	52

<b>3. Multicomponent Cyclocondensation for the Synthesis of Quinoline-core Archipelago Compounds .....</b>	<b>58</b>
MCR Advances: Three-island Archipelago Model Asphaltene Compounds.....	59
Results and Discussion .....	61
3.1. Three-island archipelago model compounds: synthesis of the aldehyde-terminated polycyclic “islands” .....	61
3.2. Initial optimization of the archipelago MCR reaction: an interim solution. ....	66
3.3. MCR optimization: testing solvent effects and oxidant concentration.....	68
3.4. Anisole as MCR solvent. An effective <i>interim</i> MCR optimization .....	75
3.5. MCR synthesis of archipelago model asphaltene compounds – scope and limitations .....	79
3.6. An application of asphaltene model quinolines: Hansen solubility parameters .....	84
Conclusion.....	87
Experimental Section.....	88
3.7. General synthetic procedure for 9-iodophenanthrene and 1-iodopyrene .....	90
3.8. General synthetic procedure of alkyl-tethered $\alpha,\omega$ -aryl aldehyde .....	91
3.9. MCR optimization: 5,6,7,8-tetrahydronaphthalen-1-amine .....	98
3.10. MCR Optimization: 4-Ethylaniline .....	101
3.11. Scope of multicomponent reaction compounds.....	102
<b>4. Investigating the Mechanistic Details of the HI-Catalyzed MCR. Enhancements in MCR Yields, Selectivity, and Scope ....</b>	<b>125</b>
4.1. Reoptimizing the reaction parameters: conditions and catalysts.....	126
4.2. The nature of the oxidant in the multicomponent cyclocondensation: defining and expanding the roles of oxygen and iodide .....	129
4.3. Proposal of the oxygen iodine redox reaction .....	137
4.4. Solving the mass balance deficiency .....	140

4.5. Ramifications of control reactions and MCR optimization: a refined mechanistic rationale.....	144
4.6. Scope of the MCR under reoptimized reaction parameters. Problematic substrates.....	148
Experimental Section.....	152
4.7. MCR optimization: general synthetic procedure.....	153
4.8. Scope of multicomponent reaction compounds. Optimized conditions.....	158
<b>5. Bi-directional MCR and Future Prospects.....</b>	<b>162</b>
5.1. Bi-directional MCRs. Synthetic approaches and preliminary results .....	162
5.2. Further investigations. The radical cation MCR .....	169
Radical Cation Catalyst .....	169
Generating Radical Cations Electrochemically.....	172
5.3. Final thoughts .....	174
Experimental Section.....	174
<b>Bibliography .....</b>	<b>177</b>
<b>Appendix I: <sup>1</sup>H and <sup>13</sup>C NMR Spectra.....</b>	<b>190</b>

# List of Figures

<b>Figure 1-1.</b> SARA analysis of bitumen.....	2
<b>Figure 1-2.</b> (1) Imaged structure of a continental compound and (2) imaged structure of archipelago-like compound.....	4
<b>Figure 1-3.</b> Asphaltene elemental composition.....	5
<b>Figure 1-4.</b> Nitrogen based compounds identified in Athabasca asphaltene by mass spectrometry .....	7
<b>Figure 1-5.</b> Actual continental-like molecule identified in bitumen.....	8
<b>Figure 1-6.</b> Fictional representation of a representative archipelago molecule. ....	9
<b>Figure 1-7.</b> Fictional representation of the archipelago model association behaviour .....	10
<b>Figure 1-8.</b> Continental model substrates explored as asphaltene mimics. ....	11
<b>Figure 1-9.</b> Small continental model compounds. ....	12
<b>Figure 1-10.</b> Oxygen containing continental-like structures.....	15
<b>Figure 1-11.</b> Heteroatom containing continental-like structures. ....	15
<b>Figure 1-12.</b> Functionalized perylene structures as asphaltene model compounds. ....	16
<b>Figure 1-13.</b> Continental and archipelago-like carboxylic acid model compounds .....	17
<b>Figure 1-14.</b> Selected biomarker components identified in fossil fuels: tricyclic terpane, (left top), hopane-type pentacyclic triterpane (left bottom), vanadyl-ethioporphyrin III (middle), and sterane (right) .....	25
<b>Figure 2-1.</b> Cyclic compound classification, with representative examples.....	30
<b>Figure 2-2.</b> Select examples of azaheterocyclic derivatives capable of therapeutic purposes.....	31
<b>Figure 2-3.</b> Nitrogen cores typically found in natural and unnatural products.....	31
<b>Figure 2-4.</b> Examples for nomenclature rules for naming heterocycles. ....	33
<b>Figure 2-5.</b> Multi-catalytic vs. domino/cascade and tandem one-pot reactions.....	40
<b>Figure 2-6.</b> Fictitious example of a potential two-island archipelago model asphaltene.....	43

<b>Figure 2-7.</b> Suggested steroid fused biomarker molecules identified in heavy crude oil .....	46
<b>Figure 3-1.</b> Synthesized PAH tethered alkyl-tethered $\alpha,\omega$ -aryl aldehyde.....	66
<b>Figure 3-2.</b> Two available ortho-positions for the cyclization.....	76
<b>Figure 3-3.</b> Synthesized asphaltene-like quinoline model compounds incorporating various methyl and ethyl substituents.....	80
<b>Figure 3-4.</b> Ortho-positions available for cyclization is limited due to substitution.....	80
<b>Figure 3-5.</b> Extended saturated and unsaturated synthesized quinoline-core asphaltene-like compounds.....	81
<b>Figure 3-6.</b> Testing the generality of the MCR by introducing electron donating/withdrawing substituents.....	82
<b>Figure 3-7.</b> Varying the terminal island in the MCR: pyrene vs phenanthrene.....	83
<b>Figure 3-8.</b> All quinoline-core compounds synthesized by our initial optimal conditions.....	84
<b>Figure 3-9.</b> Quinoline-core archipelago model compound studied using HSPs.....	86
<b>Figure 4-1.</b> Examples of hypervalent iodide III and V species.....	138
<b>Figure 4-2.</b> The formation of the iodonium cation from iodide in the presence of $H_2O_2$ .....	138
<b>Figure 4-3.</b> Equilibria equations postulated in neutral and acidic reaction media.....	139
<b>Figure 4-4.</b> <i>n</i> -Butylphenanthrene from oxidative decomposition of aldehyde <b>151</b> .....	142
<b>Figure 4-5.</b> Isolated quinoline-core compounds synthesized using NaI as the iodide source in Chapter 3.....	149
<b>Figure 4-6.</b> Three-island quinoline-core archipelago-like structures synthesized from the new optimal conditions.....	150

# List of Schemes

<b>Scheme 1-1.</b> Synthesis of HBC derivatives.....	14
<b>Scheme 1-2.</b> Early model compound synthesis of the two island systems in unreported yields.....	18
<b>Scheme 1-3.</b> Synthesis of a three-island bipyridine archipelago model compound.....	19
<b>Scheme 1-4.</b> Multi-island synthesis of archipelago models .....	22
<b>Scheme 1-5.</b> Stepwise synthesis of fused naphthenic benzoquinolines. ....	23
<b>Scheme 2-1.</b> Traditional quinoline synthesis.....	34
<b>Scheme 2-2.</b> Skraup reaction and mechanism.....	35
<b>Scheme 2-3.</b> Conrad-Limpach and Combes quinoline synthesis. ....	36
<b>Scheme 2-4.</b> Pfitzinger reaction. ....	37
<b>Scheme 2-5.</b> Povarov quinoline synthesis.....	38
<b>Scheme 2-6.</b> Efficient synthesis of benzo(naphtho)quinoline and alkaloid derivatives.....	44
<b>Scheme 2-7.</b> Proposed (literature) mechanism for iodine-catalyzed MCR quinoline synthesis ..	45
<b>Scheme 2-8.</b> Two-step procedure of steroid-derived naphthoquinolines.....	47
<b>Scheme 3-1.</b> I <sub>2</sub> -catalyzed quinoline synthesis using two aliphatic aldehydes.....	58
<b>Scheme 3-2.</b> Quinoline MCR using two aliphatic aldehydes.....	59
<b>Scheme 3-3.</b> Lewis acid catalyzed substituted quinoline synthesis and identification of secondary amine by-product .....	61
<b>Scheme 3-4.</b> Practical, large-scale synthesis of variable tethered alkyl-tethered $\alpha,\omega$ -aryl aldehyde.....	63
<b>Scheme 3-5.</b> Copper-catalyzed aromatic halide exchange reaction converting bromoarene to iodoarene.....	63
<b>Scheme 3-6.</b> Formation of product and side-product from the MCR reaction using two alkyl aldehydes.....	68

<b>Scheme 4-1.</b> Qualitative test designed for testing the presence of H <sub>2</sub> O <sub>2</sub> .....	130
<b>Scheme 4-2.</b> Background reactions to determine undesirable side reactions resulting in decreased MCR yields. ....	141
<b>Scheme 4-3.</b> The effect of a sacrificial aldehyde addition (pivaldehyde or an excess of substrate) to inhibit decomposition of the aldehyde <b>151</b> .....	143
<b>Scheme 4-4.</b> Protonation of imine to form the activated diene iminium intermediate.....	145
<b>Scheme 4-5.</b> Cyclization process to form the tetrahydroquinoline intermediate. ....	145
<b>Scheme 4-6.</b> Proposed MCR mechanism which incorporates the new oxidants identified from the control reactions.....	147
<b>Scheme 4-7.</b> Potential subsequent 1,5 hydride shifts that may occur during the final stages of the MCR.....	151
<b>Scheme 5-1.</b> Synthesis of the mono- <i>N</i> -alkylimine in a highly concentrated solvent solution. ..	167
<b>Scheme 5-2.</b> Wang's proposed radical MCR mechanism .....	171
<b>Scheme 5-3.</b> Hypothetical synthesis which combines Gen 1 and MCR approaches. ....	172

# List of Equations

<b>Equation 1-1.</b> Sonogashira alkynylation and subsequent catalytic hydrogenation affording a tetrasubstituted alkyl pyrene in an unreported yield. ....	13
<b>Equation 1-2.</b> Sonogashira coupling/catalytic hydrogenation forming three-island/two-island compounds .....	21
<b>Equation 1-3.</b> MCR synthesis of the 5- $\alpha$ -cholestanone quinoline model compounds. ....	24
<b>Equation 1-4.</b> Mixed biomarker model compounds. ....	25
<b>Equation 1-5.</b> Synthesis of archipelago-like metalloporphyrins. ....	26
<b>Equation 2-1.</b> Doebner-von Miller quinoline synthesis.....	35
<b>Equation 2-2.</b> Ugi 4-component MCR. ....	39
<b>Equation 2-3.</b> Imino Diels-Alder reaction of tetrahydroquinolines catalyzed by iodine.....	41
<b>Equation 2-4.</b> A highly efficient domino reaction to synthesize 1,2,3,4- tetrahydroquinoline derivatives. ....	41
<b>Equation 2-5.</b> Aza-Diels-Alder Povarov synthesis of tetrahydroquinolines .....	42
<b>Equation 2-6.</b> Synthesis of cyclopenta[ <i>c</i> ]naphtho[2,3- <i>f</i> ]quinoline derivatives .....	46
<b>Equation 2-7.</b> Steroid-derived multicomponent reaction. ....	48
<b>Equation 2-8.</b> Stryker and co-workers MCR conditions for determination of the optimal H <sub>2</sub> O content.....	48
<b>Equation 2-9.</b> Re-evaluation of MCR yield for steroid-derived naphthoquinoline. ....	50
<b>Equation 2-10.</b> Hypothetical MCR quinoline syntheses incorporating alkyl-tethered $\alpha,\omega$ -aryl aldehyde aldehydes. ....	51
<b>Equation 3-1.</b> Synthetic approach to new three-island archipelago model compounds.....	60
<b>Equation 3-2.</b> Reduction of the <i>N</i> -alkylimine to the secondary amine.....	60
<b>Equation 3-3.</b> Synthetic plan to assemble the desired alkyl-tethered $\alpha,\omega$ -aryl aldehyde. ....	62

<b>Equation 3-4.</b> Phosphine ligands used to promote the migratory Heck reaction using aryl bromides.....	62
<b>Equation 3-5.</b> Migratory Heck reaction to afford the linear and branched alkyl-tethered $\alpha,\omega$ -aryl aldehyde. ....	64
<b>Equation 3-6.</b> Kinetic vs. thermodynamic insertion of the alkene at room temperature. ....	65
<b>Equation 3-7.</b> Initial reaction conditions for the synthesis of 2-(4-(phenanthren-9-yl)butyl)-3-(3-(phenanthren-9-yl)propyl)-7,8,9,10-tetrahydrobenzo[ <i>h</i> ]quinoline. ....	67
<b>Equation 3-8.</b> Quinoline-core archipelago compounds synthesized using catalytic HI in ethanol. ....	69
<b>Equation 3-9.</b> MCR using ethanol as solvent: competitive formation of the aldehyde cyclic trimer.....	70
<b>Equation 3-10.</b> Reaction optimization investigating the affect of catalyst/oxygen concentration. ....	71
<b>Equation 3-11.</b> Screening MCR conditions as a function of solvent.....	72
<b>Equation 3-12.</b> Investigating the MCR using catalytic I <sub>2</sub> with and without a D <sub>2</sub> O additive. ....	73
<b>Equation 3-13.</b> Quinoline synthesis using benzene as solvent. Amplified formation of secondary amine.....	74
<b>Equation 3-14.</b> MCR conditions used to screen for the effects of oxygen concentration. ....	74
<b>Equation 3-15.</b> General MCR screening for optimal reaction conditions using 4-ethylaniline as the aniline substrate.....	77
<b>Equation 3-16.</b> Reaction conditions for the generalized synthesis of three-island archipelago compounds. ....	78
<b>Equation 3-17.</b> Mathematical equations for Hansen solubility parameters.....	85
<b>Equation 4-1.</b> Semi-optimal conditions identified from Chapter 3. ....	126
<b>Equation 4-2.</b> Reaction equation for the formation of H <sub>2</sub> O <sub>2</sub> . ....	129
<b>Equation 4-3.</b> Reaction conditions investigating the role of Brønsted acid catalysts and H <sub>2</sub> O <sub>2</sub>	131
<b>Equation 4-4.</b> General reaction parameters to investigate the differences in iodide additives..	136

<b>Equation 4-5.</b> Undesired secondary amine formation resulting from aromatization to generate the final quinoline compound. ....	146
<b>Equation 4-6.</b> Optimal reaction conditions implemented to form a few quinoline-cored three island archipelago compounds.....	148
<b>Equation 5-1.</b> Hypothetical synthetic route to new five-island archipelago model compounds .....	1633
<b>Equation 5-2.</b> Synthesis of continental-like archipelago compounds using a bi-directional MCR. ....	163
<b>Equation 5-3.</b> Bi-directional synthesis using four equivalents of an alkyl-tethered $\alpha,\omega$ -aromatic aldehyde .....	164
<b>Equation 5-4.</b> Bi-directional MCR using 1,8-diaminonaphthylene to acquire 2,11-bis(4-(phenanthren-9-yl)butyl)-3,10-bis(3-(phenanthren-9-yl)propyl)quinolino[7,8- <i>h</i> ]quinoline. ....	166
<b>Equation 5-5.</b> Unsuccessful synthesis of the 1,8 bis-imine in dilute ethanol. ....	167
<b>Equation 5-6.</b> Synthesis of (1 <i>E</i> ,1' <i>E</i> )- <i>N,N'</i> -(naphthalene-1,5-diyl)bis(5-(phenanthren-9-yl)pentan-1-imine).....	168
<b>Equation 5-7.</b> Bi-directional MCR using the semi-optimal/enhanced conditions identified in Chapter 3/4.....	169
<b>Equation 5-8.</b> Catalytic radical cation MCR proof of principle. ....	170
<b>Equation 5-9.</b> Prospective double-MCR model compound.....	171
<b>Equation 5-10.</b> Electrochemically generated stoichiometric $I_3^-$ for MCR application. ....	173
<b>Equation 5-11.</b> Electrochemical bi-directional MCR accomplished using stoichiometric $I_3^-$ ...	173

# List of Tables

<b>Table 1-1.</b> Composition by mass of Athabasca asphaltenes. ....	14
<b>Table 2-1.</b> Screening the effect of water concentration in the synthesis of naphthoquinolines. ....	49
<b>Table 2-2.</b> Brønsted acid catalyst screening, using identical water concentration, to evaluate the MCR.....	50
<b>Table 3-1.</b> Effects of catalyst concentration in the presence of variable O <sub>2</sub> atmosphere. ....	71
<b>Table 3-2.</b> Effect of oxygen concentration on the MCR synthesis of quinolines. ....	75
<b>Table 3-3.</b> Catalyst concentration, temperature, and additive screening for MCR optimization..	77
<b>Table 4-1.</b> Effects of catalyst loading and the presence of NaI additive on the MCR efficiency. ....	127
<b>Table 4-2.</b> Investigation of the semi-optimal conditions to define the optimal amount of water. ....	128
<b>Table 4-3.</b> Qualitative testing for the generation of H <sub>2</sub> O <sub>2</sub> under our reaction conditions.....	130
<b>Table 4-4.</b> Control reactions investigating the affect of slow addition of H <sub>2</sub> O <sub>2</sub> to the MCR.....	132
<b>Table 4-5.</b> Control reactions investigating other Brønsted acids and H <sub>2</sub> O <sub>2</sub> . ....	133
<b>Table 4-6.</b> Cationic halogen sources as additives to enhance the MCR yields.....	134
<b>Table 4-7.</b> Investigating other cationic halogen sources as catalyst to enhance the MCR yields. ....	135
<b>Table 4-8.</b> TBAI vs. NaI additives: Evaluating the difference in soluble iodide reagents. ....	136
<b>Table 4-9.</b> Effects of sacrificial aldehyde: <sup>t</sup> BuCHO vs. three equivalents of compound <b>151</b> ....	143
<b>Table 5-1.</b> MCR conditions for bi-directional synthesis of continental archipelago compounds. ....	163
<b>Table 5-2.</b> MCR bi-directional synthesis using 4 equivalents of alkyl-tethered $\alpha,\omega$ -aromatic aldehyde. ....	165

**Table 5-3.** Bi-directional MCR using 1,8-diaminonaphthylene in concentrated and dilute solvent conditions..... 166

# List of Abbreviations

acac	Acetylacetonyl
AFM	Atomic force microscopy
Ar	Aromatic
atm	Atmosphere
aq	Aqueous
BF <sub>3</sub> -OEt <sub>2</sub>	Boron trifluoride diethyl etherate
Br	Broad
<i>t</i> -BuCHO	Pivalaldehyde
<i>n</i> -Bu	Normal Butyl
<i>t</i> -Butyl	Tertiary Butyl
calcd	Calculated
CF <sub>3</sub>	Trifluoromethyl
cm <sup>-1</sup>	Wavenumbers
CN	Nitrile
Cy <sub>2</sub> NMe	<i>N, N</i> -Dicyclohexylmethylamine
d	Doublet
Da	Daltons
Db	Dibenzylideneacetone
DCM	Dichloromethane
ddd	Doublet of doublet of doublets
DDQ	2,3-Dichloro-6,6-dicyano-1,4-benzoquinone
ddt	Doublet of doublet of triplets
DFT	Density functional theory
DMEDA	<i>N, N'</i> -Dimethylethylenediamine
DMF	<i>N, N</i> -Dimethylformamide
DNA	Deoxyribonucleic acid
DOSY	Diffusion ordered spectroscopy

dppe	1,2-Bis(diphenylphosphino)ethane
dq	Doublet of quartets
dt	Doublet of triplets
E	Cohesive energy
EA	Elemental analysis
Ee	Enantiomeric excess
EI-MS	Electron impact mass spectrometry
EtOAc	Ethyl acetate
Eq	Equation
Equiv	Equivalents
ESI	Electrospray ionization
Et	Ethyl
EtOH	Ethanol
FT	Fourier transform
g	Gram
GC	Gas chromatography
h	Hours
HBC	Hexabenzocoronene
HSP	Hansen solubility parameters
<i>n</i> -Hex	Normal hexyl
HRMS	High-resolution mass spectrometry
Hz	Hertz
ICP-MS	Inductively coupled plasma mass spectrometry
IR	Infrared spectroscopy
ITC	Isothermal titration calorimetry
JPEC	Japan Petroleum Energy Center
K	Kelvin
LA	Lewis Acid
LDA	Lithium diisopropylamide
M	Molar

m	Multiplet
mA	Milliamps
MALDI	Matrix-assisted laser desorption/ionization
Me	Methyl
MeCN	Acetonitrile
mg	Milligram
MHz	Megahertz
mL	Milliliter
mm	Millimetre
mmol	Millimole
mol	Mole
MPa	Megapascal
NBS	<i>N</i> -Bromo succinimide
NCS	<i>N</i> -Chloro succinimide
NEt <sub>3</sub>	Triethylamine
NIS	<i>N</i> -Iodo succinimide
Nm	Nanometer
NMR	Nuclear magnetic resonance
OAc	Acetoxy
OMe	Methoxy
OTf	Triflate
Ph	Phenyl
PhMe	Toluene
ppm	Parts per million
<i>i</i> Pr	Isopropyl
psig	Pounds per square inch gauge
q	Quartet
quint	Quintet
R <sub>0</sub>	Interaction radius
R <sub>a</sub>	Distance between Hansen parameters in Hansen space

RBF	Round-bottom flask
RED	Relative energy difference
RF	Retention factor
RNA	Ribonucleic acid
RT	Room temperature
s	Singlet
SANS	Small-angle neutron scattering
sh	Sharp
STM	Scanning tunneling microscope
t	Triplet
td	Triplet of doublets
tdd	Triplet of doublet of doublets
tt	Triplet of triplets
TBACl	Tetra- <i>n</i> -butylammonium chloride
TBAI	Tetra- <i>n</i> -butylammonium iodide
TBPA <sup>+</sup>	Tris(4-bromophenyl)ammoniumyl hexachloroantimonate
TEMPO	2,2,6,6-Tetramethylpiperidin-1-yl)oxyl
TFA	Trifluoroacetic acid
THF	Tetrahydrofuran
TLC	Thin layer chromatography
TOF	Time of flight
TsOH	<i>p</i> -Toluenesulfonic acid
UV	Ultraviolet
V	Molar volume
VPO	Vapor pressure osmometry
w	Weak
wt%	Weight percent
°C	Degrees Celsius
μL	Microliter

# 1. History of Asphaltene Model Compound Synthesis

## Fossil Fuels– The Composition of Bitumen

The demand for fossil-based fuels and petrochemicals continues to grow rapidly across the globe. However, this is mirrored by a depletion of easily accessible light crude oils, which are typically processed into fossil fuels. This trend has forced producers to spend increasing amounts of capital to develop heavier, less accessible, crude oil sources, such as those found in the Alberta Oil Sands.<sup>[1–3]</sup> Vast amounts of heavy crude oil (approximately 170 billion barrels) are found in the Oil Sands, located in the Athabasca and Cold Lake regions of Alberta.<sup>[4]</sup> In addition, other oil sands and heavy petroleum resources are being developed around the world.<sup>[5]</sup> However, the chemical composition and resulting physical properties of these heavy crude oils lead to significant challenges in transporting and refining the raw material into fuels and petrochemicals. Heavy crude oils and bitumen contain a disproportionate fraction of high molecular weight molecules/aggregates, which further agglomerate in an uncontrolled manner, under processing conditions. With the increased use of heavy crude oils, associated draw-backs are magnified, both physically and chemically. These issues include asphaltene precipitation during transport and/or storage and catalyst deactivation caused by thermal coke formation.<sup>[6–15]</sup> Therefore, innovative technologies to convert this valuable resource into transportation fuels and petrochemical feed stocks has become a high priority.

Bitumen, a black tarry petroleum resource having a density  $< 1000 \text{ kg/m}^3$ , is comprised of mainly large cyclic and acyclic organic heavy hydrocarbon molecules along with some complexed metals (predominantly Ni and V). Its bulk properties are due to thousands of complex structures and abundant functionality, including polycyclic aromatics, polar functional groups, and heteroatoms.<sup>[11,16,17]</sup> For the raw commodity to have value, the bitumen must be separated from the

geological matrix and subjected to extensive upgrading/refining, *via* processes such as fractional distillation and hydrotreatment.<sup>[18]</sup> The most valuable component of raw bitumen is the alkane-soluble maltene fraction, which is composed of volatile saturated and aromatic molecules, as well as heavier resins (see the SARA method Figure 1-1).<sup>[19,20]</sup> This portion of bitumen is typically processed into fuels and petrochemicals. The heavier fraction of bitumen, referred to as the asphaltenes, is insoluble in alkanes but soluble in aromatic solvents (e.g. toluene). The asphaltenes constitute the heaviest, most poorly characterized, and least understood fraction of bitumen.<sup>[21]</sup>

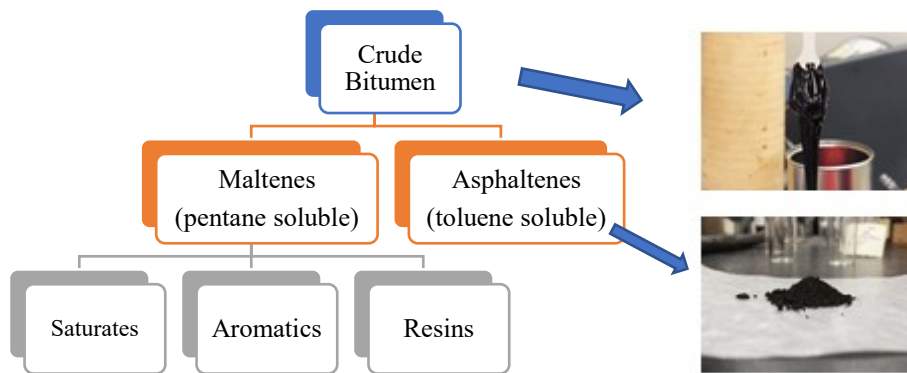


**Figure 1-1.** SARA analysis of bitumen.<sup>[19–21]</sup>

The limited knowledge about the asphaltenes results from the high molecular weights, functional group diversity, and complex intermolecular interactions characteristic of its constituent molecules.<sup>[22]</sup> There is ongoing debate regarding the average molecular weight of asphaltene constituents. Early estimates based on mass spectrometric and molecular diffusion techniques posited an average molecular weight of 600-750 Da.<sup>[12,17,23–27]</sup> but advances in mass spectrometry has resulted in a significant upward revision of that number to 2800-3600 Da. Nonetheless, considerable disagreement persists.<sup>[28–31]</sup> In addition, the possible chemical structures of asphaltene constituent molecules, along with the nature of the inter- and intramolecular

interactions, remain poorly understood and vigorously debated. No reliable technique has as yet been developed to determine the exact molecular arrangement of individual asphaltene molecules or their aggregates; however, much research continues to be dedicated to this area.<sup>[22]</sup>

### **1.1. Advances in asphaltene analytical science**

Much of the data used to construct structural models for asphaltenes is derived from a suite of analytical techniques used to probe natural asphaltenes. These techniques include modern mass spectrometry (ICP-MS) and vapor phase osmometry (VPO) for determining molecular weight distribution,<sup>[32–38]</sup> small-angle neutron scattering (SANS) for identifying asphaltene aggregates,<sup>[39]</sup> fluorescence depolarization to measure the molecular size of aggregates,<sup>[40,41]</sup> infrared spectroscopy (IR) for characterizing intermolecular interactions (e.g. hydrogen bonding),<sup>[42]</sup> isothermal titration calorimetry (ITC) for revealing asphaltene self-association,<sup>[43]</sup> and atomic force/scanning tunneling microscopies (AFM, STM)<sup>[44–46]</sup> for single molecule imaging.<sup>[44]</sup>

More recently, AFM, STM, and several novel mass spectrometric techniques, have revealed at least partial structural identification of individual constituents in asphaltenes. This has greatly refined our understanding and guided the targeted design of more representative model compounds. For example, Gross and co-workers, using coal-derived asphaltenes, combined AFM and STM to identify a range of individual continental-like compounds (Figure 1-2, e.g. **1**) and, in one case, an archipelago-like heteroaromatic structure (Figure 1-2, e.g. **2**).<sup>[44]</sup> Each compound appears to have peripheral substituents, but these could not be imaged with precision. While ground-breaking, this study must be interpreted with some caution: the compounds imaged lacked sophisticated functionality and the actual ‘parent’ molecules may not have survived the high

temperature (900 K) flash sublimation techniques used to coat the Cu(1 1 1) molecular imaging substrate.

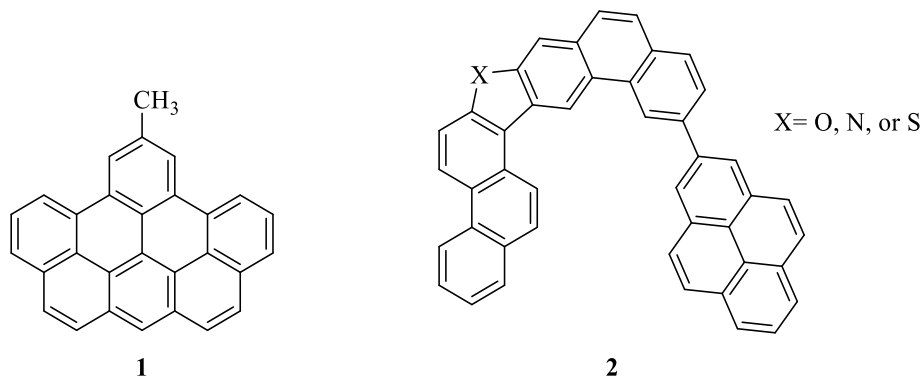


**Figure 1-2. (1)** Imaged structure of a continental compound and **(2)** imaged structure of archipelago-like compound.<sup>[44]</sup>

In 2017, imaging of *synthetic* archipelago model compounds was conducted by high-resolution noncontact atomic force microscopy.<sup>[45]</sup> The structural features clearly defined included planar polycyclic aromatic molecules, as well as linear alkyl and cycloaliphatic functionality. The authors conclude that the application of AFM for structural investigation of asphaltenes has become a superior analytical technique for individual molecule identification, and suggest that there may be a significantly higher number of archipelago compounds than had been previously determined.<sup>[44]</sup> This advance in characterization bodes well for future identification of both aromatic and aliphatic moieties in authentic asphaltene samples. Asphaltene aggregates, however, remain out of analytical reach.

## 1.2. Chemical composition of asphaltenes

Evidence from the analysis of asphaltenes has established that the constituent molecules are principally medium-to-large polycyclic aromatic ring systems (PAHs). The PAHs often

incorporate heteroatoms (sulphur, oxygen, and nitrogen; see Figure 1-3) in the cyclic core and are decorated by either terminal or tethering saturated alkyl chains. In addition, the molecules contain many cyclic and acyclic polar functional groups (carboxylic acids, phenols, thioethers, and polycyclic derivatives of pyrrole, indole, pyridine, quinoline, etc.), residual biomarkers (e.g. elaborated porphyrins, hopanes), and ligated transition metals (mostly vanadium and nickel).<sup>[11,20,47-50]</sup>

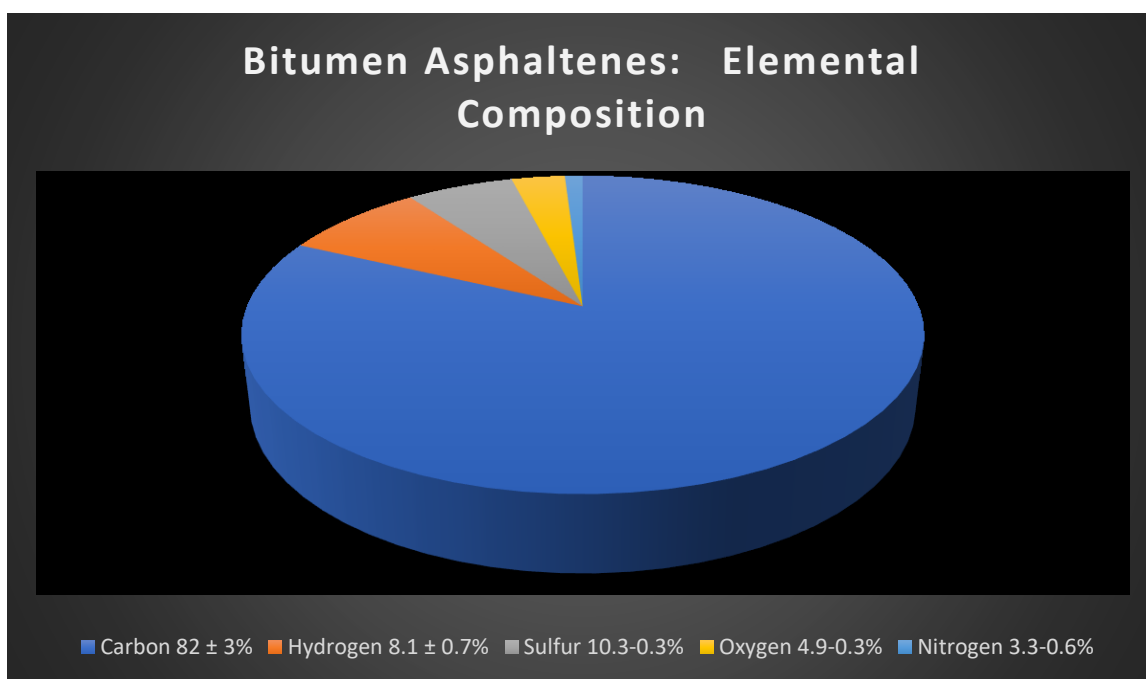


**Figure 1-3.** Asphaltene elemental composition.<sup>[20]</sup>

Heteroatoms such as nitrogen, sulphur and oxygen comprise a minority of the mass of bitumen; nevertheless, the polar intermolecular interactions resulting from their presence are of great importance for understanding the bulk behaviour of asphaltenes. The most abundant heteroatom found in asphaltenes is sulphur, accounting for as much as 10% of the total mass, while nitrogen is least abundant (typically < 3.5%).<sup>[49,51,52]</sup> The heteroatom content of asphaltenes can vary

widely, particularly for oxygen and sulfur. This is generally attributed to the geological environment in which the oil developed and how the crude oil was processed, e.g., during diagenesis and catagenesis, incorporation of sulfur comes from elemental sulfur deposits or sulfur-containing minerals.<sup>[49,53]</sup> Furthermore, the majority of oxygen is incorporated during diagenesis/catagenesis, however, the amount of oxygen is further increased when the petroleum reservoir is exposed to atmospheric oxygen.<sup>[49,53]</sup> Sulfur in asphaltenes occurs mainly in benzothiophenes, dibenzothiophenes, and naphthenic benzothiophenes. In addition, other sulfur-containing compounds have been identified, including dialkyl, alkyl/aryl, and diaryl sulfides.<sup>[49,51]</sup> Conversely, oxygen atoms are usually found in molecules primarily identified as carboxylic acids, phenols, and diarylketones. Thus, most oxygen atoms in petroleum are limited to peripheral aliphatic chains, instead of being incorporated into heterocycles.<sup>[49,51,52,54]</sup> Nitrogen atoms, on the other hand, are found almost exclusively in heterocyclic molecules, with pyrrole rings being the most abundant reservoir of this heteroatom. In addition, a significant amount of nitrogen in asphaltenes is found in pyridine, quinoline, and benzoquinoline ring systems (compounds **4-10**), as well as in a few four-ring aromatic species.<sup>[49,51,52,54-57]</sup> Non-basic nitrogen species such as carbazole and derivatives (e.g., **3**) are also found in asphaltenes.<sup>[54]</sup> The molecular assignments for nitrogen, oxygen, and sulphur were made based on data obtained from analytical separations and mass spectrometric analysis, as well as chemical degradation (Figure 1-4).<sup>[49,51,52,54-58]</sup> Nitrogen contain heterocycles, particularly quinolines and benzoquinolines, will be the focus of this dissertation, partly because they give rise to strong associative interactions (e.g., acid/base reactions and/or hydrogen bonding), but more importantly because the strategies used for constructing such molecular cores also allow for rapid, modular synthesis of very large alkyl-tethered polycyclic aromatic structures which are of critical importance to modelling the behaviour

of asphaltenes. Thus, the molecules I am synthesizing are quinoline-like compounds; which will comprise a new library of archipelago model structures. The design and preparation of model compounds will be further discussed in the remaining sections of this chapter, and again, in Chapter 2.

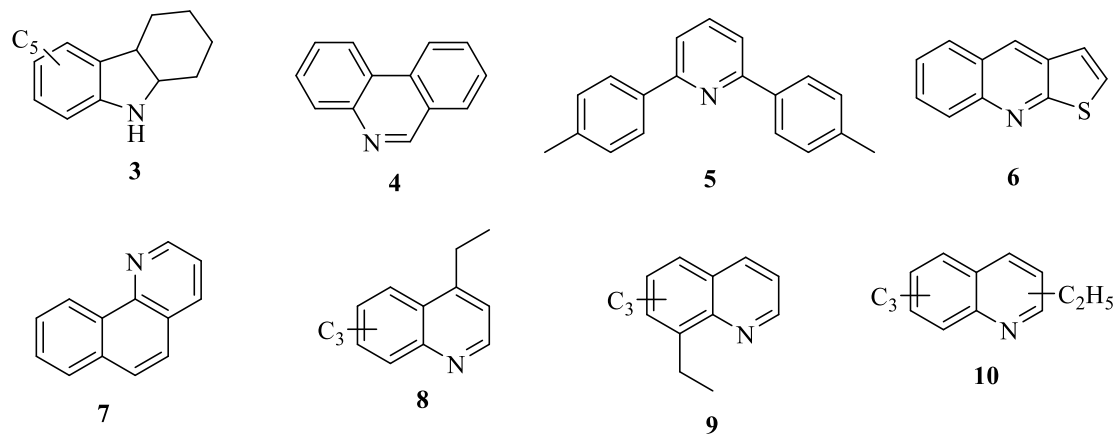


**Figure 1-4.** Nitrogen based compounds identified in Athabasca asphaltene by mass spectrometry.<sup>[51,52,54,55,57]</sup>

### 1.3. Asphaltene structural models

The high molecular weight and highly unsaturated compounds found in asphaltenes are thought to be best represented by a combination of two distinct structural motifs. These conceptual models attempt to explain the fragmentation patterns seen in mass spectrometric analysis, as well as the bulk aggregation behaviour well-established for asphaltenes. The Yen-Mullins “*continental*” model (originally termed the Yen model) defines the “average” asphaltene compound as a single highly condensed polycyclic aromatic compound, functionalized by peripheral alkyl substituents of various lengths, with incorporation of ring heteroatoms (S, N, and O, in descending order of abundance) (Figure 1-5).<sup>[49]</sup> The primary aggregation motif is identified as face-to-face  $\pi$ - $\pi$

stacking interactions of the quasi-graphitic cores. However, experimental evaluation of the aggregation behaviour of simpler, unfunctionalized model continental-like molecules (e.g., hexabenzocoronene) reveals that  $\pi$ - $\pi$  association energy alone cannot account for the total aggregation behaviour found in authentic asphaltene samples.

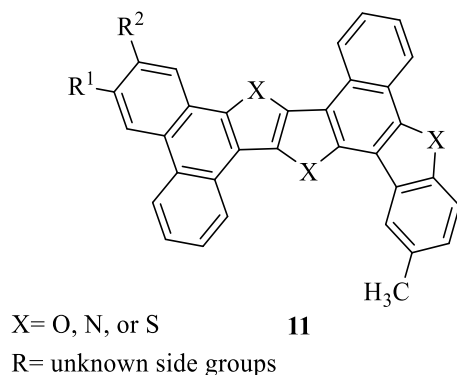
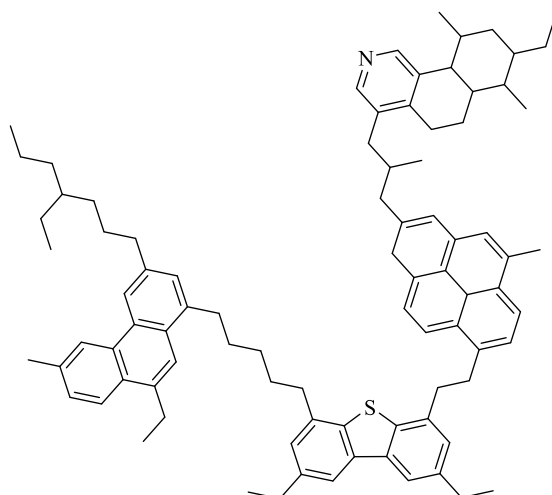


**Figure 1-5.** Actual continental-like molecule identified in bitumen.<sup>[44]</sup>

A structural model accounting for all the inter- and intramolecular associative interactions was therefore necessary. To represent the diversity of associative interactions, a second structural hypothesis was conceptualized and termed the “*archipelago*” model (Figure 1-6).<sup>[25,44]</sup> The archipelago model depicts asphaltene molecules as being composed of smaller condensed aromatic and naphthenic (partially aromatic) “islands,” decorated with alkyl sidechains and tethered together by saturated alkyl (C2-C6) and thioether bridges. The aromatic “islands” incorporate the heteroatoms and the molecule can be further decorated with complex functionality, e.g., steroidal biomarker residues and porphyrin-like rings.<sup>[59]</sup>



12

**Figure 1-6.** Fictional representation of a representative archipelago molecule.

The range of intermolecular interactions available to ‘archipelago’ molecules better correlates with the aggregation forces observed in authentic asphaltene samples. A cartoon rendering of an asphaltene aggregate composed of archipelago molecules (Figure 1-7) implicates a variety of cooperative intra- and intermolecular interactions: hydrogen bonding, acid-base interactions,  $\pi$ - $\pi$  stacking, hydrophobic pockets, small molecule inclusion complexes, and metal-ligand complexation.<sup>[11]</sup> Taken together, these interactions more accurately depict supramolecular interactions anticipated in authentic asphaltenes. Indeed, modelling studies support this hypothesis – the aggregation behaviour of archipelago model compounds is more representative than that observed for continental compounds.<sup>[60]</sup> Using molecular dynamics simulation, Cañas-Marín and co-workers showed that archipelago structures have the flexibility to maximize Van der Waals interactions, thus increasing overall aggregation energy. The comparable lack of flexibility in the large polycyclic aromatic cores of continental structures, even with flexible peripheral alkyl chains, has the net effect of reducing the volume of Van der Waals interactions, thus limiting aggregation energy.<sup>[61]</sup> However, a *combination* of both model systems, perceived as one

continental-archipelago construct, may further enhance the aggregation profile, more accurately representing natural asphaltenes.

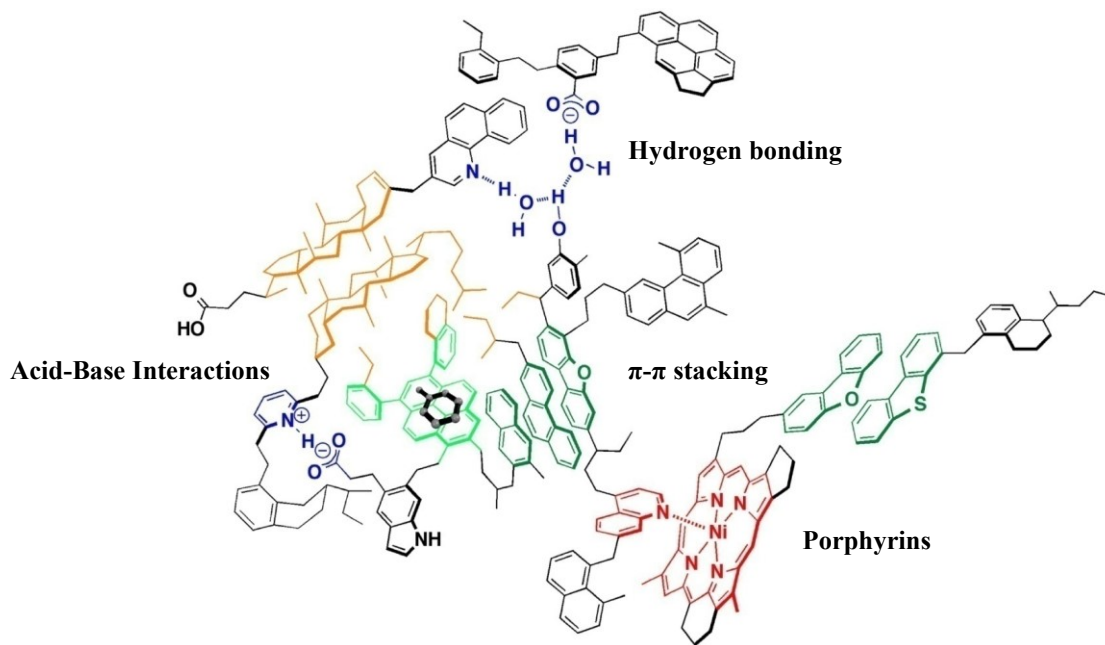


**Figure 1-7.** Fictional representation of the archipelago model association behaviour. (Adapted with permission from Gray M.R., Tykwinski R.R., Stryker J.M., Tan X. Supramolecular assembly model for aggregation of petroleum asphaltenes *Energy Fuels*, **2011**, 25, 3125-3134. Copyright 2012 American Chemical Society).<sup>[11]</sup>

### Asphaltene Model Compounds

Historically, the complex physical properties of asphaltenes have been modelled by experimental<sup>[62-74]</sup> and computational studies,<sup>[41,75-79]</sup> using only commercially-available PAHs. Both carbocyclic and heterocyclic compounds with varying degrees of alkyl substitution/bridging have been used for this purpose.<sup>[78,80-82]</sup> Even more elaborate compounds, including biomarker analogues (e.g. porphyrins) and over functionalized organic dyes (e.g. perylenediimides) have also found use as models for asphaltene constituents. Unfortunately, these model compounds are overly simplified compared to the vastly more complex asphaltene phase, not to mention compositionally irrelevant. Thus, the quality and applicability of the information obtained has been inherently

limited. In addition, most commercially available compounds are continental compounds (Figure 1-8), leaving the archipelago hypothesis completely untested. Thus, the absence of experimental data validating the archipelago hypothesis has raised a pressing demand for the synthesis of new classes of rationally designed model compounds, for use as truly representative molecular mimics of natural asphaltenes.

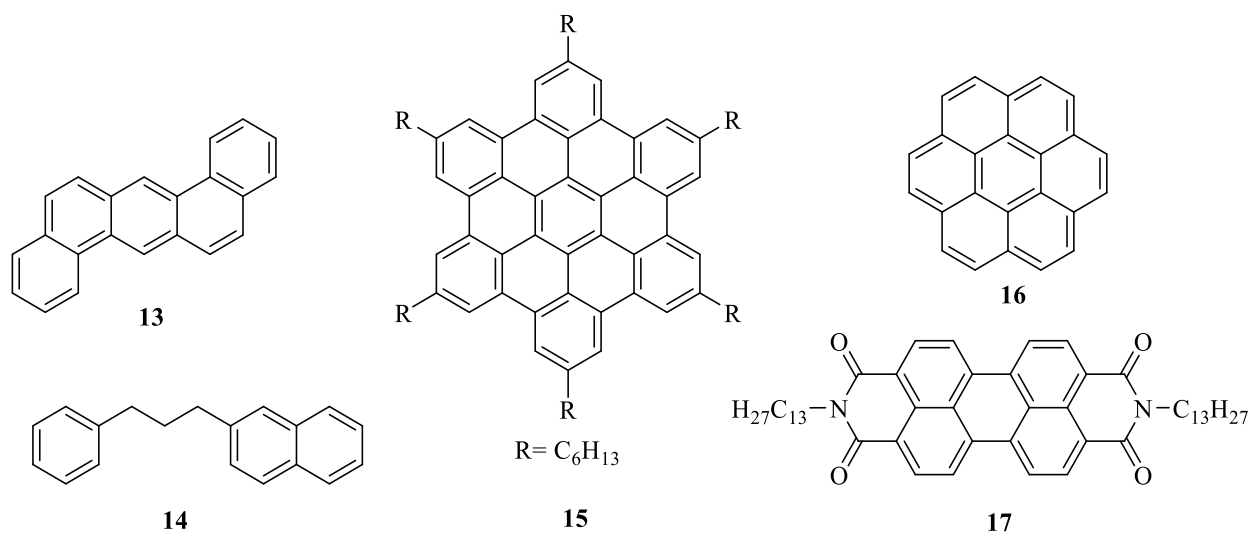


**Figure 1-8.** Continental model substrates explored as asphaltene mimics.

#### 1.4. Synthetic continental model compounds

The earliest efforts to model asphaltenes using custom-synthesized model compounds were focused on supporting the continental model. The unsubstituted core ring systems ranged from anthracenyl to coronene (Figure 1-9);<sup>[41,68,69,75]</sup> the analytical methods consisted of standard EI-MS characterization (molecular weight, fragmentation patterns) and solution self-aggregation. Unfortunately, most of these compounds show only weak association behaviour and lack the

appropriate functionality to truly represent asphaltenes. As a result, more elaborate compounds containing alkyl substituents and heteroatoms were targeted by future synthetic design.

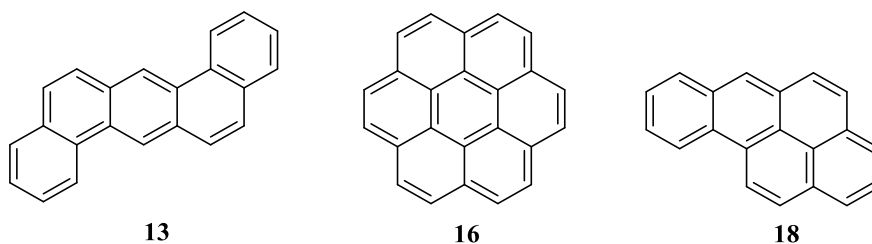
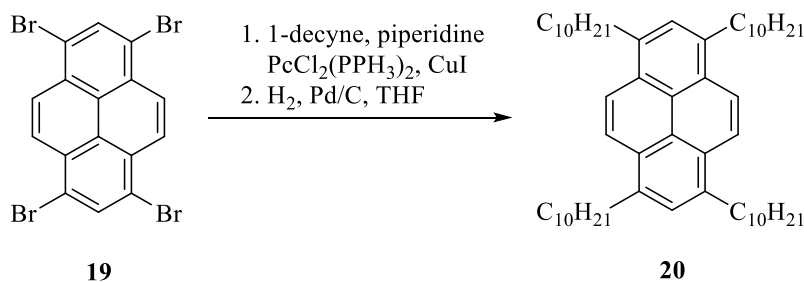


**Figure 1-9.** Small continental model compounds.

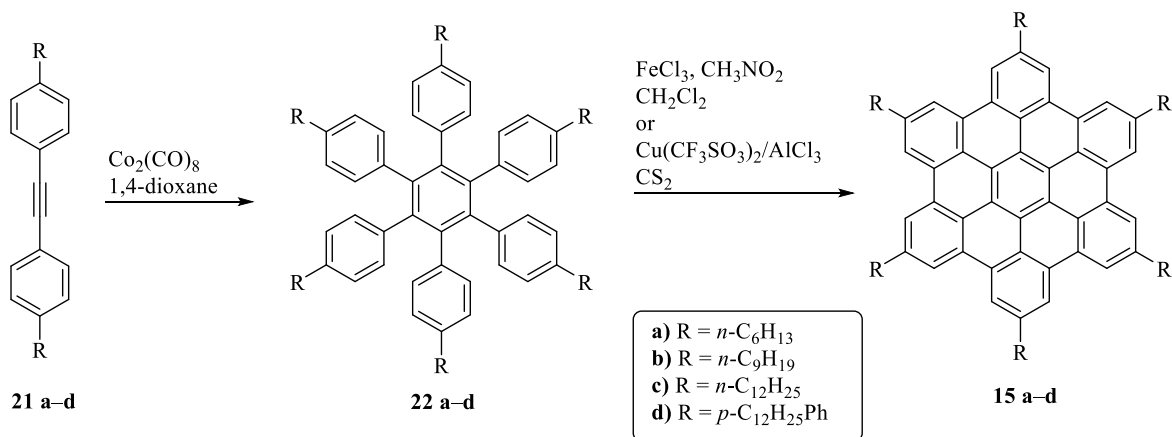
The first alkylated synthetic continental compounds were “small-core” pyrene analogues. Gray and co-workers prepared and investigated model alkyl-pyrenes using VPO, SANS, and DFT. No aggregation was observed using VPO and SANS; additionally, DFT computations suggested that pyrene, absent of any functionality, lacks the ability to propagate strong aggregation.<sup>[78,83]</sup> It was hypothesized that the installation of *n*-alkyl substituents on the pyrene core would lead to enhanced solubility, encouraging aggregation by increasing Van der Waals binding (Eq. 1-1).<sup>[84,85]</sup> However, solution aggregation of the alkylated analogues was negligible; such compounds are poor models of authentic asphaltenes. In response to this failure, researchers then explored larger continental-type compounds, in search of stronger aggregation behaviour.<sup>[60]</sup>



**Equation 1-1.** Sonogashira alkyne arylation and subsequent catalytic hydrogenation affording a tetrasubstituted alkyl pyrene in an unreported yield.

Higher molecular weight continental compounds, most notably hexa-alkyl-*peri*-hexabenzocoronenes (HBCs), were explored, anticipating a significant increase in intermolecular interactions and more desirable aggregation behaviour.<sup>[35,67]</sup> These HBC derivatives (Scheme 1-1, **15a-d**) are easily accessed synthetically using a cobalt-catalyzed trimerization of tolanes **21a-d**, followed by Lewis acid mediated ring fusion (the Scholl reaction).<sup>[86-89]</sup> The HBCs display improved self-association relative to pyrene,<sup>[86,90]</sup> forming persistent dimers in solution at 75 °C (toluene) and 100 °C (*o*-dichlorobenzene).<sup>[86]</sup> DFT calculations attribute this to a combination of stronger  $\pi$ - $\pi$  stacking and *intermolecular* alkyl-alkyl hydrophobic interactions, which together induce aggregation.<sup>[86]</sup> Unfortunately, the results also show virtually no associative  $\pi$ - $\pi$  stacking interactions between HBC **15c** and a second polycyclic system, in this case a metalloporphyrin, limiting the use of such molecules as mimics for the more complex asphaltene aggregates.<sup>[91]</sup> Furthermore, the highly symmetric nature of the HBC models, along with the absence of heteroatoms, are not representative of the molecular structures as characterized by ICP-MS and advanced imaging techniques. The size of the polycyclic HBC core is larger than that suggested by asphaltene analysis (average 4-10 fused ring systems)<sup>[25]</sup>, and the aggregation behaviour is, at best, much weaker when compared to authentic asphaltenes. Continental-type compounds

intermediate in size, but incorporating heteroatoms, were therefore targeted as the next iteration in synthetic asphaltene modeling.



**Scheme 1-1.** Synthesis of HBC derivatives.

The absence of heteroatoms in early synthetic model compounds was among the most glaring impediments to applying the compounds, with any accuracy, to model the behavior of asphaltenes. Elemental composition analysis reveals that heteroatoms comprise greater than 10% of the total mass of asphaltenes in Athabasca crude (Table 1-1).<sup>[20]</sup>

**Table 1-1.** Composition by mass of Athabasca asphaltenes.

Compound	C	H	N	O	S
Athabasca Asphaltenes	80.5 ± 3.5	8.1 ± 0.4	1.1 ± 0.3	2.5 ± 1.2	7.9 ± 1.1

In response to this, Wiehe<sup>[92]</sup> investigated aromatic polyethers **23** and polyesters **24** to model low molecular weight continent-type model compounds (Figure 1-10). These compounds were used to model thermal coke formation, which is a common reaction for asphaltene compounds. However, the high oxygen content of 2,3,6,7,10,11-hexaoxytriphenylene **23** (9.6%) and benzenehexa-*n*-

hexanoate **24** (25.2%) for these model compounds relative to Athabasca asphaltenes ( $2.5\% \pm 1.2$ ), renders the results of limited relevance.<sup>[20,92]</sup>

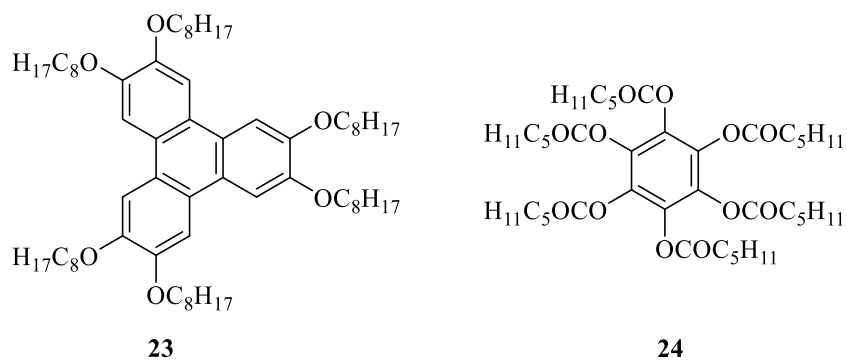


**Figure 1-10.** Oxygen containing continental-like structures.<sup>[92]</sup>

Compounds with more appropriate heteroatom content, such as dibenzofuran, thiophene, and 2,2'-dithiophene derivatives have also been explored, but the low molecular weights disqualify these as authentic asphaltene model compounds.<sup>[85,93-95]</sup> Higher molecular weight fused-ring structures were then targeted (Figure 1-11).<sup>[96,97]</sup>

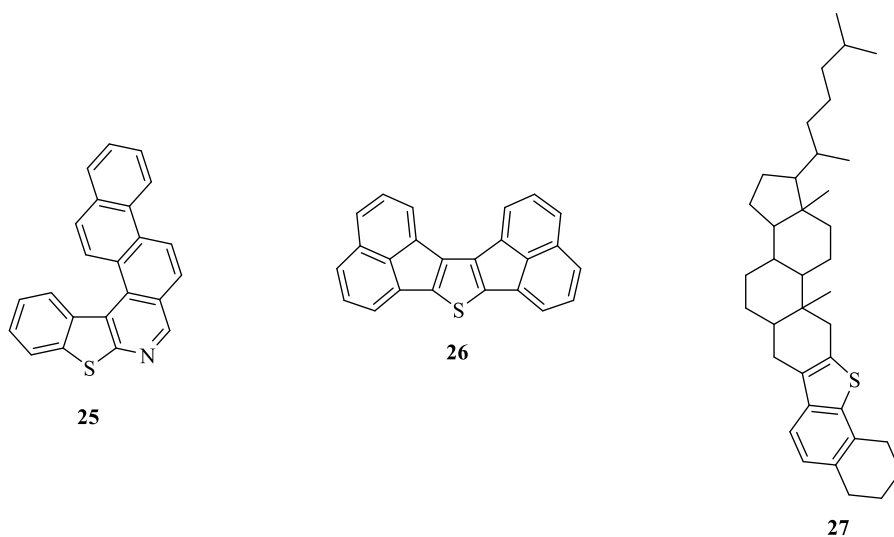


**Figure 1-11.** Heteroatom containing continental-like structures.

## 1.5. Unorthodox continental model compounds

Perylene dyes, which include cyclic anhydrides,<sup>[69]</sup> diimides,<sup>[25,69]</sup> and asphaltene-relevant ethers, ketones, and esters,<sup>[98–100]</sup> have been utilized as higher molecular weight continental model compounds. Juyal and co-workers identified the presence of perylene derivatives in crude oil,<sup>[101]</sup> and Sjöblom and co-workers synthesized many perylene diimide (PDI) model asphaltenes (Figure 1-12, **17a-d**).<sup>[25,69,98,102–110]</sup> These compounds were designed to resemble naphthenic acid derivatives, which are key components in asphaltenes.<sup>[11]</sup> While these compounds do display characteristics relevant to asphaltene modeling, the compounds themselves are poor mimics, partly due to inflated heteroatom content and uncharacteristically large number of functional groups (ketones, alcohols, esters, etc.) relative to the naturally occurring asphaltene samples.

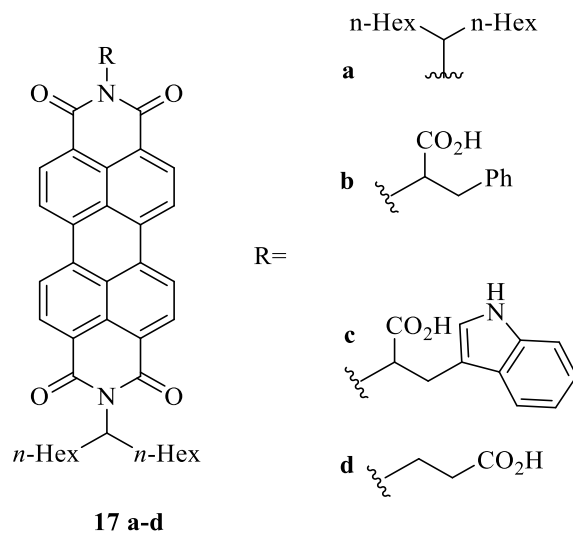


**Figure 1-12.** Functionalized perylene structures as asphaltene model compounds.

Other oxygen-rich compounds such as esters and carboxylic acids have been synthesized and studied as model asphaltenes (Figure 1-13).<sup>[105]</sup> Unfortunately, the chemical composition and

functional group structures, limit the relevance of inferences drawn from such data. [105,107,108,111–113]

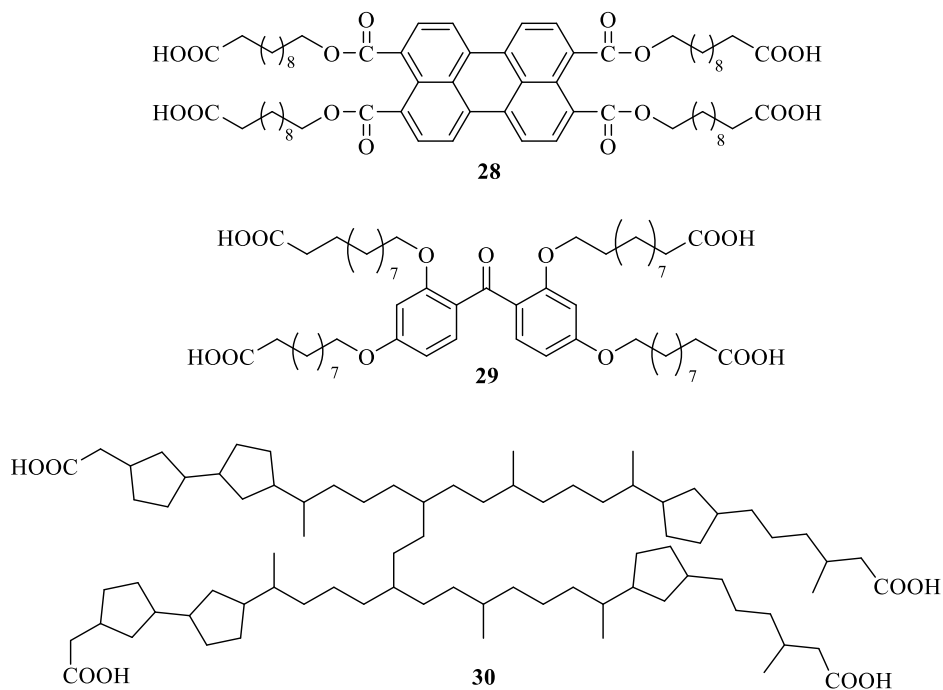


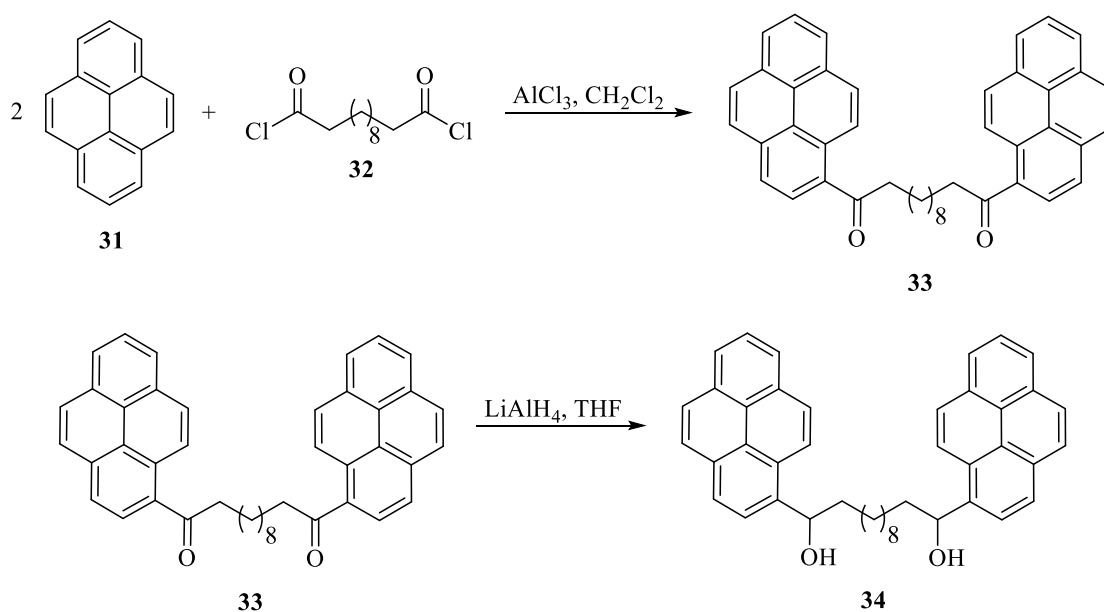
**Figure 1-13.** Continental and archipelago-like carboxylic acid model compounds.<sup>[105]</sup>

### 1.6. Early synthetic methods for preparing archipelago model compounds

The absence of significant aggregation in continental-type compounds, relative to the naturally occurring asphaltenes, precipitated a shift to the synthesis of archipelago-type molecules as potentially better models. Following the failures with continental-type molecules, archipelago compounds were designed to specifically incorporate relevant structural features that promote aggregation, while at the same time reproducing the typical elemental composition seen in asphaltenes. The presence of archipelago-like compounds in asphaltenes is strongly supported by data from oxidative degradation of the constituent aromatic cores. The abundance of  $\alpha,\omega$ -

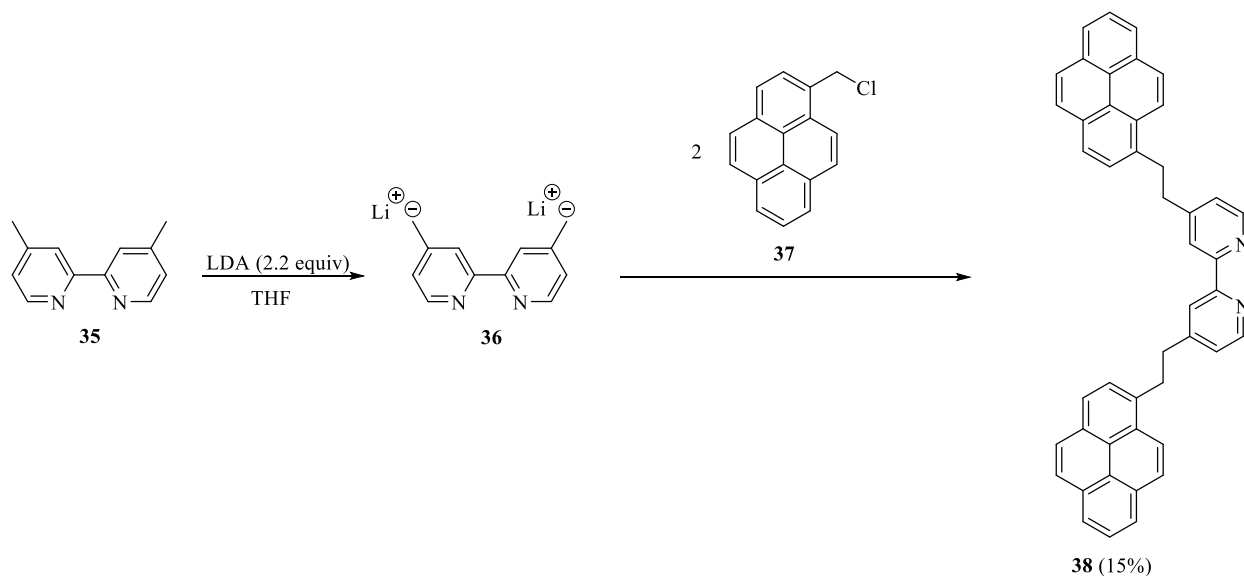
dicarboxylic acids linked by saturated alkyl chains is considered diagnostic for the presence of molecules consisting of two or more PAHs linked together by short, saturated alkyl segments.<sup>[11]</sup> Synthetic archipelago compounds have consequently become important targets for modeling asphaltene behaviour.

In one early example, Akbarzadeh, et al., prepared 1,10-di(pyrenyl)decanediol **34** using a double Friedel-Crafts acylation to tether two pyrene residues (Scheme 1-2).<sup>[83]</sup> The diketone intermediate **33** and the final diol product **34** were both found to self-associate in solution (by dimerization), partly attributed to the presence of the polar functional groups. Unfortunately, based on the chemical composition of asphaltene molecules (see Section 1.2) the position along the alkyl chain of these polar functional groups (ketones and alcohols) are not features prominently found in the asphaltene matrix, so the behavior of these model compounds **33/34** offers limited insight.<sup>[60]</sup> It is unclear why the fully reduced hydrocarbon was not investigated.



**Scheme 1-2.** Early model compound synthesis of the two island systems in unreported yields.<sup>[83,114]</sup>

To include more relevant heteroatom functionality, as well as prepare more elaborate archipelago-type compounds, Fenniri and co-workers synthesized a ‘three-island’ pyridine/pyrene archipelago system (Scheme 1-3).<sup>[60]</sup> Benzylic deprotonation of 4,4’-dimethyl-2,2’-bipyridine **35** afforded dilithiated compound **36**, which undergoes double benzylic alkylation upon addition of 1-(chloromethyl)pyrene **37**, giving the three-island archipelago compound **38**. The model is notable because it incorporates simple, saturated alkyl tethers along with a basic nitrogen heterocycle; both features are common in authentic asphaltenes.<sup>[60]</sup> Unfortunately, the overall yield of compound **38** was very low and the high symmetry of this compound is uncommon in asphaltene. Nevertheless, the synthetic strategy – building the necessary components and then assembling them into the final product in one, convergent synthetic step – set the stage for the next-generation of model compound synthesis methods.

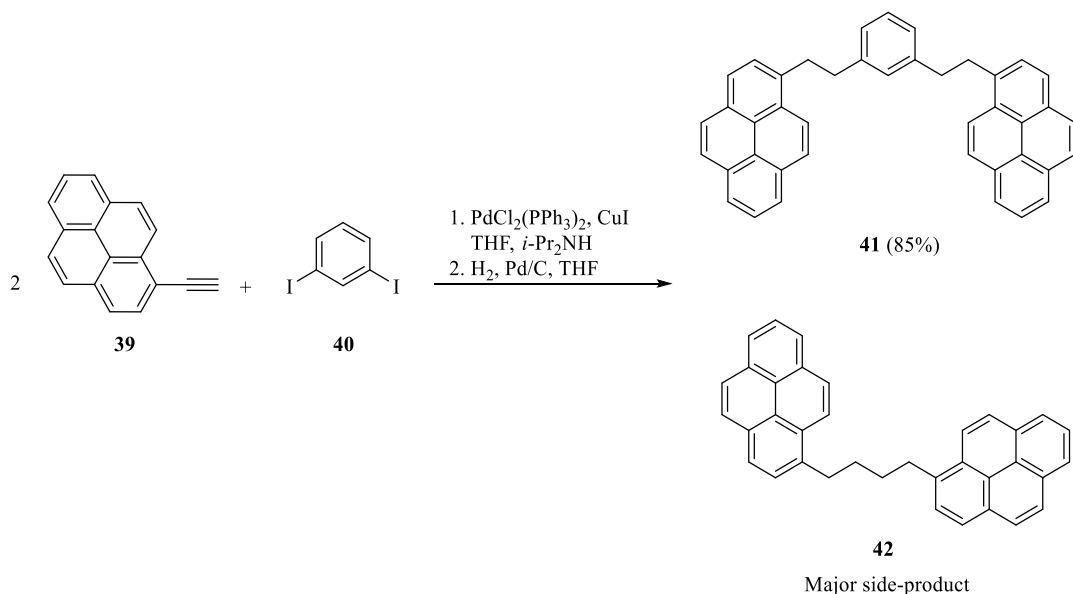


**Scheme 1-3.** Synthesis of a three-island bipyrindine archipelago model compound.<sup>[60]</sup>

Archipelago compound **38** was used to investigate potential aggregation motifs. Spectroscopic experiments ( $^1\text{H}$  NMR) were conducted in the presence of water, which is abundant in all petroleum deposits and could easily play an essential role in driving asphaltene aggregation.<sup>[11]</sup> Gray and co-workers found that even a low concentration of water leads to dimerization of **38** in chloroform.<sup>[115]</sup> Computational methods suggested that a water-bridged dimer had assembled, hydrogen bonding to *two* nitrogen atoms and supported by associative  $\pi$ - $\pi$  interactions. Theoretical investigations suggest that hydrogen-bonding, rather than  $\pi$ - $\pi$  interactions, drives the dimer formation.<sup>[116,117]</sup> This aggregation study can be interpreted to indicate that an accumulation of individually modest associative interactions is likely responsible for the irreversible aggregation characteristic of asphaltenes.<sup>[11]</sup>

### **1.7. Advanced synthetic methodology for archipelago model compounds**

To build on this design, Tykwinski, Stryker, and co-workers reported an efficient and more general strategy for the synthesis of three-island model compounds, broadly varying the central aromatic system (Eq. 1-2). Palladium-catalyzed Sonogashira alkylation<sup>[118]</sup> followed by catalytic hydrogenation of the internal bis(alkyne) provided a range of two-carbon tethered archipelago compounds in high yields.<sup>[84]</sup>

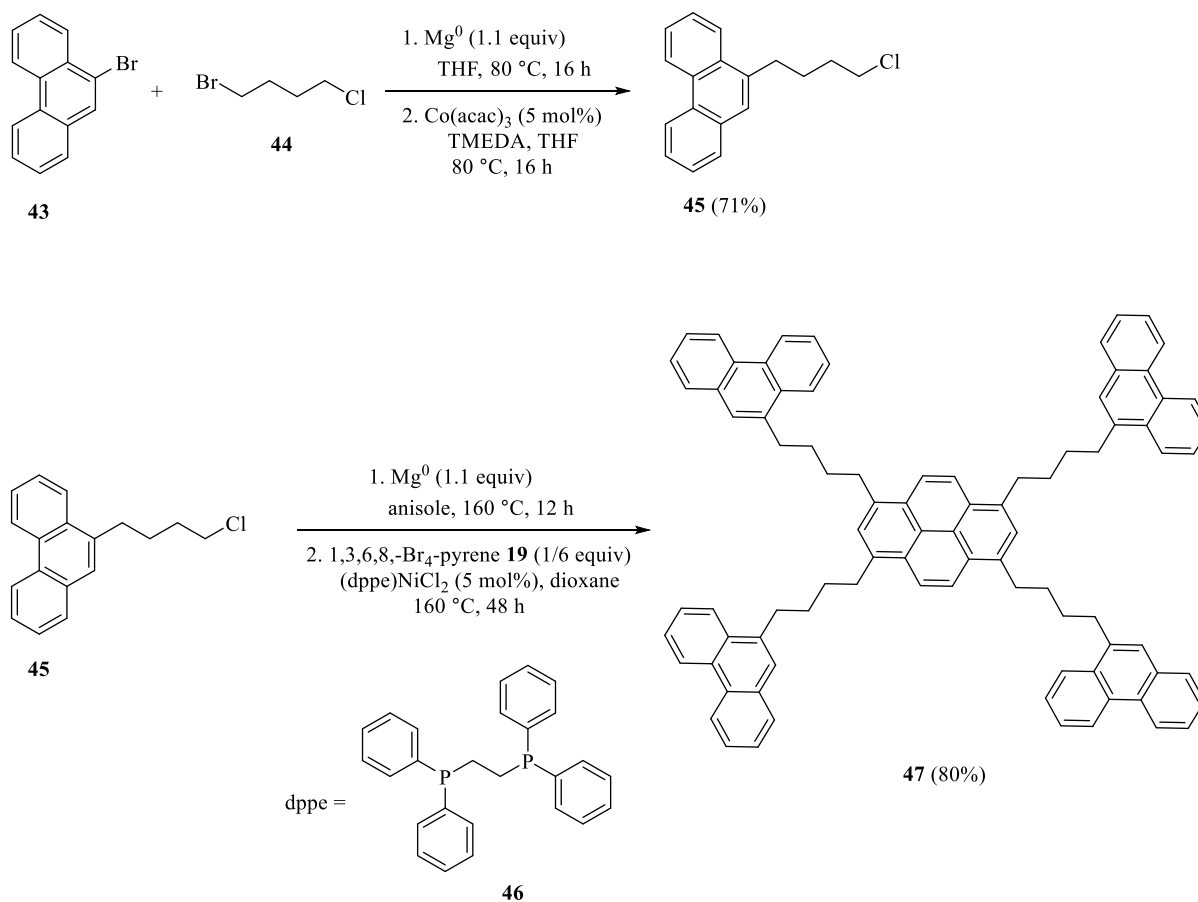


**Equation 1-2.** Sonogashira coupling/catalytic hydrogenation forming three-island/two-island compounds.<sup>[84]</sup>

Unfortunately, the methodology is flawed and not general. Two-island by-products are obtained from competitive alkyne homo-coupling **42**, requiring chromatographic separation.<sup>[119]</sup> More importantly, catalytic hydrogenation of the internal alkynes becomes less selective as the size of the aromatic system increases. The transition metal, binding competitively to the extended  $\pi$ -surfaces, leads to *kinetically competitive* hydrogenation of the arene core. In addition, the activation energy for the arene hydrogenation is influenced by the change in aromaticity during the reaction. In extended (*not* “large”)  $\pi$ -systems, the overall change in aromaticity may be enthalpically favorable, although this is not always the case.

To avoid the challenges associated with alkynylation/hydrogenation, the Stryker group developed an alternative synthetic strategy, making use of simple Kumada-type nickel-catalyzed cross-coupling reactions. Beginning with a cobalt-catalyzed arylation of  $\alpha,\omega$ -bromochloroalkanes, I synthesized 9-(4-chlorobutyl)phenanthrene **45** cleanly from 9-bromophenanthrene and 1-bromo-4-chlorobutane on a 20 g scale.<sup>[120]</sup> Then, using this compound, Colin Diner implemented the

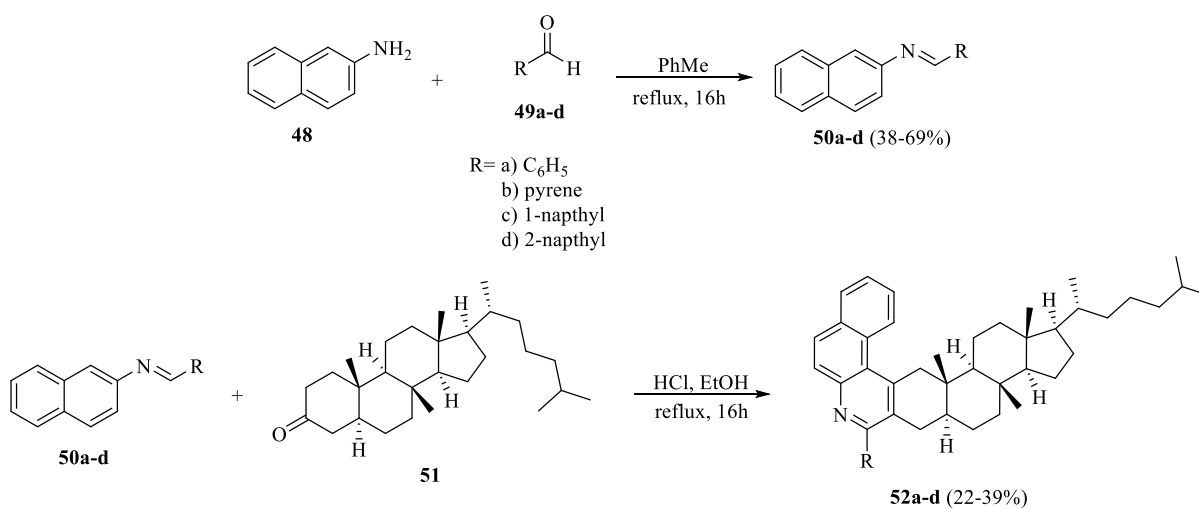
nickel-catalyzed cross-coupling<sup>[121,122]</sup> to make a series of pyrene- and phenanthrene-based archipelago model compounds comprising two-, three-, four-, and five-island aromatic systems. The archipelago compounds were prepared on gram scale and purified without the use of chromatography (Scheme. 1-4).<sup>[123]</sup> Also synthesized were analogous 4-*N*-butylcarbazole derivatives, incorporating non-basic nitrogen heterocycles also known to be present in the asphaltenes.



**Scheme 1-4.** Multi-island synthesis of archipelago models.<sup>[120,123]</sup>

The high symmetry of this series is not representative of asphaltene constituents. Thus, a new generation of model compounds were designed, adapting and extending a known multicomponent

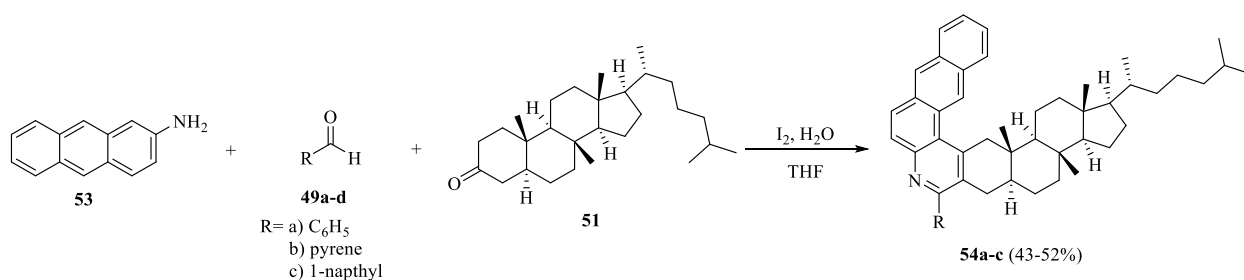
cyclocondensation reaction<sup>[124]</sup> to synthesize lower-symmetry model compounds containing basic nitrogen heterocycles. Tykwinski and co-workers initially resorted to a two-step procedure, combining  $\beta$ -naphthylamine **48** and an aromatic aldehyde to afford imines **49a-d**, which were subsequently treated with 5- $\alpha$ -cholestanone **51** (Scheme 1-5) to complete the cyclocondensation.<sup>[125]</sup> The product, fused naphthenic benzoquinoline **52**, represents an unmodeled class of highly unsymmetrical continental-like compounds. This product features a strongly basic quinoline-core fused to an extensive, conformationally rigid, hydrophobic region of steroid-derived chirality. Unfortunately, the yields were unacceptably low.



**Scheme 1-5.** Stepwise synthesis of fused naphthenic benzoquinolines.

An efficient one-pot MCR version of the cyclocondensation process was developed by Tykwinski, Stryker, and co-workers, exploiting the I<sub>2</sub>-catalyzed procedure reported by Wang and co-workers. Adapting this process to accommodate our targets required considerable modification (Eq. 1-3).<sup>[124,126]</sup> The reaction proved to be highly concentration-dependent and sensitive to water concentration, a necessary additive not recognized in published work. Following re-optimization,

the one-pot cyclocondensation of 2-aminoanthracene **53**, an aromatic aldehyde **49a-c**, and commercial 5- $\alpha$ -cholestanone **51** was used to synthesize a library of naphthenic benzonaphthoquinoline compounds.<sup>[125,126]</sup> Having succeeded in the synthesis of high molecular weight nonplanar continental structures, Stryker and co-workers next optimized the MCR methodology for convergent synthesis of three-island archipelago model compounds. This work features prominently in this thesis and is discussed at length in Chapters 3 and 4.



**Equation 1-3.** MCR synthesis of the 5- $\alpha$ -cholestanone quinoline model compounds.

In addition to steroidal components, other “biomarker residues” have been incorporated into synthetic model compounds; such fragments are relatively abundant in authentic asphaltenes.<sup>[127]</sup> With complex structures reflecting their biological origin, biomarker analysis is used to identify the geographic source of the material.<sup>[128,129]</sup> Many structural classes of biomarkers have been identified in natural asphaltenes, including chiral perinaphthenic arrays (terpanes, steranes), branched poly-isoprenoid segments, and heteroatom-rich metallated porphyrin derivatives (Figure 1-14).<sup>[127,129–132]</sup>

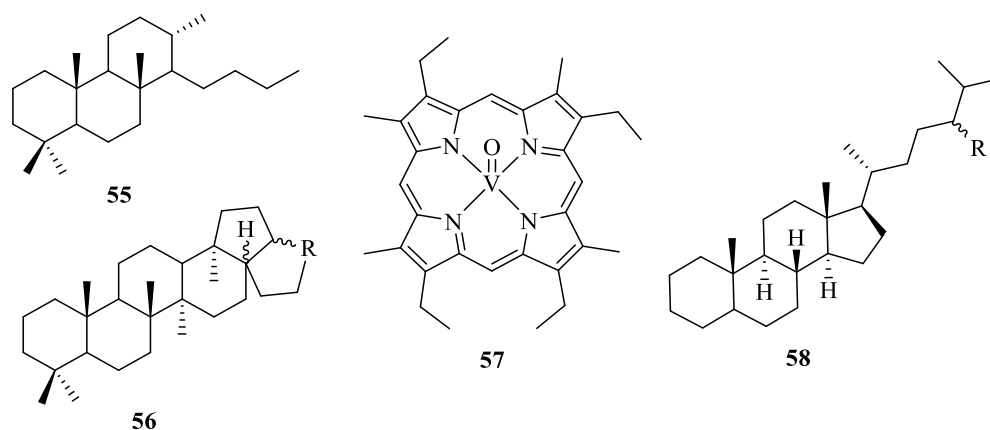
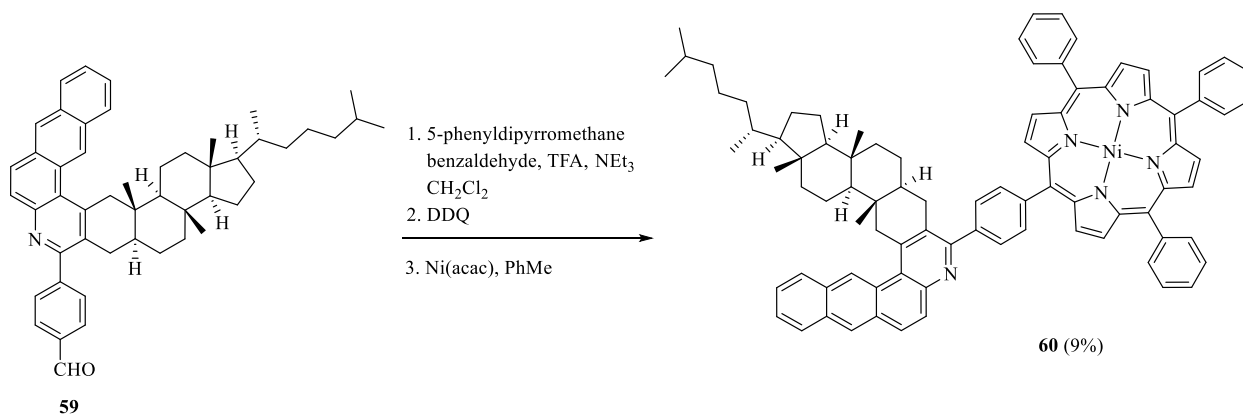


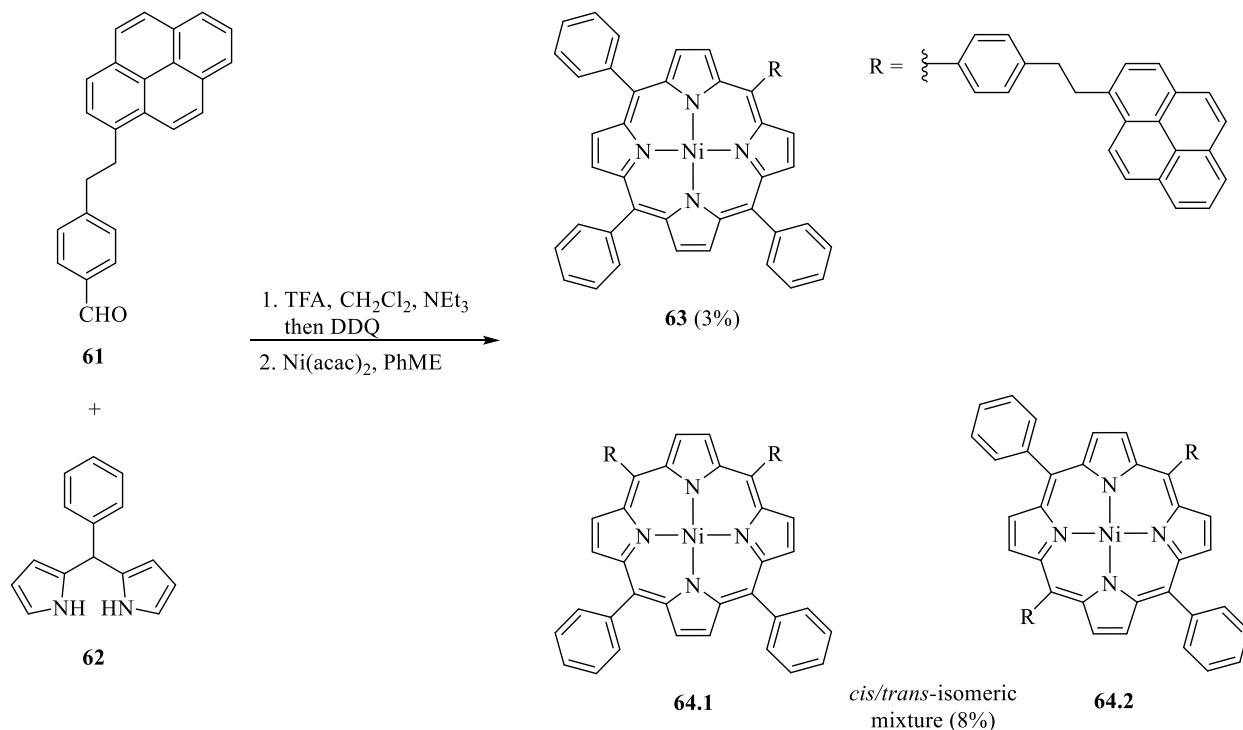
**Figure 1-14.** Selected biomarker components identified in fossil fuels: tricyclic terpane, (left top), hopane-type pentacyclic triterpane (left bottom), vanadyl-ethioporphyrin III (middle), and sterane (right).<sup>[133]</sup>

Tykwinski and co-workers expanded the MCR scope, preparing densely functionalized porphyrinic compounds representative of both continental and archipelago systems.<sup>[134]</sup> Elaborating on the previously-reported naphthoquinoline aldehyde **59** and exploiting the Lindsey porphyrin synthesis,<sup>[135]</sup> subsequent metallation afforded a unique, *nonrigid* porphyrinic continental model compound **60** (Eq. 1-4). This protocol efficiently combines two biomarker beacons into one elaborate, continental asphaltene model compound.



**Equation 1-4.** Mixed biomarker model compounds.

Archipelago-like porphyrin derivatives were also reported, incorporating  $\omega$ -arylalkyl substituents (Eq. 1-5). Thus, for example, 4-(2-pyrenylethyl)benzaldehyde **61** was transformed into a mixture of two- and three-island metallated porphyrins **63** and **64**, in yields typical for porphyrin assembly.<sup>[136]</sup>



**Equation 1-5.** Synthesis of archipelago-like metalloporphyrins.

### Limitations to Model Compound Synthesis

Initial asphaltene model compounds were simple to prepare (or purchase) and overly symmetric. The infinitely complex asphaltene constituents are neither simple nor symmetric. Asphaltenes contain a vast array of different compounds and large libraries of model compounds are required to accurately represent the material. New asphaltene characterizations have demonstrated that more elaborate compound design is required. However, the limitations of stepwise synthesis

restrict the range of synthetic compounds needed to develop an accurate representation of asphaltene.

Three specific developments were thus targeted to move the field forward:

- *Molecular weight range/target relevance* – With recent advances in analytical technology, very high molecular weight compounds incorporating multiple heteroatoms have been identified in the asphaltene matrix. Such targets pose a very significant synthetic challenge.
- *Scale* – For engineering studies related to industrial asphaltene processing, multi-gram quantities of synthetic materials are required. Milligram-scale procedures do not address the need.
- *Novel synthetic methodology* – New strategies and methodology must be introduced or adapted to address the dearth of relevant asphaltene models in the current literature.

### **Research Objectives**

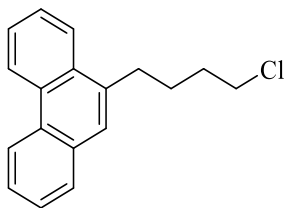
The goal of my dissertation research was to develop new structurally relevant libraries of archipelago model compounds. For this objective, our convergent MCR cyclocondensation was modified substantially and re-optimized for the combination of two *aliphatic* aldehydes and a range of substituted aniline derivatives, a procedure unexplored in the contemporary literature. Identification of the active catalysts derived from iodine was pursued, along with mechanistic investigations into the aerobic  $I^-/I^+$  redox cycle, which was identified for the first time. The optimized procedure requires only limited chromatography.

## Experimental Section

Manipulations of air-sensitive materials were performed in a well-maintained Braun dry box (<1 ppm O<sub>2</sub>) under an atmosphere of prepurified nitrogen or, at larger scale, using standard Schlenk techniques. Dioxane was distilled from sodium under nitrogen. THF was distilled from sodium/benzophenone ketyl under nitrogen. All other solvents and reagents were used without further drying or purification.

NMR spectra were recorded on Agilent/Varian instruments (500 MHz for <sup>1</sup>H NMR) at ambient temperature. Chemical shifts were referenced to residual solvent protium peaks (δ in parts per million (ppm) CHCl<sub>3</sub> <sup>1</sup>H: 7.26 ppm). Coupling constants were assigned as observed. <sup>1</sup>H NMR coupling constants are rounded to nearest 1.0 Hz.

### 9-(4-Chlorobutyl)phenanthrene (45)



In a dry three-neck 150 mL RBF attached to a condenser fitted to a nitrogen inlet were placed magnesium turnings (0.31 g, 13.0 mmol) and THF (12 mL). Ethylene bromide (48 μL, 0.6 mmol) was added and the mixture heated to reflux for 1 h. The reaction mixture was cooled to rt, and 9-bromophenanthrene (3.04 g, 11.8 mmol) in THF (12 mL) was added. The reaction mixture was heated to reflux overnight and then cooled to rt. Into a separate dry 250 mL three-neck RBF attached to a condenser fitted to a nitrogen inlet was added Co(acac)<sub>3</sub> (0.22 g, 0.62 mmol), THF

(6 mL), TMEDA (90  $\mu$ L, 0.60 mmol) and 4-chlorobromobutane (1.34 mL, 11.6 mmol). The solution was cooled to 0  $^{\circ}$ C in an ice bath, and the mixture of 9-phenanthrylmagnesium bromide was cannula transferred into the reaction flask. After 4 h at 0  $^{\circ}$ C, the solution was heated to reflux overnight, cooled to rt, and quenched with 1 M HCl (100 mL). The mixture was washed with 50 mL of ether and the phases were separated. The organic layer was washed with brine (50 mL) and dried over Na<sub>2</sub>SO<sub>4</sub>. The solution was filtered, and the solvent was removed under reduced pressure. The resulting crude product was recrystallized in hot 2-propanol to afford an off-white solid 2.25 g (71%).

<sup>1</sup>H NMR (CDCl<sub>3</sub>, 500 MHz):  $\delta$  8.76 (dd,  $J$  = 10.0, 2.0 Hz, 1H), 8.67 (d,  $J$  = 9.0 Hz, 1H), 8.11 (dd,  $J$  = 7.0, 3.0 Hz, 1H), 7.85 (dd,  $J$  = 7.0, 2.0 Hz, 1H), 7.57-7.70 (m, 5H), 3.63 (t,  $J$  = 6.0 Hz, 2H), 3.18 (t,  $J$  = 7.0 Hz, 2H), 1.98 (m, 4H).

Full characterization of the compound is found in Colin Diner's Thesis as well as the JOC publication titled "Scalable, Chromatography-free synthesis of alkyl-tethered pyrene-based materials. Application to first-generation "archipelago model" asphaltene compounds."<sup>[123,137]</sup>

## 2. Synthetic Approaches to Quinoline Derivatives

### General Introduction to Nitrogen Heterocycles

Organic heterocycles are a large, important class of molecules, comprising more than half of all organic compounds.<sup>[138,139]</sup> Heterocycles differ from *carbocyclic* compounds in that they contain at least one non-carbon atom in the ring, with nitrogen, oxygen, and sulfur being the most commonly encountered heteroatoms.<sup>[140,141]</sup> While inorganic molecules, such as borazine **65**, strictly meet the definition of heterocycles, this discussion is limited to *organic heterocycles* such as pyridine **67**, which feature carbon atoms along with one or more heteroatom(s) in the ring system (Figure 2-1).<sup>[138,140]</sup>

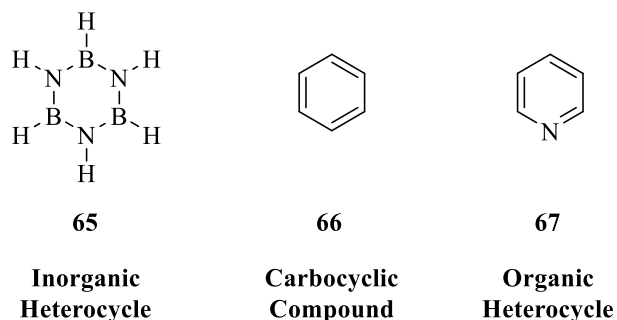


**Figure 2-1.** Cyclic compound classification, with representative examples.

Heterocycles, particularly those containing nitrogen, are ubiquitous in nature and featured in many synthetic and natural bioactive molecules. Heterocycles are found in important biomolecules such as DNA (purine **68** and pyrimidine **69** bases), RNA, vitamins *etc.* (Figure 2-2).<sup>[142,143]</sup> In addition many therapeutic compounds, e.g. antimalarial compound **70**<sup>[144–146]</sup> and antibacterial compound **71**,<sup>[147–150]</sup> contain one or more heterocycles.

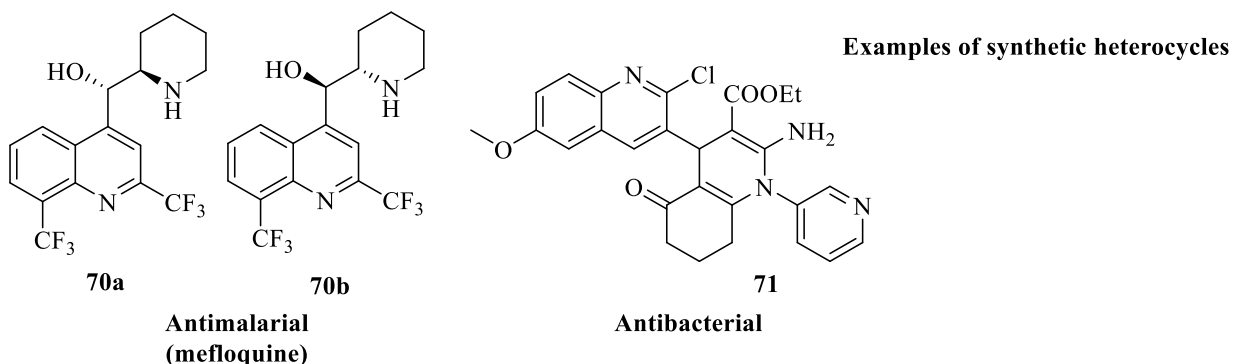
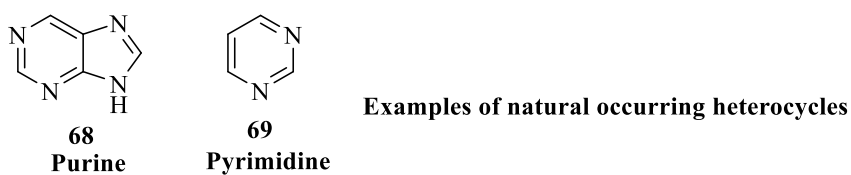


**Figure 2-2** Select examples of azaheterocyclic derivatives capable of therapeutic purposes.<sup>[144,147,151]</sup>

The most common nitrogen heterocycles are pyrroles **72**, pyridines **67**, pyrimidines **69** and fused-ring analogues, including quinolines **73**, benzo[*h*]quinolines **7**, and isoquinolines **75** (Figure 2-3). This dissertation focuses almost entirely on quinoline derivatives because of their pertinence to modeling asphaltene behaviour (Section 1.2). As previously discussed in Chapter 1, most of the nitrogen containing molecules found in asphaltenes are pyrrolic **72**, however, pyridine and quinoline based compounds are believed to represent most of the remaining nitrogen heterocycles.<sup>[49,51,52,54-57]</sup>

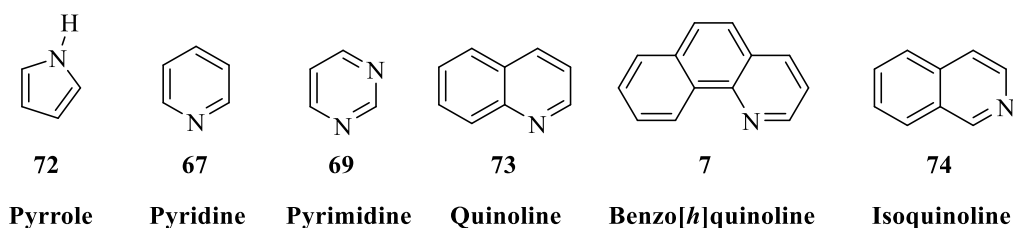


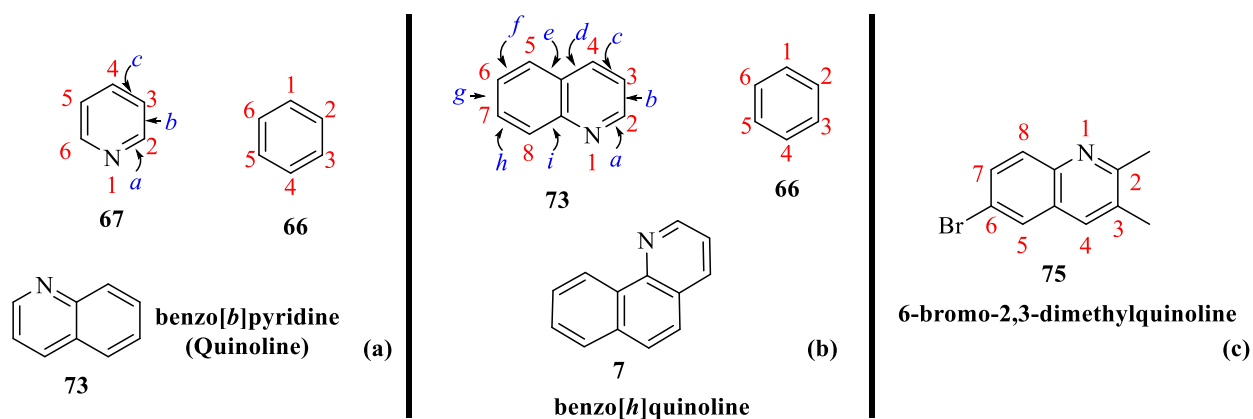
**Figure 2-3.** Nitrogen cores typically found in natural and unnatural products.

Quinoline is comprised of two fused six-membered rings, one unsubstituted and one substituted with a nitrogen. Quinolines are alternatively referred to as “benzopyridine”. Isoquinolines also share this basic structure, but the rings are fused at the distal positions (Figure 2-3). While the simple quinoline molecule has only a few uses, derivatives decorated by alkyl and functionalized substituents in diverse substitution patterns are attractive synthetic targets for many applications, in many research areas.

### 2.1. Substituted quinoline heterocycles: a little nomenclature

The diversity and complexity of the quinolines, and indeed all organic heterocycles, necessitates a well-established set of nomenclature rules. For brevity, only a limited subset of these rules is necessary for this discussion. The simplest quinolines are named as if the benzene and pyridine rings were separate molecules (Figure 2-4 (a)), with the least-saturated heterocyclic system (pyridine in this case) deemed the parent compound. The fusing ring (‘benzene’ in this case) is denoted by a prefix (e.g. benzo-), and the position at which the two rings fuse is indicated by an italic letter: *a*, *b*, *c*, etc. Thus compound **73**, the simplest quinoline molecule, is properly termed benzo[*b*]pyridine (Figure 2-4 (a)).<sup>[152,153]</sup> For substituted or polycyclic quinolines, the entire quinoline-core is treated as the ‘the least-saturated heterocyclic’ parent ring, but the same numbering and lettering patterns for pyridine are still used. Thus compound **7** is a benzo[*h*]quinoline (Figure 2-4 (b)), indicating that the benzene ring is fused to the quinoline-core at the ‘*h*’ position. The location of alkyl and other substituents on the quinoline-core is indicated by a number, taking care that the nitrogen atom of the quinoline is assigned position 1 and that the lowest possible numbering is assigned for the substituents (e.g., 6-bromo-2,3-dimethylquinoline **75**, Figure 2-4 (c)). While the compounds used for this illustration (Figure 2-4) are relatively

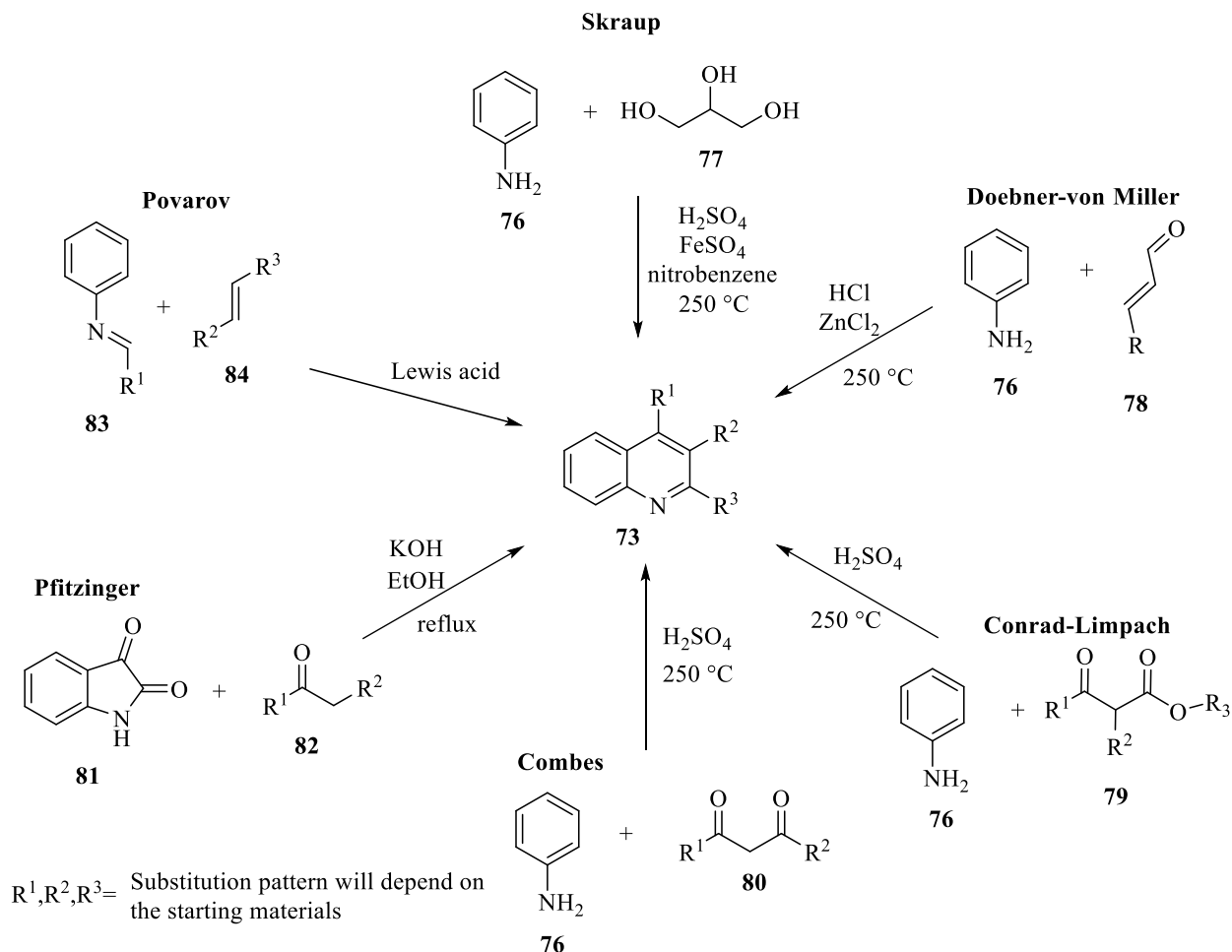
simple, the naming convention is successfully used to describe much more complex molecules bearing the quinoline-core, and several such examples arise later in this discussion.

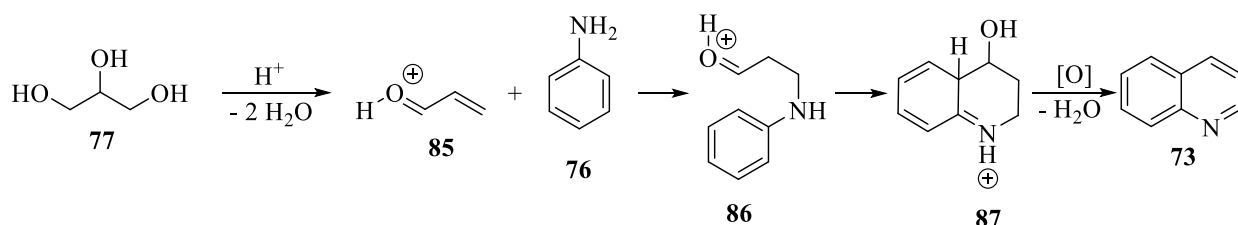
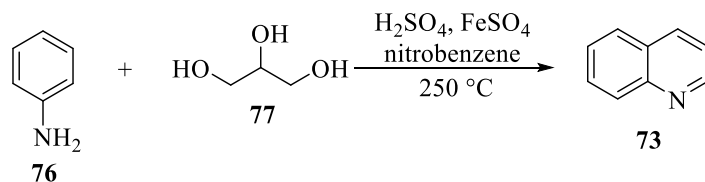


**Figure 2-4.** Examples for nomenclature rules for naming heterocycles.

## 2.2. Classical strategies for quinoline synthesis

The most important synthetic methods for preparing quinolines include many long-standing name reactions, including the Skraup,<sup>[154,155]</sup> Doebner-von Miller,<sup>[156]</sup> Conrad-Limpach,<sup>[157]</sup> Combes,<sup>[158]</sup> Pfitzinger,<sup>[159]</sup> and Povarov reactions,<sup>[160,161]</sup> as summarized in Scheme 2-1 and discussed briefly below.

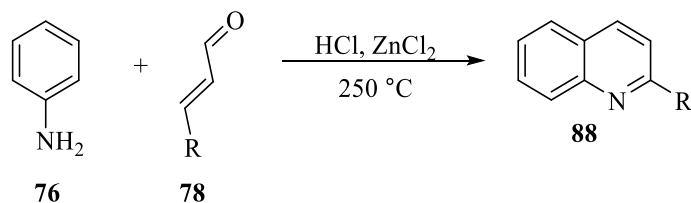




**Scheme 2-2.** Skraup reaction and mechanism.

The Doebner-von Miller reaction is an adaptation of the Skraup reaction. Aqueous HCl is used as solvent, replacing the nitro-aromatic compounds. Additional Lewis acid is required, typically using ZnCl<sub>2</sub> to promote conjugate addition and condensation of the aniline and acrolein.<sup>[156,164]</sup>

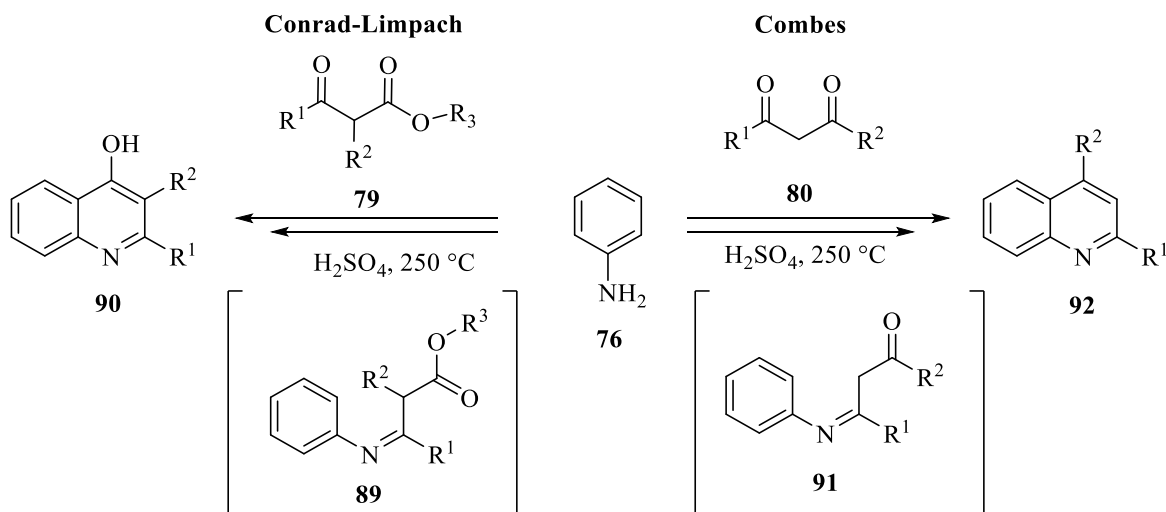
The mechanism of the Doebner-von Miller reaction is the same as the Skraup mechanism, except for the direct addition of acrolein to the reaction mixture (Eq. 2-1). This reaction is a minor improvement on the Skraup procedure, but unfortunately it does not address the synthesis of more complicated systems.



R= Functionality will depend on the starting materials

**Equation 2-1.** Doebner-von Miller quinoline synthesis.

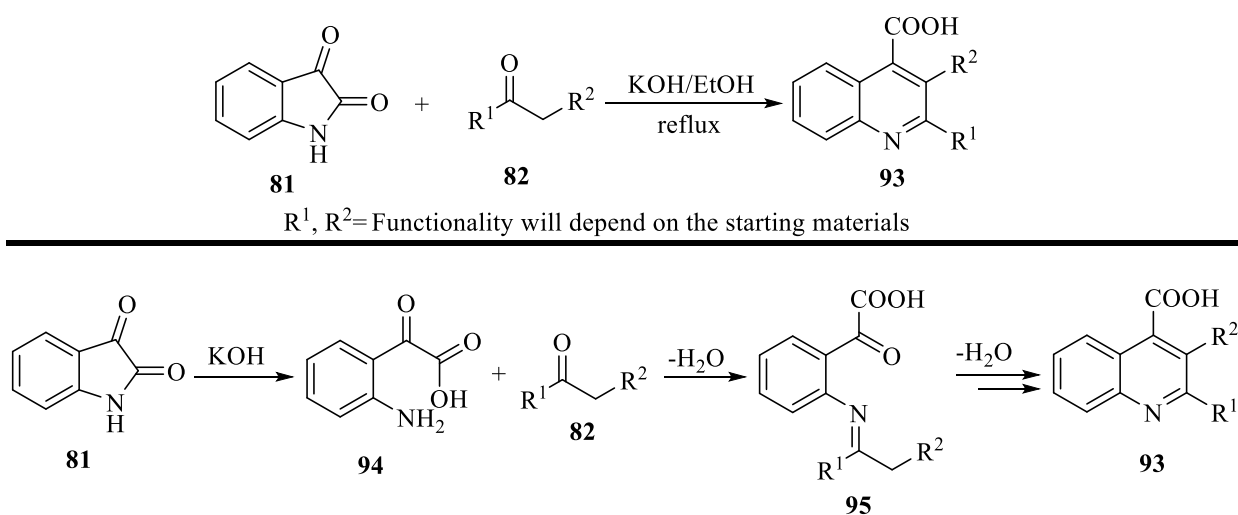
Two closely related quinoline syntheses address the issue of functionalization. The Conrad-Limpach and the Combes syntheses are acid-catalyzed cyclocondensation reactions involving a  $\beta$ -ketoester **79** or  $\beta$ -diketone **80**, respectively (Scheme 2-3).<sup>[157,158]</sup>



**Scheme 2-3.** Conrad-Limpach and Combes quinoline synthesis.

The difference in substitution patterns obtained from the Conrad-Limpach and Combes syntheses is a result of the difference in the corresponding substrates. In the Conrad-Limpach reaction, the aniline reacts with the ketone of the  $\beta$ -ketoester to form a Schiff base **89**. The intermediate then undergoes condensation and rearomatization to provide the 2,3-disubstituted 4-hydroxyquinoline **90** (Scheme 2-3).<sup>[165,166]</sup> In contrast, the Combes synthesis provides the 2,4-disubstituted quinoline, with the R-groups of the  $\beta$ -diketone dictating a preferential attack at one of the two carbonyl groups, giving Schiff base **91**. This intermediate then undergoes condensation and rearomatization to provide quinoline **92** (Scheme 2-3).<sup>[167]</sup> Unfortunately, both Conrad-Limpach and Combes syntheses still require harsh reaction conditions.

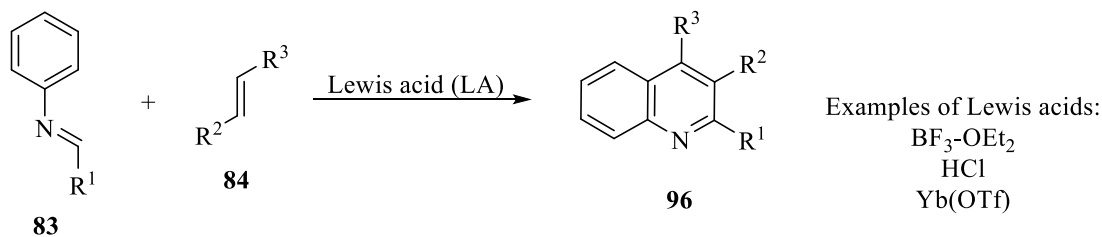
The Pfitzinger synthesis addressed the need for milder reaction conditions, as well as enhanced functionality in the quinoline product. In this process, isatin **81** reacts with ketone **82** in the presence of base,<sup>[159]</sup> affording 2,3-disubstituted quinoline-4-carboxylic acids **93** (Scheme 2-4).<sup>[168,169]</sup> Here, isatin first hydrolyzes to the 2-aminophenyl keto-acid **94**, which condenses with an equivalent of the ketone, generating an imine. Intramolecular cyclocondensation between the enamine tautomer and the keto-acid generates the 2,3-disubstituted quinoline-4-carboxylic acid **93** (Scheme 2-4).<sup>[168,169]</sup> This is a reliable reaction, but the scope is limited and, in the event that carboxylic acids are not desired, an efficient alternative is needed.



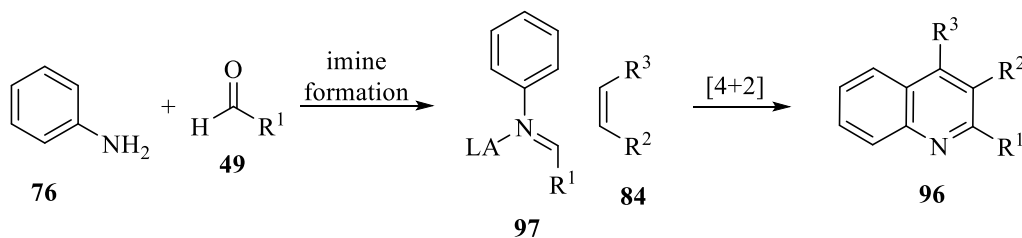
**Scheme 2-4.** Pfitzinger reaction.

The Povarov reaction, in contrast, is a powerful synthetic tool for quinoline synthesis, providing access to highly-substituted tetrahydroquinolines under very mild catalytic conditions.<sup>[170]</sup> Fundamentally, the Povarov reaction is an inverse-demand Diels-Alder cycloaddition of an *N*-arylimine and an electron-rich olefin. The preformed *N*-arylimine **83** serves as the heterodiene, which undergoes a [4+2] cycloaddition with an electron-rich dienophile (**84**; typically, an enol

ether or enamine) to form the quinoline directly (top, Scheme 2-5).<sup>[161]</sup> The reaction can be promoted by the coordination of a Lewis acid, giving a more electron-deficient diene, **97**. The Povarov reaction is particularly pertinent to this discussion because the two-step sequence can be performed as a single multicomponent reaction.



$R^1, R^2, R^3 =$  Functionality will depend on the starting materials

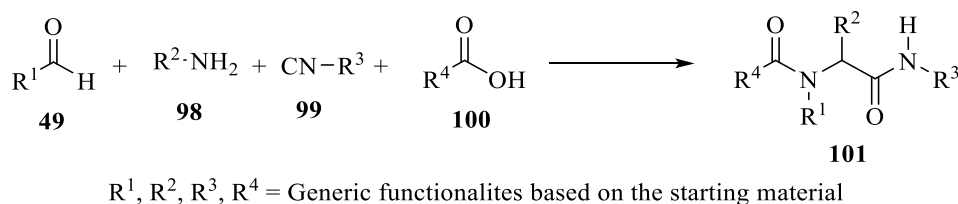


**Scheme 2-5.** Povarov quinoline synthesis.

## Multicomponent Reactions – A General Introduction

Multicomponent reactions (MCR) are one-pot procedures, typically involving three or more starting materials that are combined into a single product. A synthesis is deemed to be an MCR if the reaction mixture contains all of the components at the outset.<sup>[171]</sup> Multicomponent reactions hold several advantages over traditional sequential synthesis: high atom economy, efficiency (in time and energy), and lower environmental impact as a result of reduced solvent use.<sup>[172]</sup> Furthermore, this is an attractive methodology because it allows for isolation of complex “final” products without the need to purify an intermediate.

Many different reactions meet these criteria and are classified as MCRs – the scientific literature is replete with examples. The first generally acknowledged MCR was published by Strecker in 1850, which produces an  $\alpha$ -amino nitrile from a mixture of aldehyde, ammonia, and hydrogen cyanide.<sup>[173,174]</sup> Among the most widely known and broadly used MCR is the Ugi reaction, which combines equimolar aldehyde **49**, amine **98**, isonitrile **99**, and carboxylic acid **100** to afford amidoamide **101** (Eq. 2-2).<sup>[175]</sup>



**Equation 2-2.** Ugi 4-component MCR.

Fogg and dos Santos provide useful distinctions among the major sub-categories of one-pot reactions.<sup>[176]</sup> Domino/cascade, tandem, and multi-catalytic reactions are all defined as one-pot reactions, differentiated by specific reaction details. In the domino/cascade and tandem reactions, all the starting materials and catalysts are added at once. The reaction proceeds iteratively from intermediate to intermediate until the final product is obtained (Figure 2-5).<sup>[176,177]</sup> In multi-catalytic reactions, all of the starting materials are present, but to avoid catalyst incompatibility, the catalysts are added sequentially throughout the reaction. The first catalyst is added to give an intermediate, and once formed, a second catalyst is introduced to give the final product (Figure 2-5).<sup>[176,178]</sup> For this discussion, I will focus on the domino/cascade subset of multicomponent cyclocondensation reactions putatively catalyzed by molecular iodine, which are particularly relevant to this dissertation.

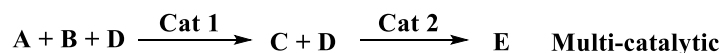
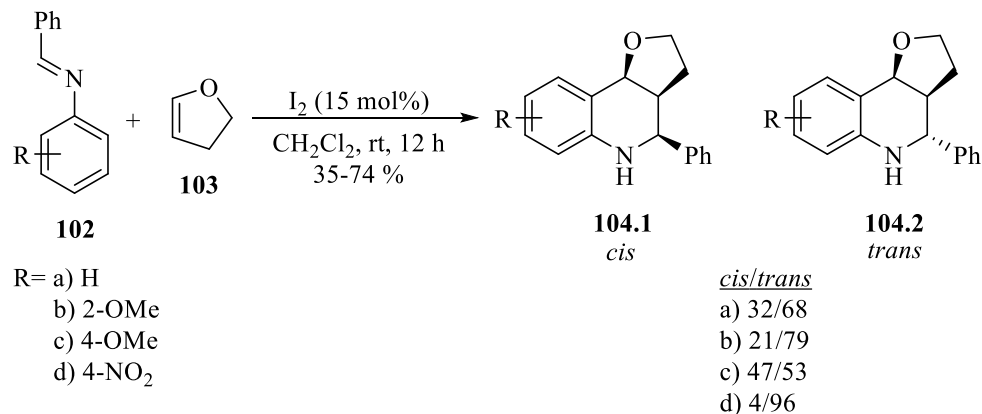


**Figure 2-5.** Multi-catalytic vs. domino/cascade and tandem one-pot reactions.

Molecular iodine is widely used to catalyze the cyclocondensation MCRs, *nominally* as a Lewis acid catalyst, because it is inexpensive and reasonably non-toxic.<sup>[179]</sup> Further, iodine is tolerant of air and moisture, and can be easily separated from reaction mixtures.<sup>[180]</sup> Iodine catalysis is featured in a plethora of nitrogen heterocycle syntheses; in particular, those reactions involving an imine intermediate en-route to tetrahydroquinolines and quinolines, all of which have a substantial history (Sections 2.3. and 2.4.).<sup>[181]</sup>

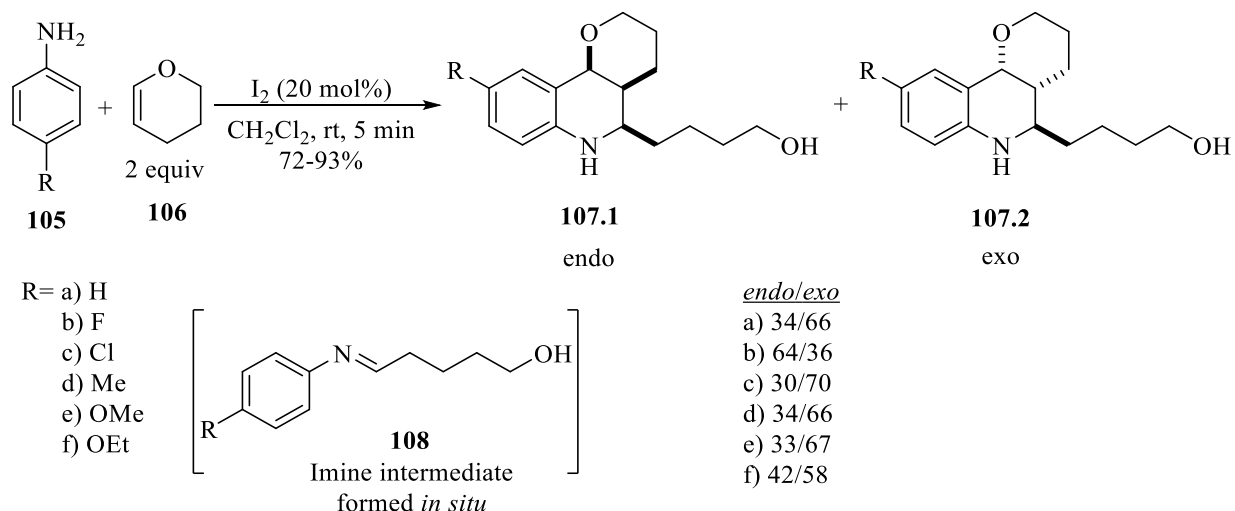
### 2.3. MCR synthesis of tetrahydroquinolines by iodine catalysis

Tetrahydroquinolines are widely studied, comprising a common substructure of important natural products and synthetic compounds.<sup>[182]</sup> While various catalytic procedures have been used to prepare tetrahydroquinolines,<sup>[145,161,182–185]</sup> many report the use of catalytic iodine as optimal.<sup>[180,181,186–189]</sup> In 2006, Li and co-workers prepared tetrahydroquinolines *via* the iodine-catalyzed imino-Diels-Alder reaction of preformed imines with enol ethers (Eq. 2-3).<sup>[187]</sup> This is the first example of an iodine-promoted reaction for the synthesis of a tetrahydroquinoline. The reaction was rudimentary, requiring a preformed imine, and the yields of tetrahydroquinoline were poor to moderate.



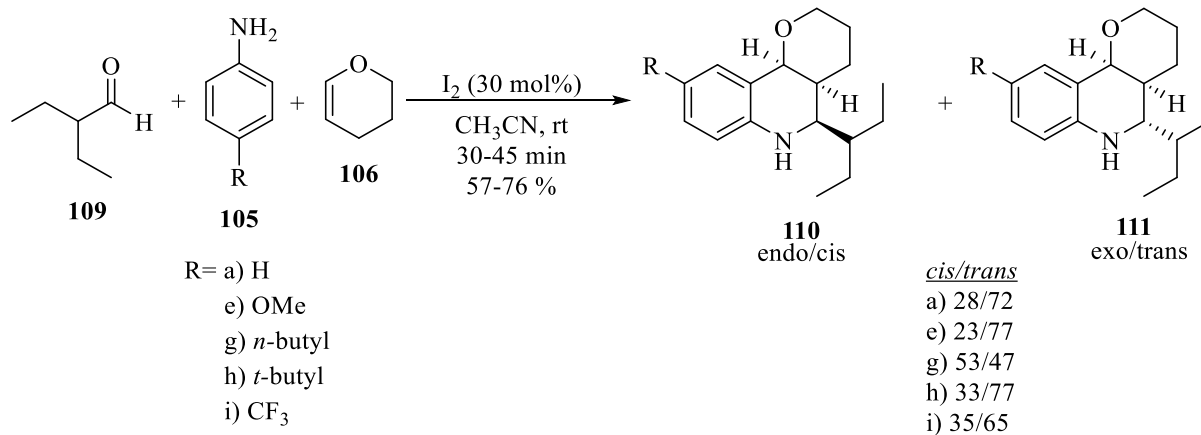
**Equation 2-3.** Imino Diels-Alder reaction of tetrahydroquinolines catalyzed by iodine.

A more efficient variant of Li's tetrahydroquinoline synthesis was subsequently reported by Lin and co-workers. High yields of tetrahydroquinolines were obtained in as little as five minutes, starting with an aniline and two equivalents of pyran **106** (Eq. 2-4).<sup>[186]</sup> In this reaction *N*-alkylimine **108**, generated *in situ*, undergoes an aza-Diels-Alder reaction with the second equivalent of pyran, affording tetrahydroquinoline derivatives **107.1** and **107.2**.



**Equation 2-4.** A highly efficient domino reaction to synthesize 1,2,3,4- tetrahydroquinoline derivatives.

Rai and co-workers extended Lin's method by incorporating aldehydes instead of enol ethers, allowing for substituent variability in the 2-position of tetrahydroquinolines (Eq. 2-5).<sup>[189]</sup>



**Equation 2-5.** Aza-Diels-Alder Povarov synthesis of tetrahydroquinolines.<sup>[189]</sup>

In this Povarov-type MCR, the *N*-alkylimine is formed *in situ* from aniline and an aliphatic aldehyde before undergoing cyclization with the enol ether. Before this report, Povarov MCRs were limited to aromatic aldehydes, because *N*-alkylimines are hydrolytically unstable and comparatively reactive. The incorporation of aliphatic aldehydes allows for greater diversity in benzoquinoline substituents, but more importantly, suggests that additional aromatic cores could be readily *tethered* to the central quinoline, separated by an arbitrary number of carbon atoms (Figure 2-6).

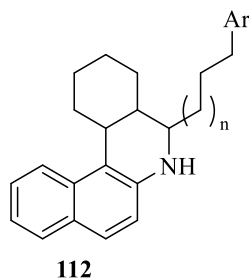
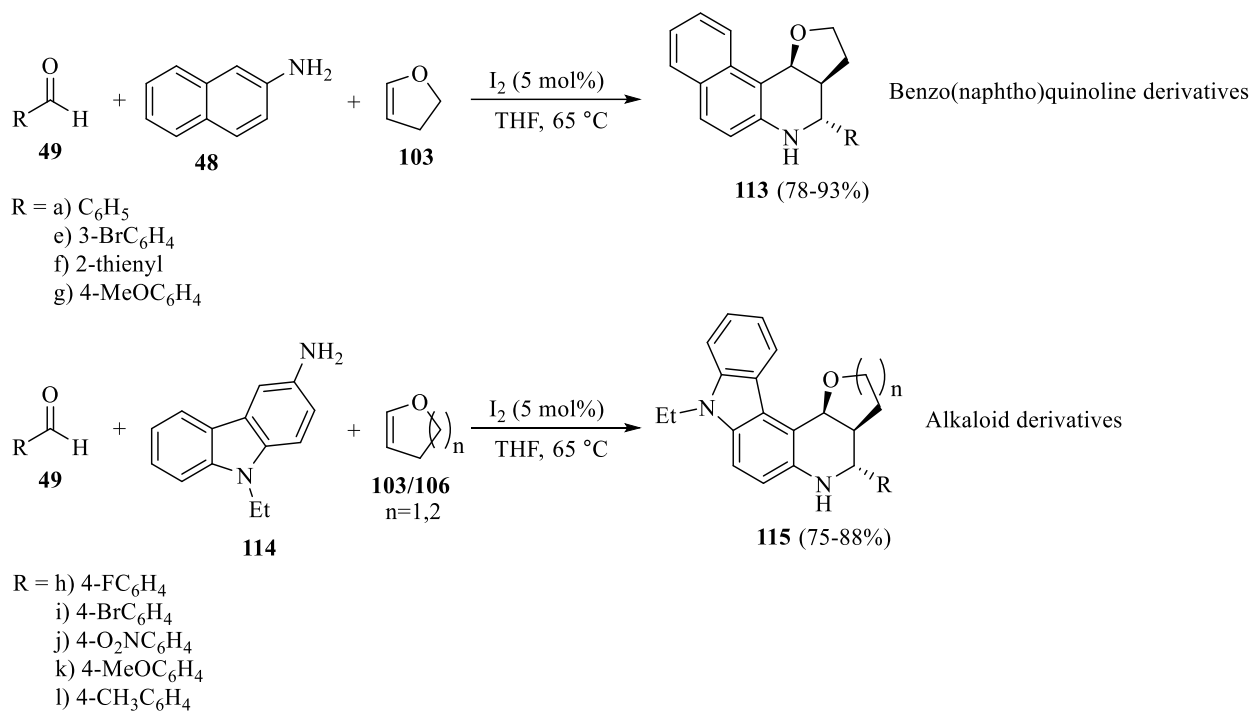


**Figure 2-6.** Fictitious example of a potential two-island archipelago model asphaltene.

The amount of iodine required to catalyze the aza-Diels-Alder reaction can be lowered substantially by using elevated reaction temperatures. Wang and co-workers showed that only five mol% of I<sub>2</sub> is required when the reaction mixture is heated to 65 °C, compared to the 15-30 mol% catalyst needed at room temperature. Higher reaction temperature also led to greater yields of tetrahydroquinolines. Under these ‘optimized’ reaction conditions, functionalized polycycles such as **114** were readily incorporated into the tetrahydroquinoline core (Scheme 2-6), leading to compounds that more closely resemble natural products as well as the ‘central islands’ of interest for model asphaltene compounds.<sup>[190,191]</sup>

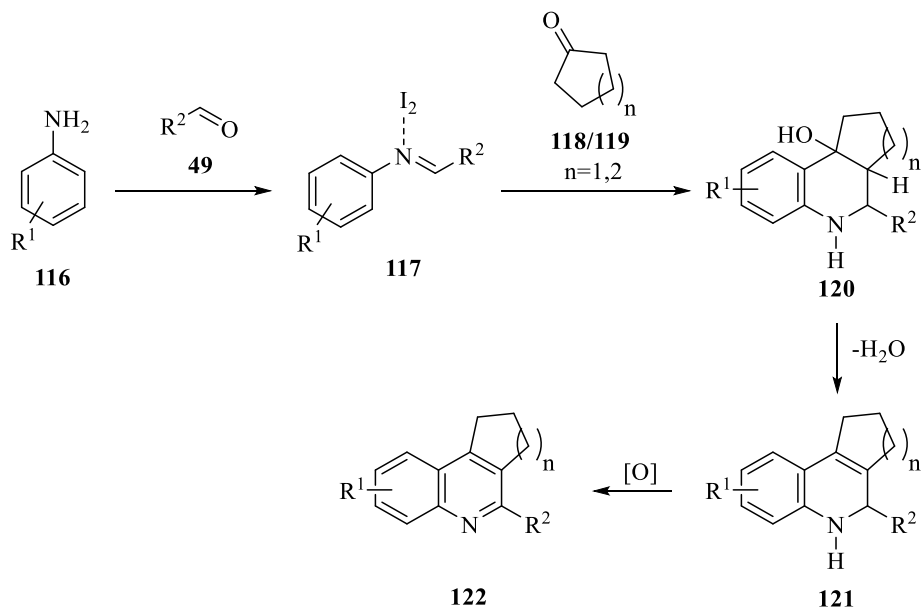


**Scheme 2-6.** Efficient synthesis of benzo(naphtho)quinoline and alkaloid derivatives.<sup>[190,191]</sup>

#### 2.4. Condensed quinolines – extended quinoline-core compounds

Fundamentally, the synthesis of quinolines by iodine-catalyzed MCR cyclocondensation is very similar to that of tetrahydroquinolines, with the significant addition of an oxidative aromatization to the reaction mechanism. Both reactions begin by imine formation from the aniline and aldehyde. The enol tautomer of the second aldehyde (or ketone) undergoes what is effectively an aza-Diels-Alder reaction, although it may proceed *via* a stepwise mechanism under some conditions. The intermediate alcohol **120** is key to the formation of quinoline: elimination affords dihydroquinoline **121**, which then aromatizes under aerobic conditions to give the quinoline compound **122** (Scheme 2-7).<sup>[180]</sup> Molecular oxygen is posited to be the oxidant, but this conclusion is not, as it turns out, entirely accurate. This, among other questions, is addressed in detail in Chapter 3 and 4. In prior work, it is generally accepted that I<sub>2</sub> functions as a mild Lewis acid catalyst by activating the imine

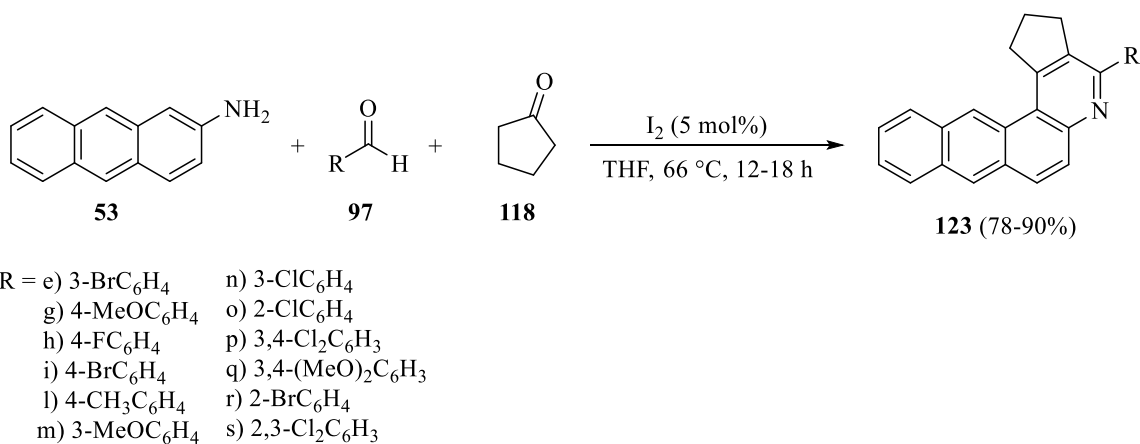
towards nucleophilic attack; however, our results show that the role of iodine is considerably more complicated, and nuanced.



$\text{R}^1, \text{R}^2$  = Functionality depends on the starting material

**Scheme 2-7.** Proposed (literature) mechanism for iodine-catalyzed MCR quinoline synthesis.<sup>[180]</sup>

Iodine-catalyzed MCR methodology is well documented by now, but Wang's 2008 report, describing the convergent formation of large polycyclic quinolines from aromatic aldehydes, aromatic amines, and ketones, is particularly relevant to our objectives.<sup>[124]</sup> The adducts reported by Wang, for example cyclopenta[*c*]naphtho[2,3-*f*]quinoline derivatives **123** (Eq. 2-6),<sup>[192]</sup> resemble continental-like asphaltene model compounds of interest to our collaborators. Wang's choice of reagents for this MCR is deliberate; aromatic aldehydes do not enolize and condense more rapidly with the aniline, giving a hydrolytically stable *N*-arylimine. This imine cyclizes with the only available enol, in equilibrium with the ketone.



**Equation 2-6.** Synthesis of cyclopenta[*c*]naphtho[2,3-*f*]quinoline derivatives.<sup>[192]</sup>

Tykwinski and co-workers adapted Wang's MCR procedure to synthesize several quinoline-based model asphaltenes;<sup>[124,126]</sup> however, several challenges arose during the course of this work. The reactions were irreproducible under strictly anhydrous conditions and particularly problematic for polycyclic anilines and some cyclic ketones. They were particularly interested in incorporating the cyclic ketone steroid biomarker 5- $\alpha$ -cholestanone into the molecules because it is an identifying feature of large hopane molecules, found in heavy crude oil (Figure 2-7).<sup>[127]</sup>

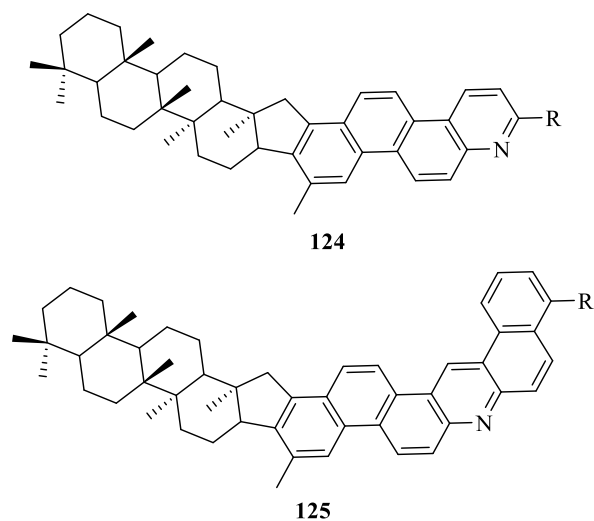
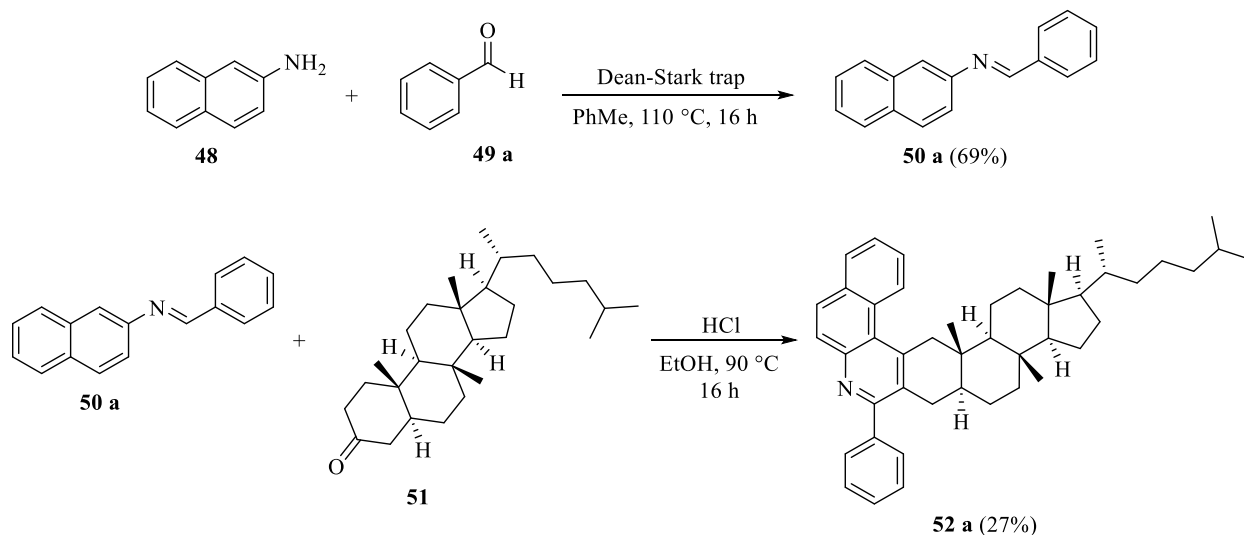


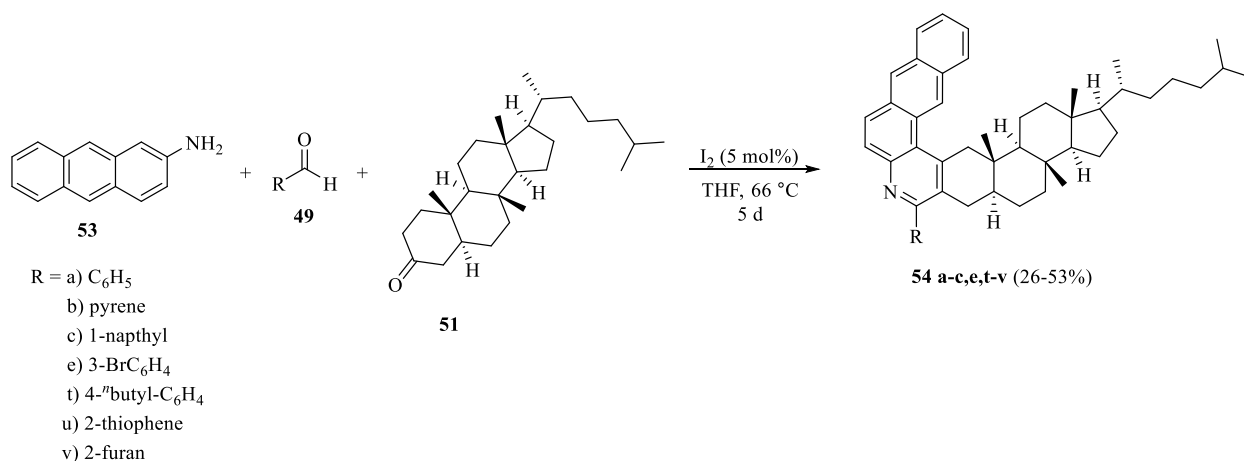
**Figure 2-7.** Suggested steroid fused biomarker molecules identified in heavy crude oil.<sup>[127]</sup>

Reproducible results were only obtained by conducting the reaction in two independent steps, using Kozlov's procedures, with tedious isolation of the imine intermediate, **50a**, resulting in poor yields of the desired cycloadducts (Scheme 2-8).<sup>[125]</sup> These issues led us to reoptimize the MCR procedure, with special emphasis on determining the identity of the active catalyst.



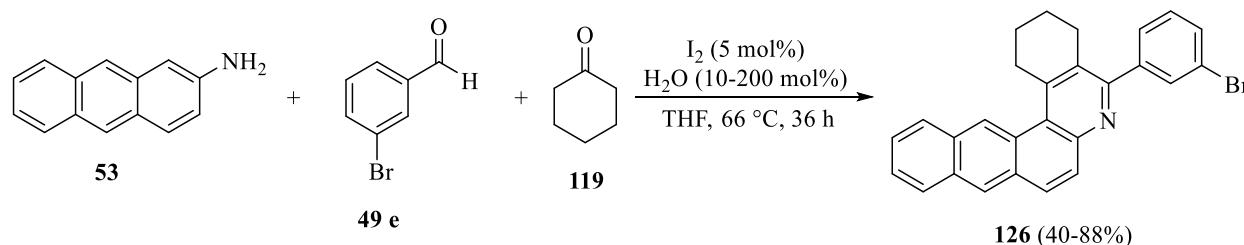
**Scheme 2-8.** Two-step procedure of steroid-derived naphthoquinolines.

Given the obvious limitations of the two-step approach to steroid-derived naphthoquinolines, we sought to apply the MCR protocol, based on Wang's procedure,<sup>[124]</sup> to prepare a small library of steroid-derived naphthoquinoline asphaltene model compounds (Eq. 2-7). This effort was led by Matthias Schulze, a collaborator from the Tykwinski group. In this reaction, cyclohexanone was replaced by 5- $\alpha$ -cholestanone and a number of compounds were synthesized, in disappointingly low to moderate yields.



**Equation 2-7.** Steroid-derived multicomponent reaction.

To improve the product yields, I began by assessing the role of water in the multicomponent reaction. To do this, the combination of 2-aminoanthracene **53**, 3-bromobenzaldehyde **49e**, and cyclohexanone **119** was used as the model reaction for this optimization (Eq. 2-8).



**Equation 2-8.** Stryker and co-workers MCR conditions for determination of the optimal H<sub>2</sub>O content.<sup>[126]</sup>

When run under rigorously anhydrous conditions, or even using HPLC-grade THF, the isolated yields of quinoline varied significantly (7-65%). However, using reagent-grade THF, which contains  $\leq 0.05\%$  residual water, higher yields and more reproducible results were obtained (Table 2-1). I conducted several reactions with varying amounts of water added to a known volume (6 mL) of anhydrous THF (distilled from Na under inert atmosphere) and from this determined that

the water to solvent ratio required to achieve high and consistent yields was roughly 150 mol% (Table 2-1, entry 4). Adding additional water, at least up to 200 mol%, had a negligible effect on the yield of the product. It is possible that increasing the water concentration beyond 200 mol% may impede the reaction, but this was not tested.

**Table 2-1.** Screening the effect of water concentration in the synthesis of naphthoquinolines.

Entry	H <sub>2</sub> O content (mol%)	Yield (%)
1	10	40
2	27	44
3	75	55
4	150	88
5	200	85

Reactions were performed in refluxing dry, degassed THF (6 mL) with catalytic I<sub>2</sub> (5 mol%) for 12 h under a N<sub>2</sub>-atmosphere, followed by an additional stir period of 24 h open to air. In all cases the amine, aldehyde and ketone were in a 1:1:1 stoichiometric mixture.

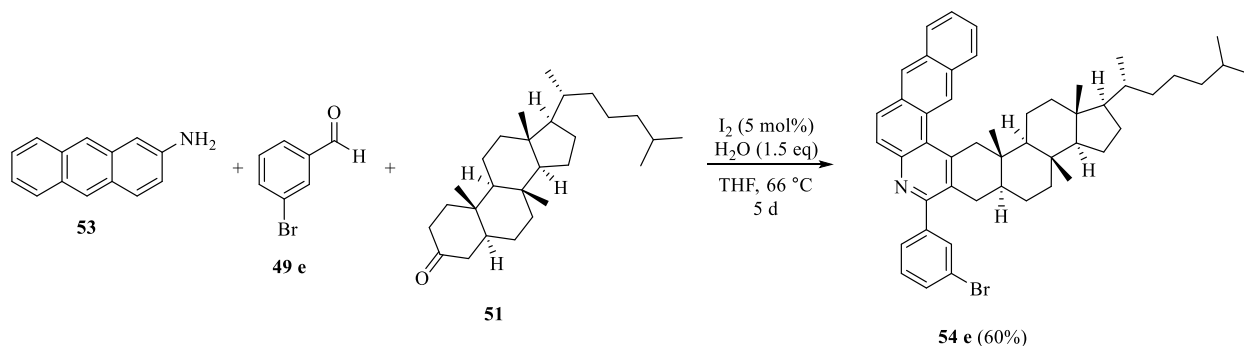
From well-established precedent, hydroiodic acid (HI), formed *in situ* from the reaction of iodine with water,<sup>[193]</sup> became the obvious catalyst candidate. To confirm this hypothesis, I used aqueous HI (57%) as the catalyst instead of the I<sub>2</sub>/H<sub>2</sub>O mixture, and obtained identical results (Table 2-2, compare entries 1 and 2). Surprisingly, *the iodide counterion proved to be equally essential*. No more than 10% product was isolated when other Brønsted acids, such as HCl and H<sub>2</sub>SO<sub>4</sub>, were used under otherwise identical conditions (Table 2-2). These results show that iodine is a *precatalyst* and that iodide is intimately involved in the reaction mechanism. The precise role (or roles) of the iodide counterion is discussed in detail in subsequent chapters.

**Table 2-2.** Brønsted acid catalyst screening, using identical water concentration, to evaluate the MCR.

Entry	Catalyst	H <sub>2</sub> O (mol%)	Yield (%)
1	HI	27	43
2	I <sub>2</sub>	27	44
3	HCl	27	10
4 <sup>a</sup>	H <sub>2</sub> SO <sub>4</sub>	27	trace

Reactions were performed in refluxing dry, degassed THF for 12 h under a N<sub>2</sub>-atmosphere, followed by an additional stir period of 24 h open to air. In all cases the amine, aldehyde and ketone were in a 1:1:1 stoichiometric mixture. Amount of catalyst added is 5 mol% unless otherwise specified. <sup>a</sup>Amount of catalyst added is 2.5 mol%.

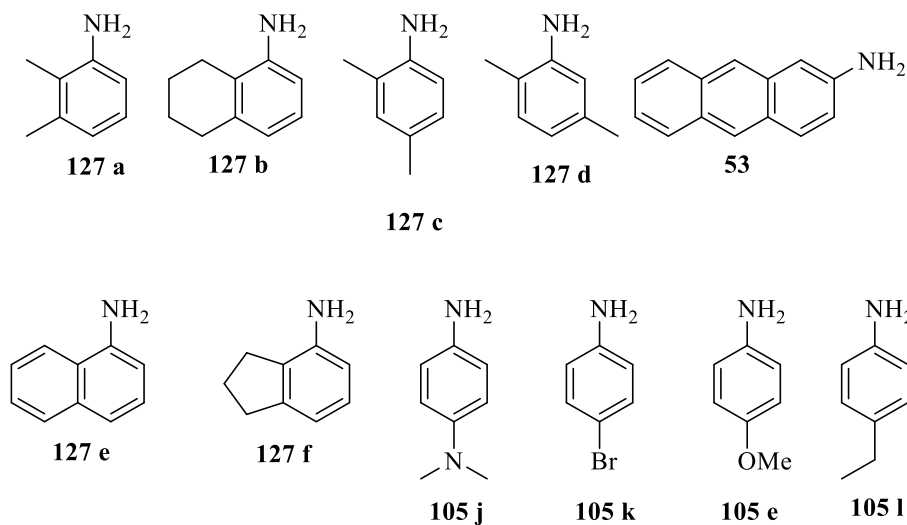
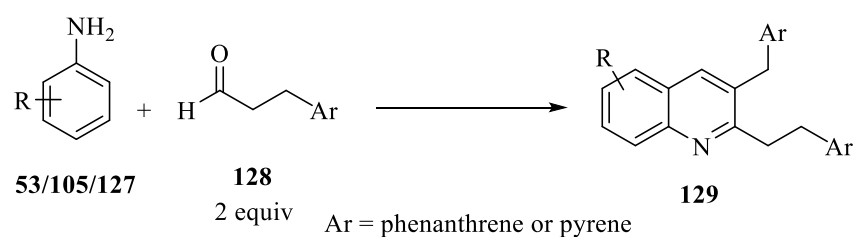
Following the optimization for catalyst and water, Matthias Schulze adopted my procedures and repeated the initial MCR with 5- $\alpha$ -cholestanone to synthesize the steroid-fused model compound **54e**. The reaction was only performed once by Matthias Schulze, obtaining **54e** (Eq. 2-9) in improved yield, and it was anticipated that similar improvements in MCR yield and reproducibility would be universally realized.



**Equation 2-9.** Re-evaluation of MCR yield for steroid-derived naphthoquinoline.

With an optimized procedure in hand, I envisioned that an extensive library of quinoline-based archipelago compounds could be synthesized by extension of the HI-catalyzed MCR. For this

series, two equivalents of an alkyl-tethered  $\alpha,\omega$ -aryl aldehyde must react with the substituted aniline, a combination of components not previously reported (Eq. 2-10). It is worth noting that very few examples of MCR quinoline syntheses incorporating two alkyl aldehydes have been reported.<sup>[184,194–196]</sup> Furthermore, no archipelago-type compounds have been prepared using this methodology. The following chapters will detail the issues, challenges, and advances made in adapting this MCR to prepare a range of archipelago model compounds. To accomplish this goal, a substantial mechanistic investigation was conducted, resulting in iterative improvements in reaction scope, selectivity, and yield.



**Equation 2-10.** Hypothetical MCR quinoline syntheses incorporating alkyl-tethered  $\alpha,\omega$ -aryl aldehydes.

## Summary

The investigation of the identity and role of the active catalyst, as well as the optimal solvent and water concentrations slowly emerged as a prominent vein of synthetic research in the Stryker group. As described in the chapter, at the outset little was known about the mechanistic role of the iodine; none of the early work on iodine-catalyzed MCRs addresses the nuances of catalyst generation, regeneration, and overall reaction mechanism. In the subsequent chapters, the mechanistic details of this catalytic reaction are interrogated experimentally and, for the most part, defined. Optimization of temperature, solvent, and source of oxidant are determined, along with a substantial extension of reaction scope, leading to the efficient synthesis of a new class of quinoline-core archipelago model asphaltene compounds.

## Experimental Section

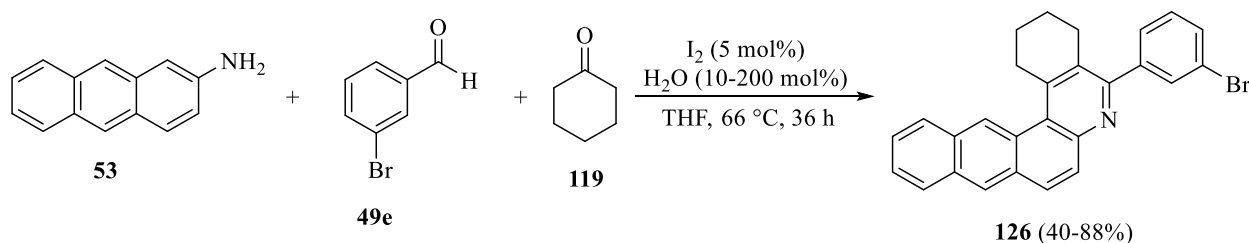
All manipulations of air-sensitive materials were performed in a well-maintained Braun dry box under an atmosphere of prepurified nitrogen or, on larger scale, using standard Schlenk techniques. Dioxane was distilled from sodium under nitrogen. THF was distilled from sodium/benzophenone ketyl, also under nitrogen. 2-Aminoanthracene, 3-bromobenzaldehyde, cyclohexanone, I<sub>2</sub>, aqueous HI (57 wt.%), aqueous HCl (37 wt.%), and H<sub>2</sub>SO<sub>4</sub> (conc.) were purchased from commercial sources and used as received. TLC analyses were performed using 0.5 mm analytical TLC plates from Macherey-Nagel (ALUGRAM<sup>®</sup> SIL G/UV<sub>254</sub>) and visualized by using UV-light of 254 nm and/or 366 nm. For flash column chromatography, silica gel 60 M (0.040–0.063 mm) from Macherey-Nagel was used.

NMR spectra were recorded on an Agilent/Varian instrument (400 MHz for <sup>1</sup>H NMR) at ambient temperature. Chemical shifts were referenced to residual solvent protium peaks ( $\delta$  in parts per

million (ppm)  $\text{CHCl}_3$   $^1\text{H}$ : 7.26 ppm). Coupling constants were assigned as observed.  $^1\text{H}$  NMR coupling constants are rounded to nearest 1.0 Hz.

Complete diagnostic data for compound **126** is found in a co-authored publication and in Matthias Schulze's Ph.D. dissertation.<sup>[126,197]</sup> Here, only the  $^1\text{H}$  NMR spectrum is reported.

**General procedure for screening the affect of water concentration in the synthesis of naphthoquinoline 126.**<sup>[126]</sup>



2-Aminoanthracene **53** (0.10 g, 0.52 mmol) was added to a dry 25 mL three-neck RBF flask and purged three times with vacuum/nitrogen. 3-Bromobenzaldehyde **49e** (96 mg, 60  $\mu\text{L}$ , 0.52 mmol),  $\text{I}_2$  (6.6 mg, 0.026 mmol), dry/distilled THF (6 mL), and  $\text{H}_2\text{O}$  (10–200 mol %), were sequentially added and the mixture stirred for 1 h at rt under  $\text{N}_2$  atmosphere. Cyclohexanone **119** (51 mg, 54  $\mu\text{L}$ , 0.52 mmol) was then added, and the mixture stirred at reflux for 12 h under  $\text{N}_2$  atmosphere. The reaction mixture was exposed to air and heating to reflux was continued for 24 h. The reaction mixture was cooled to rt and the solvent was removed under reduced pressure.  $\text{CH}_2\text{Cl}_2$  (100 mL) and saturated  $\text{Na}_2\text{CO}_3$  (100 mL) were added. The organic layer was separated, washed with saturated  $\text{Na}_2\text{CO}_3$  (2 x 100 mL), dried over  $\text{Na}_2\text{SO}_4$ , filtered, and the solvent was removed under reduced pressure. The crude material was purified by column chromatography (hexanes followed

by CH<sub>2</sub>Cl<sub>2</sub>) to give 5-(3-bromophenyl)-1,2,3,4-tetrahydro-naphtho[2,3-*a*]phenanthridine **126** as a light tan powder (40–88%).

<sup>1</sup>H NMR (CDCl<sub>3</sub>, 400 MHz) δ 9.12 (s, 1H), 8.33 (s, 1H), 8.09–8.00 (m, 2H), 7.89 (d, *J* = 9.0 Hz, 1H), 7.81 (d, *J* = 9.0 Hz, 1H), 7.75–7.74 (m, 1H), 7.60–7.56 (m, 3H), 7.49 (d, *J* = 8.0 Hz, 1H), 7.37 (t, *J* = 8.0 Hz, 1H), 3.65 (t, *J* = 5.0 Hz, 2H), 2.86 (t, *J* = 6.0 Hz, 2H), 1.91–1.87 (m, 4H)

**(T2-1.1) 10 mol% H<sub>2</sub>O.** The general procedure was used, with 10 mol% H<sub>2</sub>O (0.90 μL), giving phenanthridine **126** as a light tan powder, 0.91 g (40%).

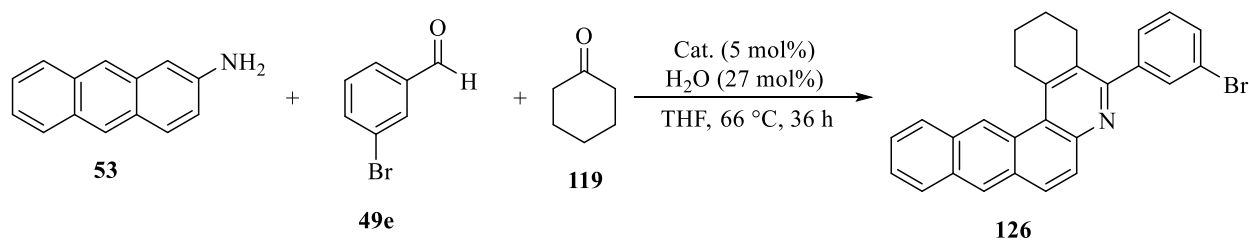
**(T2-1.2) 27 mol% H<sub>2</sub>O.** The general procedure was used, with 27 mol% H<sub>2</sub>O (2.50 μL), giving phenanthridine **126** as a light tan powder 0.99 g (44%).

**(T2-1.3) 75 mol% H<sub>2</sub>O.** The general procedure was used, with 75 mol% H<sub>2</sub>O (7.0 μL), giving phenanthridine **126** as a light tan powder, 0.12 g (55%).

**(T2-1.4) 150 mol% H<sub>2</sub>O.** The general procedure was used, with 150 mol% H<sub>2</sub>O (14.0 μL), giving phenanthridine **126** as a light tan powder, 0.20 g (88%).

**(T2-1.5) 200 mol% H<sub>2</sub>O.** The general procedure was used, with 200 mol% H<sub>2</sub>O (19.0 μL), giving phenanthridine **126** as a light tan powder, 0.19 g (85%).

## General procedure for Brønsted acid catalyst screening <sup>[126]</sup>



2-Aminoanthracene **53** (0.10 g, 0.52 mmol) was added to a dry 25 mL three-neck RBF flask and purged three times with vacuum/nitrogen. 3-Bromobenzaldehyde **49e** (96 mg, 60  $\mu$ L, 0.52 mmol), Brønsted acid (detailed below), dry/distilled THF (6 mL), and H<sub>2</sub>O (detailed below), were sequentially added and the mixture stirred for 1 h at rt under N<sub>2</sub>. Cyclohexanone **119** (51 mg, 54  $\mu$ L, 0.52 mmol) was then added, and the mixture stirred at reflux for 12 h. The reaction mixture was exposed to air and heating was continued for 24 h. The reaction mixture was cooled to rt and the solvent was removed under reduced pressure. CH<sub>2</sub>Cl<sub>2</sub> (100 mL) and saturated Na<sub>2</sub>CO<sub>3</sub> (100 mL) were added. The organic layer was separated, washed with saturated Na<sub>2</sub>CO<sub>3</sub> (2 x 100 mL), dried over Na<sub>2</sub>SO<sub>4</sub>, filtered, and the solvent was removed under reduced pressure. The crude material was purified by column chromatography (hexanes followed by CH<sub>2</sub>Cl<sub>2</sub>) to give 5-(3-bromophenyl)-1,2,3,4-tetrahydro-naphtho[2,3-*a*]phenanthridine **126** as a light tan powder.

Because of the water content (amounting to 27 mol%) of commercially available HI, the necessary amount of water was added to standardize the conditions for the reactions using other commercial Brønsted acids.

### Calculations for water addition as a function of Brønsted acid water content

For the following catalysts,  $2.6 \times 10^{-5}$  mol of mineral acid was used.

#### Amount of water in HI (57%):

$$(2.585 \times 10^{-5} \text{ mol}) \times (127.91 \text{ g/mol}) = (0.00331 \text{ g}) / (0.57 \text{ weight \%}) = \underline{0.0058 \text{ g}} \text{ of total solution}$$

$$(0.0058 \text{ g}) / (1.701 \text{ g/mL}) = 0.00342 \text{ mL} = \mathbf{3.41 \mu\text{L}}$$

$$\text{Total H}_2\text{O concentration: } (0.0058 \text{ g}) \times (0.43 \text{ weight \%}) = (\underline{0.00249 \text{ g}}) / (18.02 \text{ g/mol}) = (1.38 \times 10^{-4} \text{ mol}) / (2.585 \times 10^{-5} \text{ mol}) = 5.35 \text{ mol of H}_2\text{O for 1 mol HI} = (5.35 \text{ mol H}_2\text{O}) \times (5 \text{ mol \%}) = \mathbf{26.7 \text{ mol\% of H}_2\text{O}}$$

#### Additional water for I<sub>2</sub>:

$$(2.585 \times 10^{-5} \text{ mol}) \times (253.8 \text{ g/mol}) = 0.007 \text{ g of I}_2$$

H<sub>2</sub>O: Add **2.49 μL**

#### Additional water for H<sub>2</sub>SO<sub>4</sub>:

In this case, the catalyst loading is 2.5 mol% ( $1.293 \times 10^{-5}$  mol, 0.689 μL)

H<sub>2</sub>O: Add **2.49 μL**

#### Additional water for HCl:

$$(2.585 \times 10^{-5} \text{ mol}) \times (36.46 \text{ g/mol}) = (9.42 \times 10^{-4} \text{ g}) / (0.37 \text{ weight \%}) = \underline{0.0026 \text{ g}} \text{ of total solution}$$

$$(0.0026 \text{ g}) / (1.2 \text{ g/mL}) = 0.00213 \text{ mL} = \mathbf{2.13 \mu\text{L}}$$

H<sub>2</sub>O:  $(0.0026 \text{ g}) \times (0.63 \text{ weight \%}) = 0.00161 \text{ g of H}_2\text{O}$

0.00249 - 0.00161 = Add **0.88  $\mu\text{L}$**

(T2-2.1) The general procedure was used, HI (3.4  $\mu\text{L}$ ), giving phenanthridine **126** as a light tan powder, 0.098 g (43%).

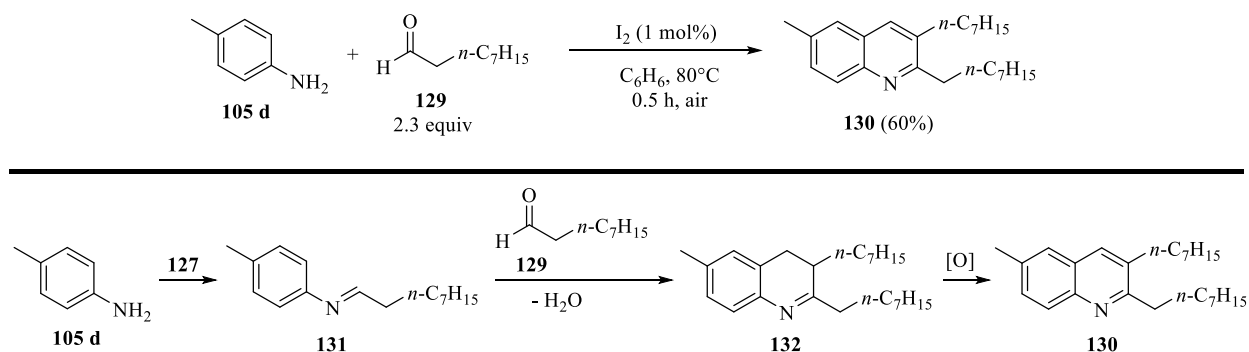
(T2-2.2) The general procedure was used, I<sub>2</sub> (6.6 mg, 0.026 mmol) and H<sub>2</sub>O (2.49  $\mu\text{L}$ ), giving phenanthridine **126** as a light tan powder, 0.099 g (44%).

(T2-2.3) The general procedure was used, HCl (2.6 mg, 2.1  $\mu\text{L}$ , 0.026 mmol) and H<sub>2</sub>O (0.88  $\mu\text{L}$ ), giving phenanthridine **126** as a light tan powder, 0.022 g (10%).

(T2-2.4) The general procedure was used, H<sub>2</sub>SO<sub>4</sub> (1.3 mg, 0.69  $\mu\text{L}$ , 0.013 mmol) and H<sub>2</sub>O (2.49  $\mu\text{L}$ ), giving phenanthridine **126** as a light tan powder, proceeding to less than 50% conversion, producing a low (unquantified) yield.

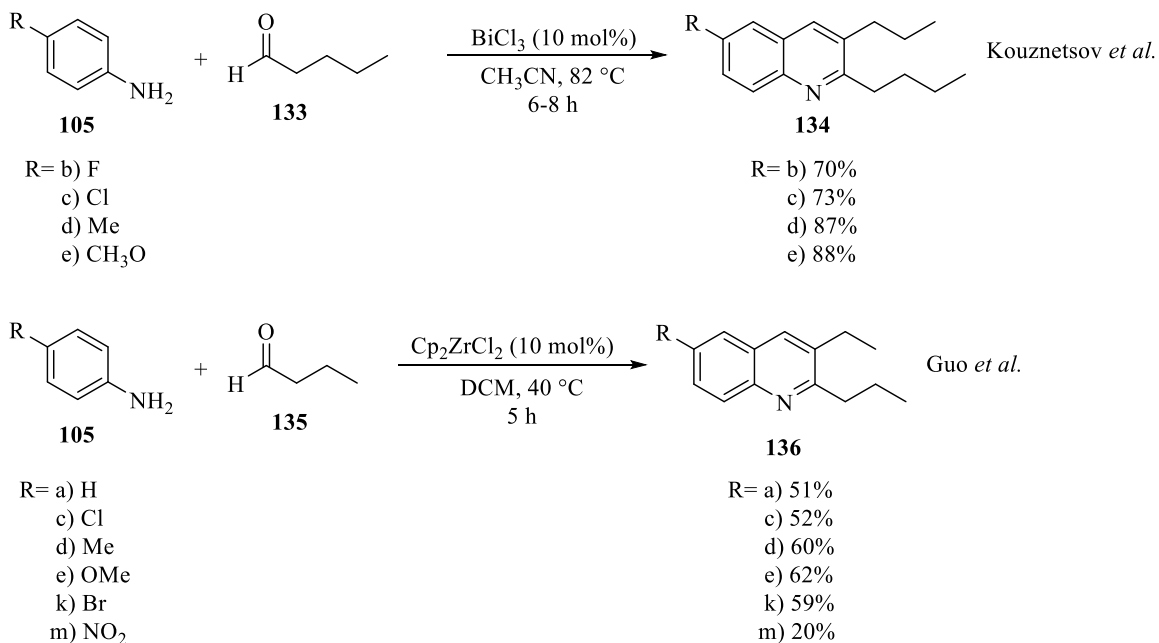
### 3. Multicomponent Cyclocondensation for the Synthesis of Quinoline-core Archipelago Compounds

The first publication incorporating two aliphatic aldehydes in an MCR cyclocondensation appeared in 1909.<sup>[198]</sup> The field lay dormant until 2006, when a more general MCR incorporating two aliphatic aldehydes was described (Scheme 3-1, top).<sup>[199]</sup> In this reaction, the *N*-alkylimine **131** presumably reacts with the enol tautomer of a second aldehyde, affording the dihydroquinoline **132**, which undergoes aerobic oxidation (bottom, Scheme 3-1).<sup>[199]</sup>



**Scheme 3-1.**  $I_2$ -catalyzed quinoline synthesis using two aliphatic aldehydes.

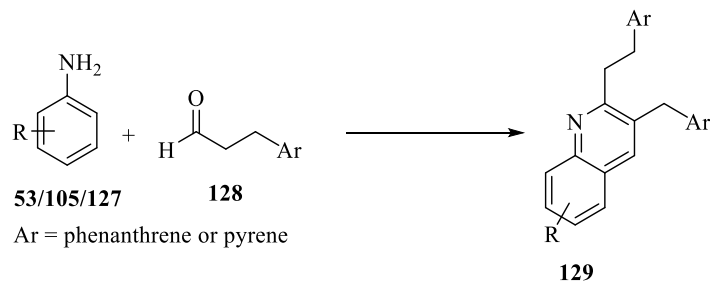
Until the present work, this reaction has remained relatively unexplored and unoptimized. The substrate scope is narrow; only a few aliphatic aldehydes and simple anilines have been used. While various catalysts, including Lewis acids and ionic liquids, have been explored (Scheme 3-2), by far the simplest of the catalysts is HI.<sup>[184,194–196]</sup> We sought to optimize the Wang MCR conditions, focusing on the direct use of catalytic HI, to synthesize new archipelago-like model asphaltene compounds. As will be discussed, this entailed further refinement of reaction conditions, to suppress significant side-reactions.



**Scheme 3-2.** Quinoline MCR using two aliphatic aldehydes.<sup>[184,195]</sup>

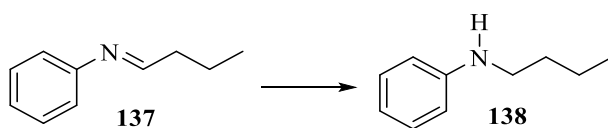
### MCR Advances: Three-island Archipelago Model Asphaltene Compounds

One of the benefits of the MCR strategy is that it can be implemented to prepare a broad range of three-island archipelago model compounds. The MCR envisioned must proceed using two equivalents of an alkyl-tethered  $\alpha,\omega$ -aromatic aldehyde and a range of substituted aniline derivatives (Eq. 3-1). Ideally, the MCR adduct should display two satellite polycyclic aromatic islands tethered to a central quinoline-core by short (2-5 carbon) saturated alkyl chains. Phenanthrene was used almost exclusively as the satellite polycyclic aromatic island for this exploration. These archipelago molecules are of great interest to petroleum researchers, including our collaborators at the Japan Petroleum Energy Center (JPEC), as models for benchmarking ICP-MS analysis of native asphaltenes and assessing the aggregation behaviour of basic asphaltenes.



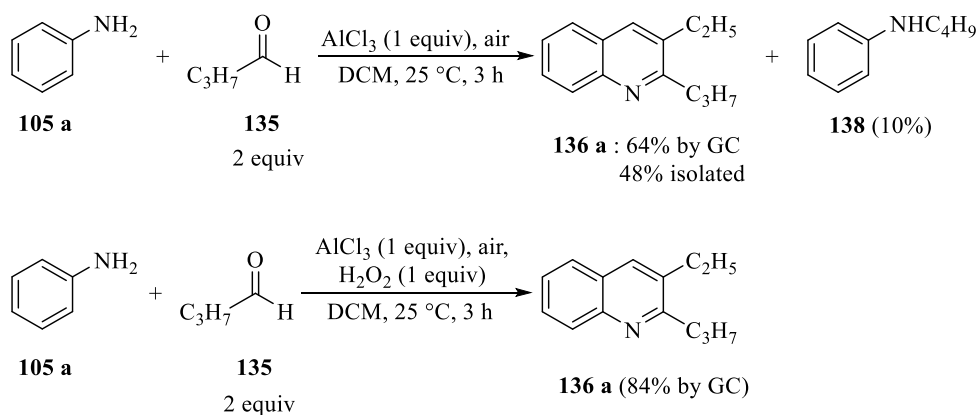
**Equation 3-1.** Synthetic approach to new three-island archipelago model compounds.

Several synthetic challenges are involved in adapting the MCR to the use of two equivalents of an aliphatic aldehyde. The most significant issue is the formation of secondary amine **138** as a side-product, arising from the reduction of the *N*-alkylimine intermediate **137** formed during the reaction (Eq. 3-2).



**Equation 3-2.** Reduction of the *N*-alkylimine to the secondary amine.

Guo and co-workers proposed that in the absence of  $\text{H}_2\text{O}_2$  in the reaction medium, greater amounts of secondary amine are formed, at the expense of MCR yields. The authors attributed this to the protonated *N*-alkylimine acting as the oxidant in the final aromatization step.<sup>[196]</sup> When the authors added a stoichiometric quantity of  $\text{H}_2\text{O}_2$  as an external oxidant, yields increased and side-product formation decreased (Scheme 3-3). This result raises the question of whether peroxide is actually formed *in situ* under HI-catalyzed MCR conditions. This question is addressed, conclusively, in Chapter 4 of this thesis.



**Scheme 3-3.** Lewis acid catalyzed substituted quinoline synthesis and identification of secondary amine by-product.<sup>[196]</sup>

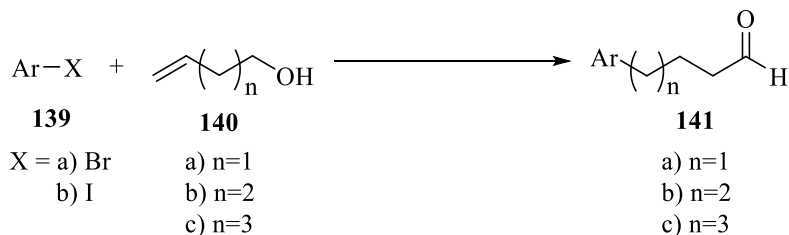
Another issue associated with the use of aliphatic aldehydes is that electronic, steric, and conformational effects of substituents on the alkyl chain or polycyclic aromatic terminus significantly influence reactivity. In literature examples, simple, unsubstituted aliphatic aldehydes are used with few issues.<sup>[184,194–196]</sup> However, the large polycyclic aromatic residues tethered to our aldehydes introduce potential solubility and structural affects. Furthermore, the electronic effects of substituent(s) on the aniline is expected to be an important factor in the efficiency of the MCR.

## Results and Discussion

### 3.1. Three-island archipelago model compounds: synthesis of the aldehyde-terminated polycyclic “islands”

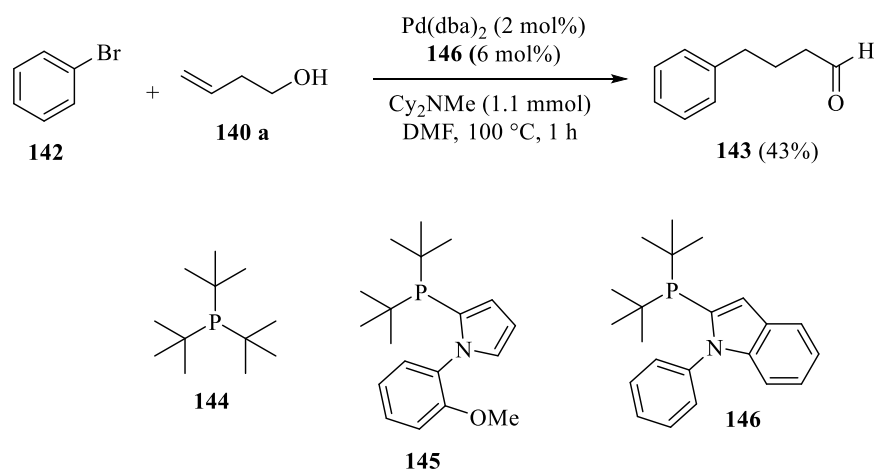
The asphaltene-like model compounds we envisioned can be assembled starting from a range of alkyl-tethered  $\alpha,\omega$ -aryl aldehydes. For our purposes, the aldehyde-terminated polycyclic “islands” needed for the three-island archipelago MCR reaction must be synthesized on large scale from readily available starting materials. In addition, the aldehydes should ideally be easily purified on this scale, preferably without chromatography. The most efficient synthetic procedure to

accomplish this transformation is the well-known migratory Heck reaction between the appropriate aryl halide and various  $\alpha,\omega$ -allylic alcohols (Eq. 3-3).<sup>[200,201]</sup>



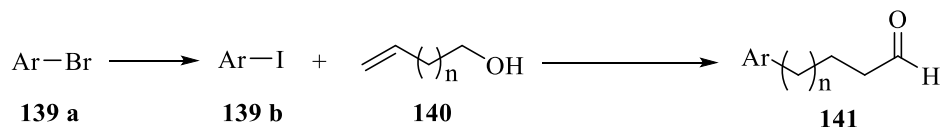
**Equation 3-3.** Synthetic plan to assemble the desired alkyl-tethered  $\alpha,\omega$ -aryl aldehyde.

The migratory Heck reaction can be accomplished using aryl bromides directly. The requirement for bulky, electron-rich phosphine ligands to promote this reaction is essential (Eq. 3-4).<sup>[201]</sup>



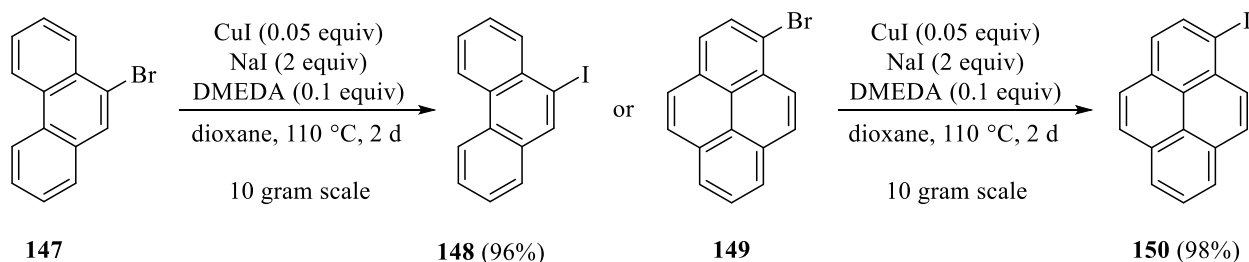
**Equation 3-4.** Phosphine ligands used to promote the migratory Heck reaction using aryl bromides.<sup>[201]</sup>

Unfortunately, the phosphine ligands are air-sensitive and expensive, impractical for large-scale synthesis. Instead, a two-step sequence of halogen exchange followed by a “ligand-free” migratory Heck procedure became our preferred approach (Scheme 3-4).



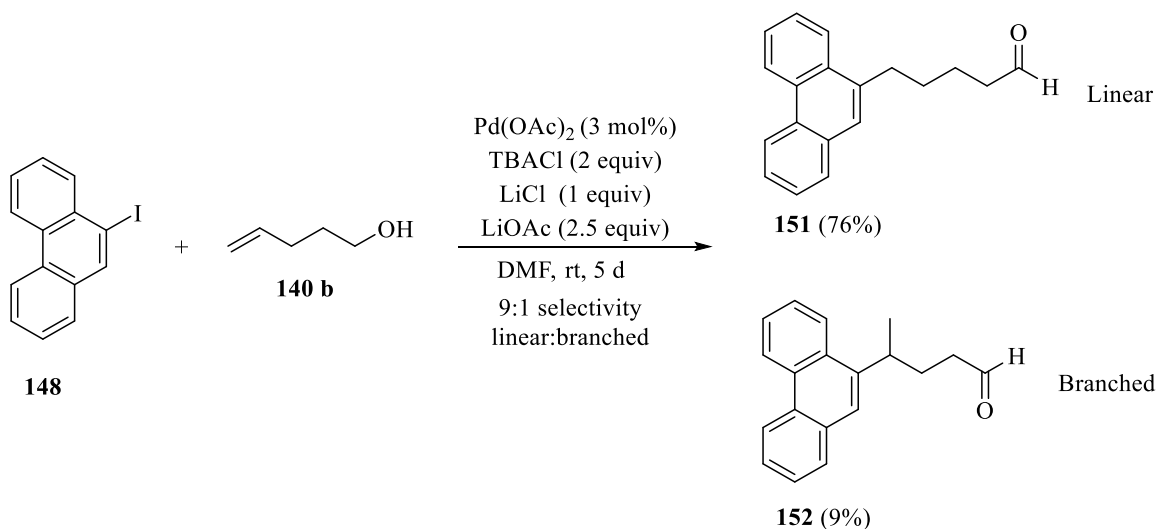
**Scheme 3-4.** Practical, large-scale synthesis of variable tethered alkyl-tethered  $\alpha,\omega$ -aryl aldehyde.

Aryl iodides are best prepared from the corresponding commercially available (or easily synthesized)<sup>[202]</sup> aryl bromides *via* copper-catalyzed halogen exchange.<sup>[203]</sup> For our purposes, 9-bromophenanthrene and 1-bromopyrene were selected as the starting ‘islands,’ which were converted to the corresponding iodide on a multigram scale (Scheme 3-5). For this reaction, the use of freshly purified CuI is crucial to obtain high yields of pure aryl iodide.



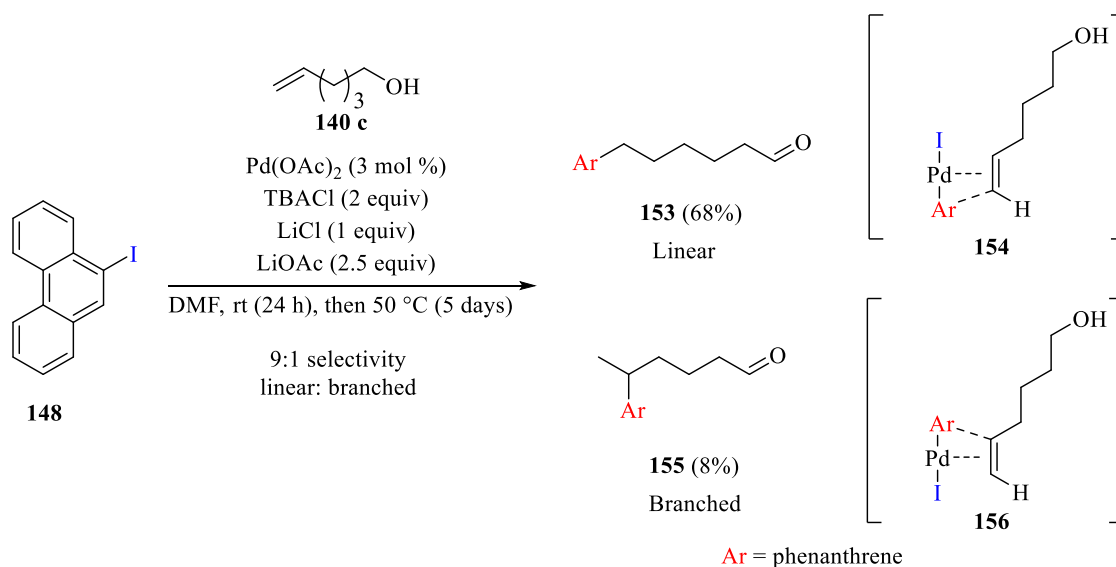
**Scheme 3-5.** Copper-catalyzed aromatic halide exchange reaction converting bromoarene to iodoarene.<sup>[203]</sup>

Larock’s palladium-catalyzed migratory Heck reaction using commercial  $\alpha,\omega$ -alkenyl alcohols was then used to prepare the tethered aliphatic aldehydes.<sup>[200]</sup> The reaction was optimized using 9-iodophenanthrene **148** and 4-penten-1-ol **140b**, producing the expected mixture of linear and branched products **151** and **152**, respectively (Eq. 3-5).



**Equation 3-5.** Migratory Heck reaction to afford the linear and branched alkyl-tethered  $\alpha,\omega$ -aryl aldehyde.

Larock determined that the linear to branched ratio was governed by the reaction temperature.<sup>[200]</sup> When the temperature is maintained at 22-25 °C, greater selectivity for the linear product is observed. Upon heating, increasing amounts of branched product are obtained. Indeed, we found that any deviation from the published reaction conditions leads to increased formation of the undesired branched aldehyde. This is especially problematic when using longer-chain allylic alcohols ( $\geq 6$  carbons). To obtain acceptable conversion in a reasonable timeframe, gentle heating is necessary. However, the increased temperature also results in almost complete loss of selectivity (linear : branched  $\sim 1 : 1$ ). As an alternative, we found that delaying the onset of heating for 24 h results in an improved linear-to-branched ratio. Following this period, heating the reaction mixture to 50 °C for five additional days gives the alkene migrations time to equilibrate fully. Using delayed heating, the desired terminal adduct was formed in a 9 : 1 selectivity (Eq. 3-6). Unfortunately, all attempts to extend the tether length beyond six carbons were impractical, as a result of our inability to separate mixtures of regioisomeric aldehydes by either column chromatography or fractional recrystallization.



**Equation 3-6.** Kinetic vs. thermodynamic insertion of the alkene at room temperature.

The separation of the linear aldehydes from the branched isomers produced in the migratory Heck reaction is challenging in general. While these reactions are successful on multigram scale (Figure 3-1), it is not possible to remove the small amount of the branched isomer by flash column chromatography. Instead, iterative recrystallization (up to three times) proved to be the only method to give isomerically pure material, as identified by  $^1\text{H}$  and  $^{13}\text{C}$  NMR spectroscopy. The pure aldehydes, synthesized on > 1 gram scale, are stable solids that can be stored indefinitely at room temperature in the air with no decomposition.

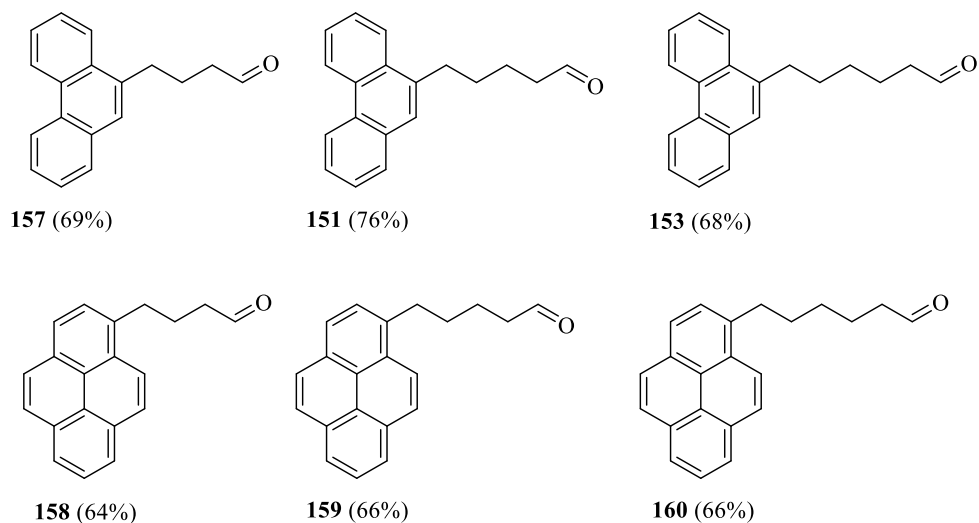
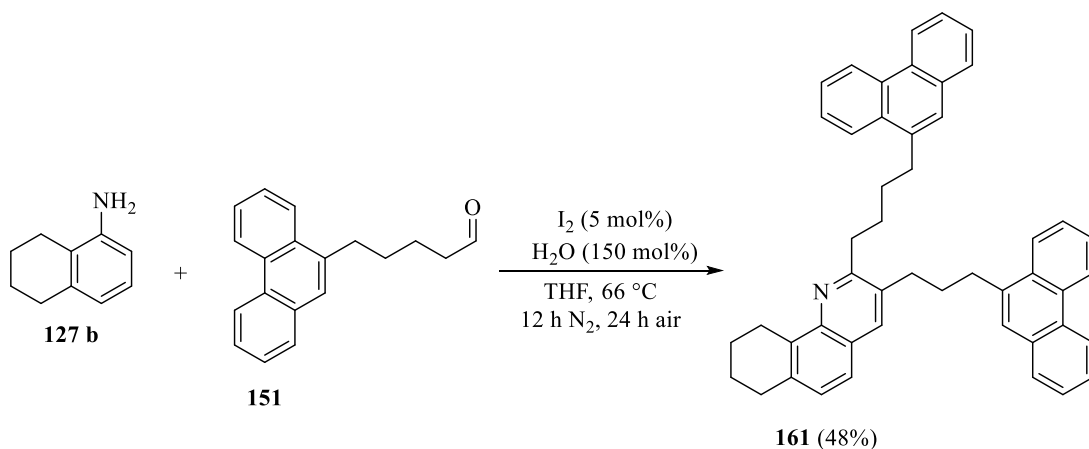


**Figure 3-1.** Synthesized PAH tethered alkyl-tethered  $\alpha,\omega$ -aryl aldehyde.

### 3.2. Initial optimization of the archipelago MCR reaction: an interim solution.

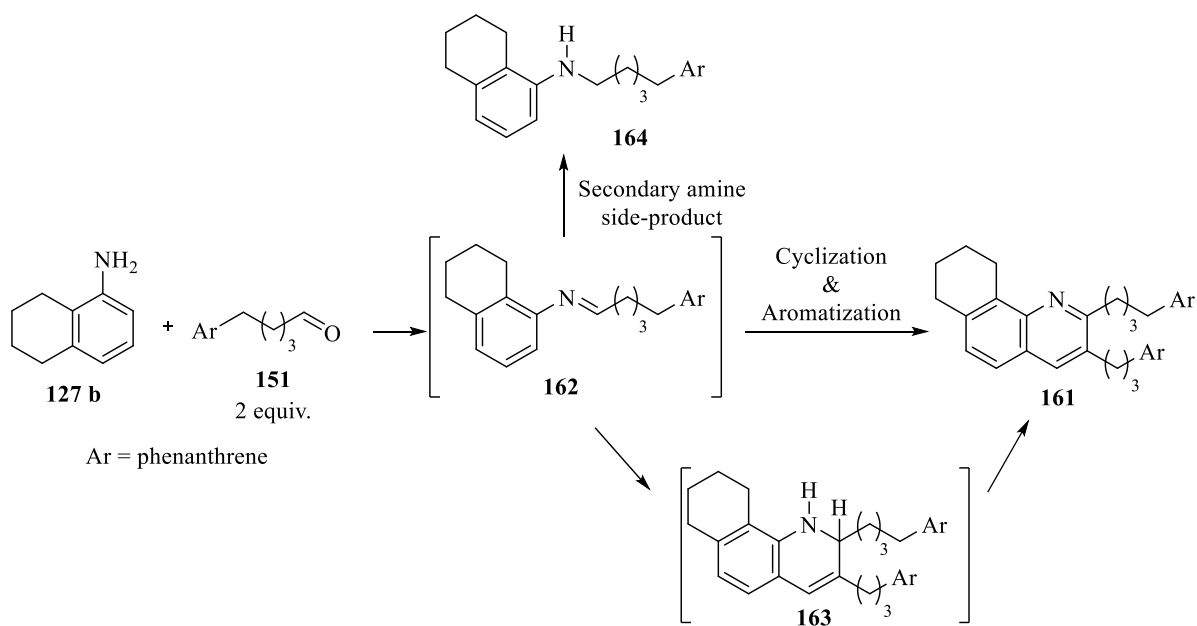
With the alkyl-tethered  $\alpha,\omega$ -aryl aldehydes in hand, we turned our attention to the synthesis of three-island archipelago-like model compounds. Using previously published conditions from our laboratory – catalytic iodine and water – the reaction of two equivalents of 5-(phenanthren-9-yl)pentanal and one equivalent of 5,6,7,8-tetrahydronaphthyl-1-amine, led to the formation of the three-island cycloadduct 161 in 48% isolated yield (Eq. 3-7).



**Equation 3-7.** Initial reaction conditions for the synthesis of 2-(4-(phenanthren-9-yl)butyl)-3-(3-(phenanthren-9-yl)propyl)-7,8,9,10-tetrahydrobenzo[*h*]quinoline.

This promising result indicated that the synthetic aldehydes are indeed compatible with the MCR methodology. However, the yield of the reaction was low, for three reasons: (i) competition from the formation of a secondary amine side-product (here, ~17%), (ii) incomplete cyclocondensation reaction, and (iii) unproductive loss of the aldehyde. Discussion of the latter is deferred to Chapter 4.

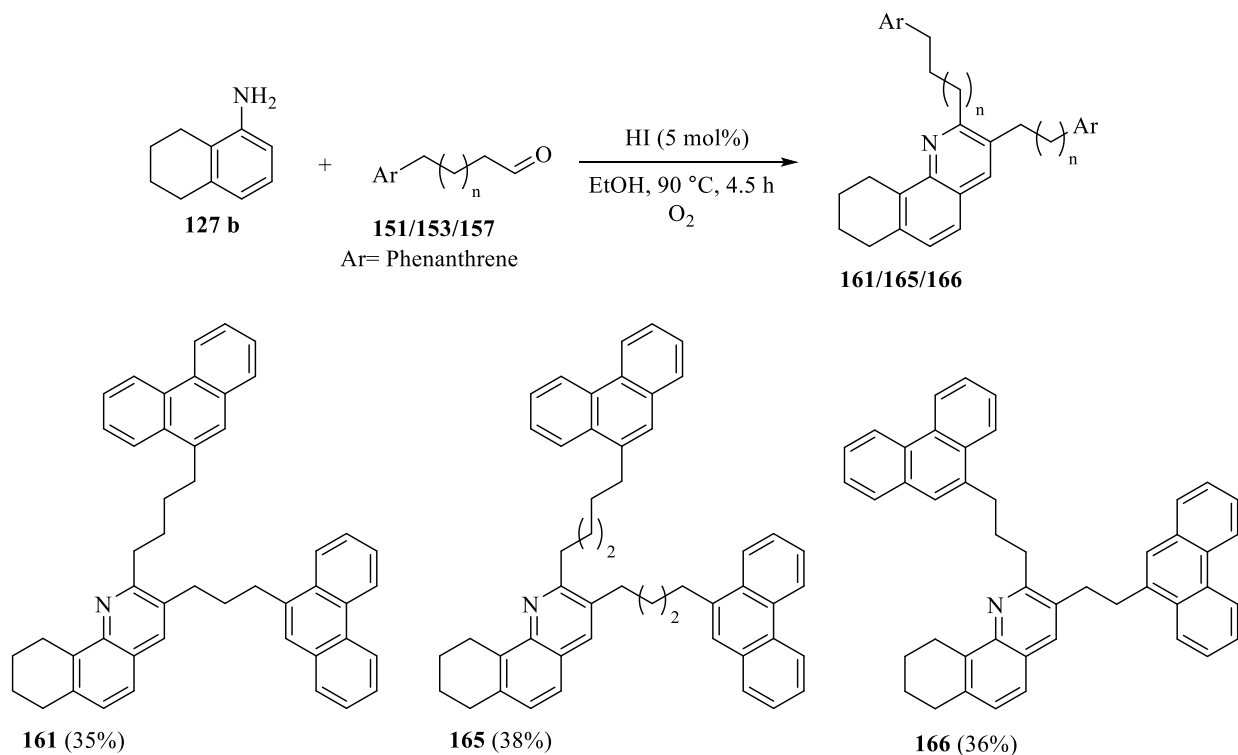
During the reaction, the *N*-alkylimine intermediate **162** undergoes hydride reduction to give the secondary amine, a consequence of insufficient oxidant in solution to mediate the aromatization of intermediate **163** (Scheme 3-6). Thus, addition of an external oxidant, such as pure oxygen, was expected to suppress imine reduction. In addition, we presumed that increasing the aldehyde enol concentration would increase the rate of cyclocondensation. The increased concentration of intermediate **163** in the presence of an effective external oxidant, should afford higher overall yields.



**Scheme 3-6.** Formation of product and side-product from the MCR reaction using two alkyl aldehydes.

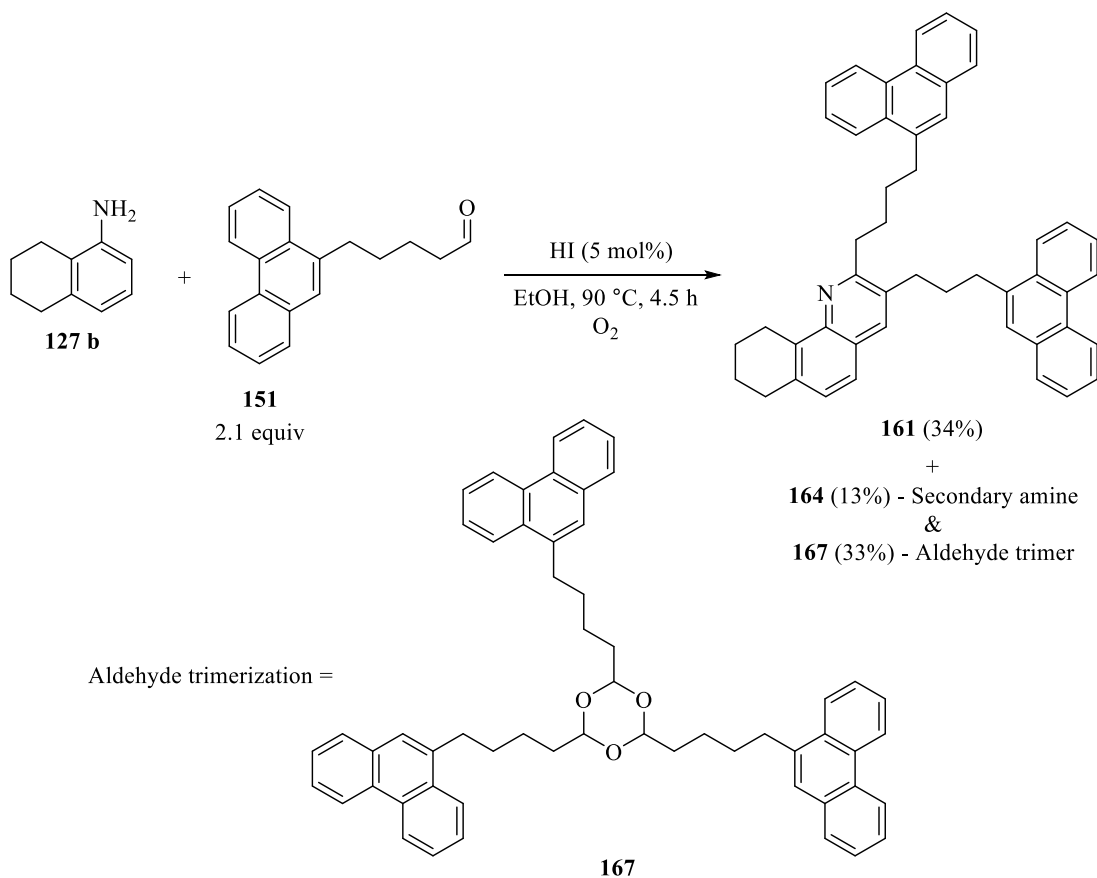
### 3.3. MCR optimization: testing solvent effects and oxidant concentration

The first solvent explored was ethanol, in the hope that a polar, protic medium would stabilize the enol tautomer of the aldehyde, increasing its steady-state concentration.<sup>[204,205]</sup> In addition, the catalyst of choice was HI (57%) rather than iodine, based on observations from our previously published work.<sup>[126]</sup> Using these reaction conditions, I synthesized a few quinoline-core archipelago compounds (Eq. 3-8) on one gram scale, regardless of yield, to supply compounds needed by our collaborators at JPEC. The yields, unfortunately, were low.



**Equation 3-8.** Quinoline-core archipelago compounds synthesized using catalytic HI in ethanol.

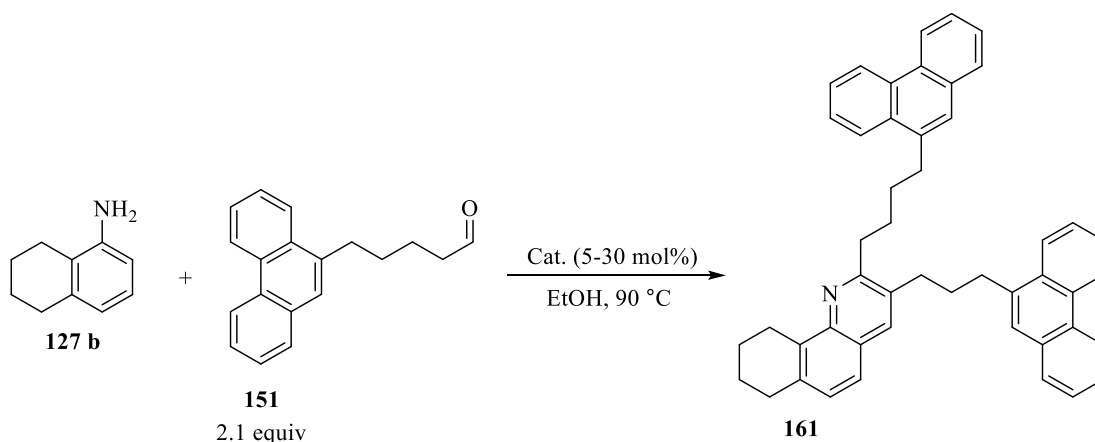
Under these reaction conditions, the formation of secondary amine was limited (~13% of the crude mixture). Unfortunately, however, the acidic reaction conditions induced competitive trimerization of the aldehyde, giving undesired 1,3,5-trioxane **167** (Eq. 3-9). The prevalence of this trimeric product, coupled with the low solubility of the starting materials in ethanol, led to the conclusion that a polar, protic medium must not be optimal for our purposes.



**Equation 3-9.** MCR using ethanol as solvent: competitive formation of the aldehyde cyclic trimer.

Before changing solvents, I briefly explored whether the low availability of oxidant in solution, resulting in slow oxidation of the intermediate, was a more significant problem. The results from varying oxidizing conditions and catalyst loadings are recorded in Table 3-1. Increasing the oxygen concentration by conducting the reaction in pure O<sub>2</sub> atmosphere (instead of air) allowed the catalyst loading to be lowered to achieve comparable conversion (compare entries 1 and 3). The reaction in pure oxygen can be run with as little as five mol% catalyst, but the reaction time must be lengthened significantly (entry 4). Following this reaction by TLC revealed complete consumption of aldehyde, although the yield of the quinoline was only 34%. All components of

the mixture were isolated and quantified, with the aldehyde trimerization **167** being most abundant (Eq. 3-9).



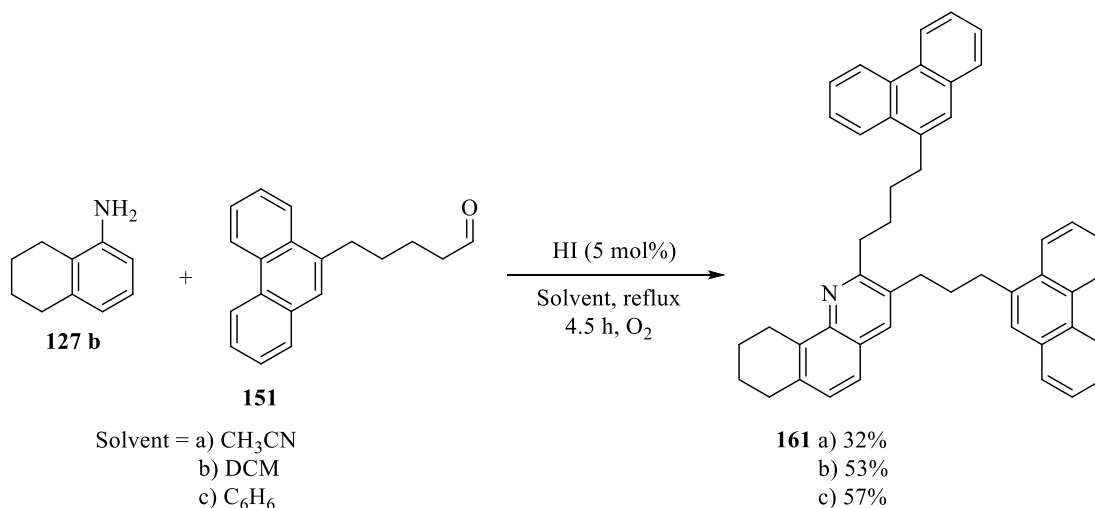
**Equation 3-10.** Reaction optimization investigating the affect of catalyst/oxygen concentration.

**Table 3-1.** Effects of catalyst concentration in the presence of variable O<sub>2</sub> atmosphere.

Entry	Catalyst	Time (h)	Oxidant	<sup>1</sup> H NMR Conversion (%) <sup>a</sup>
1	HI (30 mol%)	2.5	air	42 <sup>a</sup>
2	HI (30 mol%)	1.5	2 atm O <sub>2</sub>	35 <sup>a,c</sup>
3	HI (10 mol%)	2.5	O <sub>2</sub>	43 <sup>a,c</sup>
4	HI (5 mol%)	4.5	O <sub>2</sub>	34 <sup>b</sup>
5	I <sub>2</sub> (5 mol%)	1.5	2 atm O <sub>2</sub>	41 <sup>a,c</sup>

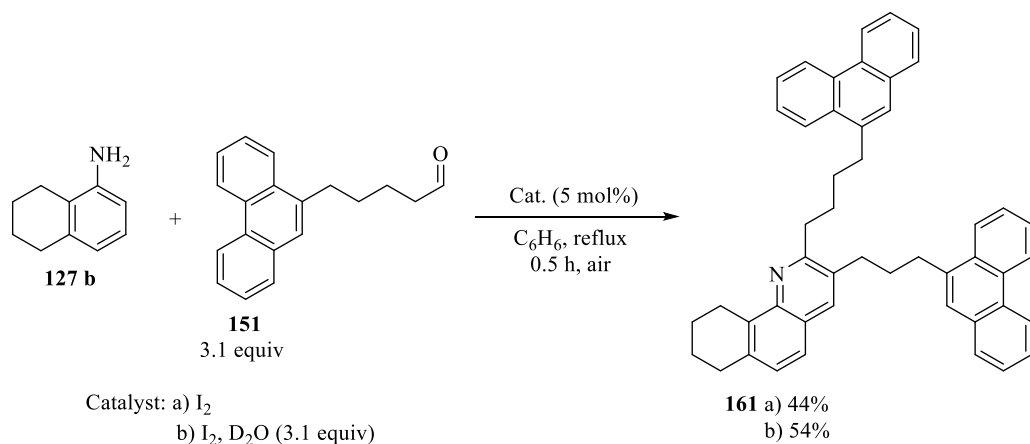
Reactions were conducted at reflux temperatures. <sup>a</sup>Yield based on <sup>1</sup>H NMR spectroscopy, quantified by using an internal standard of hexamethyldisiloxane. <sup>b</sup>Isolated yield. <sup>c</sup>Reactions requiring two atm O<sub>2</sub> were conducted in a sealed Fischer-Porter bottle. The pressurized reactions were conducted behind a blast shield as a precaution. The amount of secondary amine by-product was not quantified.

The persistence of the aldehyde trimerization product in the ethanolic reactions led us to abandon this solvent entirely. Several other solvents, along with other variations in catalyst loading and reaction time, were therefore explored to suppress the formation of this undesired product.



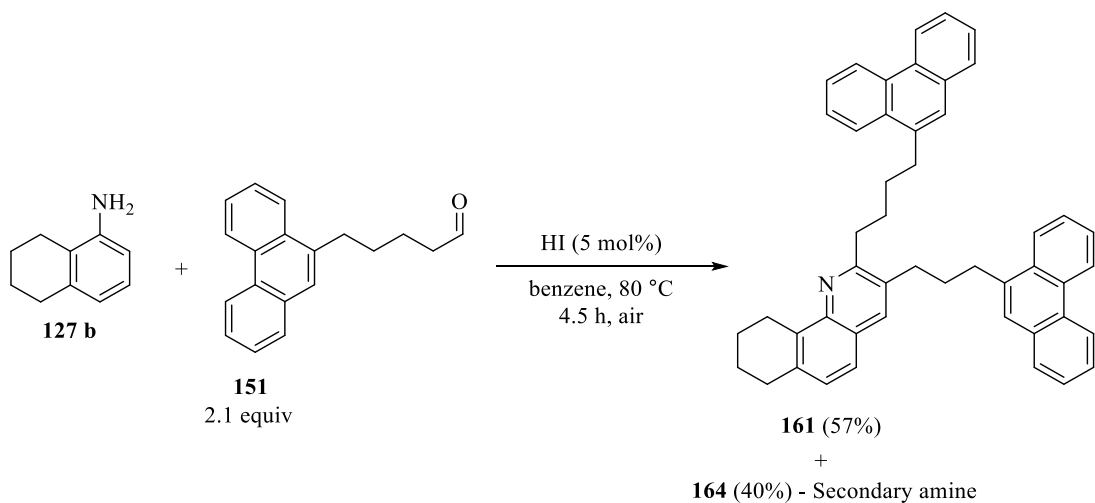
**Equation 3-11.** Screening MCR conditions as a function of solvent. Compound yields for the reactions using CH<sub>3</sub>CN and DCM were determined by <sup>1</sup>H NMR spectroscopy. The yield of the reaction using benzene was determined by isolation after purification by column chromatography.

Both dichloromethane and benzene proved to be better solvents (Eq. 3-11),<sup>[199]</sup> affording improved but moderate yields of the desired quinoline and, importantly, no aldehyde trimerization. Our focus turned to benzene for subsequent reactions, given the higher reflux temperature, which is beneficial. Furthermore, from preliminary reactions using I<sub>2</sub> as the catalyst in hot benzene, the reaction was complete after only 0.5 h (Eq. 3-12).



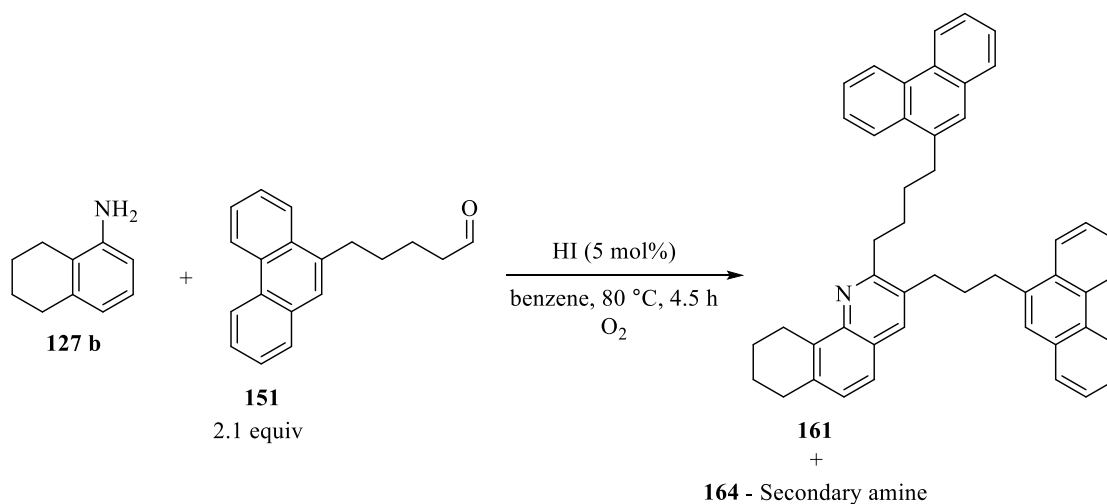
**Equation 3-12.** Investigating the MCR using catalytic I<sub>2</sub> with and without a D<sub>2</sub>O additive.

Unfortunately, the yields of both I<sub>2</sub> and I<sub>2</sub>/D<sub>2</sub>O reactions (Eq. 3-12) were low and the ratio of product to side-product was a disappointing 1 : 1. Conducting the reaction under air and using benzene as solvent, afforded the desired product in 44% yield. We suspected that an unfavourable keto-enol tautomerization rate in benzene may limit conversion, so a stoichiometric quantity of D<sub>2</sub>O was added in an attempt to stabilize the transient enol.<sup>[206,207]</sup> The resulting increase in yield (approx. 10%) confirmed this hypothesis, but even then, significant secondary amine was present (Eq. 3-12). I then decreased the amount of aldehyde from three to two equivalents and extended the reaction time (based on TLC progress). However, a significant amount of secondary amine (~40%) remains, significantly higher in comparison to reactions conducted in THF or EtOH (compare Eq. 3-7 and Eq. 3-8 with Eq. 3-13).



**Equation 3-13.** Quinoline synthesis using benzene as solvent. Amplified formation of secondary amine.

I therefore turned my attention to using pure oxygen, in the hopes that the rate of oxidation to the final quinoline would increase, resulting in a decrease of *N*-alkylimine (Eq. 3-14, Table 3-2).



**Equation 3-14.** MCR conditions used to screen for the effects of oxygen concentration.

**Table 3-2.** Effect of oxygen concentration on the MCR synthesis of quinolines.

Entry	Time (h)	Oxidant	<sup>1</sup> H NMR Conversion (%)	Yield of amine (%)
1	4.5	air	57	40
2	4.5	O <sub>2</sub>	59	40
3 <sup>a</sup>	4.5	2 atm O <sub>2</sub>	82	<sup>b</sup>
4 <sup>a</sup>	1.5	2 atm O <sub>2</sub>	74	<sup>b</sup>

All reactions were conducted in benzene at 85 °C using 5 mol% HI catalyst. <sup>a</sup>Reactions conducted in a sealed Fischer Porter bottle. The pressurized reactions, due to flammable solvent in the presence of oxygen, are conducted behind a blast shield as a precaution. Yields of secondary amine in entries 1 and 2 were determined by <sup>1</sup>H NMR spectroscopy. <sup>b</sup>The amount of secondary amine was reduced significantly, but not quantified. Conversions acquired by <sup>1</sup>H NMR, with an internal standard of hexamethyldisiloxane.

In the control reactions, switching from a static air headspace with rapid stirring (~20% O<sub>2</sub>) to sparging pure oxygen gas provided little benefit (Table 3-2, entry 2), suggesting that the solution was already oxygen-saturated under air alone. To our delight, however, pressurizing the reaction vessel to two atmospheres of oxygen (30 psig) improved conversion and partitioning dramatically (Table 3-2, entry 3). After heating only 1.5 h under oxygen pressure, the reaction is 74 % complete (Table 3-2, entry 4). While this result was encouraging, heating under pressurized oxygen is neither safe nor practical for large-scale synthesis.

### 3.4. Anisole as MCR solvent. An effective *interim* MCR optimization

At this point, we found 4-ethylaniline to be a better substrate for optimization studies: 4-ethylaniline is less expensive and less air-sensitive than 5,6,7,8-tetrahydronaphthyl-*l*-amine. In addition, the MCR adduct is statistically favored for this aniline; cyclization can occur at either the 2- or 6-positions (Figure 3-2).

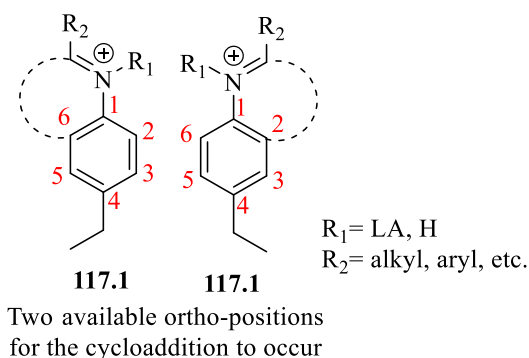


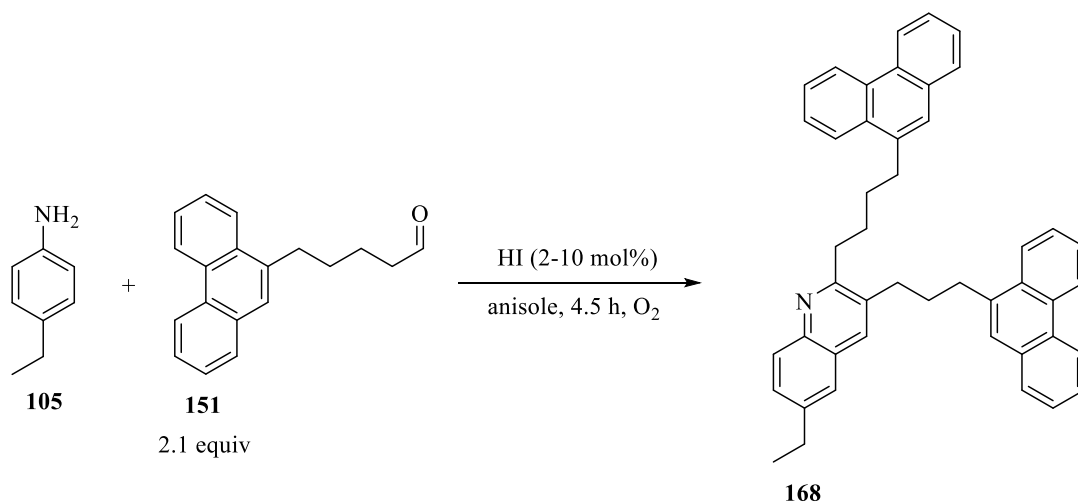
**Figure 3-2.** Two available ortho-positions for the cyclization.

To maximize the efficiency of the oxidative aromatization, we also adopted an aromatic solvent that effectively increases the concentration of soluble oxygen, yet still dissolves our substrates. Anisole proved to be ideal, supporting higher concentrations of dissolved oxygen relative to benzene<sup>[208–210]</sup> and easily dissolving the functionalized aldehydes. In this solvent, the use of oxygen at one atmosphere becomes highly effective, avoiding an oxygen overpressure.

An added benefit to using anisole is its high boiling point, allowing the reaction temperature to be increased. Interestingly, in anisole, the reaction requires higher temperature to provide complete conversion. At 100 °C, the conversion is underwhelming (Table 3-3, entry 1). However, by heating the reaction mixture to 130 °C, the yield increases to 77% after 4.5 h (Table 3-3, entry 2).

The effects of catalyst concentration were then investigated. Five mol% aqueous HI proved optimal;<sup>[126]</sup> decreasing the acid concentration to two mol% led to a decrease in conversion from 77% to 67% (Table 3-3, entries 2 and 3). Increasing the catalyst concentration from five mol% to 10 mol% had a similarly deleterious effect (entry 4), with the conversion falling to 65%. We attribute the latter to excess water concentration in the reaction medium, a sensitivity we previously

identified.<sup>[126]</sup> However, this result remains puzzling: the reaction time was identical, yet only a minimal drop in conversion was observed.



**Equation 3-15.** General MCR screening for optimal reaction conditions using 4-ethylaniline as the aniline substrate.

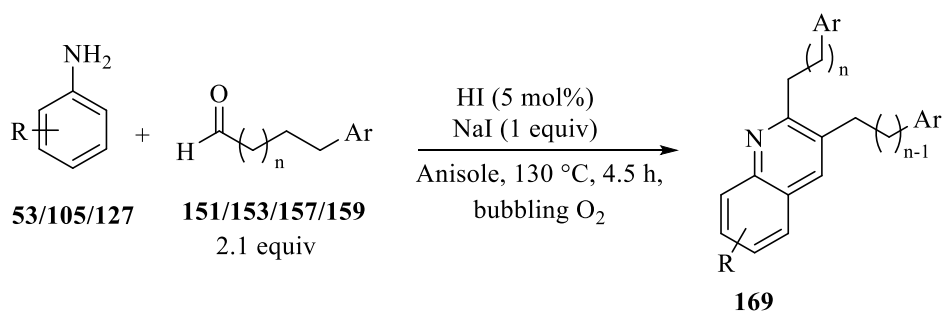
**Table 3-3.** Catalyst concentration, temperature, and additive screening for MCR optimization.

Entry	Catalyst	Temp. (°C)	Additive	<sup>1</sup> H NMR Conversion (%)
1	HI (5 mol%)	100	–	43
2	HI (5 mol%)	130	–	77
3	HI (2 mol%)	130	–	67
4	HI (10 mol%)	130	–	65
5	HI (5 mol%)	130	NaI (1 equiv)	> 95
6	HI (5 mol%)	130	NaI (2 equiv)	51

Reactions are run in anisole for 4.5 h under a constant, rapid bubbling of oxygen, unless otherwise stated. Note, higher temperatures (up to 160 °C which is the boiling point of anisole) may well improve the yield but excessive heating of organic solvents in pure oxygen gas is ill-advised and the reaction temperature was limited to 130 °C. The amount of secondary amine was not quantified during these control reactions. Conversions acquired by <sup>1</sup>H NMR, with an internal standard of hexamethyldisiloxane.

Following the catalyst experiments, we considered the potential importance of *iodide anion* concentration, in combination with acid concentration, on product formation. The addition of one molar equivalent of partially-soluble sodium iodide to the reaction medium surprisingly resulted in a nearly quantitative conversion of the quinoline (Table 3-3, entry 5). However, upon addition of a second equivalent of sodium iodide, conversion is strongly inhibited. Intrigued, a deeper investigation into the causes and effects of iodide concentration was conducted, as presented in Chapter 4.

Following this initial optimization, a limited investigation of the scope of the reaction was conducted to survey the synthetic generality of our reaction. In this study, we varied the aldehyde tether length and sampled several substituted anilines. For these reactions, we used identical conditions: NaI (1 equiv), O<sub>2</sub> sparge, five mol% HI (57%), at 130 °C for 4.5 h (Eq. 3-16). Importantly, the series of synthetic compounds produced in this investigation also served the immediate needs of our collaborators.



**Equation 3-16.** Reaction conditions for the generalized synthesis of three-island archipelago compounds.

### 3.5. MCR synthesis of archipelago model asphaltene compounds – scope and limitations

The range of substrates selected represents structural features and/or compositional characteristics observed in authentic asphaltenes. The most important aspect for our model compounds is the tolerance of diverse aniline substitution. Specifically, we investigated methyl and ethyl substituents positioned in patterns representative of the short terminal alkyl chains identified in all authentic asphaltenes. Furthermore, extended saturated and unsaturated anilines were also investigated, to increase the size of the quinoline-core and to provide contrast to simple methyl/ethyl substitutions. Some of the substrates were selected to challenge the MCR process, as determined from prior experimentation. In addition, electronic effects were assessed, using electron-withdrawing and electron-donating substituents that range well outside the functionality found in authentic asphaltenes, but good indicators of generality. The scope also encompassed tethered aldehydes ranging from 4-6 carbons, to examine the impact of positioning the aromatic islands at different distances from the reactive aldehyde. One final variation was to include pyrene as the terminal island motif.

Variations in aniline substitution proved illuminating (Figure 3-3). Surprisingly, aniline itself does not afford a high yield, despite the similarity to 4-ethylaniline. This suggests that even remote substituents are important. The results from the three dimethylanilines demonstrate that alkyl substituents in the ortho- and meta-positions (**171**, **172**, and **173**) also have a negative impact on the yield of the MCR.

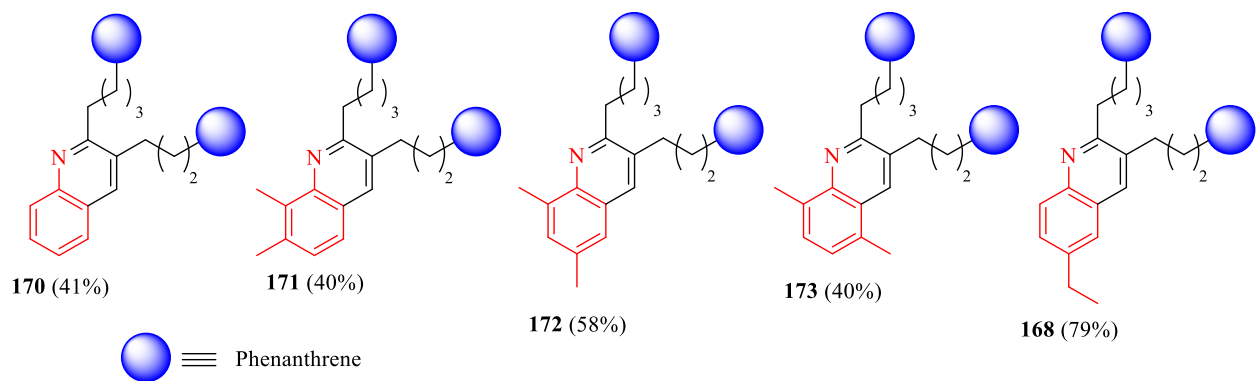


**Figure 3-3.** Synthesized asphaltene-like quinoline model compounds incorporating various methyl and ethyl substituents.

Some decrease in yield was anticipated, as an ortho-substituent eliminates one of the potential positions for cyclization, but the significant difference was unexpected (Figure 3-4, compounds **117.1** vs. **117.2**).

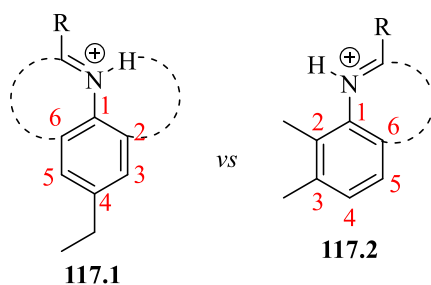


**Figure 3-4.** Ortho-positions available for cyclization is limited due to substitution.

The contrast in yields between **172** and **171/173** (Figure 3-3) suggests that a substituent in a meta-position has a significant influence on the effectiveness of the cyclocondensation, possibly changing the mechanism of the process from concerted asynchronous to stepwise. To prove this hypothesis, extensive mechanistic studies – or a computational investigation – are required. But given the underwhelming results from simple aniline derivatives, we became increasingly concerned with the narrow scope of the reaction.

An expanded range of aniline substrate was thus investigated. Fused bicyclic anilines (Figure 3-5, **161**, **165**, **166**, and **175**) provided marginally better yields compared to 2,3-dimethylaniline **171**. The series of 5,6,7,8-tetrahydronaphthyl-1-amine derivatives **161**, **165**, and **166** did show that the tether length is unimportant, giving no significant changes in yield. Interestingly, the size of the saturated ring does not seem to influence the reaction (**175**) but extended aromatic amines (**174** and **176**) gives significantly lower yields.

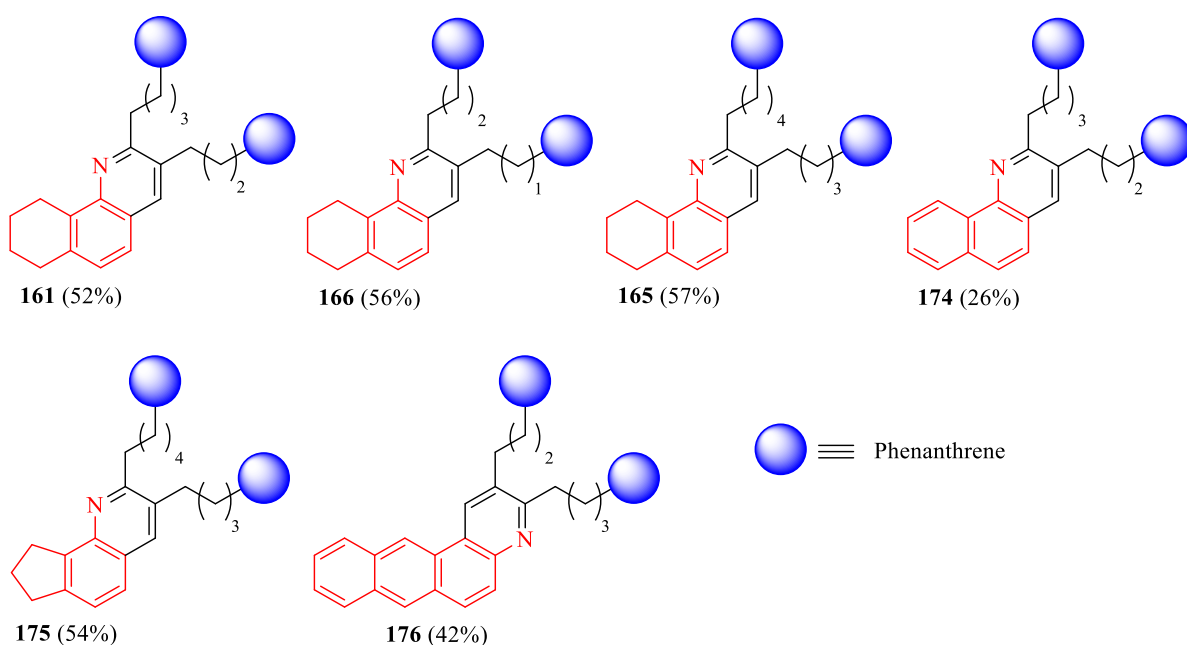


**Figure 3-5.** Extended saturated and unsaturated synthesized quinoline-core asphaltene-like compounds.

To assess substituent electronic effects, a few *para*-substituted electron-donating and electron-withdrawing groups were studied (Figure 3-6). The yield of the reaction of electron-deficient 4-bromoaniline **178** was quite low in comparison to 4-ethylaniline **168**. This decline in yield may be associated with a decrease in nitrogen basicity, which inhibits the rate of imine protonation and nucleophilic addition of the enol. On the other hand, the electron-donating substituent in *p*-

anisidine **177** returns a moderate yield. This result was unexpected: the methoxy group increases the basicity of the nitrogen, promoting protonation and imine formation. Furthermore, in the case of *N,N'*-dimethyl-*p*-phenylenediamine **179** the overall yield suffers exceptionally. This decrease is surprising, because we believed that increasing the donation of the substituent would enhance the reaction. Unfortunately, the opposite occurred, and the reaction suffered. These results strongly suggest that there remain uncontrolled variables in the cyclocondensation reaction, beyond simple substitution effects.

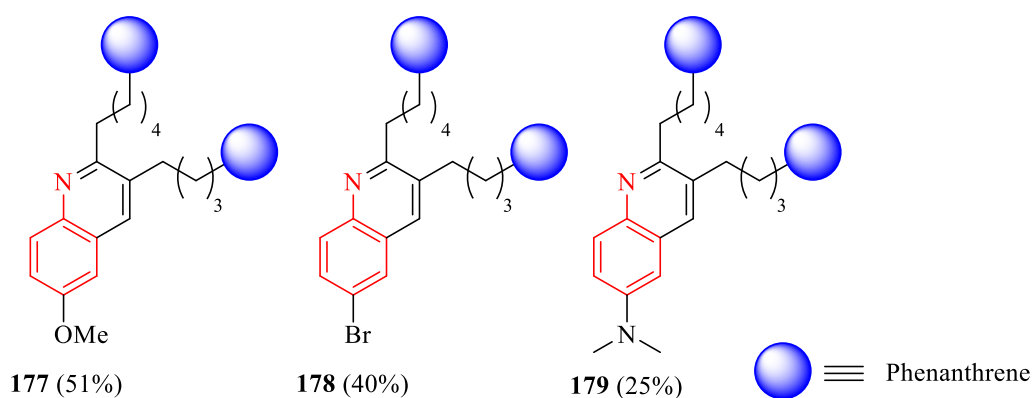


**Figure 3-6.** Testing the generality of the MCR by introducing electron donating/withdrawing substituents. The reaction scale for archipelago synthesis incorporating *p*-anisidine **177** and 4-bromoaniline **178** was 0.5 g and for *N,N'*-dimethyl-*p*-phenylenediamine **179**, 0.16 g. Each reaction was conducted just one time, as an initial test for generality.

To control for the effects of changing terminal islands, 4-ethylaniline was also condensed with 5-(pyren-1-yl) pentanal, resulting in notably lower conversion and reduced yield (Figure 3-7, **168** and **180**). One hypothesis is that the electron deficiency in the pyrene ring affects the reactivity of the imine or enolized aldehyde, slowing the MCR, assuming that step occurs in advance of, or is, the turnover-limiting step. It bears noting that the yields fall within the typical range of other



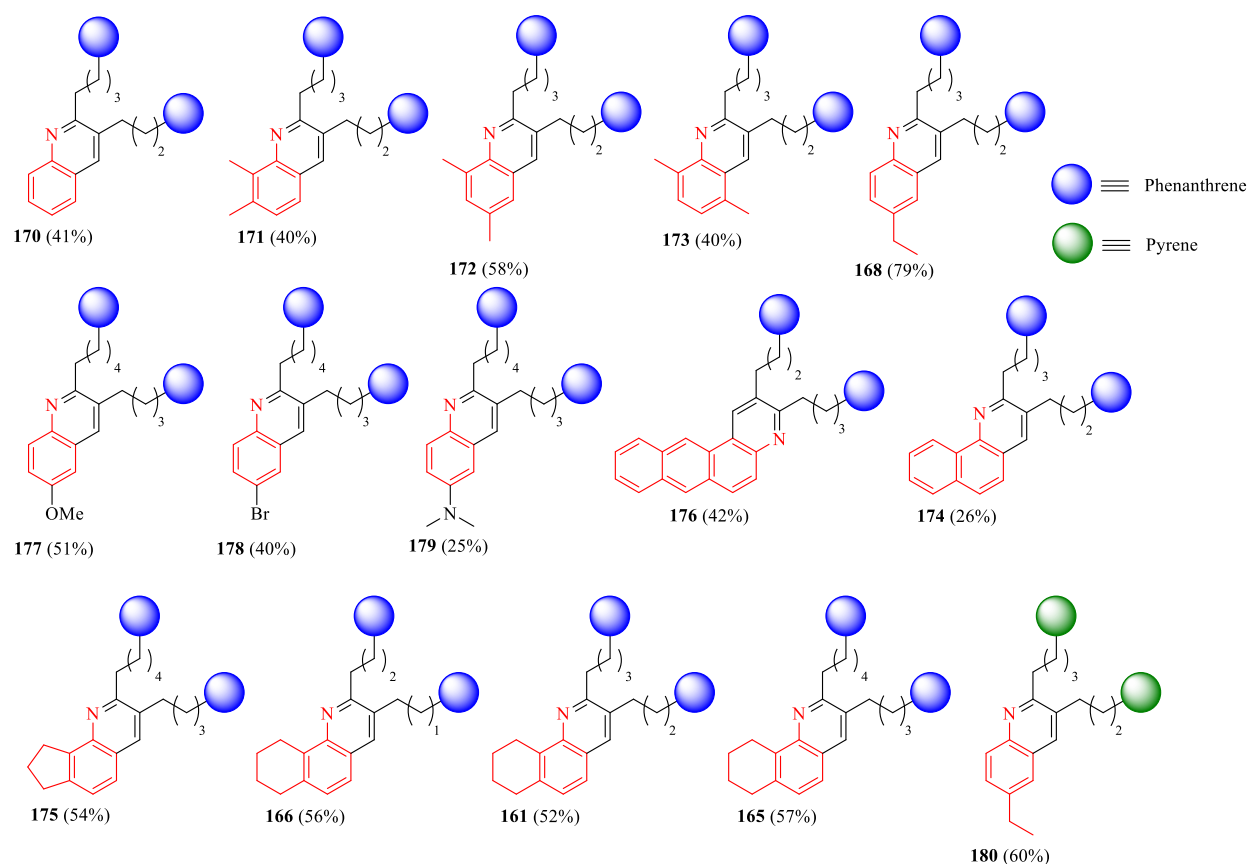


**Figure 3-8.** All quinoline-core compounds synthesized by our initial optimal conditions.

### 3.6. An application of asphaltene model quinolines: Hansen solubility parameters

The purified model compounds listed in Figure 3-8 (above) were shipped to our JPEC (Japan Petroleum Energy Center) collaborators for analysis. Our collaborators assessed the compound's solubility characteristics using Hansen solubility parameters, to correlate with those of authentic bitumen samples. For any meaningful interpretation of the results, a brief précis on Hansen solubility parameters is necessary.

The asphaltene fraction of bitumen is typically defined based on solubility (see earlier discussion on the SARA method) and therefore, it is important to engineers to understand the solution behaviour of both the authentic material and the synthesized model compounds. The most widely

used method for accurately evaluating solubility involves determining the Hansen solubility parameters (HSP).<sup>[211]</sup> These parameters have been typically used to study authentic asphaltenes,<sup>[212–215]</sup> but Yamamoto and co-workers published a study using synthetic asphaltene model compounds, including mine, in order to make comparisons with bitumen-derived material.<sup>[216]</sup>

Hansen solubility parameters serve fundamentally as a predictive tool for assessing whether or not one material will dissolve in another. Hansen solubility parameters are an extension of the older Hildebrand solubility parameter  $\delta_t = (E/V)^{1/2}$ , where E, cohesive energy, is measured in J/mol and V, molar volume, is measured in cm<sup>3</sup>/mol.<sup>[217]</sup> However, in the Hansen solubility parameters, the equation separates the cohesive energy into dispersion forces ( $E_d$ ), dipolar intermolecular forces ( $E_p$ ), and hydrogen bonding ( $E_h$ ) (Eq. 3-17), accounting implicitly for steric and electronic factors.<sup>[211,216]</sup>

$$\begin{aligned}
 E &= E_d + E_p + E_h \\
 \delta_d &= (E_d/V)^{1/2}, \delta_p = (E_p/V)^{1/2}, \delta_h = (E_h/V)^{1/2} \\
 \delta_t^2 &= \delta_d^2 + \delta_p^2 + \delta_h^2 \\
 R_a &= [4(\delta_{d1} - \delta_{d2})^2 + (\delta_{p1} - \delta_{p2})^2 + (\delta_{h1} - \delta_{h2})^2]
 \end{aligned}$$

**Equation 3-17.** Mathematical equations for Hansen solubility parameters.

The affinity of two molecules to form solutions is calculated from the parameters ( $R_a$  (MPa<sup>1/2</sup>)) and will determine the likelihood the substances will dissolve. If the value of the  $R_a$  is small, the result indicates that the forces between the two molecules are similar and should be miscible. To determine if the molecules in question are within range, the parameters are plotted on a three-dimensional graph and a spherical boundary can be drawn to evaluate all solvents; this is termed

the interaction radius ( $R_0$ ). Once  $R_a$  and  $R_0$  are determined, the relative energy difference can be calculated ( $RED = R_a/R_0$ ). If the RED is  $< 1$ , the molecules will dissolve, if RED = 1 only partial solubility is anticipated, and when RED is  $\geq 1$  no solubility is expected.<sup>[211]</sup> Therefore, using these equations a series of model compounds are interrogated to determine the HSPs and compare the results to authentic material.

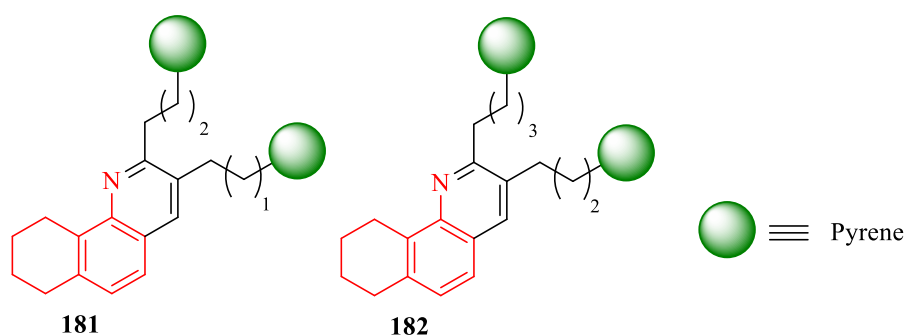


**Figure 3-9.** Quinoline-core archipelago model compound studied using HSPs.

The solution behaviour of compound **183** (Figure 3-9), which I synthesized, has been evaluated using HSP. In a 2018 publication, Yamamoto used both experimental and modeling techniques to investigate the behaviour of archipelago model **183** along with several other archipelago-like compounds, such as pyrene-based models, steroidal naphthoquinolines, and continental structures such as hexabenzocoronene and nickel porphyrin-derived compounds.<sup>[216]</sup> Using a number of different of organic solvents, the experimental results indicate that there is a large variation in the types of solvents that can be used, with no single solvent being universal for all compounds. Critically, an accurate solubility prediction based solely on chemical structure (functional groups, heteroatoms, ring sizes, etc.) is not easily achieved; however, when the prediction is combined with comparable experimental HSP analysis, solubility characteristics can be successfully determined. In addition, the interaction radius  $R_0$  varies significantly with minimal structural

differences, such as which heteroatom is incorporated and where in the molecule it is located. Overall, the HSP and  $R_0$  values were determined for the series of model compounds with a range from:  $\delta_d = 18.7\text{--}21.0 \text{ MPa}^{1/2}$ ,  $\delta_p = 2.7\text{--}8.1 \text{ MPa}^{1/2}$ ,  $\delta_h = 2.2\text{--}6.5 \text{ MPa}^{1/2}$ , and  $R_0 = 3.5\text{--}8.5 \text{ MPa}^{1/2}$ .<sup>[216]</sup> Though this data falls within the range of the authentic material, over-interpretation of the results must be restrained (Canadian oil sand bitumen is 19, 4, 4  $\text{MPa}^{1/2}$ ).<sup>[212–215]</sup> This method, however, will be beneficial for the design of new targets and for exploring mixed model systems.

In addition to HSP investigation, our model compounds will be used to develop and validate other techniques for analyzing asphaltenes. In particular, much work will be focused on the mass spectrometry techniques used by our collaborators at JPEC. Specifically, the fragmentation patterns of our model compounds may help identify molecules in authentic asphaltenes with similar substructures. Furthermore, isothermal titration calorimetry measurements of model compounds will provide a useful reference point for comparing data obtained from authentic material. In addition, diffusion ordered spectroscopy (DOSY) can be used to study intermolecular interactions, revealing the concentrations needed for the onset of aggregation, and possibly the size of these aggregates. This data would then become a reference point for interpreting the DOSY spectra of asphaltene samples. Finally, subjecting our model compounds to AFM/STM measurements will be invaluable for developing, refining and validating techniques for imaging archipelago-type compounds in authentic asphaltene samples.

## **Conclusion**

With various archipelago model compounds assembled, we recognized that the reaction was far from general enough to move the field forward. For this reason, we needed to revisit, again, our optimization process, to understand what was neglected during our initial investigations. Hence,

we decided to thoroughly interrogate catalyst systems and reaction mechanisms, probing each of the problems identified in this chapter.

### **Experimental Section**

All manipulations of air-sensitive materials were performed in a well-maintained Braun dry box under an atmosphere of prepurified nitrogen or, on larger scale, using standard Schlenk techniques. Dioxane was distilled from sodium under nitrogen. THF was distilled from sodium/benzophenone ketyl, also under nitrogen. Sodium iodide (NaI) was purchased and dried in a vacuum oven for two days and stored in the dry box. Freshly purchased copper iodide needed no further purification; however, if stored on a shelf, purification was performed using a literature procedure.<sup>[218]</sup> All other solvents and reagents were used without further purification. TLC analyses were performed using 0.5 mm analytical TLC plates from Macherey-Nagel (ALUGRAM<sup>®</sup> SIL G/UV<sub>254</sub>) and visualized by using UV-light of 254 nm and/or 366 nm. For flash column chromatography, silica gel 60 M (0.040–0.063 mm) from Macherey-Nagel was used.

NMR spectra were recorded on Agilent/Varian instruments (400, 500 and 700 MHz for <sup>1</sup>H NMR and 101, 126 and 176 MHz for <sup>13</sup>C NMR) at ambient temperature. Chemical shifts were referenced to residual solvent protium peaks ( $\delta$  in parts per million (ppm) CHCl<sub>3</sub> <sup>1</sup>H: 7.26 ppm; <sup>13</sup>C: 77.0 ppm). Coupling constants were assigned as observed. <sup>1</sup>H NMR coupling constants are rounded to nearest 1.0 Hz and <sup>13</sup>C NMR values are reported to the nearest 0.1 Hz.

High-resolution mass spectra (HRMS) were recorded on several instruments (Agilent Technologies 6220 TOF, Bruker 9.4T Apex-Qe FTICR, or Kratos Analytical MS-50G) and acquired by the department analytical technology staff. Elemental analyses (C, H, N) of purified

compounds were obtained by the Department of Chemistry Instrumentation Laboratory, supervised by Mr. Wayne Moffat, using a Thermo Carlo Erba EA1108 or ThermoScientific Flash 2000 analyzer.

Most of the quinoline compounds prepared by this method do not pass elemental analysis due to low values for carbon content. Multiple cases were run for reproducibility; however, the results are self-consistent. This is not uncommon for compounds incorporating adjacent quaternary carbons, which do not completely combust.<sup>[219–222]</sup> To rectify this issue, the instrument requires a continuous oxygen flow to ensure complete combustion.

The <sup>1</sup>H NMR spectra for the aldehydes and quinoline-based compounds have signals in the aliphatic region that show a splitting pattern that appears as an ordinary triplet or overlapping doublet of doublets. However, the resonance arises from second-order coupling; at this field strength, the complex signal is deceptively simple.<sup>[223]</sup> Thus, the symbol  $J_{app}$  is used to designate the appearance of second order systems seen in the spectrum data below.

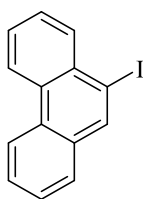
For aldehyde synthesis, I performed initial reactions and determined reaction conditions and purification methods. However, I was assisted during the scale-up process by two (then) undergraduate co-workers, Jose F. Rodriguez and Mark Aloisio.

Compound **181** was initially made by Jose F. Rodriguez, while working as a C403 student under my supervision. However, I repeated the reaction to obtain the purified product in order to satisfy the request made by JPEC.

### 3.7. General synthetic procedure for 9-iodophenanthrene and 1-iodopyrene<sup>[203]</sup>

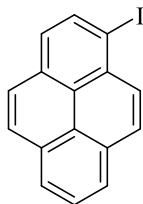
In the presence of purified copper (I) iodide (5 mol%), and dry sodium iodide (2 equiv), 9-bromophenanthrene or 1-bromopyrene, were added into a 100 mL three-neck round-bottom flask, equipped with a reflux condenser, placed under inert atmosphere, and diluted with dioxane. To this mixture, *N, N'*-dimethylethylenediamine (10 mol%) was added and the solution was heated to 120 °C (bath temperature) for 48 h. The reaction mixture was cooled to rt, after which excess ammonium hydroxide (30% aq) was added. The resulting blue solution was poured into water and extracted using DCM. The organic layer was separated, washed with saturated brine, dried over Na<sub>2</sub>SO<sub>4</sub>, filtered, and the solvent was removed under reduced pressure. The solid was dissolved in the minimal amount of DCM, then the solution was filtered through silica gel and the solvent was removed under reduced pressure.

#### 9-Iodophenanthrene (148).



The general procedure was used, 9-bromophenanthrene (10.0 g, 39.0 mmol), purified copper (I) iodide (0.37 g, 1.9 mmol), dry sodium iodide (11.7 g, 77.8 mmol), dioxane (40 mL), and *N, N'*-dimethylethylenediamine (0.42 mL, 3.9 mmol) was heated to 120 °C (bath temperature) for 48 h. The resulting product was an off-white solid to yield 11.1 g (96%): spectroscopic data is identical to previously published work.<sup>[224]</sup>

## 1-Iodopyrene (150).

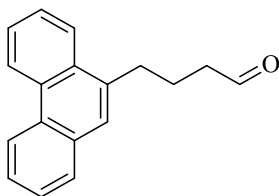


The general procedure was used, 1-bromopyrene (10.0 g, 36.0 mmol), purified copper (I) iodide (0.34 g, 1.8 mmol), dry sodium iodide (10.7 g, 71.1 mmol), dioxane (40 mL), and *N, N'*-dimethylethylenediamine (0.38 mL, 3.6 mmol) was added and the solution was heated 110 °C (bath temperature) for 48 h. The resulting product was an off white solid to yield 11.5 g (98%): spectroscopic data is identical to previously published work.<sup>[224]</sup>

### 3.8. General synthetic procedure of alkyl-tethered $\alpha,\omega$ -aryl aldehyde<sup>[200]</sup>

A mixture of aromatic iodide (1 equiv), palladium acetate (Pd(OAc)<sub>2</sub>) (3 mol%), tetra-*n*-butylammonium chloride (TBACl) (2 equiv), lithium chloride (LiCl) (1 equiv), and lithium acetate (LiOAc) (2.5 equiv) was added to a 3-neck round-bottom flask under inert atmosphere and diluted in dry, degassed dimethylformamide (DMF). To the stirred suspension, the alkenyl alcohol (1 equiv) was added and the solution was stirred for 4 – 6 days (required heat and time depend on the length of the alkenyl alcohol). The reaction was quenched with deionized water and washed with ethyl acetate. The organic layer was separated, washed with saturated brine, dried over Na<sub>2</sub>SO<sub>4</sub>, filtered, and the solvent was removed under reduced pressure. The crude mixture was passed through a silica gel column of hexanes and ethyl acetate (85:15). The solvent was removed under reduced pressure, and the resulting solid was recrystallized. The recrystallization was repeated with the filtrate to maximize the yield.

**4-(Phenanthren-9-yl) butanal (157).**



The general procedure was used, with 9-iodophenanthrene (1.0 g, 3.3 mmol), Pd(OAc)<sub>2</sub> (0.022 g, 0.099 mmol), TBACl (1.83 g, 6.58 mmol), LiCl (0.14 g, 3.3 mmol), LiOAc (0.54 g, 8.2 mmol), dry degassed DMF (8 mL), and 3-buten-1-ol (0.28 mL, 3.3 mmol) was stirred at rt for 4 days. The resulting orange solid was recrystallized in hot ethyl acetate layered with hot hexanes. The reaction afforded an orange solid 0.56 g (69%).

**IR (FTIR):** 3104 (w), 3062 (w), 3031 (w), 2935 (m), 2893 (m), 2869 (m), 2816 (m), 2727 (m), 1718 (s)

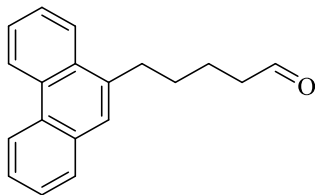
**<sup>1</sup>H NMR** (CDCl<sub>3</sub>, 500 MHz): δ 9.84 (s, 1H), 8.78 – 8.76 (m, 1H), 8.69 (d, *J* = 8.0 Hz, 1H), 8.16 – 8.14 (m, 1H), 7.87 – 7.85 (m, 1H), 7.70 – δ 7.60 (m, 5H), 3.19 (apparent dd, second order coupling, *J*<sub>app</sub> = 8.0, 7.0 Hz, 2H), 2.61 (td, *J* = 7.0, 1.0 Hz, 2H), 2.20 (quint, *J* = 7.0 Hz, 2H)

**<sup>13</sup>C NMR** (CDCl<sub>3</sub>, 126 MHz): δ 202.2, 135.4, 131.7, 131.0, 130.8, 129.8, 128.1, 126.7, 126.7, 126.5, 126.3, 126.1, 124.3, 123.3, 122.5, 43.5, 32.6, 22.4

**HRMS** (ESI) exact mass *m/z* calculated for C<sub>18</sub>H<sub>16</sub>O (M<sup>+</sup>) is 248.1201, found 248.1198

**EA anal.** calcd for C<sub>18</sub>H<sub>16</sub>O: C, 87.06 %; H, 6.49 %; O, 6.44 %. Found: C, 86.86 %; H, 6.54 %; O, 6.59 %. Repeat found: C, 87.07 %; H, 6.56 %; O, 6.37 %

**5-(Phenanthren-9-yl) pentanal (151).**



The general procedure was used, with 9-iodophenanthrene (3.00 g, 9.86 mmol), Pd(OAc)<sub>2</sub> (66.4 mg, 0.296 mmol), TBACl (5.48 g, 19.7 mmol), LiCl (0.42 g, 9.9 mmol), LiOAc (1.63 g, 24.7 mmol), dry and degassed DMF (21 mL), and 4-penten-1-ol (1.02 mL, 9.86 mmol) was stirred at rt for 4 days. The resulting orange solid was recrystallized in hot ethyl acetate layered with hot hexanes. The reaction afforded an orange solid 1.98 g (76%).

**IR (FTIR):** 3104 (w), 3077 (m), 3031 (w), 2928 (s), 2885 (m), 2862 (m), 2822 (m) and 2722 (m), 1718 (s)

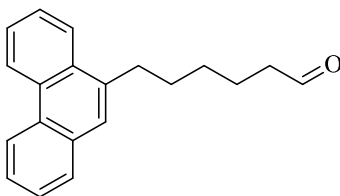
**<sup>1</sup>H NMR** (CDCl<sub>3</sub>, 500 MHz): δ 9.80 (t, *J* = 2.0 Hz, 1H), 8.78 – 8.76 (m, 1H), 8.69 (d, *J* = 8.0 Hz, 1H), 8.14 – 8.10 (m, 1H), 7.87 – 7.85 (m, 1H), 7.71 – δ 7.59 (m, 5H), 3.17 (apparent dd, second order coupling, *J*<sub>app</sub> = 8.0, 7.0 Hz, 2H), 2.52 (td, *J* = 7.0, 2.0 Hz, 2H), 1.91 – 1.82 (m, 4H)

**<sup>13</sup>C NMR** (CDCl<sub>3</sub>, 126 MHz): δ 202.4, 136.0, 131.8, 131.1, 130.7, 129.7, 128.0, 126.6, 126.5, 126.2, 126.1, 126.0, 124.3, 123.3, 122.4, 43.8, 32.2, 29.6, 22.0

**HRMS** (ESI) exact mass *m/z* calculated for C<sub>19</sub>H<sub>18</sub>O (M<sup>+</sup>) is 262.1358, found 262.1354

**EA anal.** calcd for C<sub>19</sub>H<sub>18</sub>O: C, 86.99 %; H, 6.92 %; O, 6.10 %. Found: C, 85.94 %; H, 6.89 %; O, 7.17 %. Repeat found: C, 85.62 %; H, 6.86 %; O, 7.52 %

**6-(Phenanthren-9-yl) hexanal (153).**



The general procedure was used, with 9-iodophenanthrene (1.00 g, 3.29 mmol), Pd(OAc)<sub>2</sub> (22.3 mg, 0.0993 mmol), TBACl (1.83 g, 6.58 mmol), LiCl (0.14 g, 3.3 mmol), LiOAc (0.54 g, 8.2 mmol), dry degassed DMF (8 mL), and 5-hexen-1-ol (0.40 mL, 3.3 mmol) was stirred at rt for 24 h then heated to 50 °C for 5 days. The resulting orange solid was recrystallized in hot ethyl acetate layered with hot hexanes. The reaction afforded an orange solid 0.62 g (68%).

**IR (FTIR):** 3104 (w), 3075 (w), 3030 (w), 2931 (s), 2884 (m), 2859 (m), 2827 (m) and 2735 (m), 1714 (s)

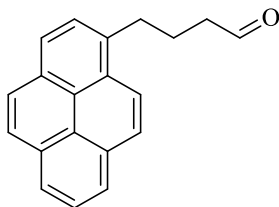
**<sup>1</sup>H NMR** (CDCl<sub>3</sub>, 500 MHz): δ 9.80 (t, *J* = 2.0 Hz, 1H), 8.80 – 8.74 (m, 1H), 8.68 (d, *J* = 8.0 Hz, 1H), 8.14 – 8.08 (m, 1H), 7.88 – 7.84 (m, 1H), 7.72 – 7.64 (m, 2H), 7.64 – 7.58 (m, 3H), 3.15 (apparent dd, second order coupling, *J*<sub>app</sub> = 8.0, 8.0 Hz, 2H), 2.47 (td, *J* = 7.0, 2.0 Hz, 2H), 1.88 (quint, *J* = 7.0 Hz, 2H), 1.75 (quint, *J* = 7.0 Hz, 2H), 1.58 – 1.51 (m, 2H)

**<sup>13</sup>C NMR** (CDCl<sub>3</sub>, 126 MHz): δ 202.6, 136.4, 131.9, 131.2, 130.7, 129.6, 128.0, 126.6, 126.5, 126.1, 126.1, 125.9, 124.3, 123.2, 122.4, 43.8, 33.2, 29.9, 29.3, 22.0

**HRMS** (ESI) exact mass *m/z* calculated for C<sub>20</sub>H<sub>20</sub>O (M<sup>+</sup>) is 276.1514, found 276.1516

**EA anal.** calcd for C<sub>20</sub>H<sub>20</sub>O: C, 86.99 %; H, 6.92 %; O, 6.10 %. Found: C, 86.35 %; H, 7.35 %; O, 6.30 %. Repeat found: C, 86.29 %; H, 7.22 %; O, 6.49 %

**4-(Pyren-1-yl) butanal (158).**



The general procedure was used, with 1-iodopyrene (1.00 g, 3.03 mmol), Pd(OAc)<sub>2</sub> (20 mg, 0.089 mmol), TBACl (1.68 g, 6.06 mmol), LiCl (0.13 g, 3.0 mmol), LiOAc (0.50 g, 7.6 mmol), dry degassed DMF (7 mL), and 3-buten-1-ol (0.26 mL, 3.0 mmol) was stirred at rt for 4 days. The resulting yellow solid was recrystallized in hot ethyl acetate layered with hot hexanes. The reaction afforded a yellow solid 0.53 g (64%).

**IR (FTIR):** 3113 (w), 3039 (m), 2950 (m), 2894 (m), 2883 (m), 2816 (m) and 2707 (s), 1726 (s)

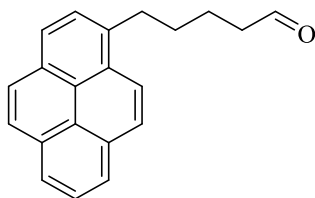
**<sup>1</sup>H NMR** (CDCl<sub>3</sub>, 500 MHz): δ 9.83 (t, *J* = 1.0 Hz, 1H), 8.31 (d, *J* = 9.0 Hz, 1H), 8.20 (dd, *J* = 8.0, 4.0 Hz, 2H), 8.15 (dd, *J* = 9.0, 6.0 Hz, 2H), 8.09 – 8.00 (m, 3H), 7.87 (d, *J* = 8.0 Hz, 1H), 3.41 (apparent dd, second order coupling, *J*<sub>app</sub> = 8.0, 8.0 Hz, 2H), 2.60 (td, *J* = 7.0, 1.0 Hz, 2H), 2.23 (quint, *J* = 7.0 Hz, 2H)

**<sup>13</sup>C NMR** (CDCl<sub>3</sub>, 126 MHz): δ 202.1, 135.5, 131.4, 130.9, 130.0, 128.7, 127.5, 127.4, 127.3, 127.0, 126.8, 125.9, 125.1, 125.0, 124.8, 123.2, 122.3, 43.4, 32.6, 24.0

**HRMS** (ESI) exact mass *m/z* calculated for C<sub>20</sub>H<sub>16</sub>O (M<sup>+</sup>) is 272.1201, found 272.1199

**EA anal.** calcd for C<sub>20</sub>H<sub>16</sub>O: C, 87.21 %; H, 5.99 %; O, 5.87 %. Found: C, 87.17 %; H, 6.01 %; O, 6.82 %. Repeat found: C, 87.25 %; H, 5.98 %; O, 6.77 %

**5-(Pyren-1-yl) pentanal (159).**



The general procedure was used, with 1-iodopyrene (5.00 g, 15.2 mmol), Pd(OAc)<sub>2</sub> (0.10 g, 0.46 mmol), TBACl (6.92 g, 30.4 mmol), LiCl (0.644 g, 15.2 mmol), LiOAc (2.51 g, 38.0 mmol), dry degassed DMF (38 mL), and 4-penten-1-ol (1.57 mL, 15.2 mmol) was stirred at rt for 4 days. The resulting yellow solid was recrystallized in hot ethyl acetate layered with hot hexanes. The reaction afforded a yellow solid 2.9 g (66%).

**IR (FTIR):** 3063 (w), 3046 (w), 2935 (s), 2923 (s), 2881 (m), 2858 (m), 2833 (m), 2735 (w), 1712 (s)

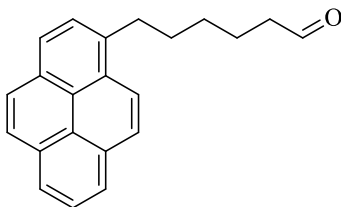
**<sup>1</sup>H NMR** (CDCl<sub>3</sub>, 500 MHz) δ 9.80 (t, *J* = 2.0 Hz, 1H), 8.28 (d, *J* = 9.0 Hz, 1H), 8.19 (dd, *J* = 8.0, 4.0 Hz, 2H), 8.16 – 8.09 (m, 2H), 8.05 (d, *J* = 2.0 Hz, 2H), 8.02 (t, *J* = 8.0 Hz, 1H), 7.89 (d, *J* = 8.0 Hz, 1H), 3.40 (apparent dd, second order coupling, *J*<sub>app</sub> = 8.0, 7.0 Hz, 2H), 2.53 (td, *J* = 7.0, 2.0 Hz, 2H), 1.98 – 1.78 (m, 4H)

**<sup>13</sup>C NMR** (CDCl<sub>3</sub>, 126 MHz) δ 202.3, 136.2, 131.4, 130.9, 129.9, 128.6, 127.5, 127.3, 127.2, 126.6, 125.8, 125.1, 125.0, 124.9, 124.8, 124.7, 123.2, 43.8, 33.3, 31.2, 22.1

**HRMS** (ESI) exact mass *m/z* calculated for C<sub>21</sub>H<sub>18</sub>O (M<sup>+</sup>) is 286.1358, found 286.1359

**EA anal.** calcd for C<sub>21</sub>H<sub>18</sub>O: C, 88.08 %; H, 6.34 %; O, 5.59 %. Found: C, 88.04 %; H, 6.39 %; O, 5.57 %. Repeat Found: C, 87.85 % H, 6.41 %; O, 5.74 %

**6-(Pyren-1-yl) hexanal (160).**



The general procedure was used, with 1-iodopyrene (1.00 g, 3.03 mmol), Pd(OAc)<sub>2</sub> (20 mg, 0.09 mmol), TBACl (1.68 g, 6.06 mmol), LiCl (0.13 g, 3.0 mmol), LiOAc (0.50 g, 7.6 mmol), dry degassed DMF (7 mL), and 5-hexen-1-ol (0.36 mL, 3.0 mmol) was stirred at rt for 24 h then heated to 50 °C for 5 days. The resulting yellow solid was recrystallized in hot ethyl acetate layered with hot hexanes. The reaction afforded a yellow solid 0.60 g (66 %).

**IR (FTIR):** 3056 (w), 2934 (m), 2921 (m), 2880 (w), 2857 (w), 2833 (w), 2736 (w), 1711 (s)

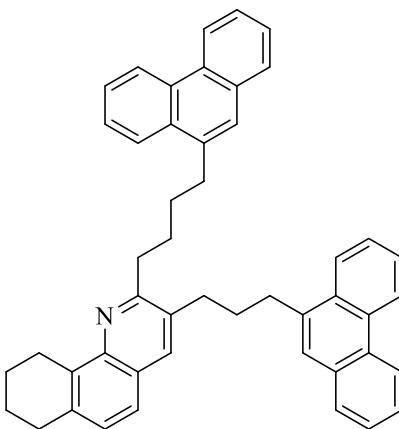
**<sup>1</sup>H NMR** (CDCl<sub>3</sub>, 500 MHz): δ 9.79 (t, *J* = 2.0 Hz, 1H), 8.29 (d, *J* = 9.0 Hz, 1H), 8.19 (dd, *J* = 8.0, 5.0 Hz, 2H), 8.13 – 8.09 (m, 2H), 8.10 – 7.97 (m, 3H), 7.86 (d, *J* = 8.0 Hz, 1H), 3.35 (apparent dd, second order coupling, *J*<sub>app</sub> = 8.0, 8.0 Hz, 2H), 2.46 (td, *J* = 7.0, 2.0 Hz, 2H), 1.89 (quint, *J* = 8.0 Hz, 2H), 1.75 (quint, *J* = 7.0 Hz, 2H), 1.59 – 1.51 (m, 2H)

**<sup>13</sup>C NMR** (CDCl<sub>3</sub>, 126 MHz) δ 202.6, 136.7, 131.4, 130.9, 129.8, 128.6, 127.5, 127.2, 126.6, 125.8, 125.1, 125.0, 124.8, 124.8, 124.7, 123.3, 43.8, 33.3, 31.6, 29.2, 22.0

**HRMS** (ESI) exact mass *m/z* calculated for C<sub>22</sub>H<sub>20</sub>O (M<sup>+</sup>) is 300.1514, found 300.1519

**EA anal.** calcd for C<sub>22</sub>H<sub>20</sub>O: C, 87.96 %; H, 6.71 %; O, 5.33 %. Found: C, 85.93 %; H, 6.80 %; O, 7.27 %. Repeat Found: C, 85.90 %; H, 6.82 %; O, 7.28 %

### 3.9. MCR optimization: 5,6,7,8-tetrahydronaphthalen-1-amine



**(Eq. 3-7)** A mixture of 5-(phenanthren-9-yl) pentanal (0.10 g, 0.381 mmol) was added to a dry 25 mL three-neck RBF flask and purged three times with vacuum/nitrogen. 5,6,7,8-tetrahydronaphthalen-1-amine (25  $\mu$ L, 0.182 mmol), hydroiodic acid (0.7  $\mu$ L), dry/distilled THF (15 mL), and H<sub>2</sub>O (5  $\mu$ L, 150 mol%) were sequentially added and the mixture stirred for 1 h at rt under N<sub>2</sub> atmosphere. the mixture stirred at reflux for 12 h under N<sub>2</sub> atmosphere. The reaction mixture was exposed to air and heating to reflux was continued for 24 h. The reaction mixture was cooled to rt and the solvent was removed under reduced pressure. CH<sub>2</sub>Cl<sub>2</sub> (100 mL) and saturated Na<sub>2</sub>CO<sub>3</sub> (100 mL) were added. The organic layer was separated, washed with saturated Na<sub>2</sub>CO<sub>3</sub> (2 x 100 mL), dried over Na<sub>2</sub>SO<sub>4</sub>, filtered, and the solvent was removed under reduced pressure. The crude material was purified by column chromatography (hexanes/EtOAc gradient) to give an off white solid (55.4 mg, 48% isolated yield).

## General procedure for screening the various conditions for optimization of 5,6,7,8-tetrahydronaphthalen-1-amine

5-(Phenanthren-9-yl) pentanal (0.10 g, 0.381 mmol) was added to a 50 mL three-neck RBF flask equipped with a reflux condenser. 5,6,7,8-Tetrahydronaphthalen-1-amine (25  $\mu$ L, 0.182 mmol) and hydroiodic acid or I<sub>2</sub> (2-30 mol%) was dissolved in solvent (15 mL) and heated for 1.5 – 4.5 h. The reaction mixture was cooled to rt, basified with 10% aqueous NaOH, and washed with CH<sub>2</sub>Cl<sub>2</sub>. The organic layer was separated, washed with saturated sodium bisulfite (15 mL), NaBH<sub>4</sub> (100 mg) in H<sub>2</sub>O (15 mL), saturated brine and dried over Na<sub>2</sub>SO<sub>4</sub>, filtered, and the solvent was removed under reduced pressure. Hexamethyldisiloxane (4.3  $\mu$ L, 0.020 mmol) was added as an internal standard for <sup>1</sup>H NMR analysis.

**(T3-1.1)** The general procedure was used, HI (4.1  $\mu$ L), EtOH, 90 °C (bath temperature), open to air, for 2.5 h (<sup>1</sup>H NMR conversion: 42%).

**(T3-1.2)** The general procedure was used, HI (4.1  $\mu$ L), EtOH, 90 °C (bath temperature), pressurized in a Fischer Porter bottle to 2 atm of O<sub>2</sub>, for 1.5 h (<sup>1</sup>H NMR conversion: 35%).

**(T3-1.3)** The general procedure was used, HI (1.4  $\mu$ L), EtOH, 90 °C (bath temperature), oxygen sparge, for 2.5 h (<sup>1</sup>H NMR conversion: 43%).

**(T3-1.4)** The general procedure was used, HI (0.7  $\mu$ L), EtOH, 90 °C (bath temperature), oxygen sparge, for 4.5 h (Isolated yield: 34%).

**(T3-1.5)** The general procedure was used, I<sub>2</sub> (2.3 mg), EtOH, 90 °C (bath temperature), pressurized in a Fischer Porter bottle to 2 atm of O<sub>2</sub>, for 1.5 h (<sup>1</sup>H NMR conversion: 41%).

**(Eq. 3-11a)** The general procedure was used, HI (0.7  $\mu$ L), CH<sub>3</sub>CN, 85 °C (bath temperature), oxygen sparge, for 4.5 h (<sup>1</sup>H NMR conversion: 32%).

**(Eq. 3-11b)** The general procedure was used, HI (0.7  $\mu$ L), DCM, 45  $^{\circ}$ C (bath temperature), oxygen sparge, for 4.5 h ( $^1$ H NMR conversion: 53%).

**(Eq. 3-11c)** The general procedure was used, HI (0.7  $\mu$ L), C<sub>6</sub>H<sub>6</sub>, 90  $^{\circ}$ C (bath temperature), oxygen sparge, for 4.5 h (Isolated yield: 57%).

**(Eq. 3-12a)** The general procedure was used, 5-(phenanthren-9-yl) pentanal (0.300 g, 1.14 mmol), 5,6,7,8-tetrahydronaphthalen-1-amine (51  $\mu$ L, 0.37 mmol), I<sub>2</sub> (4.7 mg), C<sub>6</sub>H<sub>6</sub> (20mL), 90  $^{\circ}$ C (bath temperature), open to air, for 0.5 h (Isolated yield: 44%).

**(Eq. 3-12b)** The general procedure was used, 5-(phenanthren-9-yl) pentanal (0.300 g, 1.14 mmol), 5,6,7,8-tetrahydronaphthalen-1-amine (51  $\mu$ L, 0.37 mmol), I<sub>2</sub> (4.7 mg), D<sub>2</sub>O (19.9  $\mu$ L, 1.14 mmol), C<sub>6</sub>H<sub>6</sub> (20mL), 90  $^{\circ}$ C (bath temperature), open to air, for 0.5 h (Isolated yield: 54%).

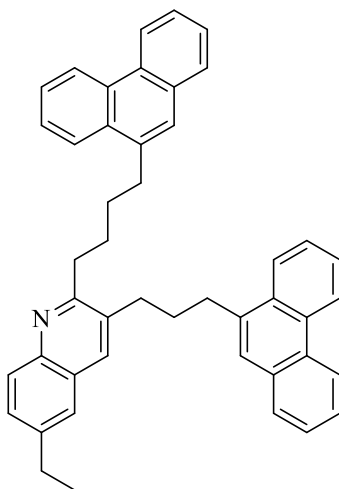
**(T3-2.1)** The general procedure was used, HI (0.7  $\mu$ L), C<sub>6</sub>H<sub>6</sub>, 90  $^{\circ}$ C (bath temperature), open to air, for 4.5 h ( $^1$ H NMR conversion: 57%).

**(T3-2.2)** The general procedure was used, HI (0.7  $\mu$ L), C<sub>6</sub>H<sub>6</sub>, 90  $^{\circ}$ C (bath temperature), oxygen sparge, for 4.5 h ( $^1$ H NMR conversion: 59%).

**(T3-2.3)** The general procedure was used, HI (0.7  $\mu$ L), C<sub>6</sub>H<sub>6</sub>, 90  $^{\circ}$ C (bath temperature), pressurized in a Fischer Porter bottle to 2 atm of O<sub>2</sub>, for 4.5 h ( $^1$ H NMR conversion: 82%).

**(T3-2.4)** The general procedure was used, HI (0.7  $\mu$ L), C<sub>6</sub>H<sub>6</sub>, 90  $^{\circ}$ C (bath temperature), pressurized in a Fischer Porter bottle to 2 atm of O<sub>2</sub>, for 1.5 h ( $^1$ H NMR conversion: 74%).

### 3.10. MCR Optimization: 4-Ethylaniline



#### General procedure for screening the various conditions for optimization of 4-ethylaniline

5-(Phenanthren-9-yl) pentanal (0.10 g, 0.38 mmol) was added to a 50 mL three-neck RBF flask equipped with a reflux condenser. 4-Ethylaniline (23  $\mu$ L, 0.18 mmol) and hydroiodic acid (2-10 mol%) was dissolved in anisole (15 mL), sparged with O<sub>2</sub> and heated to 100 – 130 °C (bath temperature) for 4.5 h. The reaction mixture was cooled to rt, basified with 10% aqueous NaOH, and washed with CH<sub>2</sub>Cl<sub>2</sub>. The organic layer was separated, washed with saturated sodium bisulfite (15 mL), NaBH<sub>4</sub> (100 mg) in H<sub>2</sub>O (15 mL), saturated brine and dried over Na<sub>2</sub>SO<sub>4</sub>, filtered, and the solvent was removed under reduced pressure. Hexamethyldisiloxane (4.3  $\mu$ L, 0.020 mmol) was added as an internal standard for <sup>1</sup>H NMR analysis.

**(T3-3.1)** The general procedure was used, HI (0.7  $\mu$ L) and heated to 100 °C (bath temperature). (<sup>1</sup>H NMR conversion: 43%).

**(T3-3.2)** The general procedure was used, HI (0.7  $\mu$ L) and heated to 130 °C (bath temperature). (<sup>1</sup>H NMR conversion: 77%).

(T3-3.3) The general procedure was used, HI (0.3  $\mu$ L) and heated to 130  $^{\circ}$ C (bath temperature), ( $^1$ H NMR conversion: 67%).

(T3-3.4) The general procedure was used, HI (1.4  $\mu$ L), and heated to 130  $^{\circ}$ C (bath temperature). ( $^1$ H NMR conversion: 65%).

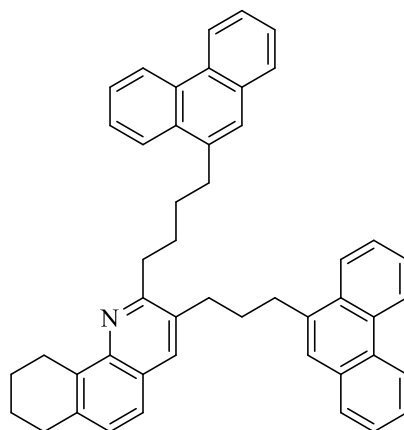
(T3-3.5) The general procedure was used, HI (0.7  $\mu$ L), NaI (27 mg, 0.18 mmol) and heated to 130  $^{\circ}$ C (bath temperature). ( $^1$ H NMR conversion: > 95%).

(T3-3.6) The general procedure was used, HI (0.7  $\mu$ L), NaI (55 mg, 0.36 mmol) and heated to 130  $^{\circ}$ C (bath temperature). ( $^1$ H NMR conversion: 51%).

### 3.11. Scope of multicomponent reaction compounds

A mixture of an alkyl-tethered  $\alpha,\omega$ -aromatic aldehyde (2.1 equiv) was added to a three-neck RBF flask equipped with a reflux condenser. Amine (1 equiv), hydroiodic acid (5 mol%), and NaI (1 equiv) was added and dissolved in anisole, sparged with O<sub>2</sub>, and heated to 130  $^{\circ}$ C (bath temperature) for 4.5 h. The reaction mixture was cooled to rt, basified with 10% aqueous NaOH, and washed with CH<sub>2</sub>Cl<sub>2</sub>. The organic layer was separated, washed with saturated sodium bisulfite, NaBH<sub>4</sub> in H<sub>2</sub>O, saturated brine and dried over Na<sub>2</sub>SO<sub>4</sub>, filtered, and the solvent was removed under reduced pressure.

**2-(4-(phenanthren-9-yl)butyl)-3-(3-(phenanthren-9-yl)propyl)-7,8,9,10-tetrahydrobenzo[*h*]quinoline (161).**



The general procedure was used, 5-(phenanthren-9-yl) pentanal (0.50 g, 0.19 mmol), 5,6,7,8-tetrahydronaphthalen-1-amine (126  $\mu$ L, 0.908 mmol), NaI (0.136 g, 0.908 mmol), HI (3.4  $\mu$ L) and anisole (86 mL). The crude material was purified by column chromatography RF=0.54 (9 : 1 Hexane/EtOAc) to afford an off white solid 0.30 g (52%).

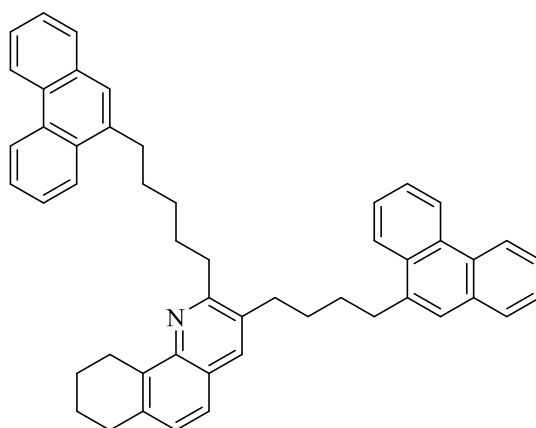
**$^1\text{H NMR}$**  ( $\text{CDCl}_3$ , 500 MHz):  $\delta$  8.73 (d,  $J = 8.0$  Hz, 1H), 8.67 – 8.64 (m, 2H), 8.59 – 8.56 (m, 1H), 8.07 – 8.02 (m, 2H), 7.81 – 7.60 (m, 3H), 7.65 (ddd,  $J = 8.0, 7.0, 1.0$  Hz, 1H), 7.60 – 7.51 (m, 9H), 7.44 (d,  $J = 8.0$  Hz, 1H), 7.15 (d,  $J = 8.0$  Hz, 1H), 3.31 (apparent dd, second order coupling,  $J_{app} = 6.0, 6.0$  Hz, 2H), 3.21 (apparent dd, second order coupling,  $J_{app} = 8.0, 7.0$  Hz, 2H), 3.10 (apparent dd, second order coupling,  $J_{app} = 8.0, 8.0$  Hz, 2H), 2.96 (apparent dd, second order coupling,  $J_{app} = 8.0, 7.0$  Hz, 2H), 2.93 – 2.89 (m, 4H), 2.20 (quint,  $J = 8.0$  Hz, 2H), 2.05 (quint,  $J = 8.0$  Hz, 2H), 1.96 – 1.83 (m, 6H)

**$^{13}\text{C NMR}$**  ( $\text{CDCl}_3$ , 126 MHz):  $\delta$  159.6, 145.2, 136.8, 136.8, 135.9, 134.7, 134.2, 132.1, 131.9, 131.7, 131.3, 131.1, 130.7, 130.6, 129.6, 129.6, 128.0, 127.9, 127.8, 126.6, 126.5, 126.5, 126.4,

126.3, 126.1, 126.0, 125.9, 125.9, 125.7, 125.0, 124.5, 124.2, 123.7, 123.2, 123.1, 122.4, 122.4, 35.1, 33.3, 33.1, 32.0, 30.6, 30.2, 30.0, 28.5, 24.7, 23.2, 23.1

**HRMS** (ESI) exact mass  $m/z$  calculated for  $C_{48}H_{43}N$  is 633.3396, found 633.3397

**3-(4-(phenanthren-9-yl)butyl)-2-(5-(phenanthren-9-yl)pentyl)-7,8,9,10-tetrahydrobenzo[*h*]quinoline (165).**



The general procedure was used, 6-(phenanthren-9-yl) hexanal (0.50 g, 0.18 mmol), 5,6,7,8-tetrahydronaphthalen-1-amine (120  $\mu$ L, 0.862 mmol), NaI (0.129 g, 0.862 mmol), HI (3.3  $\mu$ L) and anisole (86 mL). The crude material was purified by column chromatography RF=0.36 (9 : 1 Hexane/EtOAc) to afford an off white solid 0.33 g (57%).

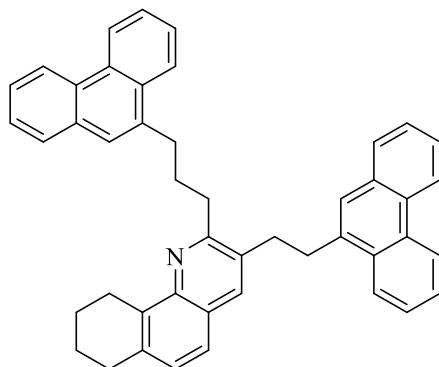
**$^1H$  NMR** ( $CDCl_3$ , 500 MHz):  $\delta$  8.77 – 8.70 (m, 2H), 8.64 (d,  $J = 8.0$  Hz, 2H), 8.13 – 8.06 (m, 2H), 7.80 – 7.76 (m, 2H), 7.71 (s, 1H), 7.68 – 7.52 (m, 10H), 7.43 (d,  $J = 8.0$  Hz, 1H), 7.16 (d,  $J = 8.0$  Hz, 1H), 3.34 (apparent dd, second order coupling,  $J_{app} = 6.0, 6.0$  Hz, 2H), 3.16 (apparent dd, second order coupling,  $J_{app} = 8.0, 7.0$  Hz, 2H), 3.12 (apparent dd, second order coupling,  $J_{app} = 8.0, 8.0$  Hz, 2H), 2.98 (apparent dd, second order coupling,  $J_{app} = 8.0, 7.0$  Hz, 2H), 2.91 (apparent

dd, second order coupling,  $J_{app} = 6.0, 6.0$  Hz, 2H), 2.82 (apparent dd, second order coupling,  $J_{app} = 8.0, 8.0$  Hz, 2H), 2.04 – 1.80 (m, 12H), 1.63 (quint,  $J = 7.0$  Hz, 2H)

$^{13}\text{C}$  NMR ( $\text{CDCl}_3$ , 126 MHz)  $\delta$ : 159.8, 137.0, 136.8, 136.4, 134.7, 134.2, 132.5, 132.0, 131.9, 131.3, 131.2, 130.7, 130.7, 129.6, 129.6, 128.0, 128.0, 127.7, 126.6, 126.5, 126.5, 126.4, 126.1, 126.1, 126.0, 126.0, 125.9, 125.8, 125.1, 124.5, 124.4, 123.8, 123.2, 123.2, 122.4, 122.4, 35.3, 33.4, 33.3, 32.4, 30.4, 30.3, 30.0, 29.8, 28.6, 24.8, 23.8, 23.2, 23.1

HRMS (MALDI-FT-ICR) exact mass  $m/z$  calculated for  $\text{C}_{50}\text{H}_{47}\text{N}$  ( $[\text{M}+\text{H}]^+$ ) is 662.3742, found 662.3771

**3-(2-(phenanthren-9-yl)ethyl)-2-(3-(phenanthren-9-yl)propyl)-7,8,9,10-tetrahydrobenzo[*h*]quinoline (166).**



The general procedure was used, 4-(phenanthren-9-yl) butanal (0.078 g, 0.31 mmol), 5,6,7,8-tetrahydronaphthalen-1-amine (21  $\mu\text{L}$ , 0.15 mmol), NaI (0.022 mg, 0.15 mmol), HI (0.5  $\mu\text{L}$ ) and anisole (14 mL). The crude material was purified by column chromatography RF=0.41 (9 : 1 Hexane/EtOAc) to afford a off white solid 0.051 g (56%).

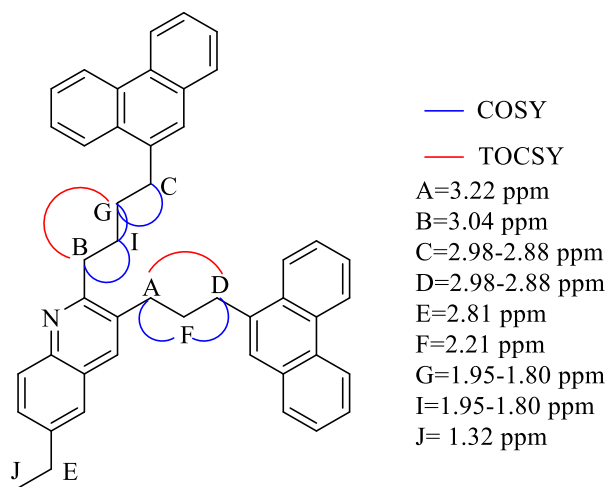
$^1\text{H}$  NMR ( $\text{CDCl}_3$ , 500 MHz):  $\delta$  8.77 (d,  $J = 8.0$  Hz, 1H), 8.72 – 8.66 (m, 2H), 8.61 (d,  $J = 8.0$  Hz, 1H), 8.16 – 8.09 (m, 2H), 7.88 (s, 1H), 7.77 – 7.72 (m, 2H), 7.69 (ddd,  $J = 8.0, 7.0, 1.0$  Hz, 1H),

7.65 – 7.46 (m, 10H), 7.20 (d,  $J = 8.0$  Hz, 1H), 3.46 – 3.40 (m, 4H), 3.31 – 3.22 (m, 4H), 3.19 (t,  $J = 7.0$  Hz, 2H), 2.96 (t,  $J = 6.0$  Hz, 2H), 2.49 (quint,  $J = 8.0$  Hz, 2H), 2.03 – 1.89 (m, 4H)

$^{13}\text{C}$  NMR ( $\text{CDCl}_3$ , 126 MHz):  $\delta$  159.2, 137.0, 136.8, 135.5, 135.1, 134.8, 134.4, 132.3, 131.9, 131.8, 131.0, 130.7, 129.8, 129.6, 128.2, 128.0, 128.0, 126.7, 126.7, 126.5, 126.4, 126.3, 126.2, 126.2, 126.2, 126.0, 125.8, 124.6, 124.1, 123.9, 123.4, 123.1, 123.0, 122.4, 122.4, 35.0, 34.1, 33.0, 32.8, 30.3, 28.5, 24.9, 23.2, 23.1

HRMS (MALDI-FT-ICR) exact mass  $m/z$  calculated for  $\text{C}_{46}\text{H}_{39}\text{N}$  ( $[\text{M}+\text{H}]^+$ ) is 606.3116, found 606.3144

**6-ethyl-2-[4-(phenanthren-9-yl)butyl]-3-[3-(phenanthren-9-yl)propyl]quinoline (168).**



The general procedure was used, 5-(phenanthren-9-yl) pentanal (1.00 g, 3.81 mmol), 4-ethylaniline (226  $\mu\text{L}$ , 1.82 mmol), NaI (271 mg, 1.82 mmol), HI (6.8  $\mu\text{L}$ ) and anisole (150 mL), The crude material was purified by column chromatography  $\text{RF}=0.20$  (9 : 1 Hexane/EtOAc) to afford an off white solid 0.82 g (79%).

**<sup>1</sup>H NMR** (CDCl<sub>3</sub>, 400 MHz): δ 8.72 (d, *J* = 8.0 Hz, 1H), 8.70 – 8.60 (m, 2H), 8.60 – 8.50 (m, 1H), 8.07 – 8.02 (m, 2H), 7.93 (d, *J* = 8.0 Hz, 1H), 7.83 – 7.76 (m, 3H), 7.64 (ddd, *J* = 8.0, 7.0, 2.0 Hz, 1H), 7.62 – 7.54 (m, 6H), 7.54 – 7.49 (m, 4H), 7.48 (s, 1H), 3.22 (apparent dd, second order coupling, *J*<sub>app(A)</sub> = 8.0, 7.0 Hz, 2H), 3.04 (apparent dd, second order coupling, *J*<sub>app(B)</sub> = 8.0, 7.0 Hz, 2H), 2.98 – 2.88 (m<sub>(C/D)</sub>, 4H), 2.81 (q, *J*<sub>(E)</sub> = 8.0 Hz, 2H), 2.21 (quint, *J*<sub>(F)</sub> = 8.0 Hz, 2H), 1.95 – 1.80 (m<sub>(G/I)</sub>, 4H), 1.32 (t, *J*<sub>(J)</sub> = 8.0 Hz, 3H)

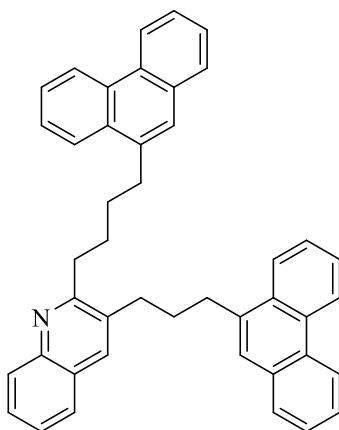
Alkyl chain assignments were acquired by COSY and TOSCY.

**<sup>13</sup>C NMR** (CDCl<sub>3</sub>, 126 MHz) δ 160.8, 145.4, 141.7, 136.7, 135.8, 134.6, 133.3, 131.9, 131.8, 131.3, 131.1, 130.8, 130.7, 129.7, 129.6, 128.4, 128.0, 128.0, 127.3, 126.7, 126.6, 126.5, 126.5, 126.4, 126.2, 126.1, 125.9, 125.8, 124.5, 124.5, 124.2, 123.3, 123.2, 122.5, 122.4, 35.7, 33.2, 33.1, 32.1, 30.7, 30.2, 29.7, 28.8, 15.4

**HRMS** (MALDI-FT-ICR) exact mass *m/z* calculated for C<sub>46</sub>H<sub>41</sub>N ([M+H]<sup>+</sup>) is 608.3273, found 608.3306

**EA** anal. calcd. for C<sub>46</sub>H<sub>41</sub>N: C, 90.90 %; H, 6.80 %; N, 2.30 %; Found: C, 90.06 %; H, 6.74 %; N, 2.32 %. Repeat found: C, 90.45 %; H, 6.83 %; N, 2.29 %

**2-(4-(phenanthren-9-yl) butyl)-3-(3-(phenanthren-9-yl) propyl) quinoline (170).**



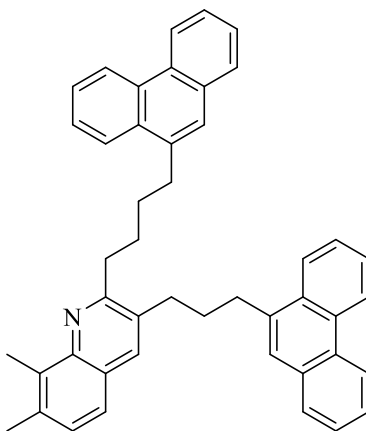
The general procedure was used, 5-(phenanthren-9-yl) pentanal (0.23 g, 0.89 mmol), aniline (39  $\mu$ L, 0.42 mmol), NaI (0.063 g, 0.421 mmol), HI (1.6  $\mu$ L) and anisole (40 mL). The crude material was purified by column chromatography RF=0.28 (9 : 1 Hexane/EtOAc) to afford a pink solid 0.10 g (41%).

**$^1\text{H NMR}$**  ( $\text{CDCl}_3$ , 500 MHz):  $\delta$  8.73 (d,  $J = 8.0$  Hz, 1H), 8.69 – 8.64 (m, 2H), 8.61 – 8.54 (m, 1H), 8.08 – 8.00 (m, 3H), 7.88 (s, 1H), 7.82 – 7.70 (m, 2H), 7.70 (dd,  $J = 8.0, 1.0$  Hz, 1H), 7.68 – 7.61 (m, 2H), 7.60 – 7.54 (m, 6H), 7.54 – 7.49 (m, 3H), 7.48 – 7.42 (m, 1H), 3.23 (apparent dd, second order coupling,  $J_{app} = 7.0, 7.0$  Hz, 2H), 3.05 (apparent dd, second order coupling,  $J_{app} = 8.0, 8.0$  Hz, 2H), 3.01 – 2.90 (m, 4H), 2.23 (quint,  $J = 8.0$  Hz, 2H), 1.93 (quint,  $J = 8.0$  Hz, 2H), 1.84 (quint,  $J = 7.0$  Hz, 2H)

**$^{13}\text{C NMR}$**  ( $\text{CDCl}_3$ , 126 MHz):  $\delta$  161.8, 146.6, 136.6, 135.7, 134.9, 133.5, 131.9, 131.7, 131.3, 131.0, 130.8, 130.7, 129.7, 129.6, 128.6, 128.5, 128.0, 128.0, 127.2, 126.9, 126.7, 126.6, 126.5, 126.5, 126.4, 126.2, 126.1, 126.0, 125.8, 125.7, 124.5, 124.2, 123.4, 123.2, 122.5, 122.4, 35.7, 33.3, 33.1, 32.2, 30.7, 30.2, 29.6

**HRMS** (ESI) exact mass  $m/z$  calculated for  $C_{44}H_{37}N$  ( $[M+H]^+$ ) is 580.2960, found 580.2995

**7,8-dimethyl-2-[4-(phenanthren-9-yl)butyl]-3-[3-(phenanthren-9-yl)propyl]quinoline (171).**



The general procedure was used, 5-(phenanthren-9-yl) pentanal (0.50 g, 1.9 mmol), 2,3-dimethylaniline (111  $\mu$ L, 0.908 mmol), NaI (136 mg, 0.908 mmol), HI (3.4  $\mu$ L) and anisole (86 mL). The crude material was purified by column chromatography  $R_F=0.36$  (9 : 1 Hexane/EtOAc) to afford a white solid 0.22 g (40%).

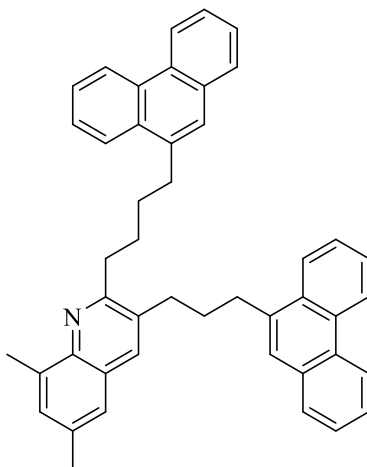
**$^1H$  NMR** ( $CDCl_3$ , 400 MHz):  $\delta$  8.73 (d,  $J = 8.0$  Hz, 1H), 8.68 – 8.64 (m, 2H), 8.59 – 8.54 (m, 1H), 8.09 – 8.01 (m, 2H), 7.82 – 7.76 (m, 3H), 7.68 – 7.60 (m, 1H), 7.64 – 7.49 (m, 9H), 7.46 (d,  $J = 8.0$  Hz, 1H), 7.26 (d,  $J = 8.0$  Hz, 1H), 3.22 (apparent dd, second order coupling,  $J_{app} = 8.0, 7.0$  Hz, 2H), 3.12 (apparent dd, second order coupling,  $J_{app} = 8.0, 8.0$  Hz, 2H), 2.97 (apparent dd, second order coupling,  $J_{app} = 8.0, 7.0$  Hz, 2H), 2.91 (apparent dd, second order coupling,  $J_{app} = 8.0, 8.0$  Hz, 2H), 2.75 (s, 3H), 2.48 (s, 3H), 2.20 (quint,  $J = 8.0$  Hz, 2H), 2.06 (quint,  $J = 8.0$  Hz, 2H), 1.87 (quint,  $J = 8.0$  Hz, 2H)

$^{13}\text{C}$  NMR ( $\text{CDCl}_3$ , 126 MHz)  $\delta$  159.7, 145.4, 136.9, 135.9, 135.8, 134.7, 133.8, 132.0, 131.7, 131.3, 131.1, 130.7, 130.6, 129.7, 129.6, 128.4, 128.0, 128.0, 126.6, 126.5, 126.5, 126.4, 126.3, 126.2, 126.0, 126.0, 125.9, 125.8, 125.3, 124.5, 124.2, 123.7, 123.3, 123.1, 122.4, 122.4, 35.2, 33.4, 33.1, 32.0, 30.5, 30.0, 28.4, 20.5, 13.1

**HRMS** (MALDI-FT-ICR) exact mass  $m/z$  calculated for  $\text{C}_{46}\text{H}_{41}\text{N}$  ( $[\text{M}+\text{H}]^+$ ) is 608.3273, found 608.3308

**EA** anal. calcd. for  $\text{C}_{46}\text{H}_{41}\text{N}$ : C, 90.90 %; H, 6.80 %; N, 2.30 %; Found: C, 89.04 %; H, 6.85 %; N, 2.27 %. Repeat found: C, 89.28 %; H, 6.81 %; N, 2.35 %. Repeat Found: C, 89.22 %; H, 6.88 %; N, 2.27 %

**6,8-dimethyl-2-[4-(phenanthren-9-yl)butyl]-3-[3-(phenanthren-9-yl)propyl]quinoline (172).**



The general procedure was used, 5-(phenanthren-9-yl) pentanal (0.5 g, 1.9 mmol), 2,4-dimethylaniline (113  $\mu\text{L}$ , 0.908 mmol), NaI (136 mg, 0.908 mmol), HI (3.4  $\mu\text{L}$ ) and anisole (86 mL). The crude material was purified by column chromatography  $\text{RF}=0.36$  (9 : 1 Hexane/EtOAc) to afford a white solid 0.32 g (58%).

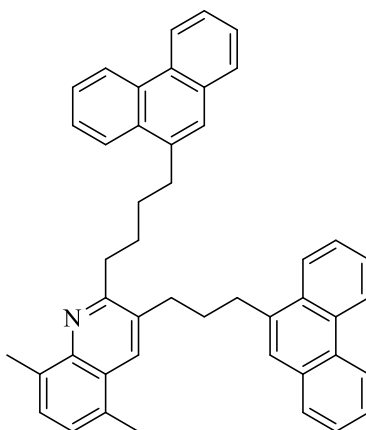
**<sup>1</sup>H NMR** (CDCl<sub>3</sub>, 500 MHz): δ 8.72 (d, *J* = 8.0 Hz, 1H), 8.68 – 8.63 (m, 2H), 8.59 – 8.54 (m, 1H), 8.07 – 8.01 (m, 2H), 7.81 – 7.76 (m, 2H), 7.73 (s, 1H), 7.67 – 7.60 (m, 1H), 7.60 – 7.49 (m, 9H), 7.30 (s, 2H), 3.22 (apparent dd, second order coupling, *J*<sub>app</sub> = 8.0, 8.0 Hz, 2H), 3.09 (apparent dd, second order coupling, *J*<sub>app</sub> = 8.0, 8.0 Hz, 2H), 2.95 (apparent dd, second order coupling, *J*<sub>app</sub> = 8.0, 7.0 Hz, 2H), 2.91 (apparent dd, second order coupling, *J*<sub>app</sub> = 8.0, 8.0 Hz, 2H), 2.74 (s, 3H), 2.45 (s, 3H), 2.20 (quint, *J* = 8.0 Hz, 2H), 2.03 (quint, *J* = 7.0 Hz, 2H), 1.86 (quint, *J* = 7.0 Hz, 2H)

**<sup>13</sup>C NMR** (CDCl<sub>3</sub>, 126 MHz) δ 158.9, 144.1, 136.9, 136.2, 135.9, 134.8, 134.2, 133.0, 132.0, 131.7, 131.3, 131.1, 130.7, 130.7, 130.6, 129.7, 129.6, 128.0, 128.0, 127.0, 126.6, 126.5, 126.5, 126.4, 126.3, 126.2, 126.0, 125.9, 125.8, 124.5, 124.2, 123.6, 123.3, 123.1, 122.4, 122.4, 35.1, 33.4, 33.1, 32.1, 30.6, 30.0, 29.7, 28.5, 21.5, 17.7

**HRMS** (MALDI-FT-ICR) exact mass *m/z* calculated for C<sub>46</sub>H<sub>41</sub>N ([M+H]<sup>+</sup>) is 608.3273, found 608.3306

**EA** anal. calcd. for C<sub>46</sub>H<sub>41</sub>N: C, 90.90 %; H, 6.80 %; N, 2.30 %; Found: C, 87.79 %; H, 6.92 %; N, 1.93 %. Repeat found: C, 87.71 %; H, 6.95 %; N, 1.92 %

**5,8-dimethyl-2-[4-(phenanthren-9-yl)butyl]-3-[3-(phenanthren-9-yl)propyl]quinoline (173).**



The general procedure was used, 5-(phenanthren-9-yl) pentanal (0.5 g, 1.9 mmol), 2,5-dimethylaniline (113  $\mu$ L, 0.908 mmol), NaI (0.136 mg, 0.908 mmol), HI (3.4  $\mu$ L) and anisole (86 mL). The crude material was purified by column chromatography RF=0.62 (7 : 3 Hexane/EtOAc) to afford a light grey solid 0.21 g (40%).

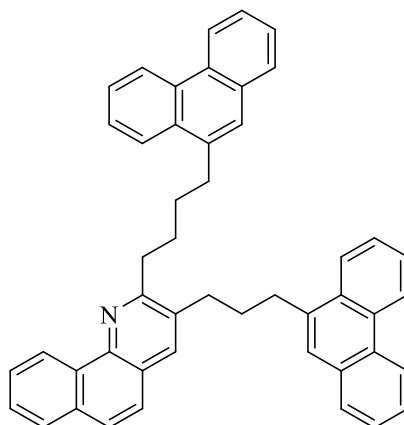
**$^1\text{H NMR}$**  ( $\text{CDCl}_3$ , 500 MHz):  $\delta$  8.73 (d,  $J = 8.0$  Hz, 1H), 8.68 – 8.64 (m, 2H), 8.59 – 8.56 (m, 1H), 8.08 – 8.02 (m, 2H), 7.97 (s, 1H), 7.82 – 7.78 (m, 2H), 7.68 – 7.57 (m, 1H), 7.62 – 7.49 (m, 9H), 7.34 (d,  $J = 7.0$  Hz, 1H), 7.15 (d,  $J = 7.0$  Hz, 1H), 3.23 (apparent dd, second order coupling,  $J_{app} = 8.0, 8.0$  Hz, 2H), 3.11 (apparent dd, second order coupling,  $J_{app} = 8.0, 8.0$  Hz, 2H), 3.00 – 2.93 (m, 4H), 2.74 (s, 3H), 2.59 (s, 3H), 2.20 (quint,  $J = 8.0$  Hz, 2H), 2.06 (quint,  $J = 8.0$  Hz, 2H), 1.87 (quint,  $J = 8.0$  Hz, 2H)

**$^{13}\text{C NMR}$**  ( $\text{CDCl}_3$ , 125 MHz):  $\delta$  159.2, 145.7, 136.9, 135.9, 134.6, 132.5, 131.9, 131.7, 131.4, 131.3, 131.2, 131.1, 130.7, 130.6, 129.7, 129.6, 128.0, 128.0, 127.9, 126.6, 126.5, 126.5, 126.4, 126.4, 126.2, 126.0, 125.9, 125.8, 125.7, 124.5, 124.2, 123.3, 123.1, 122.4, 122.4, 35.0, 33.4, 33.1, 32.4, 30.8, 30.0, 28.5, 18.5, 17.8

**HRMS** (MALDI-FT-ICR) exact mass  $m/z$  calculated for  $C_{46}H_{41}N$  ( $[M+H]^+$ ) is 608.3273, found 608.3308

**EA** anal. calcd. for  $C_{46}H_{41}N$ : C, 90.90 %; H, 6.80 %; N, 2.30 %; Found: C, 89.52 %; H, 6.87 %; N, 2.18 %. Repeat found: C, 89.44 %; H, 6.85 %; N, 2.16 %. Repeat found: C, 89.64 %; H, 6.84 %; N, 2.23 %

**2-(4-(phenanthren-9-yl)butyl)-3-(3-(phenanthren-9-yl)propyl)benzo[h]quinoline (174).**



The general procedure was used, 5-(phenanthren-9-yl) pentanal (0.20 g, 0.76 mmol), 1-aminonaphthylene (0.052 g, 0.36 mmol), NaI (0.054 g, 0.36 mmol), HI (1.4  $\mu$ L) and anisole (35 mL). The crude material was purified by column chromatography RF= (9 : 1 Hexane/EtOAc) to afford a tan solid 0.060 g (26%).

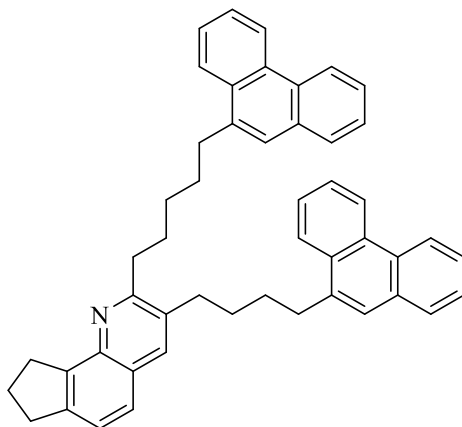
**$^1H$  NMR** ( $CDCl_3$ , 500 MHz):  $\delta$  9.33 – 9.29 (m, 1H), 8.75 – 8.71 (m, 1H), 8.69 – 8.63 (m, 2H), 8.60 – 8.55 (m, 1H), 8.11 – 8.06 (m, 1H), 8.05 – 8.03 (m, 1H), 7.90 – 7.85 (m, 2H), 7.82 – 7.76 (m, 2H), 7.72 (d,  $J$  = 9.0 Hz, 1H), 7.70 – 7.62 (m, 3H), 7.61 – 7.50 (m, 10H), 3.26 (apparent dd, second order coupling,  $J_{app}$  = 8.0, 8.0 Hz, 2H), 3.17 (apparent dd, second order coupling,  $J_{app}$  =

8.0, 8.0 Hz, 2H), 3.07 (apparent dd, second order coupling,  $J_{app} = 8.0, 8.0$  Hz, 2H), 2.99 (apparent dd, second order coupling,  $J_{app} = 8.0, 8.0$  Hz, 2H), 2.26 (quint,  $J = 7.0$  Hz, 2H), 2.15 (quint,  $J = 7.0$  Hz, 2H), 1.92 (quint,  $J = 8.0$  Hz, 2H)

$^{13}\text{C}$  NMR ( $\text{CDCl}_3$ , 125 MHz):  $\delta$  159.6, 144.1, 136.9, 135.9, 135.0, 133.9, 133.3, 132.0, 131.8, 131.5, 131.4, 131.1, 130.8, 130.7, 129.7, 129.6, 128.0, 128.0, 127.6, 127.4, 126.7, 126.6, 126.6, 126.5, 126.4, 126.4, 126.2, 126.0, 125.8, 125.0, 124.7, 124.6, 124.3, 124.2, 123.3, 123.1, 122.5, 122.4, 35.1, 33.5, 33.2, 32.1, 30.7, 30.1, 28.8

HRMS (ESI) exact mass  $m/z$  calculated for  $\text{C}_{48}\text{H}_{39}\text{N}$  ( $[\text{M}+\text{H}]^+$ ) is 630.3116, found 630.3154

**3-[4-(phenanthren-9-yl) butyl]-2-[5-(phenanthren-9-yl) pentyl]-7,8,9-cyclopenta[*h*]quinoline (175).**



The general procedure was used, 6-(phenanthren-9-yl) hexanal (0.50 g, 1.8 mmol), 4-aminodan (104  $\mu\text{L}$ , 0.862 mmol), NaI (129 mg, 0.862 mmol), HI (3.3  $\mu\text{L}$ ) and anisole (86 mL). The crude material was purified by column chromatography  $R_F=0.48$  (9 : 1 Hexane/EtOAc) to afford an off white solid 0.30 g (54%).

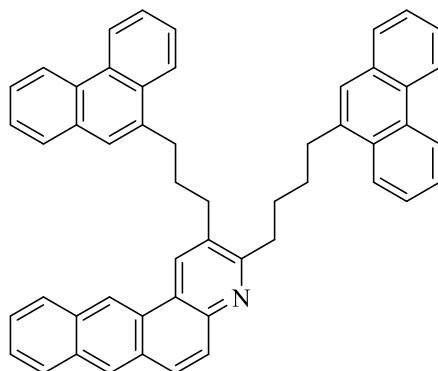
**<sup>1</sup>H NMR** (CDCl<sub>3</sub>, 500 MHz): δ 8.75 – 8.70 (m, 2H), 8.63 (d, *J* = 8.0 Hz, 2H), 8.14 – 8.06 (m, 2H), 7.81 – 7.74 (m, 3H), 7.68 – 7.53 (m, 10H), 7.50 (d, *J* = 8.0 Hz, 1H), 7.34 (d, *J* = 8.0 Hz, 1H), 3.41 (apparent dd, second order coupling, *J*<sub>app</sub> = 8.0, 7.0 Hz, 2H), 3.20 – 3.08 (m, 6H), 2.99 (apparent dd, second order coupling, *J*<sub>app</sub> = 8.0, 7.0 Hz, 2H), 2.83 (apparent dd, second order coupling, *J*<sub>app</sub> = 8.0, 7.0 Hz, 2H), 2.22 (quint, *J* = 8.0 Hz, 2H), 2.00 – 1.80 (m, 8H), 1.63 (quint, *J* = 8.0 Hz, 2H)

**<sup>13</sup>C NMR** (CDCl<sub>3</sub>, 126 MHz): δ 161.1, 144.1, 143.8, 140.9, 136.9, 136.3, 135.0, 132.4, 132.0, 131.9, 131.3, 130.8, 130.8, 129.7, 129.6, 129.6, 128.1, 128.0, 126.6, 126.6, 126.4, 126.2, 126.2, 126.1, 126.0, 126.0, 125.8, 125.5, 124.5, 124.3, 123.2, 123.1, 122.9, 122.5, 122.5, 35.4, 34.1, 33.4, 33.3, 32.4, 30.8, 30.5, 30.2, 29.9, 29.8, 28.8, 24.8

**HRMS** (MALDI-FT-ICR) exact mass *m/z* calculated for C<sub>49</sub>H<sub>45</sub>N ([M+H]<sup>+</sup>) is 648.3586, found 648.3618

**EA anal.** calcd. for C<sub>49</sub>H<sub>45</sub>N: C, 90.84 %; H, 7.00 %; N, 2.16 %; Found: C, 90.72 %; H, 7.18 %; N, 2.07 %. Repeat found: C, 90.73 %; H, 7.18 %; N, 2.01 %

**2-[4-(phenanthren-9-yl)butyl]-3-[3-(phenanthren-9-yl)propyl]-1-azatetraphene (176).**



The general procedure was used, 5-(phenanthren-9-yl) pentanal (0.50 g, 1.9 mmol), 2-aminoanthracene (0.175 g, 0.908 mmol), NaI (136 mg, 0.908 mmol) and hydroiodic acid (3.4  $\mu$ L) was dissolved in anisole (86 mL). The crude material was purified by column chromatography RF=0.42 (9 : 1 Hexane/EtOAc) to afford a tan solid 0.26 g (42%).

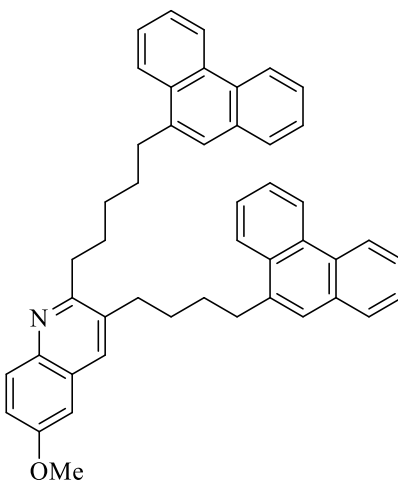
**$^1\text{H}$  NMR** ( $\text{CDCl}_3$ , 400 MHz):  $\delta$  9.02 (s, 1H), 8.77 (s, 1H), 8.75 – 8.70 (m, 1H), 8.70 – 8.62 (m, 2H), 8.61 – 8.55 (m, 1H), 8.39 (s, 1H), 8.13 – 8.03 (m, 4H), 7.97 (d,  $J = 9.0$  Hz, 1H), 7.86 – 7.77 (m, 3H), 7.68 – 7.51 (m, 12H), 3.28 (apparent dd, second order coupling,  $J_{app} = 8.0, 7.0$  Hz, 2H), 3.12 – 2.97 (m, 6H), 2.33 (quint,  $J = 8.0$  Hz, 2H), 1.96 (quint,  $J = 8.0$  Hz, 2H), 1.88 (quint,  $J = 8.0$  Hz, 2H)

**$^{13}\text{C}$  NMR** ( $\text{CDCl}_3$ , 126 MHz):  $\delta$  160.6, 146.7, 136.6, 135.8, 133.4, 132.0, 131.9, 131.9, 131.8, 131.3, 131.1, 130.8, 130.7, 130.7, 130.4, 130.0, 129.7, 129.6, 128.3, 128.2, 128.0, 127.9, 127.1, 126.7, 126.6, 126.5, 126.5, 126.3, 126.1, 126.1, 126.0, 126.0, 126.0, 125.8, 124.5, 124.3, 124.0, 123.4, 123.2, 122.5, 122.4, 121.4, 35.3, 33.3, 33.1, 32.5, 31.1, 30.2, 29.8

**HRMS** (MALDI-FT-ICR) exact mass  $m/z$  calculated for  $\text{C}_{52}\text{H}_{41}\text{N}$  ( $[\text{M}+\text{H}]^+$ ) is 680.3273, found 680.3306

**EA** anal. calcd. for  $\text{C}_{52}\text{H}_{41}\text{N}$ : C, 91.86 %; H, 6.08 %; N, 2.06 %; Found: C, 90.42 %; H, 6.12 %; N, 2.06 %. Repeat found: C, 90.38 %; H, 6.07 %; N, 2.05 %

**6-methoxy-3-[2-(phenanthren-9-yl)ethyl]-2-[3-(phenanthren-9-yl)propyl]quinoline (177).**



The general procedure was used, 6-(phenanthren-9-yl) hexanal (0.50 g, 1.8 mmol), p-anisidine (0.11 g, 0.86 mmol), NaI (0.13 g, 0.86 mmol), HI (3.2  $\mu$ L) and anisole (86 mL). The crude material was purified by column chromatography RF=0.31 (7 : 3 Hexane/EtOAc) to afford a pale-yellow solid 0.28 g (51%).

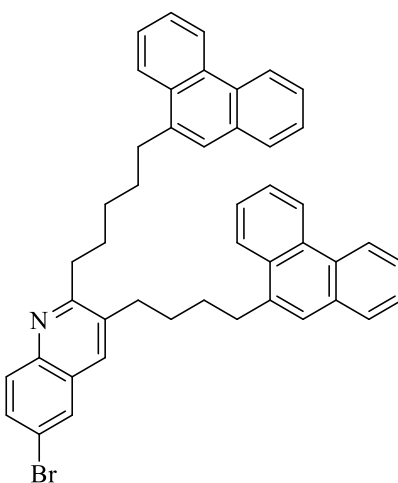
**$^1\text{H NMR}$**  ( $\text{CDCl}_3$ , 400 MHz):  $\delta$  8.76 – 8.68 (m, 2H), 8.67 – 8.60 (m, 2H), 8.12 – 8.05 (m, 2H), 7.91 (d,  $J = 9.0$  Hz, 1H), 7.81 – 7.75 (m, 2H), 7.70 (s, 1H), 7.68 – 7.51 (m, 10H), 7.28 (d,  $J = 3.0$  Hz, 1H), 6.94 (d,  $J = 3.0$  Hz, 1H), 3.90 (s, 3H), 3.17 (apparent dd, second order coupling,  $J_{app} = 8.0, 7.0$  Hz, 2H), 3.11 (apparent dd, second order coupling,  $J_{app} = 8.0, 8.0$  Hz, 2H), 2.97 (apparent dd, second order coupling,  $J_{app} = 8.0, 8.0$  Hz, 2H), 2.82 (apparent dd, second order coupling,  $J_{app} = 8.0, 8.0$  Hz, 2H), 2.00 – 1.80 (m, 8H), 1.63 (quint,  $J = 8.0$  Hz, 2H)

**$^{13}\text{C NMR}$**  ( $\text{CDCl}_3$ , 126 MHz):  $\delta$  159.3, 157.2, 142.6, 136.8, 136.3, 133.9, 133.9, 131.9, 131.8, 131.3, 131.2, 130.8, 130.7, 129.9, 129.6, 129.6, 128.0, 128.0, 126.6, 126.5, 126.4, 126.2, 126.1, 126.0, 126.0, 125.8, 124.5, 124.3, 123.3, 123.2, 122.4, 122.4, 120.9, 104.6, 55.5, 35.5, 33.3, 33.3, 32.3, 30.5, 30.1, 30.0, 29.9, 29.6

**HRMS** (MALDI-FT-ICR) exact mass  $m/z$  calculated for  $C_{47}H_{43}NO$  ( $[M+H]^+$ ) is 638.3378, found 638.3408

**EA** anal. calcd. for  $C_{47}H_{43}NO$ : C, 88.50 %; H, 6.80 %; N, 2.20 %; Found: C, 86.75 %; H, 6.94 %; N, 2.04 %. Repeat found: C, 86.78 %; H, 7.01 %; N, 2.04 %

**6-bromo-3-[2-(phenanthren-9-yl)ethyl]-2-[3-(phenanthren-9-yl)propyl]quinoline (178).**



The general procedure was used, 6-(phenanthren-9-yl) hexanal (0.50 g, 1.8 mmol), 4-bromoaniline (0.15 g, 0.86 mmol), NaI (129 mg, 0.862 mmol), HI (3.2  $\mu$ L) and anisole (86 mL). The crude material was purified by column chromatography  $RF=0.29$  (9 : 1 Hexane/EtOAc) to afford a white solid 0.23 g (40%).

**$^1H$  NMR** ( $CDCl_3$ , 400 MHz):  $\delta$  8.76 – 8.69 (m, 2H), 8.64 (apparent dd, second order coupling,  $J_{app} = 8.0, 7.0$  Hz, 2H), 8.11 – 8.04 (m, 2H), 7.85 (d,  $J = 9.0$  Hz, 1H), 7.81 – 7.74 (m, 3H), 7.68 – 7.51 (m, 12H), 3.17 (apparent dd, second order coupling,  $J_{app} = 8.0, 7.0$  Hz, 2H), 3.11 (apparent dd, second order coupling,  $J_{app} = 8.0, 8.0$  Hz, 2H), 2.96 (apparent dd, second order coupling,  $J_{app} =$

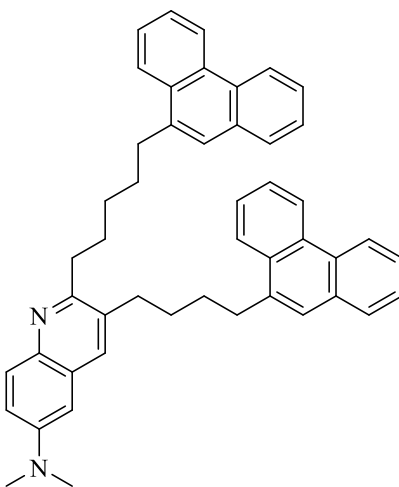
8.0, 8.0 Hz, 2H), 2.81 (apparent dd, second order coupling,  $J_{app} = 8.0, 7.0$  Hz, 2H), 1.99 – 1.79 (m, 8H), 1.65 – 1.55 (m, 2H).

$^{13}\text{C}$  NMR ( $\text{CDCl}_3$ , 101 MHz):  $\delta$  162.5, 145.1, 136.7, 136.1, 134.7, 133.7, 131.9, 131.8, 131.8, 131.3, 131.2, 130.8, 130.7, 130.3, 129.7, 129.6, 128.9, 128.3, 128.0, 128.0, 126.7, 126.6, 126.5, 126.5, 126.3, 126.2, 126.1, 126.0, 126.0, 125.9, 124.5, 124.3, 123.3, 123.2, 122.5, 122.4, 119.3, 35.7, 33.3, 33.3, 32.2, 30.1, 30.0, 29.9, 29.8, 29.2

HRMS (MALDI-FT-ICR) exact mass  $m/z$  calculated for  $\text{C}_{46}\text{H}_{40}\text{BrN}$  ( $[\text{M}+\text{H}]^+$ ) is 686.2417, found 686.2413

EA anal. calcd. for  $\text{C}_{46}\text{H}_{40}\text{BrN}$ : C, 80.45 %; H, 5.87 %; N, 2.04 %; Found: C, 80.15 %; H, 5.96 %; N, 1.97 %. Repeat Found: C, 80.02 %; H, 5.93 %; N, 1.99 %. Repeat Found: C, 80.04 %; H, 5.78 %; N, 1.99 %

***N, N*-dimethyl-3-(4-(phenanthren-9-yl)butyl)-2-(5-(phenanthren-9-yl)pentyl)quinolin-6-amine (179).**



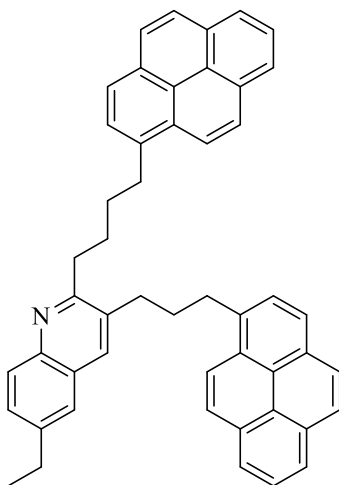
The general procedure was used, 6-(phenanthren-9-yl) hexanal (0.16 g, 0.58 mmol), *N,N*-dimethyl-*p*-phenylenediamine (0.038 g, 0.28 mmol), NaI (0.041 g, 0.28 mmol), HI (1.0  $\mu$ L) and anisole (24 mL). The crude material was purified by column chromatography RF= (7 : 3 Hexane/EtOAc) to afford a pale-yellow green solid 0.045 mg (25%).

**$^1\text{H}$  NMR** ( $\text{CDCl}_3$ , 500 MHz):  $\delta$  8.76 – 8.70 (m, 2H), 8.67 – 8.62 (m, 2H), 8.12 – 8.07 (m, 2H), 7.88 (d,  $J = 9.0$  Hz, 1H), 7.81 – 7.76 (m, 2H), 7.68 – 7.51 (m, 11H), 7.29 (apparent dd, second order coupling,  $J_{app} = 9.0, 3.0$  Hz, 1H), 6.73 (d,  $J = 3.0$  Hz, 1H), 3.17 (apparent dd, second order coupling,  $J_{app} = 8.0, 7.0$  Hz, 2H), 3.12 (apparent dd, second order coupling,  $J_{app} = 8.0, 8.0$  Hz, 2H), 3.05 (s, 6H), 2.95 (apparent dd, second order coupling,  $J_{app} = 8.0, 8.0$  Hz, 2H), 2.81 (apparent dd, second order coupling,  $J_{app} = 8.0, 8.0$  Hz, 2H), 1.96 (quint,  $J = 7.0$  Hz, 3H), 1.87 (quint,  $J = 7.0$  Hz, 6H), 1.63 (quint,  $J = 7.0$  Hz, 2H)

**$^{13}\text{C}$  NMR** ( $\text{CDCl}_3$ , 126 MHz):  $\delta$  157.8, 148.2, 140.8, 136.9, 136.3, 133.7, 133.4, 131.9, 131.9, 131.3, 130.7, 130.7, 129.6, 129.6, 129.1, 128.5, 128.0, 128.0, 126.9, 126.6, 126.5, 126.4, 126.1, 126.1, 126.0, 126.0, 126.0, 125.8, 124.5, 124.4, 123.2, 123.2, 122.4, 122.4, 118.7, 105.0, 40.9, 35.5, 33.3, 33.3, 32.4, 30.6, 30.1, 30.0, 29.9, 29.8

**HRMS** (ESI) exact mass  $m/z$  calculated for  $\text{C}_{48}\text{H}_{46}\text{N}_2$  ( $[\text{M}+\text{H}]^+$ ) is 651.3695, found 651.3732

**6-ethyl-2-[4-(pyren-1-yl) butyl]-3-[3-(pyren-1-yl) propyl] quinoline (180).**



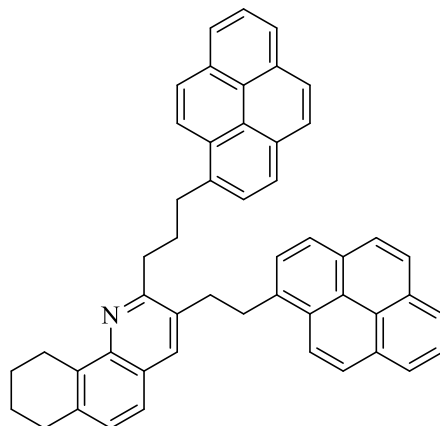
The general procedure was used, 5-(pyren-1-yl) pentanal (0.57 g, 1.9 mmol), 4-ethylaniline (108  $\mu$ L, 0.948 mmol), NaI (142 mg, 0.948 mmol), HI (3.6  $\mu$ L) and anisole (86 mL). The crude material was purified by column chromatography RF=0.27 (8 : 2 Hexane/EtOAc) to afford an off white solid 0.37 g (60%).

**$^1\text{H NMR}$**  ( $\text{CDCl}_3$ , 400 MHz):  $\delta$  8.18 (d,  $J = 9.0$  Hz, 1H), 8.16 – 8.11 (m, 3H), 8.09 – 7.95 (m, 10H), 7.94 – 7.86 (m, 4H), 7.83 (d,  $J = 8.0$  Hz, 1H), 7.79 (s, 1H), 7.72 (d,  $J = 8.0$  Hz, 1H), 7.50 – 7.44 (m, 2H), 3.43 (apparent dd, second order coupling,  $J_{app} = 8.0, 7.0$  Hz, 2H), 3.20 (apparent dd, second order coupling,  $J_{app} = 8.0, 8.0$  Hz, 2H), 1.93 – 1.75 (m, 4H), 2.80 (q,  $J = 8.0$  Hz, 2H), 2.24 (quint,  $J = 8.0$  Hz, 2H), 1.93 – 1.75 (m, 4H), 1.31 (t,  $J = 8.0$  Hz, 3H)

**$^{13}\text{C NMR}$**  ( $\text{CDCl}_3$ , 126 MHz):  $\delta$  160.8, 145.4, 141.7, 136.9, 135.9, 134.6, 133.3, 131.4, 131.4, 130.9, 130.8, 129.9, 129.7, 129.7, 128.7, 128.5, 128.3, 127.5, 127.4, 127.4, 127.3, 127.2, 127.2, 127.1, 127.1, 126.7, 126.5, 125.7, 125.7, 125.1, 125.0, 125.0, 124.9, 124.8, 124.7, 124.7, 124.7, 124.6, 124.4, 123.5, 123.1, 35.6, 33.3, 33.1, 32.3, 32.1, 31.8, 29.7, 28.8, 15.4

**HRMS** (ESI) exact mass  $m/z$  calculated for  $C_{50}H_{41}N$  ( $[M+H]^+$ ) is 656.3273, found 656.3309

**3-(2-(pyren-1-yl)-2-(3-(pyren-1-yl)propyl)-7,8,9,10-tetrahydrobenzo[*h*]quinoline (181).**



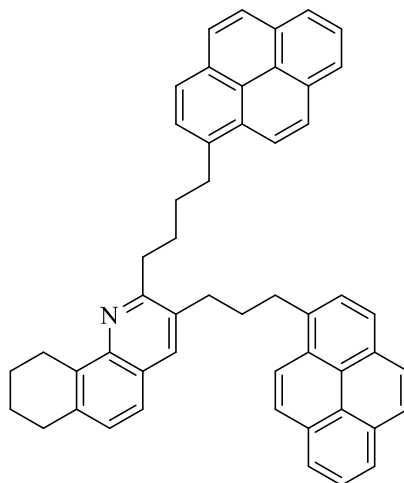
The general procedure was used, 4-(phenanthren-9-yl) butanal (0.30 g, 1.1 mmol), 5,6,7,8-tetrahydronaphthalen-1-amine (73.0  $\mu$ L, 0.53 mmol), HI (1.2  $\mu$ L) and EtOH (20 mL). The crude material was purified by column chromatography (9 : 1 Hexane/EtOAc) to afford an off white solid 0.10 g (30%).

**$^1H$  NMR** ( $CDCl_3$ , 700 MHz):  $\delta$  8.23 (apparent dd, second order coupling,  $J_{app} = 7.0, 7.0$  Hz, 2H), 8.17 (d,  $J = 7.0$  Hz, 1H), 8.13 (d,  $J = 7.0$  Hz, 2H), 8.10 (d,  $J = 7.0$  Hz, 1H), 8.05-7.95 (m, 9H), 7.88 (d,  $J = 8.0$  Hz, 1H), 7.85 (d,  $J = 8.0$  Hz, 1H), 7.83 (s, 1H), 7.55 (d,  $J = 8.0$  Hz, 1H), 7.47 (d,  $J = 8.0$  Hz, 1H), 7.19 (d,  $J = 8.0$  Hz, 1H), 3.59 (apparent dd, second order coupling,  $J_{app} = 8.0, 8.0$  Hz, 2H), 3.47 (apparent dd, second order coupling,  $J_{app} = 8.0, 8.0$  Hz, 2H), 3.44 (apparent dd, second order coupling,  $J_{app} = 6.0, 6.0$  Hz, 2H), 3.21 (apparent dd, second order coupling,  $J_{app} = 8.0, 8.0$  Hz, 2H), 3.15 (t,  $J = 7.0$  Hz, 2H), 2.95 (apparent dd, second order coupling,  $J_{app} = 6.0, 6.0$  Hz, 2H), 2.52 (quint,  $J = 8.0$  Hz, 2H), 2.05 – 1.95 (m, 2H), 1.95 – 1.90 (m, 2H)

$^{13}\text{C}$  NMR ( $\text{CDCl}_3$ , 176 MHz):  $\delta$  159.1, 145.5, 137.1, 137.0, 135.4, 135.0, 134.4, 132.1, 131.4, 131.4, 130.9, 130.8, 130.0, 129.7, 128.8, 128.5, 128.0, 127.5, 127.4, 127.1, 127.1, 127.0, 126.7, 126.5, 125.8, 125.8, 125.7, 125.2, 125.1, 125.0, 125.0, 125.0, 124.8, 124.8, 124.7, 124.6, 124.6, 123.9, 123.6, 123.4, 122.9, 34.9, 34.4, 34.3, 33.1, 30.3, 30.1, 24.9, 23.2, 23.1

HRMS (ESI) exact mass  $m/z$  calculated for  $\text{C}_{50}\text{H}_{39}\text{N}$  ( $[\text{M}+\text{H}]^+$ ) is 654.3116, found 654.3149

**2-(4-(pyren-1-yl)butyl)-3-(3-(pyren-1-yl)propyl)-7,8,9,10-tetrahydrobenzo[*h*]quinoline (182).**



The general procedure was used, 5-(pyren-1-yl) pentanal (0.20 g, 0.70 mmol), 5,6,7,8-tetrahydronaphthalen-1-amine (46  $\mu\text{L}$ , 0.33 mmol), HI (1.3  $\mu\text{L}$ ) and EtOH (15 mL). The crude material was purified by column chromatography (8 : 2 Hexane/EtOAc) to afford an off white solid 0.068 g (30%).

$^1\text{H}$  NMR ( $\text{CDCl}_3$ , 500 MHz):  $\delta$  8.18 (d,  $J = 9.0$  Hz, 2H), 8.14 (t,  $J = 7.0$  Hz, 2H), 8.05 (d,  $J = 8.0$  Hz, 4H), 8.03 – 7.95 (m, 6H), 7.94 – 7.86 (m, 2H), 7.83 (d,  $J = 8.0$  Hz, 1H), 7.77 (d,  $J = 8.0$  Hz, 1H), 7.75 (s, 1H), 7.42 (d,  $J = 8.0$  Hz, 1H), 7.15 (d,  $J = 8.0$  Hz, 1H), 3.41 (apparent dd, second

order coupling,  $J_{app} = 8.0, 8.0$  Hz, 2H), 3.35 – 3.24 (m, 4H), 2.97 – 2.84 (m, 6H), 2.23 (quint,  $J = 7.0$  Hz, 2H), 2.02 (quint,  $J = 8.0$  Hz, 2H), 1.94 – 1.81 (m, 6H)

$^{13}\text{C}$  NMR ( $\text{CDCl}_3$ , 126 MHz):  $\delta$  159.6, 145.3, 137.2, 136.8, 136.1, 134.7, 134.3, 132.2, 131.5, 131.4, 131.0, 130.9, 130.8, 129.9, 129.7, 128.7, 128.6, 127.9, 127.6, 127.5, 127.4, 127.3, 127.3, 127.3, 127.0, 126.6, 126.4, 125.8, 125.7, 125.1, 125.1, 125.0, 124.9, 124.8, 124.8, 124.7, 124.6, 123.8, 123.6, 123.4, 123.2, 35.1, 33.5, 33.2, 32.2, 32.0, 31.7, 30.3, 28.6, 24.8, 23.2, 23.1

**HRMS** (ESI) exact mass  $m/z$  calculated for  $\text{C}_{52}\text{H}_{43}\text{N}$  ( $[\text{M}+\text{H}]^+$ ) is 682.3429, found 682.3467

**EA** anal. calcd. for  $\text{C}_{52}\text{H}_{43}\text{N}$ : C, 91.59 %; H, 6.36 %; N, 2.05 %; Found: C, 89.85 %; H, 6.61 %; N, 2.02 %. Repeat Found: C, 90.21 %; H, 6.60 %; N, 2.04 %. Repeat Found: C, 89.77 %; H, 6.49 %; N, 2.04 %

## 4. Investigating the Mechanistic Details of the HI-Catalyzed MCR. Enhancements in MCR Yields, Selectivity, and Scope

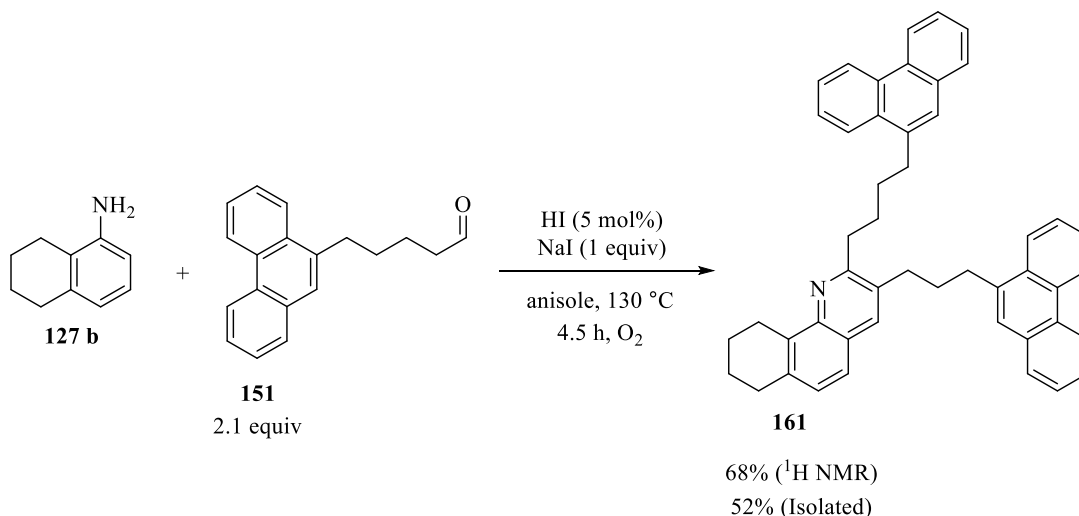
In Chapter 3, I discussed our synthetic approach to access various three-island archipelago asphaltene-like model compounds. Unfortunately, the low-to-moderate yields obtained from the MCRs limits the wide application of the method in its current sub-optimized state. Several key issues contribute to this less-than-optimal performance of the MCR approach, and this chapter is largely concerned with examining these challenges, along with highlighting the solutions developed, leading to a more efficient reaction. Naturally, from this effort, an initial, though highly tentative, picture of the step-by-step mechanism of the reaction will emerge.

Four key issues will be discussed in this chapter. Firstly, 4-ethylaniline was used almost exclusively in Chapter 3 optimization reactions, yet a *truly useful* MCR methodology requires that the reaction work for diverse anilines with varied substitution patterns. The use of bicyclic substrates such as 5,6,7,8-tetrahydronaphthyl-1-amine is more challenging in these reactions and requires further investigation. A second issue is the importance of high concentration of oxygen (ideally, sparging of oxygen gas) to obtain high yields. The working hypothesis is that oxygen is needed for *in situ* formation of hydrogen peroxide ( $\text{H}_2\text{O}_2$ ), which in turn can serve as the key oxidant in the MCR. The role of oxygen is explored further in this chapter. The significant promotional effect of excess iodide also required further exploration. The discussion that follows will show that subtle redox transformations involving iodine are central to the oxidative side of the catalytic MCR mechanism. Finally, I will discuss, the previously alluded to mass balance deficiency, which results from undesired aldehyde oxidation. After these issues are addressed, an

extension in substrate scope will be presented, revealing the full potential of the new optimized MCR procedures.

#### 4.1. Reoptimizing the reaction parameters: conditions and catalysts

Several of the reactions reported in Chapter 3 were repeated, but using 5,6,7,8 tetrahydronaphthyl-1-amine as the aniline substrate instead of 4-ethylaniline. Gratifyingly, the naphthenic quinoline product **161** was formed in 52% isolated yield using the previously described semi-optimal conditions (Eq. 4.1 and Table 4-1).



**Equation 4-1.** Semi-optimal conditions identified from Chapter 3.

As expected, the concentration of the oxidant is critical; when this MCR was performed under an air sparge, instead of pure oxygen, the yield decreased (Table 4-1, entry 2). Surprisingly, reactions performed using I<sub>2</sub> as the precatalyst, instead of HI, returned higher conversions based on NMR analysis. It should be noted, however, that isolation and purification of the archipelago compounds presents a unique challenge, as both higher conversion I<sub>2</sub> reactions and those catalyzed by HI

returned nearly identical isolated yields (Table 4-1, entries 1 and 4). This disparity between isolated yields and NMR conversions is a recurring theme.

It should be further noted that in most cases reported here, where optimization of reaction conditions is the primary concern, only  $^1\text{H}$  NMR conversions are reported. In select cases however, isolated yields are shown in brackets for comparison. A discussion of the challenges associated with isolating the products of these MCRs will follow.

**Table 4-1.** Effects of catalyst loading and the presence of NaI additive on the MCR efficiency.

Entry	Catalyst	Oxidant	Additive	$^1\text{H}$ NMR Conversion (%)
1	HI (5 mol%)	O <sub>2</sub>	NaI	68 (52)
2 <sup>a</sup>	HI (5 mol%)	air	NaI	40 (34)
3	-	O <sub>2</sub>	NaI	11
4	I <sub>2</sub> (5 mol%)	O <sub>2</sub>	NaI	83 (56)
5 <sup>a</sup>	I <sub>2</sub> (5 mol%)	air	NaI	62 (36)
6	HI (500 mol%)	O <sub>2</sub>	-	10
7	HI (100 mol%)		-	16

Reactions are run in anisole at 130 °C for 4.5 h under a constant, rapid bubbling of oxygen, and one equivalent of NaI unless otherwise stated. Yields in brackets indicate isolate yield. <sup>a</sup> During the reaction an air sparge was used in place of the pure O<sub>2</sub> sparge. The amount of secondary amine was not quantified during these control reactions. Conversions acquired by  $^1\text{H}$  NMR, with an internal standard of hexamethyldisiloxane.

Intriguingly, the presence of very high concentrations of HI leads to very low conversions, as shown in the last two entries of Table 4-1. The lower conversions could be attributed just to the excess water, as we noted in an earlier publication.<sup>[126]</sup> However, following the reactions by TLC revealed a further effect of the high acid concentration. In both cases, the formation of the *N*-alkylimine occurs very slowly. We believe that this slow formation of the *N*-alkylimine allows for side reactions to occur, as indicated by the several product spots seen by TLC. In fact, the formation of the *N*-alkylimine is quite pH sensitive: if the reaction is too acidic, imine formation is extremely

slow.<sup>[225]</sup> Thus, by decreasing the rate of *N*-alkylimine formation, the MCR is almost completely suppressed. Statistically, the difference in conversion between stoichiometric and excess HI is negligible, and these results confirm that the reaction is optimal when run using catalytic acid.

While the concentrations of HI (or I<sub>2</sub>) must be kept very low, the acid cannot be completely absent from the MCR. Results in Table 4-1 show that five mol% HI in the presence of O<sub>2</sub> and air affords 68% and 40% conversions by NMR, and 52% and 34% isolated yields, respectively. However, in the absence of HI, the reaction proceeds only to 11% conversion (Table 4-1, entry 3).

Next, the role of water in the reaction was investigated, for comparison to the results reported in a previous publication.<sup>[126]</sup> In that study, the presence of 150 mol% water was optimal for the MCR, with significant decreases observed at either higher or lower concentration. In the present case, we find no statistically significant difference in conversions when the loading of water is increased to 300 mol% (Table 4-2). Conveniently, the concentration of adventitious water in commercial anisole falls within this optimal range, where no effect is seen on the reaction outcome. Therefore, for all subsequent MCRs, anisole was used as received, without pre-drying or addition of precise quantities of water.

**Table 4-2.** Investigation of the semi-optimal conditions to define the optimal amount of water.

Entry	Added Mol% H <sub>2</sub> O	<sup>1</sup> H NMR Conversion (%)
1	-	68 (52)
2	150	73 (50)
3	300	67 (51)

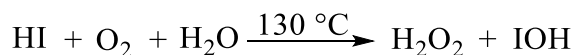
Reactions are run in anisole for 4.5 h under a constant, rapid bubbling of oxygen, unless otherwise stated. Amount of catalyst is 5 mol% HI (57%). The number of additive equivalents is quantified based on the amount of aniline substrate used. The amount of secondary amine was not quantified during these control reactions. Yield in brackets indicate isolate yield. Conversions acquired by <sup>1</sup>H NMR, with an internal standard of hexamethyldisiloxane.

Having established that our MCR procedure is suitable, at least, for 5,6,7,8 tetrahydronaphthyl-*l*-amine and other anilines (*vide infra*), I turned my attention to understanding the role of molecular oxygen and iodide.

#### 4.2. The nature of the oxidant in the multicomponent cyclocondensation: defining and expanding the roles of oxygen and iodide

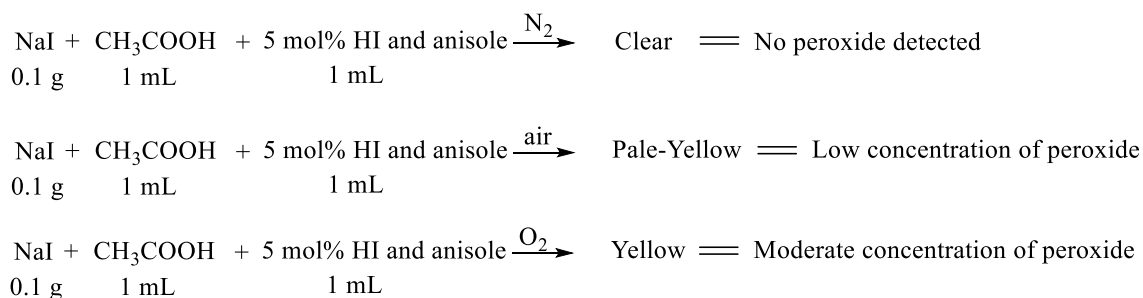
The classical MCR literature limits the role of oxygen to assisting in the final oxidative aromatization to the quinoline product.<sup>[180,181,190,199,226,227]</sup> The experiments described herein challenge this idea. While elevated oxygen pressure (30 psig) improves the yields significantly, compared to reactions conducted under air, this effect does not necessarily indicate the direct involvement of molecular oxygen in the reaction pathway. For example, Guo and co-workers demonstrated that H<sub>2</sub>O<sub>2</sub> is probably the consequential oxidant in these MCR procedures, having observed that the direct addition of one equivalent of H<sub>2</sub>O<sub>2</sub> to the reaction mixture provides improved yields, at least for simple MCRs (see Scheme 3-3).<sup>[196]</sup>

In my work, control experiments determined that heating HI (57%) under an oxygen atmosphere, similar to our MCR reactions, continuously generates a low concentration of H<sub>2</sub>O<sub>2</sub> (Eq. 4-2). This led us to postulate that H<sub>2</sub>O<sub>2</sub>, formed *in situ* under these reaction conditions, is the oxidant that participates in the reaction.



**Equation 4-2.** Reaction equation for the formation of H<sub>2</sub>O<sub>2</sub>.

To confirm the hypothesis of *in situ* formation and direct reactivity of H<sub>2</sub>O<sub>2</sub>, a series of qualitative experiments were performed to detect the presence and measure the effects of H<sub>2</sub>O<sub>2</sub> (Table 4-3). A typical reaction mixture, without aldehyde and aniline substrates, was heated under an oxygen atmosphere and aliquots of this solution were removed and analysed for the presence of H<sub>2</sub>O<sub>2</sub>. Upon adding glacial acetic acid (1 mL) and NaI (0.1 g) (Scheme 4-1), the aliquots became pale- or dark-yellow, indicating the presence of H<sub>2</sub>O<sub>2</sub>.<sup>[228–230]</sup> Unsurprisingly, a similar yellow solution is observed for multicomponent reactions where molecular oxygen is present, indicating that H<sub>2</sub>O<sub>2</sub> is consistently present, albeit in low-to-moderate concentration.<sup>[228–230]</sup> Similarly, the reaction performed under air produces a pale-yellow colouration, presumably due to the substantially lower concentration of peroxide produced. By contrast, when an inert atmosphere is used in place of either air or O<sub>2</sub>, no peroxide is formed, as evidenced by a colorless solution and poor reactivity.



**Scheme 4-1.** Qualitative test designed for testing the presence of H<sub>2</sub>O<sub>2</sub>.<sup>[228–230]</sup>

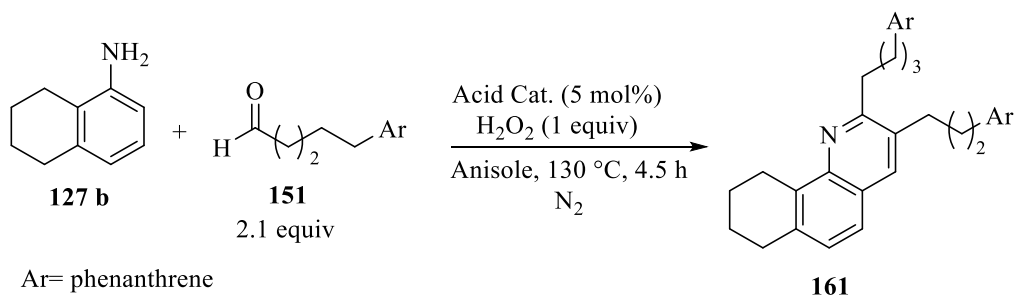
**Table 4-3.** Qualitative testing for the generation of H<sub>2</sub>O<sub>2</sub> under our reaction conditions.

Entry	Oxidant	Presence of H <sub>2</sub> O <sub>2</sub>
1	N <sub>2</sub>	No
2	air	Yes
3	O <sub>2</sub>	Yes

Reactions are run in anisole, 15 mL, for 4.5 h. The amount of catalyst added, 5 mol% HI (57%), is the same amount of catalyst added in our optimization reactions. The amount of H<sub>2</sub>O<sub>2</sub> was determined qualitatively based on a 1 mL aliquot of solution in NaI (0.1 g) /glacial acetic acid (1 mL) test. The solution colour indicates the presence of H<sub>2</sub>O<sub>2</sub>.

It bears emphasizing that these reactions are purely qualitative; no attempt was made to quantify the concentrations of H<sub>2</sub>O<sub>2</sub> produced. However, H<sub>2</sub>O<sub>2</sub> is clearly generated under our reaction conditions and, together with Guo's results, support the role of *in situ* generated H<sub>2</sub>O<sub>2</sub> as an essential oxidant in MCRs, particularly those nominally catalyzed by iodine.

To provide further confirmation, I directly investigated the effects of added H<sub>2</sub>O<sub>2</sub> on the MCR synthesis (Eq. 4-3 and Table 4-4). In order to mimic the supposed slow formation of H<sub>2</sub>O<sub>2</sub> under our reaction conditions, H<sub>2</sub>O<sub>2</sub> (30 wt.%) was added dropwise by syringe pump over the course of the reaction (4.5 h). Following the slow addition, conditions similar to those reported by Guo were evaluated by the addition of one equivalent of H<sub>2</sub>O<sub>2</sub> at the outset. The optimization reactions in sections 4.3. to 4.5. were characterized by <sup>1</sup>H NMR conversions only, used as a quick diagnostic tool for the overall efficiency of the reaction, which also reveals the extent of side-product formation, in conjunction with TLC. This was a “rapid screening” of conditions: the results shown are single point reactions, unless otherwise stated.



**Equation 4-3.** Reaction conditions investigating the role of Brønsted acid catalysts and H<sub>2</sub>O<sub>2</sub>.

**Table 4-4.** Control reactions investigating the affect of slow addition of H<sub>2</sub>O<sub>2</sub> to the MCR.

Entry	Catalyst	Oxidant	<sup>1</sup> H NMR Conversion (%)
1	5 mol% HI	H <sub>2</sub> O <sub>2</sub>	60
2	5 mol% HI	H <sub>2</sub> O <sub>2</sub> / O <sub>2</sub>	63
3	-	H <sub>2</sub> O <sub>2</sub>	12

Reactions are run in anisole for 4.5 h at 130 °C under an atmosphere of nitrogen, unless otherwise stated. The equivalents of H<sub>2</sub>O<sub>2</sub> quantified to aniline. A syringe pump administered one equivalent of H<sub>2</sub>O<sub>2</sub> over 4.5 h at 130 °C (1.0 mL solution containing 0.18 mmol of H<sub>2</sub>O<sub>2</sub>). Conversions acquired by <sup>1</sup>H NMR, with an internal standard of hexamethyldisiloxane.

When performed under an inert atmosphere, slow addition of hydrogen peroxide (Table 4-4, entry 1) returns a similar yield compared to our semi-optimized conditions (Table 4-1, entry 1). Furthermore, sparging oxygen into the reaction mixture combined with the slow addition of H<sub>2</sub>O<sub>2</sub> does not provide a significant increase in yield relative to the H<sub>2</sub>O<sub>2</sub>/inert atmosphere experiment (Table 4-4, entry 2). These results support the argument that oxygen is simply a precursor for another active oxidant, in this case H<sub>2</sub>O<sub>2</sub>. In the course of these studies we performed a range of informative control reactions. The HI catalyst was excluded, leading to a collapse in the yield of the quinoline (Table 4-4, entry 3). This result is partly attributed to the absence of the Brønsted acid catalyst, which is needed to promote the formation of the *N*-alkylimine and subsequent adducts.

Since HI is pivotal for the optimal MCR, we investigated whether other Brønsted acids could perform in a similar mannner. As seen in Table 4-5, other Brønsted acids indeed promote the MCR, however, HI remains optimal, and significantly so. No obvious structure/function relationship among these acids could be discerned, with HCl, TsOH, and HBr returning comparable results. The use of other acids was also studied while investigating the MCR sythesis of continental asphaltene structures, as previously discussed (Chapter 2, Table 2-2).

**Table 4-5.** Control reactions investigating other Brønsted acids and H<sub>2</sub>O<sub>2</sub>.<sup>a</sup>

Entry	Catalyst <sup>b</sup>	Oxidant	<sup>1</sup> H NMR Conversion (%) <sup>c</sup>
1	5 mol% HI	H <sub>2</sub> O <sub>2</sub>	84
2	5 mol% TsOH	H <sub>2</sub> O <sub>2</sub>	62
3	5 mol% HCl	H <sub>2</sub> O <sub>2</sub>	68
4	5 mol% HBr	H <sub>2</sub> O <sub>2</sub>	58
5	5 mol% CH <sub>3</sub> COOH	H <sub>2</sub> O <sub>2</sub>	NC <sup>d</sup>

<sup>a</sup>Reactions were run in anisole using 0.18 mmol H<sub>2</sub>O<sub>2</sub> for 4.5 h at 130 °C under an atmosphere of nitrogen, unless otherwise stated. The H<sub>2</sub>O<sub>2</sub> was added at the beginning of the reaction. <sup>b</sup>The Brønsted acid catalysts were added as 5% *p*-toluenesulfonic acid monohydrate, HI (57%), HCl (37%), HBr (48%) and glacial acetic acid. <sup>c</sup>Conversions determined by <sup>1</sup>H NMR spectroscopy, using an internal standard (hexamethyldisiloxane). <sup>d</sup>NC: no conversion to MCR adduct.

Interestingly, adding a stoichiometric quantity of H<sub>2</sub>O<sub>2</sub> in one portion at the beginning of the reaction, combined with the five mol% HI catalyst, affords a nearly clean conversion of the aldehyde and aniline into the quinoline product, based on inspection of the <sup>1</sup>H NMR spectrum. Only a very small amount of the secondary amine was observed and the overall conversion to the quinoline was 84% (Table 4-5, entry 1). This may be attributed to the higher concentration of H<sub>2</sub>O<sub>2</sub> intercepting the pro-aromatic reactive intermediate, suppressing the reduction of the *N*-alkylimine to secondary amine, diverting it from interfering in the MCR. Further discussion of this process appears in section 4.4.

Glacial acetic acid did not produce any MCR product. Instead, the aldehyde was oxidized to the corresponding carboxylic acid and decarboxylated to give *n*-butylphenanthrene. Only a limited (unquantified) amount of secondary amine was detected by <sup>1</sup>H NMR spectroscopy. The decarbonylation has literature precedent and will become very important in the determination of mass balances.<sup>[231]</sup>

A likely explanation for the results reported in Table 4-5 is that the more highly ionized acids will protonate the imine more readily,<sup>[232,233]</sup> activating it for the cyclocondensation, which is followed by H<sub>2</sub>O<sub>2</sub> oxidation to the final quinoline. Also, it is clear that HI has another, functionally critical role, which is a *promotional effect*, in the MCR process. Since HI is superior to all other Brønsted acids tested, the promotional effect must originate with the iodide ion. The discovery of this secondary role for HI, and the iodide counterion, was fortuitous. This detection changed the direction of our mechanistic research, which included the use of halide additives.

**Table 4-6.** Cationic halogen sources as additives to enhance the MCR yields.

Entry	Catalyst	Additive	<sup>1</sup> H NMR Conversion (%)
1	HI (5 mol%)	NaI (1 equiv)/NBS (1 equiv)	38
2	HI (5 mol%)	NaI (1 equiv)/NIS (1 equiv)	41
3	HI (5 mol%)	NaI (1 equiv)/NCS (1 equiv)	18

Reactions were conducted in anisole at 130 °C with a continuous oxygen sparge for 4.5 h. Conversions acquired by <sup>1</sup>H NMR, with an internal standard of hexamethyldisiloxane. The amount of secondary amine was not quantified.

Our initial experiments investigated the addition of stoichiometric cationic halogen sources to the reaction. The addition of N-bromosuccinimide (NBS), N-iodosuccinimide (NIS) and N-chlorosuccinimide (NCS), provided no enhancement (Table 4-6). In fact all three additives led to decreased conversion. The difference between NBS and NIS is statistically insignificant. This is not entirely surprising because cationic iodine and bromine are used interchangeably in some oxidation reactions.<sup>[234–236]</sup> On the other hand, the poor yield of the NCS reaction was not expected, especially given that catalytic HCl is a reasonable promoter for the MCR (Table 4-6, entry 3). Further experiments were conducted to understand these results.

When the reactions with N-halosuccinimides were run in the absence of HI, a startling trend was observed: catalytic NCS was now superior to the other succinimides. Interestingly, in the absence

of HI, but in the presence of a stoichiometric amount of succinimide, the use of either NBS or NIS led to a decrease in conversion. However, the opposite effect was observed in the presence of NCS. It is possible that in these reactions interhalogen compounds are formed (*i.e.* BrI, ICl) which are both strong oxidizing agents (for promoting aromatization) *and* strong Lewis acids (to promote cyclocondensation).<sup>[237,238]</sup> A combination of such factors may explain the greater effectiveness of NCS and NBS compared to NIS (Table 4-7 entries 1, 3, and 4). Increasing the concentration of the N-halosuccinimide from five mol% to 100 mol% does not improve the yields; in fact, in the case of NBS, the higher concentration actually inhibits conversion. The reasons for this are not yet apparent. It should be noted that the presence of some source of iodide remains essential; the yield of quinoline falls by over 30% if NBS is used without the addition of NaI (Table 4-7, compare entries 1 and 2). Taken together, the secondary effects of iodide ion are real, but remain unexplained.

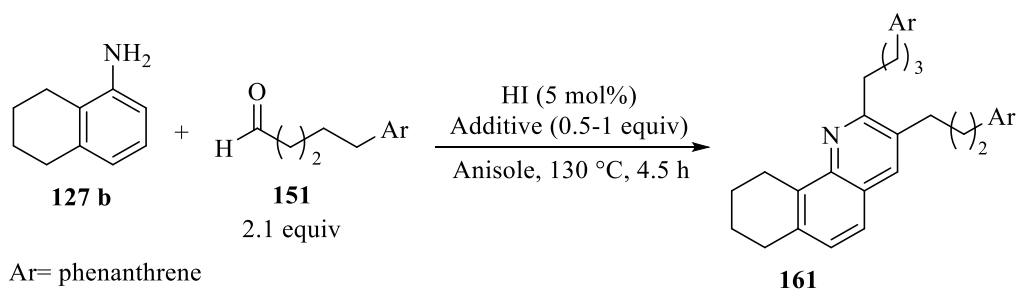
**Table 4-7.** Investigating other cationic halogen sources as catalyst to enhance the MCR yields.

Entry	Catalyst	Additive	<sup>1</sup> H NMR Conversion (%)
1	NBS (5 mol%)	NaI (1 equiv)	50
2	NBS (5 mol%)	-	21
3	NCS (5 mol%)	NaI (1 equiv)	64
4	NIS (5 mol%)	NaI (1 equiv)	37
5	-	NaI (1 equiv)/NBS (1 equiv)	25
6	-	NaI (1 equiv)/NIS (1 equiv)	30
7	-	NaI (1 equiv)/NCS (1 equiv)	63

Reactions were conducted in anisole at 130 °C with a continuous oxygen sparge for 4.5 h. Conversions acquired by <sup>1</sup>H NMR, with an internal standard of hexamethyldisiloxane. The amount of secondary amine was not quantified.

Initially, the equivalent of NaI was added to maintain a high concentration of iodide throughout the reaction, however, the solubility of NaI in anisole is low. Nevertheless, we found a correlation

between the amount of added iodide and the yield of the reaction. The addition of one equivalent of iodide increased the overall yields significantly, but excess iodide (2 equiv) suppresses the yield (see Chapter 3, Table 3-3, entries 5 and 6). This may be due to the deliquescent nature of NaI; a large excess of this salt may absorb water, which must be present in the reaction mixture to mediate proton-transfer reactions. However, for the sake of minimizing the number of additives we returned to the use of catalytic HI, and instead shifted our attention to more soluble sources of iodide.



**Equation 4-4.** General reaction parameters to investigate the differences in iodide additives.

**Table 4-8.** TBAI vs. NaI additives: Evaluating the difference in soluble iodide reagents.

Entry	Oxidant	Additive	<sup>1</sup> H NMR Conversion (%)
1	O <sub>2</sub>	NaI (1 equiv)	68
2 <sup>a</sup>	air	NaI (1 equiv)	40
<b>3</b>	<b>O<sub>2</sub></b>	<b>TBAI (1 equiv)</b>	<b>91</b>
4	O <sub>2</sub>	TBAI (0.5 equiv)	60
5 <sup>a</sup>	air	TBAI (1 equiv)	40
6 <sup>b</sup>	H <sub>2</sub> O <sub>2</sub> (1 equiv)/air	TBAI (1 equiv)	20

Reactions are run in anisole for 4.5 h at 130 °C, unless otherwise stated. The amount of catalyst added in all reactions is 5 mol% HI (57%). <sup>a</sup>The reaction was run open to air, no added oxidants. <sup>b</sup>One equivalent of H<sub>2</sub>O<sub>2</sub> was added at the beginning of the reaction. Conversions acquired by <sup>1</sup>H NMR, with an internal standard of hexamethyldisiloxane. The amount of secondary amine was not quantified.

Replacing NaI with anisole-soluble tetra-*n*-butylammonium iodide (TBAI) provides a very significant improvement in conversion (Table 4-8, entry 3). Surprisingly, this increase in conversion is only observed under pure oxygen; the corresponding reaction run under air returned a much lower yield (Table 4-8, entries 3 and 5). When the concentration of TBAI is decreased by half, the yield falls, indicating that optimized conditions require a full equivalent of TBAI (Table 4-8, entry 4). Replacing the oxygen sparge with one equivalent of H<sub>2</sub>O<sub>2</sub> added at the start of the TBAI-promoted reaction, drastically reduces conversion to quinoline (Table 4-8, entry 6). This we tentatively attribute to peroxide-induced oxidation/decarboxylation of the starting aldehyde, as <sup>1</sup>H NMR analysis of the reaction mixture shows no unreacted aldehyde. At this stage, the effect of soluble iodide is clear, although the actual role this species plays in the MCR remains much less so.

### 4.3. Proposal of the oxygen iodine redox reaction

The obvious promotional effect of iodine on the MCR requires further examination. Iodine is a heavy, electron-rich element, and the high degree of polarizability of its valence shell electrons, combined with a range of accessible oxidation states, confer it a privileged role in synthetic organic chemistry.<sup>[233]</sup> In fact, the reactivity of high-oxidation state iodine can be favourably compared to that of transition metals.<sup>[233]</sup> For our purposes, the variable oxidation state of iodine provides a useful starting point for elucidating its role in the MCR. Our working hypothesis was that the iodide is oxidized by the combination of iodide, molecular oxygen, and water, giving a hypervalent species derived from IOH, which is partially or completely converted to H<sub>2</sub>O<sub>2</sub>. It is this combination of oxidants, produced *in situ* from soluble iodide, that appear to produce optimized yields of the quinoline-core archipelago compounds.

Typically, iodine forms compounds and salts as the iodide, formally in the  $-1$  oxidation state. However, hypervalent iodide compounds are ubiquitous in organic oxidation reactions.<sup>[233]</sup> Many easily isolable and stable hypervalent iodine compounds are known, especially ones coordinated to electron-rich ligands (Figure 4-1).

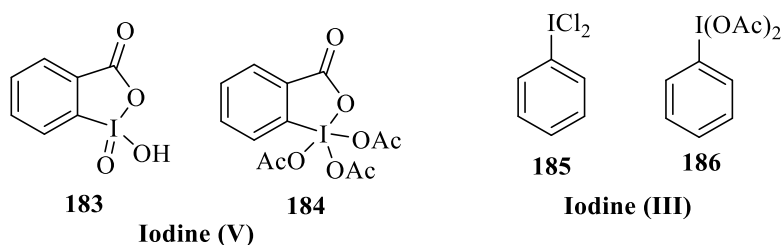


**Figure 4-1.** Examples of hypervalent iodide III and V species.

The formation of hypervalent iodine from iodide and  $\text{H}_2\text{O}_2$  is well-known, particularly in biochemical systems. One notable example is the iodination of tyrosine in thyroid follicles, which is facilitated by  $\text{I}_3^-$ , formed *in situ* from the reaction of iodide and  $\text{H}_2\text{O}_2$  (Figure 4-2).<sup>[239]</sup> We anticipate that a similar equilibrium transformation occurs during the course of the MCR, and that this hypervalent iodide species acts in place of or promotes the formation of  $\text{H}_2\text{O}_2$ .

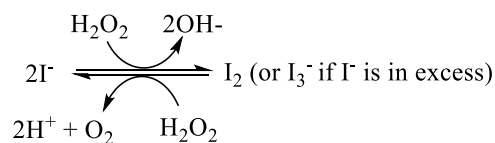


**Figure 4-2.** The formation of the iodonium cation from iodide in the presence of  $\text{H}_2\text{O}_2$ .<sup>[239]</sup>

The kinetics of hypervalent iodine production from  $\text{H}_2\text{O}_2$  is the subject of several publications, some dating as far back as the 1930's.<sup>[240–246]</sup> In 2009, Schmitz addressed the reduction of iodine(+1) by  $\text{H}_2\text{O}_2$ , catalyzed by buffers of various acidities and iodide concentrations.<sup>[247]</sup> Two

equations, in particular, help elucidate the transformations almost certainly occurring in our reactions (Figure 4-3, equation 4 and 5).

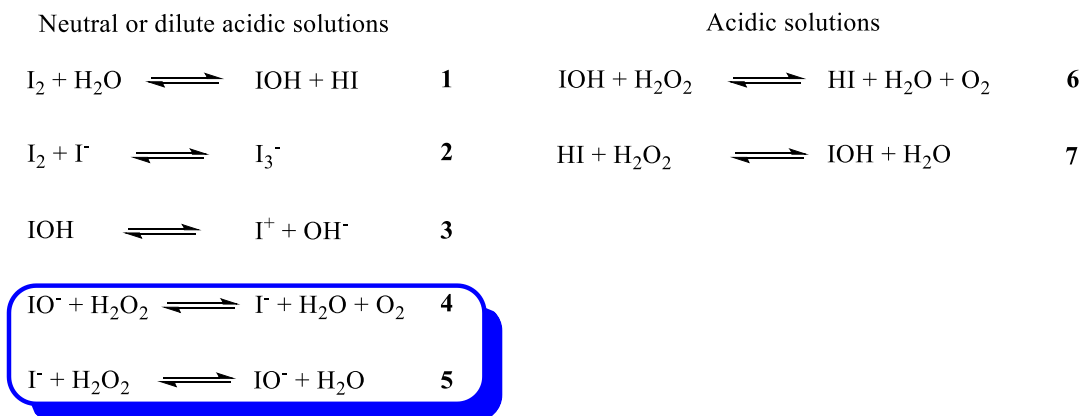


**Figure 4-3.** Equilibria equations postulated in neutral and acidic reaction media.<sup>[247]</sup>

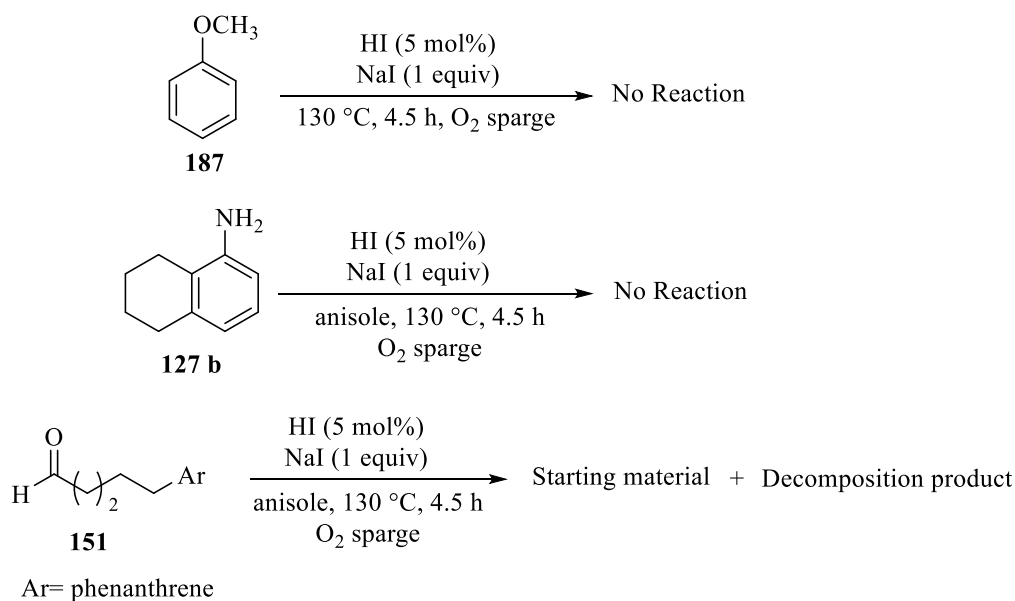
The conditions of the optimized MCR closely resembles a buffered, dilute acidic solution of iodide and a high concentration of oxygen. Thus, the equilibrium transformations shown in equations 4 and 5 (Figure 4-3) are particularly pertinent because they describe the exact reagents ( $I^-$ ,  $H_2O$ ,  $H_2O_2$ , and  $O_2$ ) present in our reaction mixtures, along with the protonated amine. In our system, the equilibrium shown in equation 4 is driven to the left: iodide, water, and  $O_2$  are transformed concomitantly to  $IO^-$  and  $H_2O_2$ , both active oxidants. The  $IO^-$  is metastable in the presence of water (Figure 4-3, Eq. 5), proceeding to hydrogen peroxide and regenerating iodide, *closing a catalytic cycle*.

These equations provide insight into why added water is critical to the MCR, as determined by previous work from our group.<sup>[126]</sup> In addition, the high concentration of iodide ions shifts the equilibrium position of equation 4 to the left, promoting the formation of  $IO^-$  and  $H_2O_2$ . Excess iodide can also combine with  $I_2$ , which can be generated in solution (Figure 4-3, Eq. 1), to form  $I_3^-$  (Figure 4-3, Eq. 2). Equation 5 indicates that at high concentration of iodide, some  $H_2O_2$  is

converted into  $\text{IO}^-$ , returning  $\text{H}_2\text{O}$  to the system. Thus,  $\text{IO}^-$  (sometimes represented as  $\text{I}^+$ ) and  $\text{H}_2\text{O}_2$  are constantly being (re)generated. It can be surmised that  $\text{H}_2\text{O}_2$  can be both an oxidant for product formation and for the generation of  $\text{I}^+$ , some of which is also generated directly from oxygen according to equation 6. Therefore, it is conceivable that this combination (oxygen-derived  $\text{H}_2\text{O}_2/\text{I}^+$ ) works in tandem to promote the oxidation, avoiding diversion of the iminium intermediate. Unfortunately, we cannot easily determine the precise mixture of active oxidant(s) involved, but it does allow us to propose a more detailed mechanistic pathway for the MCR cyclocondensation (Section 4.5.).

#### **4.4. Solving the mass balance deficiency**

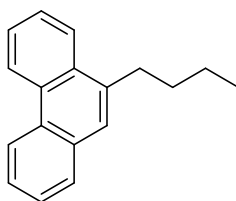
In the ideal, MCR cyclocondensations are highly efficient and atom-economical. We were thus particularly concerned with the mass balance issue observed for many of our core anilines. In one specific optimization reaction (Scheme 4-2), we obtained  $^1\text{H}$  NMR evidence for at least some aldehyde decomposition. We wondered to what extent such decomposition accounts for the low yields obtained from problematic substrates.



**Scheme 4-2.** Background reactions to determine undesirable side reactions resulting in decreased MCR yields.

Background control reactions were conducted to determine the nature and extent of the problem. Our initial inclination was to focus on anisole iodination/oxidation and, more importantly, aniline oxidation and/or electrophilic aromatic substitution. However, control reactions in which HI, O<sub>2</sub>, NaI and aniline were heated in anisole, most of the starting aniline was recovered (Scheme 4-2). Conversely, subjecting one of the aldehydes to identical reaction conditions (Scheme 4-2, bottom reaction) led to the formation of significant aldehyde loss. Although the extent was unquantified, the qualitative data are definitive. This loss of aldehyde can occur by various pathways, including oxidation to carboxylic acid and decarbonylation to the corresponding alkane. Powers and co-workers described a similar oxidation of aldehydes to carboxylic acid in the presence of oxygen and a range of hypervalent iodine reagents.<sup>[248]</sup> In our case, however, no carboxylic acid is produced. Instead, in the presence of H<sub>2</sub>O<sub>2</sub>, the aldehyde undergoes decarbonylation or, once oxidized, rapid decarboxylation. The latter is not an uncommon process, one that has been identified and studied in the decarboxylation of pyruvic acid.<sup>[249]</sup> In our case, the formation of

H<sub>2</sub>O<sub>2</sub> in high concentration leads to the formation of *n*-butylphenanthrene **188**, isolated by column purification (Figure 4-4). In addition, at the elevated reaction temperature, the potential for aldehyde decarbonylation is also possible. However, without the use of a transition metal catalyst (typically palladium or rhodium), decarbonylation is likely too slow to be competitive with oxidation/decarboxylation.<sup>[250,251]</sup>

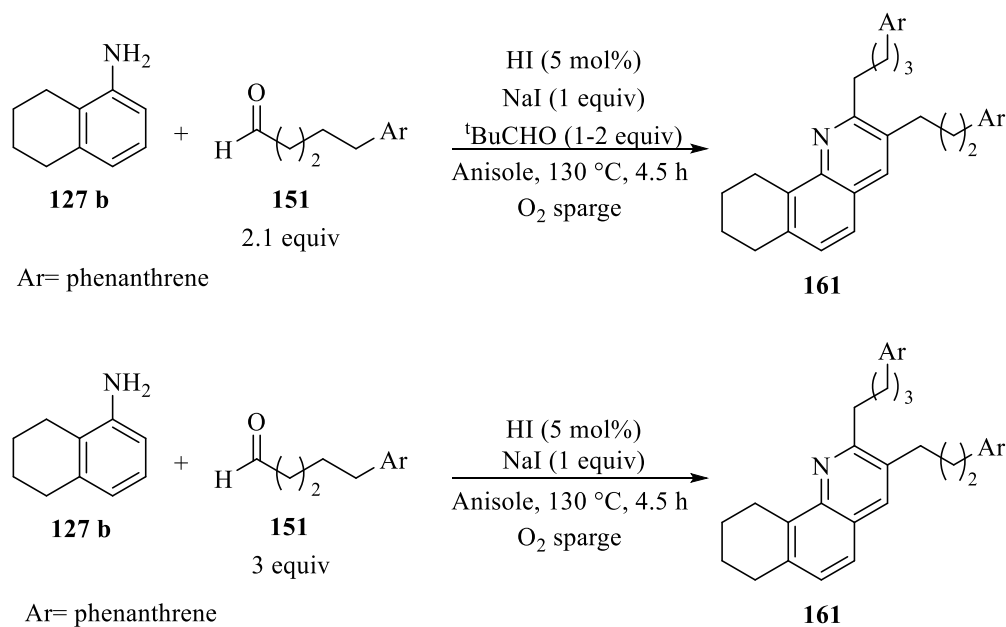


**188**

**Figure 4-4.** *n*-Butylphenanthrene from oxidative decomposition of aldehyde **151**.

We sought to limit oxidative decomposition of our valuable aldehyde by conducting the reaction in the presence of a more reactive sacrificial aldehyde that would not compete with MCR imine formation. The presence of one equivalent of pivaldehyde indeed suppresses undesired decarboxylation, increasing the isolated yields significantly (Scheme 4-3, Table 4-9, entry 1). By comparison, a reaction performed without pivaldehyde, but under otherwise identical conditions returns only 68% of the desired quinoline (see Table 4-8, entry 1, above). This procedure, however, requires that the *N*-alkylimine be pre-formed stoichiometrically before the pivaldehyde is added. Without this change, a mixture of *N*-alkylimines was obtained, presumably due to competitive imine formation. In any case, this result clearly indicates that the MCR aldehyde suffers from oxidative decarboxylation, leading to diminished MCR yields. The addition of a second equivalent of pivaldehyde has an unexpectedly deleterious effect (Scheme 4-3, Table 4-9, entry 2): the sacrificial aldehyde evidently reacts competitively and irreversibly with the external oxidants

(H<sub>2</sub>O<sub>2</sub> or IO<sup>-</sup>) present in the medium, leading again to secondary amine formation. In this experiment, a significant, but unquantified amount of the secondary amine was recovered.



**Scheme 4-3.** The effect of a sacrificial aldehyde addition (pivaldehyde or an excess of substrate) to inhibit decomposition of the aldehyde **151**.

**Table 4-9.** Effects of sacrificial aldehyde: <sup>t</sup>BuCHO vs. three equivalents of compound **151**.

Entry	Solvent	Temp. (°C)	Oxidant	Additive	<sup>1</sup> H NMR Conversion (%)
1 <sup>a</sup>	anisole	130	O <sub>2</sub>	<sup>t</sup> BuCHO (1 equiv)	85
2 <sup>a</sup>	anisole	130	O <sub>2</sub>	<sup>t</sup> BuCHO (2 equiv)	34
3	anisole	130	O <sub>2</sub>	<b>151</b> (3 equiv)	> 95

Reactions were conducted using five mol% HI (57%) over a reaction period of 4.5 h. All reactions included NaI (1 equiv). <sup>a</sup>Entries one and two, the reaction is performed step wise with the imine generated *in situ* in the presence of the HI catalyst. Once the imine is formed, the second equivalent of aldehyde and pivaldehyde is added and the reaction run for the allotted time. Conversions acquired by <sup>1</sup>H NMR, with an internal standard of hexamethyldisiloxane. The amount of secondary amine obtained as a biproduct was not quantified.

To circumvent aldehyde decomposition and suppress secondary amine formation, we resorted to the addition of an extra equivalent of “precious” substrate aldehyde, a benign (but inelegant)

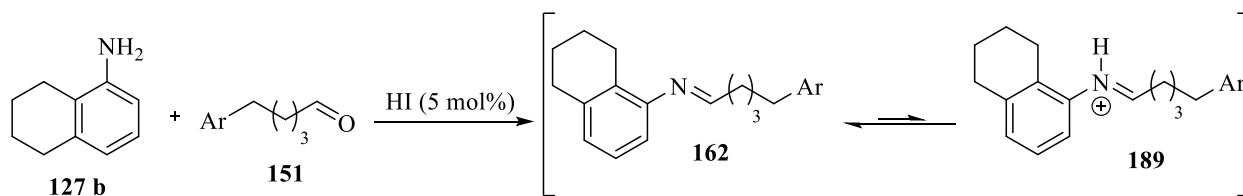
sacrificial reductant. In the presence of three equivalents of compound **151**, an almost quantitative yield of quinoline was isolated (Scheme 4-3, Table 4-9, entry 3). Obviously, using excess substrate aldehyde is not acceptable synthetically, given that the compound is neither commercially available nor trivial to prepare.

#### **4.5. Ramifications of control reactions and MCR optimization: a refined mechanistic rationale**

The cumulative results obtained allow for a plausible, dual-catalytic mechanism to be proposed for the cyclocondensation between alkyl-tethered  $\alpha,\omega$ -aryl aldehydes and substituted anilines. The mechanistic proposal builds on typical proposals from the literature, but introduces significant variations, particularly as it relates to the role of iodide.

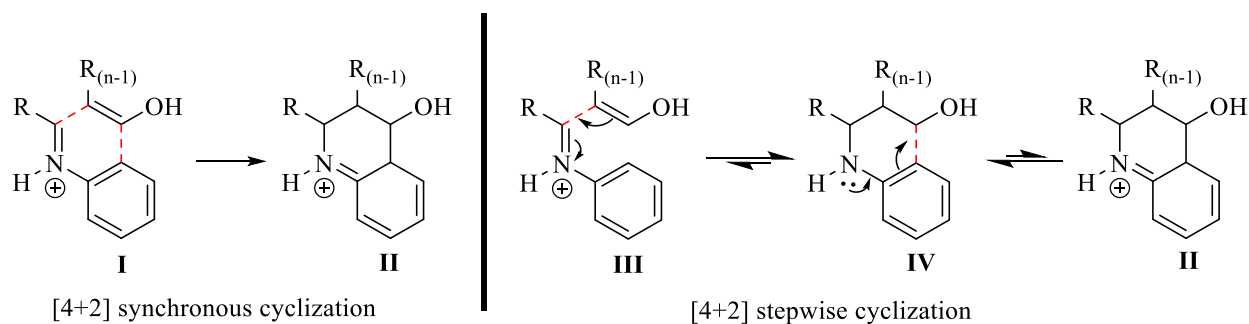
The first step in the MCR is a simple acid-catalyzed condensation between one equivalent of aldehyde **151** and aniline **127b** to give the neutral imine **162** and a catalytic amount of iminium cation **189** (Scheme 4-4). Beyond this point, there are divergent proposals regarding the fate of the imine, depending on substrate and reaction parameters. Traditional rationales invoke either an imino-Diels-Alder reaction or a stepwise Mannich-like cyclocondensation of the imine with the enol tautomer of the second aldehyde. Another, less frequently invoked rationale,<sup>[183]</sup> requires equilibrium formation of an enamine tautomer, which then undergoes one-electron oxidation to give a radical cation intermediate (further discussed in Chapter 5).

In the imino Diels-Alder/Mannich-like cycloaddition, the iminium cation **189** (Scheme 4-4) is highly electrophilic, inducing much lower activation barrier(s) for subsequent condensation/cyclization steps.



**Scheme 4-4.** Protonation of imine to form the activated diene iminium intermediate.

The cyclocondensation occurs either by a stepwise or concerted process. The aldehyde enol can act as the dienophile in an inverse electron-demand Diels-Alder reaction (Scheme 4-5, **I**→**II**). Or, a completely asynchronous (i.e., stepwise) pathway where the enol initially adds to the iminium intermediate, followed by electrophilic arylation of the pendant protonated aldehyde. This is, essentially, a Friedel-Crafts reaction (Scheme 4-5, **III**→**IV**→**II**).

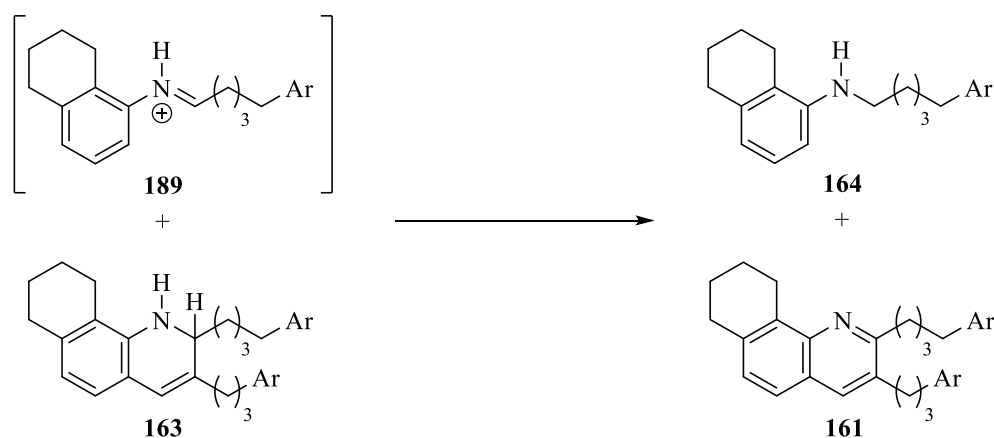


**Scheme 4-5.** Cyclization process to form the tetrahydroquinoline intermediate.

Extensive density functional theory (DFT) has been conducted to discern the mechanistic pathway of the closely related Povarov reaction.<sup>[252,253]</sup> DFT computations by Domingo and co-workers showed that the mechanism can be *both* concerted and stepwise processes, depending on the reaction conditions.<sup>[252]</sup> Based on our results, we suggest that this cyclocondensation proceeds via a stepwise process. This hypothesis is based on the analysis of the scope of the reaction (Chapter 3), which indicates that the cyclization is highly sensitive to slight variations in the position and

electronic nature of the aniline substituents. Furthermore, we speculate that the cyclization event is likely to be comparatively much slower than the iminium reaction, possibly due to torsional distortions that inhibit good orbital overlap (Scheme 4-5, **IV**). This prediction requires further extensive experimentation or, better, computational modeling.

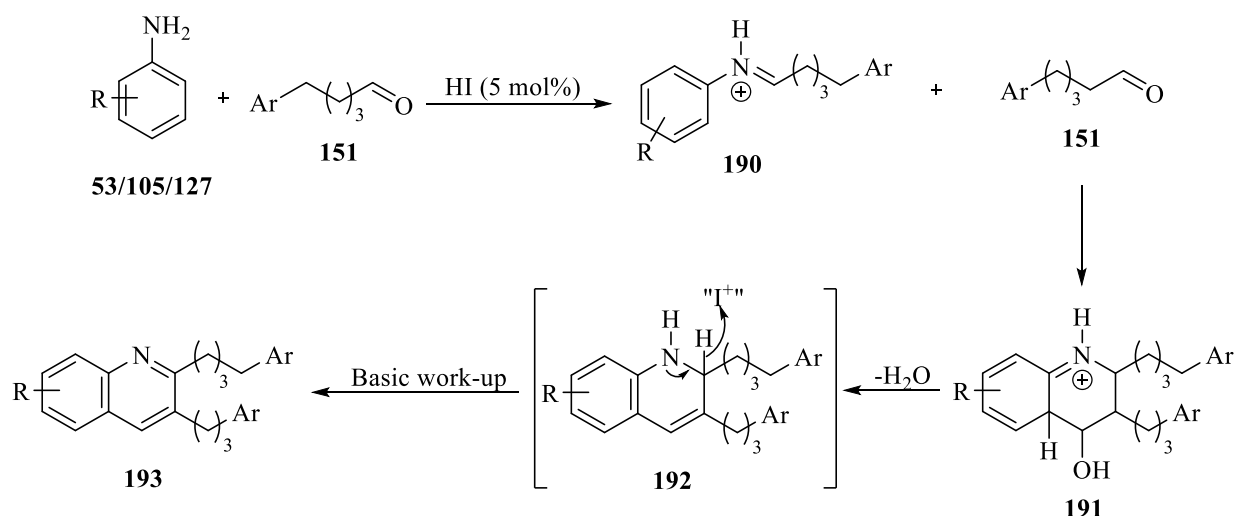
At this point, our mechanistic proposal diverges from well-established precedent and literature proposals. Among the most significant challenges in this reaction is to suppress the participation of the protonated *N*-alkylimine as the oxidant for the aromatization step, leading to the formation of the undesired secondary amine **164** (Eq. 4-5).



**Equation 4-5.** Undesired secondary amine formation resulting from aromatization to generate the final quinoline compound.

To inhibit the formation of secondary amine, we focused on increasing the concentration of ‘external’ oxidants,  $\text{H}_2\text{O}_2/\Gamma^+$ , by elucidating and optimizing the native oxidants involved in the aromatization step. As a result, the unproductive imine reduction was reduced substantially or eliminated entirely.

The culmination of the individual events can be combined into a full catalytic mechanism (Scheme 4-6). Subsequent to acid-catalyzed *N*-alkylimine formation, the iminium intermediate condenses with the enol tautomer, which undergoes a stepwise dipolar cyclization to generate the transient iminium intermediate **191**. Tautomerization and dehydration affords the partially rearomatized dihydroquinoline **192**. From control reactions run with a deficiency of oxidant, the concentration of peroxide is too low to trap the pro-aromatic intermediate, leaving only the hydride transfer to the iminium intermediate. However, with efficient formation of the  $I^+/H_2O_2$  combination, the inorganic oxidation effectively competes with the unproductive consumption of the *N*-alkylimine.



**Scheme 4-6.** Proposed MCR mechanism which incorporates the new oxidants identified from the control reactions.

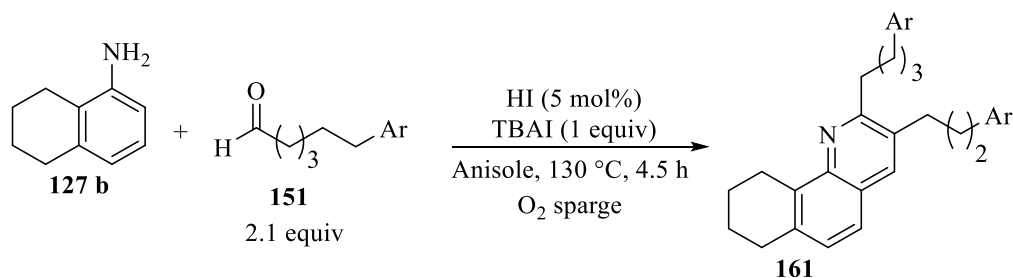
Although, it is unclear which oxidant is kinetically dominant, it is likely the entire mixture of species (IOH,  $I_3^-$ , and  $H_2O_2$ ) act together to enhance the rate of productive aromatization. The rearomatization is believed to occur by one of two potential pathways: (1) hydrogen peroxide formally abstracts hydride to yield the fully aromatized quinoline,<sup>[196,254]</sup> or (2) in the presence of iodide/iodine(I), a catalytic oxidation occurs, with regeneration of buffered HI, the active (dual)

catalyst (see Figure 4-3). In either event, when the concentration of soluble oxidant(s) is high, the undesirable reactions are inhibited, substantially enhancing product yields.

#### 4.6. Scope of the MCR under reoptimized reaction parameters. Problematic substrates

In conjunction with our improved understanding of the active catalysts and redox systems, we re-evaluated the cyclocondensation reaction for a limited number of substituted anilines. The compounds were selected to highlight differences with the partly optimized conditions described in Chapter 3 and to confirm the generality of the revised oxidation conditions. The compounds represent the most challenging aniline derivatives; all returned low yields yet remain substrates of particular interest to our collaborators.

The precise conditions implemented retain the use of anisole as solvent, combining the aniline substrate (1 equiv), 5-(phenanthren-9-yl) pentanal (2.1 equiv), HI catalyst (5 mol%, 57% aq), and TBAI (1 equiv) under an oxygen sparge, with heating to 130 °C (bath temperature). A reaction time of 4.5 h was sufficient for all of the reactions to reach completion (Eq. 4-6).



**Equation 4-6.** Optimal reaction conditions implemented to form a few quinoline-cored three island archipelago compounds.

Using these conditions, four anilines were reinvestigated: aniline, 5,6,7,8-tetrahydronaphylen-*l*-amine, 2,3-dimethylaniline, and 1-aminonaphthylene, shown as red fragments in Figure 4-5. Yields of the archipelago adducts, as reported in Chapter 3, were 52% (**161**), 41% (**170**), 40% (**171**), and 26% (**178**), respectively (Figure 4-5).

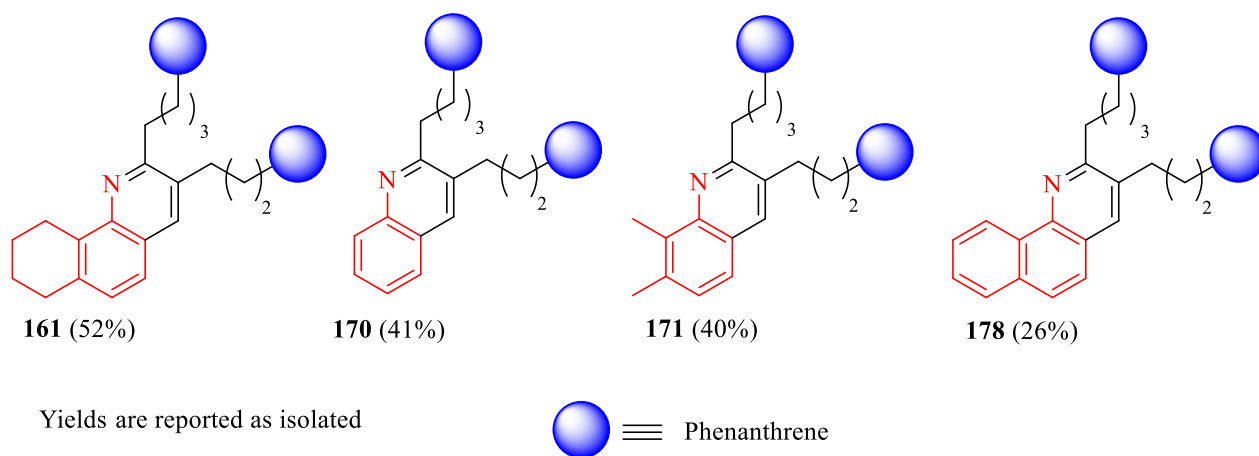


**Figure 4-5.** Isolated quinoline-core compounds synthesized using NaI as the iodide source in Chapter 3.

The new reaction conditions resulted in a significant enhancement for all but one of the substrates. In particular, the yields for 5,6,7,8-tetrahydronaphylen-*l*-amine, aniline, and 1-aminonaphthylene derivatives increased (Figure 4-6). For both 5,6,7,8-tetrahydronaphylen-*l*-amine and aniline, <sup>1</sup>H NMR yields increased to ≥ 90%. The <sup>1</sup>H NMR yield from 1-aminonaphthylene, the most challenging substrate, nearly doubled, giving a still modest 50% yield of benzoquinoline **178** (Figure 4-6). Only 2,3-dimethylaniline failed to afford a significantly improved yield.

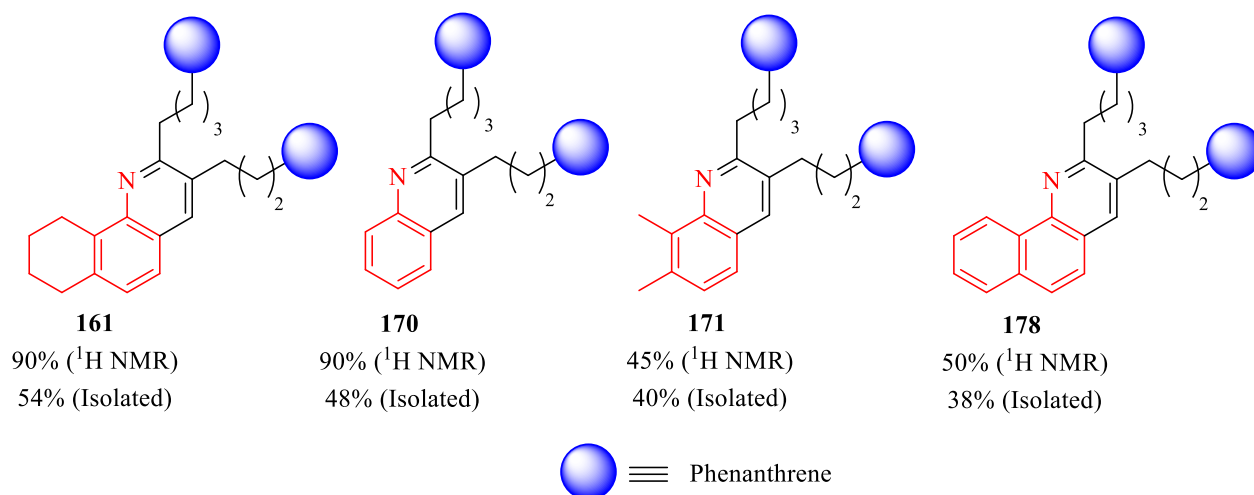
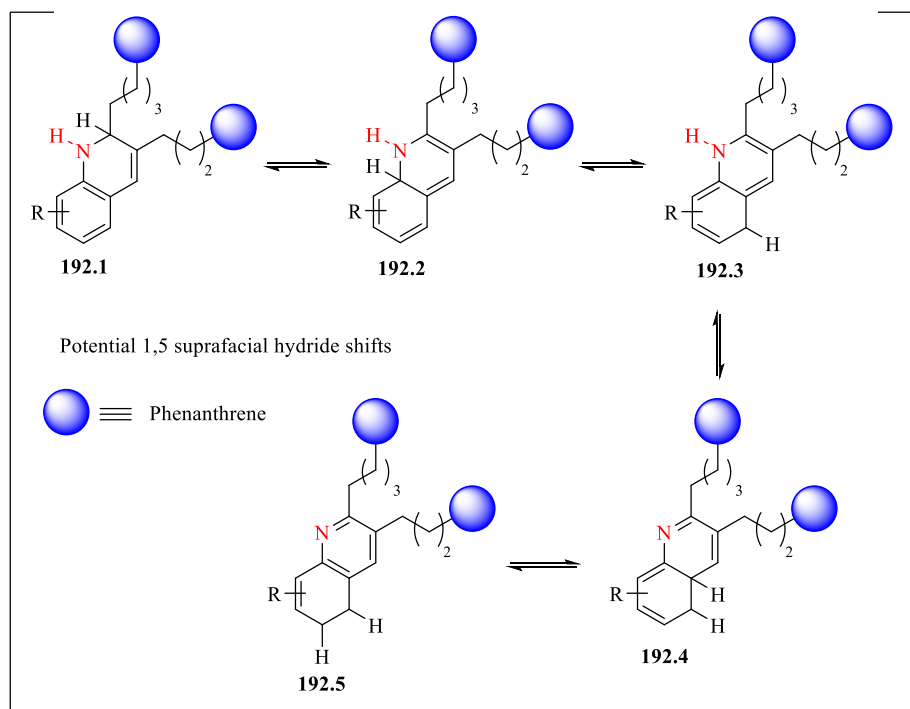


**Figure 4-6.** Three-island quinoline-core archipelago-like structures synthesized from the new optimal conditions.

For 2,3-dimethylaniline, close inspection of product mixture showed that the amount of secondary amine by-product was approximately equivalent to that of the desired product. One reasonable explanation is that subtle differences in the conformations of the pro-aromatic intermediates alter the relative effectiveness of the inorganic oxidants (i.e., Scheme 4-6, intermediate **192**). More likely, perhaps, is that the loss of hydride is extremely facile for this intermediate, outpacing the rate of peroxide/iodonium generation. Among other contributions, the high reaction temperature (130 °C) raises the possible intervention of suprafacial 1,5-hydride shift(s) prior to oxidative aromatization, changing the relative accessibility of the hydride location (Scheme 4-7). This possibility has not been investigated.



**Scheme 4-7.** Potential subsequent 1,5 hydride shifts that may occur during the final stages of the MCR.

At this stage, the most noteworthy deficiency in the archipelago MCR process is isolation of pure, crystalline products in yields comparable to the NMR yields. Purification of the benzoquinoline compounds by recrystallization has not proved fruitful. Column chromatography, which is perhaps the most ubiquitous bench-scale separation technique in synthetic organic chemistry, is of only limited utility here. In Chapter 3, the desired products were easily obtained from the column in high purity, albeit in low yields. However, after the reaction was optimized, the same adducts behave much differently – only a portion of the desired material is eluted from the column. Chromatography on basic alumina is equally unsuccessful. I suspect a combination of self-association and irreversible absorption to the Lewis acidic sites on the chromatography support prevents elution, leaving much of the adduct on the column. The most common solution to this challenge is to ‘prewash’ the column with triethylamine – a strong enough base to passivate the

most acidic binding sites. This procedure also fails to improve the elution of the quinoline. Efforts continue to address this problem, either with reverse-phase supports or the use of amine-functionalized silica gel, which is known to simplify purification of strongly basic eluents.<sup>[255]</sup>

Purification issues aside, we recently re-discovered that sunlight and oxygen induce decomposition of polycyclic quinolines.<sup>[256–258]</sup> We now understand that a similar decomposition *on the benchtop* plays a significant role in the purification challenges we encountered. In order to address this problem, we are currently investigating procedures that will allow us to purify the products under strictly anaerobic conditions. Other potential options are discussed in Chapter 5, along with some unpromising results.

In summary, we have successfully synthesized a range of difficult-to-prepare highly elaborated benzoquinoline model compounds, providing (for now) optimized reaction conditions and continued diversification of accessible structures. This procedure has afforded gram quantities of pure archipelago model asphaltene, which our collaborators are using for a comprehensive investigation of aggregation and precipitation behaviour, as well as standards for developing new analytical methods to characterize the heaviest fractions of crude oils.

## **Experimental Section**

General experimental information can be found in Chapter 3. I<sub>2</sub>, aqueous HI (57 wt.%), aqueous HCl (37 wt.%), HBr (48 wt.%), H<sub>2</sub>O<sub>2</sub> (30 wt.%), *p*-toluenesulfonic acid monohydrate, NBS, NCS, NIS, NaI, TBAI, pivaldehyde, and anisole were purchased from commercial sources and used as received.

The structural characterization of the MCR quinoline compounds depicted in section 4.1.9. is provided in Chapter 3. For the MCR optimizations, I was assisted by (then) undergraduate co-worker, Mark Aloisio.

#### 4.7. MCR optimization: general synthetic procedure

5-(Phenanthren-9-yl) pentanal (0.10 g, 0.38 mmol) was added to a 50 mL three-neck RBF flask equipped with a reflux condenser. 5,6,7,8-Tetrahydronaphthalen-1-amine (25  $\mu$ L, 0.18 mmol), additives (1 equiv), Brønsted acid catalyst (5-500 mol%) was dissolved in anisole (15 mL) and heated 130 °C (bath temperature) for 4.5 h. The reaction mixture was cooled to rt, basified with 10% aqueous NaOH, and washed with CH<sub>2</sub>Cl<sub>2</sub>. The organic layer was separated, washed with saturated sodium bisulfite (15 mL), NaBH<sub>4</sub> (100 mg) in H<sub>2</sub>O (15 mL), saturated brine and dried over Na<sub>2</sub>SO<sub>4</sub>, filtered, and the solvent was removed under reduced pressure. Hexamethyldisiloxane (4.3  $\mu$ L, 0.020 mmol) was added as an internal standard for <sup>1</sup>H NMR analysis.

(T4-1.1) The general procedure was used, NaI (0.027 mg, 0.18 mmol) and HI (0.7  $\mu$ L) (<sup>1</sup>H NMR conversion: 68%, Isolated yield: 52%)

(T4-1.2) The general procedure was used, NaI (0.027 g, 0.18 mmol), HI (0.7  $\mu$ L), open to air (<sup>1</sup>H NMR conversion: 40%, Isolated yield: 34)

(T4-1.3) The general procedure was used, NaI (0.027 g, 0.18 mmol) (<sup>1</sup>H NMR conversion: 11%)

(T4-1.4) The general procedure was used, NaI (0.027 g, 0.18 mmol) and I<sub>2</sub> (0.002 g) (<sup>1</sup>H NMR conversion: 83%, Isolate yield: 56%)

(T4-1.5) The general procedure was used, NaI (0.027 g, 0.18 mmol), I<sub>2</sub> (0.002 g), and open to air (<sup>1</sup>H NMR conversion: 62%, Isolate yield: 36%)

(T4-1.6) The general procedure was used and HI (68 μL) (<sup>1</sup>H NMR conversion: 10%)

(T4-1.7) The general procedure was used and HI (14 μL) (<sup>1</sup>H NMR conversion: 16%)

(T4-2.1) The general procedure was used, NaI (0.027 g, 0.18 mmol) and HI (0.7 μL) (<sup>1</sup>H NMR conversion: 68%, Isolated yield: 52%)

(T4-2.2) The general procedure was used, NaI (0.027 g, 0.18 mmol), H<sub>2</sub>O (4.9 μL, 0.27 mmol) and HI (0.7 μL) (<sup>1</sup>H NMR conversion: 73%, Isolated yield: 50%).

(T4-2.3) The general procedure was used, NaI (0.027 g, 0.18 mmol), H<sub>2</sub>O (9.8 μL, 0.55 mmol), and HI (0.7 μL) (<sup>1</sup>H NMR conversion: 67%, Isolated yield: 51%).

(T4-3.1) A mixture of anisole (15 mL) and hydroiodic acid (0.7 μL) was added into a 25 mL round-bottom flask equipped with a magnetic stir bar and heated to 130 °C (bath temperature), under inert atmosphere, for 1 h. Following the 1 h stir period, a 1 mL aliquot of solution was removed and added to a mixture of glacial acetic acid (1 mL) and NaI (0.1 g). The resulting solution remained clear indicating no peroxide formation.

(T4-3.2) A mixture of anisole (15 mL) and hydroiodic acid (0.7 μL) was added into a 25 mL round-bottom flask equipped with a magnetic stir bar and heated to 130 °C (bath temperature), open to air, for 1 hr. Following the 1 h stir period, a 1 mL aliquot of solution was removed and added to a mixture of glacial acetic acid (1 mL) and NaI (0.1 g). The resulting solution turned pale-yellow indicating a low concentration of peroxide has formed.

**(T4-3.3)** A mixture of anisole (15 mL) and hydroiodic acid (0.7  $\mu$ L) was added into a 25 mL round-bottom flask equipped with a magnetic stir bar, sparged with O<sub>2</sub>, and heated to 130 °C (bath temperature) for 1 h. Following the 1 h stir period, a 1 mL aliquot of solution was removed and added to a mixture of glacial acetic acid (1 mL) and NaI (0.1 g). The resulting solution turned yellow indicating a medium concentration of peroxide has formed.

**(T4-4.1)** The general procedure was used, HI (0.7  $\mu$ L), H<sub>2</sub>O<sub>2</sub> (30 wt%, 6  $\mu$ L in 1 mL of anisole, 0.18 mmol) was added by syringe pump under inert atmosphere (<sup>1</sup>H NMR conversion: 60%)

**(T4-4.2)** The general procedure was used, HI (0.7  $\mu$ L) and H<sub>2</sub>O<sub>2</sub> (30 wt%, 6  $\mu$ L in 1 mL of anisole, 0.18 mmol) was added by syringe pump with sparging O<sub>2</sub> (<sup>1</sup>H NMR conversion: 63%)

**(T4-4.3)** The general procedure was used, H<sub>2</sub>O<sub>2</sub> (30 wt%, 6  $\mu$ L in 1 mL of anisole, 0.18 mmol) was added by syringe pump under inert atmosphere (<sup>1</sup>H NMR conversion: 12%)

**(T4-5.1)** The general procedure was used, HI (0.7  $\mu$ L), H<sub>2</sub>O<sub>2</sub> (30 wt%, 6  $\mu$ L, 0.18 mmol), under inert atmosphere (<sup>1</sup>H NMR conversion: 84%)

**(T4-5.2)** The general procedure was used, *p*-toluenesulfonic acid monohydrate (1.7 mg, 0.009 mmol), H<sub>2</sub>O<sub>2</sub> (30 wt%, 6  $\mu$ L, 0.18 mmol), under inert atmosphere (<sup>1</sup>H NMR conversion: 62%)

**(T4-5.3)** The general procedure was used, HCl (0.3  $\mu$ L), H<sub>2</sub>O<sub>2</sub> (30 wt%, 6  $\mu$ L, 0.18 mmol), under inert atmosphere (<sup>1</sup>H NMR conversion: 68%)

**(T4-5.4)** The general procedure was used, HBr (0.5  $\mu$ L), H<sub>2</sub>O<sub>2</sub> (30 wt%, 6  $\mu$ L, 0.18 mmol), under inert atmosphere (<sup>1</sup>H NMR conversion: 58%)

**(T4-5.5)** The general procedure was used, glacial acetic acid (0.5  $\mu$ L), H<sub>2</sub>O<sub>2</sub> (30 wt%, 6  $\mu$ L, 0.18 mmol), under inert atmosphere (NC = no conversion).

**(T4-6.1)** The general procedure was used, NaI (0.027 g, 0.18 mmol), HI (0.7  $\mu$ L), NBS (0.032 g, 0.18 mmol) ( $^1\text{H}$  NMR conversion: 38%)

**(T4-6.2)** The general procedure was used, NaI (0.027 g, 0.18 mmol), HI (0.7  $\mu$ L), NIS (0.041 g, 0.18 mmol) ( $^1\text{H}$  NMR conversion: 41%)

**(T4-6.3)** The general procedure was used, NaI (0.027 g, 0.18 mmol), HI (0.7  $\mu$ L), NCS (0.024 g, 0.18 mmol) ( $^1\text{H}$  NMR conversion: 18%)

**(T4-7.1)** The general procedure was used, NaI (0.027 g, 0.18 mmol), NBS (0.002 g, 0.009 mmol) ( $^1\text{H}$  NMR conversion: 50%)

**(T4-7.2)** The general procedure was used, NaI (0.027 g, 0.18 mmol), NBS (0.002 g, 0.009 mmol) ( $^1\text{H}$  NMR conversion: 21%)

**(T4-7.3)** The general procedure was used, NaI (0.027 g, 0.18 mmol), NCS (0.001 g, 0.009 mmol) ( $^1\text{H}$  NMR conversion: 64%)

**(T4-7.4)** The general procedure was used, NaI (0.027 g, 0.18 mmol), NIS (0.002 g, 0.009 mmol) ( $^1\text{H}$  NMR conversion: 37%)

**(T4-7.5)** The general procedure was used, NaI (0.027 g, 0.18 mmol), NBS (0.032 g, 0.18 mmol) ( $^1\text{H}$  NMR conversion: 25%)

**(T4-7.6)** The general procedure was used, NaI (0.027 g, 0.18 mmol), NIS (0.041 g, 0.18 mmol) ( $^1\text{H}$  NMR conversion: 30%)

**(T4-7.7)** The general procedure was used, NaI (0.027 g, 0.18 mmol), NCS (0.024 g, 0.18 mmol) ( $^1\text{H}$  NMR conversion: 63%)

**(T4-8.1)** The general procedure was used, NaI (0.027 g, 0.18 mmol), HI (0.7  $\mu$ L) ( $^1$ H NMR conversion: 68%).

**(T4-8.2)** The general procedure was used, NaI (0.027 g, 0.18 mmol), HI (0.7  $\mu$ L), open to air ( $^1$ H NMR conversion: 40%).

**(T4-8.3)** The general procedure was used, TBAI (0.067 g, 0.18 mmol), HI (0.7  $\mu$ L) ( $^1$ H NMR conversion: 91%)

**(T4-8.4).** The general procedure was used, TBAI (0.034 g, 0.091 mmol), HI (0.7  $\mu$ L) ( $^1$ H NMR conversion: 60%)

**(T4-8.5).** The general procedure was used, TBAI (0.067 g, 0.18 mmol), HI (0.7  $\mu$ L), open to air ( $^1$ H NMR conversion: 40%)

**(T4-8.6)** The general procedure was used, TBAI (0.067 g, 0.18 mmol), H<sub>2</sub>O<sub>2</sub> (30 wt%, 6  $\mu$ L, 0.18 mmol), HI (0.7  $\mu$ L), open to air ( $^1$ H NMR conversion: 20%)

**(Control 1)** A mixture of NaI (27 mg, 0.182 mmol), and hydroiodic acid (0.7  $\mu$ L) was dissolved in anisole (15 mL), sparged with O<sub>2</sub>, and heated to 130 °C (bath temperature) for 4.5 h. No background reaction was identified.

**(Control 2)** A mixture of 5,6,7,8-tetrahydronaphthalen-1-amine (25  $\mu$ L, 0.182 mmol), NaI (27 mg, 0.182 mmol) and hydroiodic acid (0.7  $\mu$ L) was dissolved in anisole (15 mL), sparged with O<sub>2</sub>, and heated to 130 °C (bath temperature) for 4.5 h. No background reaction was identified.

**(Control 3)** A mixture of 5-(phenanthren-9-yl) pentanal (0.10 g, 0.381 mmol), NaI (27 mg, 0.182 mmol) and hydroiodic acid (0.7  $\mu$ L) was dissolved in anisole (15 mL), sparged with O<sub>2</sub>, and heated

to 130 °C (bath temperature) for 4.5 h. The result of this experiment showed that there is minor decomposition of the aldehyde but was not quantified.

**(T4-9.1)** The general procedure was used, and the reaction is performed stepwise. The imine is first generated by stirring HI (0.7 μL), amine and one equivalent of aldehyde at rt for 1 h. Once formed, as indicated by TLC analysis the second equivalent of aldehyde, NaI (0.027 g, 0.18 mmol), and <sup>t</sup>BuCHO (20 μL, 0.18 mmol) is added and heating is started (<sup>1</sup>H NMR conversion: 85%)

**(T4-9.2)** The general procedure was used, and the reaction is performed step wise. The imine is first generated by stirring HI (0.7 μL), amine and one equivalent of aldehyde at rt for 1 h. Once formed, as indicated by TLC analysis the second equivalent of aldehyde, NaI (0.027 g, 0.18 mmol), and <sup>t</sup>BuCHO (20 μL, 0.18 mmol) is added and heating is started (<sup>1</sup>H NMR conversion: 34%)

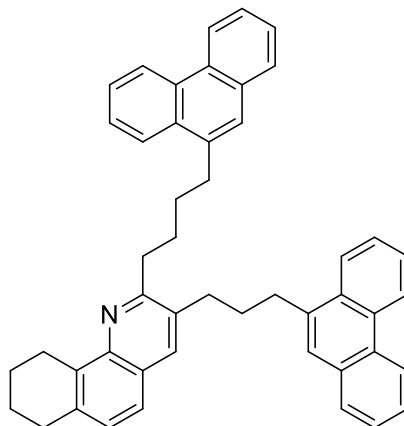
**(T4-9.3)** The general procedure was used, 5-(phenanthren-9-yl) pentanal (0.14 g, 0.55 mmol), NaI (0.027 g, 0.18 mmol) and HI (0.7 μL) (<sup>1</sup>H NMR conversion: >95%)

#### **4.8. Scope of multicomponent reaction compounds. Optimized conditions**

##### **General procedure for optimized MCR synthesis**

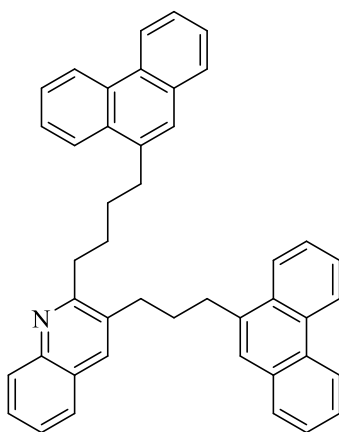
A mixture of an alkyl-tethered  $\alpha,\omega$ -aromatic aldehyde (2.1 equiv) was added to a three-neck RBF flask equipped with a reflux condenser. Amine (1 equiv), hydroiodic acid (5 mol%), and TBAI (1 equiv) was added and dissolved in anisole, sparged with O<sub>2</sub>, and heated to 130 °C (bath temperature) for 4.5 h. The reaction mixture was cooled to rt, basified with 10% aqueous NaOH, and washed with CH<sub>2</sub>Cl<sub>2</sub>. The organic layer was separated, washed with saturated sodium bisulfite, NaBH<sub>4</sub> in H<sub>2</sub>O, saturated brine and dried over Na<sub>2</sub>SO<sub>4</sub>, filtered, and the solvent was removed under reduced pressure.

**2-(4-(phenanthren-9-yl)butyl)-3-(3-(phenanthren-9-yl)propyl)-7,8,9,10-tetrahydrobenzo[*h*]quinoline (161).**



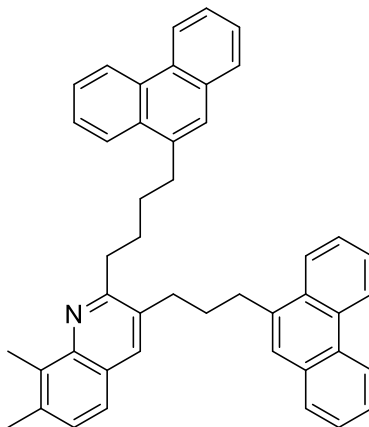
The general procedure was used, 5-(phenanthren-9-yl) pentanal (0.10 g, 0.38 mmol), 5,6,7,8-tetrahydronaphthalen-1-amine (25  $\mu$ L, 0.18 mmol), TBAI (0.066 g, 0.18 mmol) and hydroiodic acid (0.7  $\mu$ L) was dissolved in anisole (15 mL). Hexamethyldisiloxane (4.3  $\mu$ L, 0.020 mmol) was added as an internal standard ( $^1\text{H}$  NMR yield: 90%). The crude material was purified by column chromatography RF=0.54 (9 : 1 Hexane/EtOAc) to afford an off white solid 0.062 g (54%).

**2-(4-(phenanthren-9-yl) butyl)-3-(3-(phenanthren-9-yl) propyl) quinoline (170).**



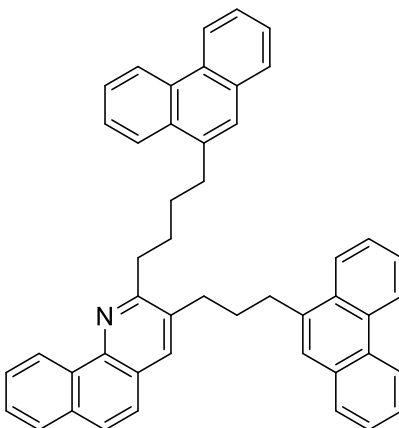
The general procedure was used, 5-(phenanthren-9-yl) pentanal (0.10 g, 0.38 mmol), aniline (17  $\mu\text{L}$ , 0.18 mmol), TBAI (0.067 mg, 0.18 mmol) and hydroiodic acid (0.7  $\mu\text{L}$ ) was dissolved in anisole (15 mL). Hexamethyldisiloxane (4.3  $\mu\text{L}$ , 0.020 mmol) was added as an internal standard ( $^1\text{H}$  NMR yield: 90%). The crude material was purified by column chromatography RF=0.28 (9 : 1 Hexane/EtOAc) to afford a pink solid 0.050 g (48%).

**7,8-dimethyl-2-[4-(phenanthren-9-yl)butyl]-3-[3-(phenanthren-9-yl)propyl]quinoline (171).**



The general procedure was used, 5-(phenanthren-9-yl) pentanal (0.10 g, 0.38 mmol), 2,3-dimethylaniline (22  $\mu\text{L}$ , 0.18 mmol), TBAI (0.067 g, 0.18 mmol) and hydroiodic acid (0.7  $\mu\text{L}$ ) was dissolved in anisole (15 mL). Hexamethyldisiloxane (4.3  $\mu\text{L}$ , 0.020 mmol) was added as an internal standard ( $^1\text{H}$  NMR yield: 45%). The crude material was purified by column chromatography RF=0.36 (9 : 1 Hexane/EtOAc) to afford a white solid 0.044 g (40%).

**2-(4-(phenanthren-9-yl)butyl)-3-(3-(phenanthren-9-yl)propyl)benzo[*h*]quinoline (174).**



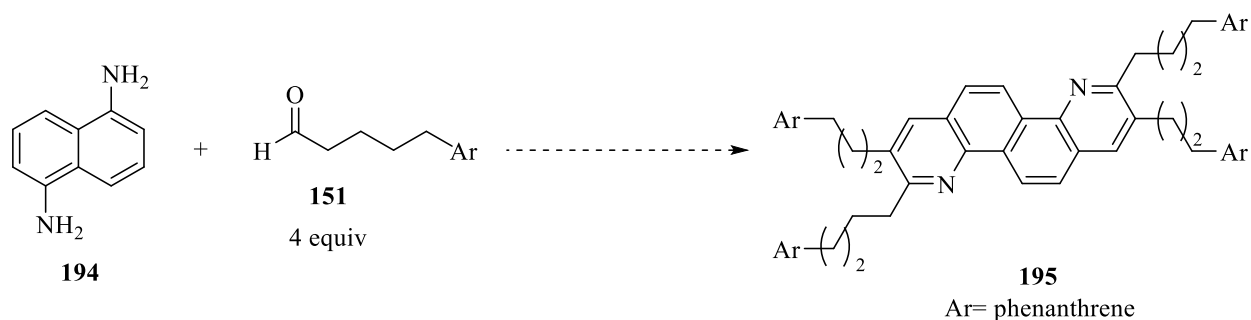
The general procedure was used, 5-(phenanthren-9-yl) pentanal (0.10 g, 0.38 mmol), 1-aminonaphthylene (0.052 g, 0.18 mmol), TBAI (0.067 g, 0.18 mmol) and hydroiodic acid (0.7  $\mu$ L) was dissolved in anisole (15 mL). Hexamethyldisiloxane (4.3  $\mu$ L, 0.020 mmol) was added as an internal standard ( $^1$ H NMR yield: 50%). The crude material was purified by column chromatography RF= (9 : 1 Hexane/EtOAc) to afford a tan solid 0.043 g (38%).

## 5. Bi-directional MCR and Future Prospects

In Chapters 3 and 4, highly substituted novel benzoquinoline archipelago model compounds were prepared by an MCR. This synthetic route involves fewer steps than the previous strategies, affords pure materials, and the procedures are reproducible. Furthermore, using variety of commercially-available aniline derivatives, along with our alkyl-tethered  $\alpha,\omega$ -aromatic aldehydes, we can generate a diversified library of new quinoline compounds. Such molecules are critical to our collaborators for use in modeling asphaltene behavior. Other diversifications that may be pursued includes varying the alkyl chain lengths and terminal aromatic appendages. With an optimized synthetic procedure in hand, the next logical step is to prepare higher molecular weight compounds that incorporate a greater number of heteroatoms, as better asphaltene models. Our collaborators at JPEC are particularly anxious to have access to higher molecular weight (~1500-2000 g/mol) model compounds, with the added requirement that these new molecules should feature multiple cyclic and acyclic nitrogen and sulfur atoms.

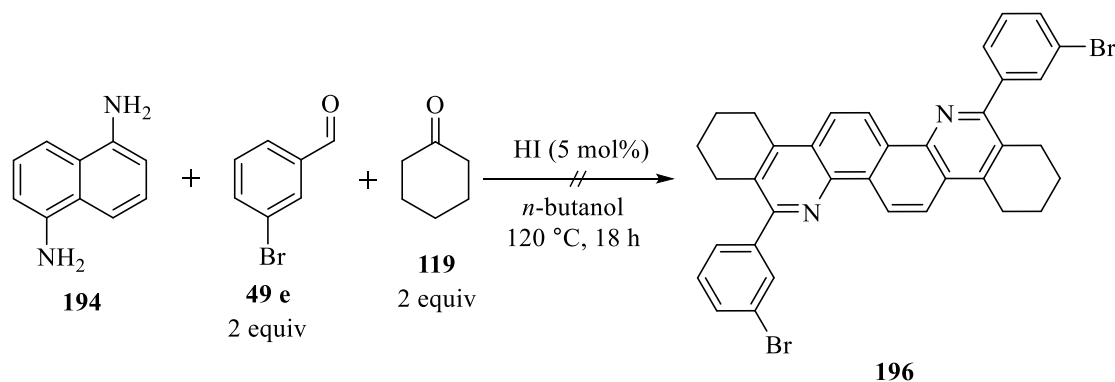
### 5.1. Bi-directional MCRs. Synthetic approaches and preliminary results

The most obvious method to access such alkyl-tethered polycyclic aromatic hydrocarbons is to apply our MCR strategy, but use diaminoarenes for *bi-directional synthesis*.<sup>[259–262]</sup> For example, one potential reaction could access a new five-island archipelago compound incorporating four equivalents of our alkyl-tethered  $\alpha,\omega$ -aromatic aldehydes and 1,5-diaminonaphthelene (Eq. 5-1).



**Equation 5-1.** Hypothetical synthetic route to new five-island archipelago model compounds.

This foray into the bi-directional molecular architecture is not entirely new to our research. As part of earlier optimization reactions, the combination of 1,5-diaminonaphthalene with two equivalents each of 3-bromobenzaldehyde and cyclohexanone (Eq. 5-2) was investigated, in a failed attempt to prepare a bis-bromophenyl-octahydrophenanthridinophenanthridine **196**.



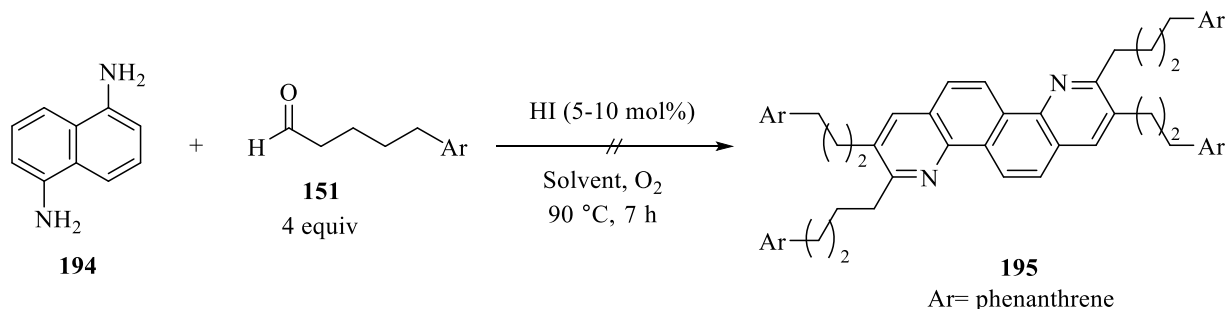
**Equation 5-2.** Synthesis of continental-like archipelago compounds using a bi-directional MCR.

**Table 5-1.** MCR conditions for bi-directional synthesis of continental archipelago compounds.

Entry	Solvent	Oxidant	Yield
1	<i>n</i> -butanol	air	NC
2 <sup>a</sup>	<i>n</i> -butanol	O <sub>2</sub>	NC

A mixture 1,5-diaminonaphthalene (0.5 g, 3.2 mmol), 3-bromobenzaldehyde (1.2 g, 6.3 mmol), cyclohexanone (0.6 g, 6.3 mmol), butanol (20 mL), and HI (12  $\mu$ L) is added 50 mL round bottom flask and stirred at 120  $^\circ$ C for 18 h. <sup>a</sup>Reaction run under a constant, rapid bubbling of oxygen. NC = no conversion to product.

This reaction was conducted in butanol, which we believed to be optimal at the time, but no MCR product was obtained (see Chapter 3, section 3.3 for details). Nevertheless, we decided to explore a variation of this strategy, using 1,5-diaminonaphthalene and four equivalents of aldehyde, under partially optimized conditions (Eq. 5-3 and Table 5-2).



**Equation 5-3.** Bi-directional synthesis using four equivalents of an alkyl-tethered  $\alpha,\omega$ -aromatic aldehyde

Preparing quinolino[8,7-*h*]quinoline core model compounds from diamionaphthalene via bi-directional MCR proved severely challenging. Both 1,5-diaminonaphthalene and 1,8-diaminonaphthalene were used as the starting scaffold. When 1,5-diaminonaphthylene was used, no conversion to the desired product **197** was obtained, despite numerous trials (Eq. 5-3 and Table 5-2).

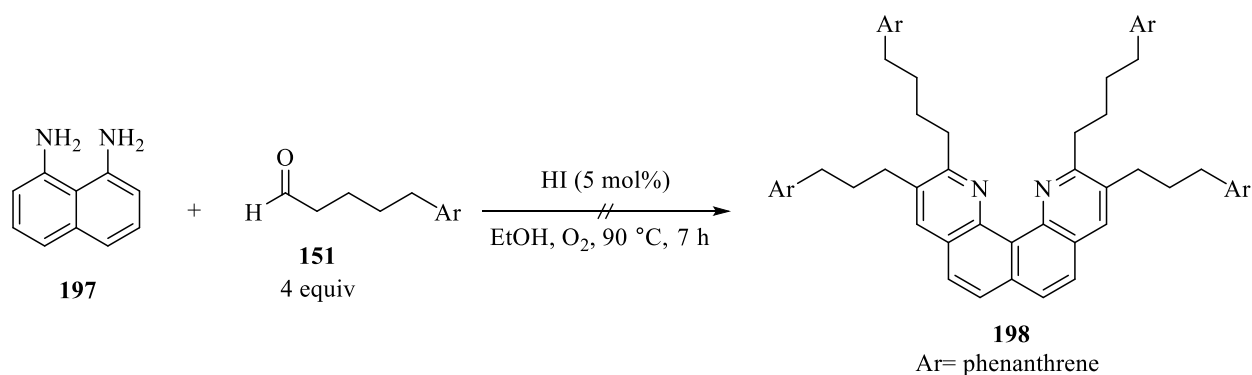
**Table 5-2.** MCR bi-directional synthesis using 4 equivalents of alkyl-tethered  $\alpha,\omega$ -aromatic aldehyde.

Entry	Solvent	Catalyst	Yield
1	EtOH	HI (5 mol%)	NC
2	EtOH	HI (10 mol%)	NC
3 <sup>a</sup>	EtOH	HI (10 mol%)	NC
4 <sup>b</sup>	THF:EtOH (9:1)	HI (10 mol%)	NC
5 <sup>c</sup>	EtOH:H <sub>2</sub> O (95:5)	HI (10 mol%)	NC

A mixture 1,5-diaminonaphthalene (0.02 g, 0.13 mmol), 5-(phenanthren-9-yl) pentanal (0.15 g, 0.51 mmol), ethanol (4 mL), and HI (0.8  $\mu$ L) is added 25 mL round bottom flask and stirred at 90 °C for 7 h under a constant, rapid bubbling of oxygen. <sup>a</sup> The amount of solvent was doubled in volume. <sup>b</sup> Ethanol:THF (0.8 mL:7.2 mL). <sup>c</sup> Ethanol:H<sub>2</sub>O (7.6 mL:0.4 mL). NC= no conversion to product.

I believe this reaction failed because our synthetic aldehyde is only partially soluble in EtOH (see Chapter 3). To improve solubility, we increased the volume of solvent (Table 5-2, entry 3) and switched to a dual solvent system of THF and ethanol (Table 5-2, entry 4) but neither modification led to product. Finally, we investigated whether a higher loading of catalyst (from five mol% to 10 mol% per aromatic amine) would lead to the archipelago compound, but this too was unsuccessful (Table 5-2, entries 2 to 5).

When 1,8-diaminonaphthalene was used as the starting diamine, (Eq. 5-4 and Table 5-3), no MCR product was obtained, presumably for the reasons outlined above. It should be noted that for both diaminoarene substrates, neither the mono- nor bis-imine intermediates were detected and, as such, were unlikely to have been generated *in situ*, excluding the possibility of conversion.



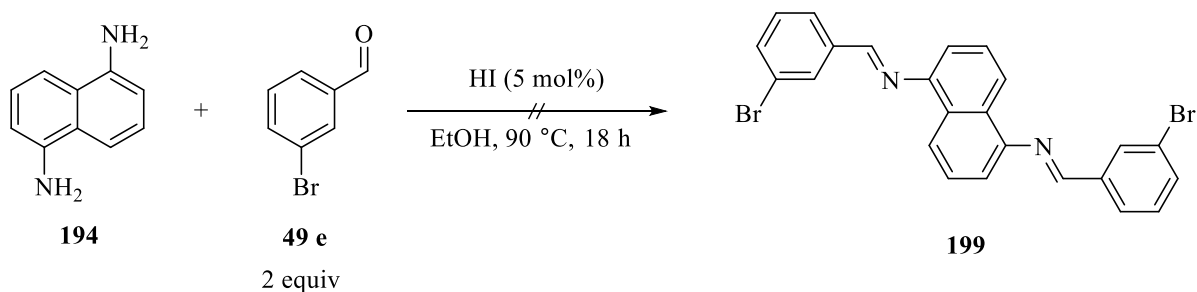
**Equation 5-4.** Bi-directional MCR using 1,8-diaminonaphthylene to acquire 2,11-bis(4-(phenanthren-9-yl)butyl)-3,10-bis(3-(phenanthren-9-yl)propyl)quinolino[7,8-*h*]quinoline.

**Table 5-3.** Bi-directional MCR using 1,8-diaminonaphthylene in concentrated and dilute solvent conditions.

Entry	Solvent	Catalyst	Yield
1	EtOH	HI (5 mol%)	NC
2 <sup>a</sup>	EtOH	HI (5 mol%)	NC

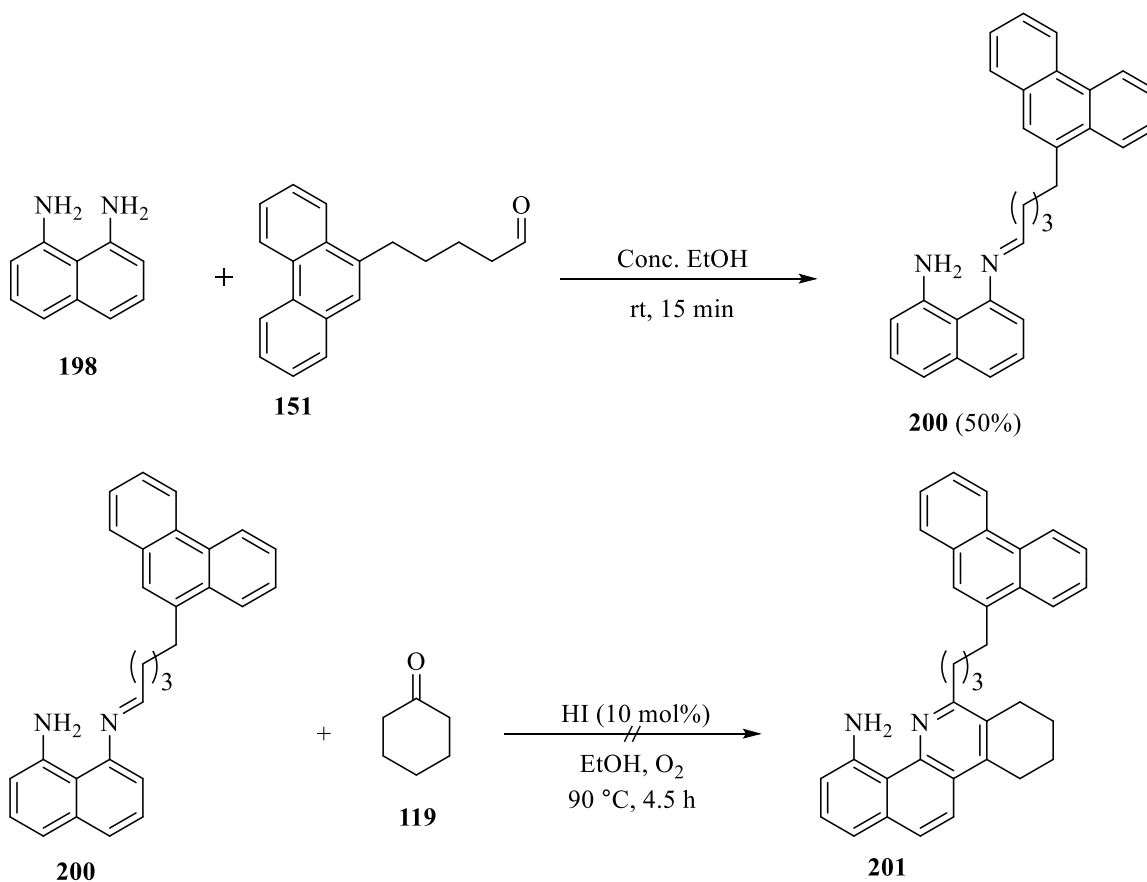
A mixture 1,8-diaminonaphthalene (0.3 g, 1.8 mmol), 5-(phenanthren-9-yl) pentanal (1.9 g, 7.6 mmol), ethanol (20 mL), and HI (12  $\mu$ L) is added 50 mL round bottom flask and stirred at 90  $^\circ$ C for 7 h under a constant, rapid bubbling of oxygen. <sup>a</sup> The amount of solvent was doubled in volume. NC = no conversion to product.

At this stage of the investigation, we focused on promoting the formation of the bis-imine, as a first step toward the bi-directional MCR. Once formed, these imines could undergo an imino Diels-Alder/Mannich-like cycloaddition with a second equivalent of aldehyde to form the desired adduct. Strictly speaking, this two-step approach is antithetical to the concept of an MCR, but it would at least provide a starting point for subsequent optimization. Attempts to synthesize the bis-arylnaphthylimine **201** using 3-bromobenzaldehyde, however, did not afford an imine. Dilute ethanol proved to be a poor choice of solvent, as previously noted (Eq. 5-5).



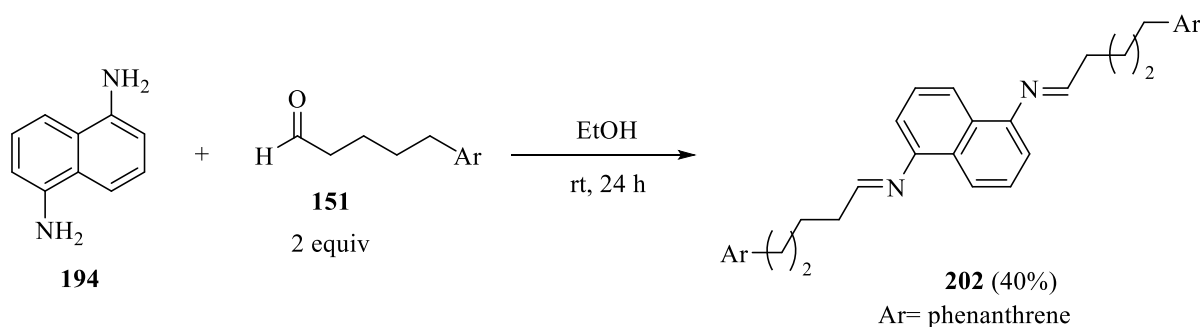
**Equation 5-5.** Unsuccessful synthesis of the 1,8 bis-imine in dilute ethanol.

The 1,8-diaminonaphthalene series, in contrast did afford the mono-imine. Imine **200** is generated in a matter of minutes at very high concentration and can be isolated to afford a light pink/purple solid in a 50% yield (Scheme 5-1, top). Unfortunately, no cyclocondensation proceeded upon addition of cyclohexanone, at least in ethanol (Scheme 5-1, bottom).



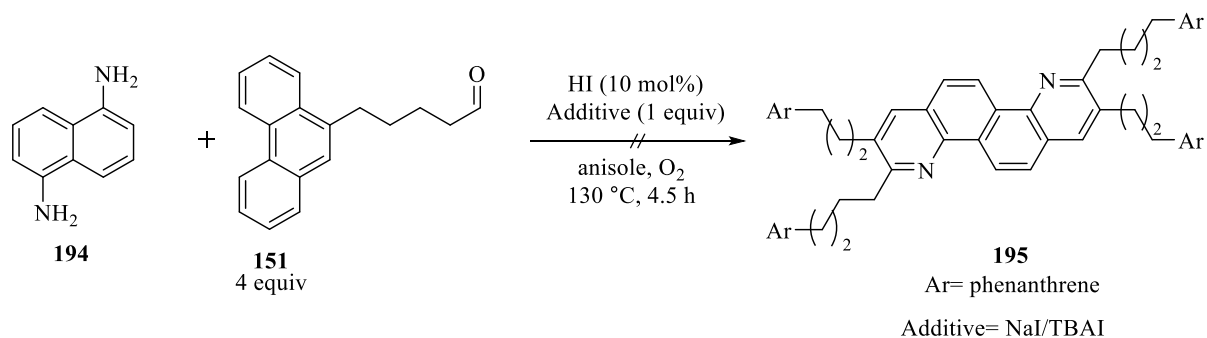
**Scheme 5-1.** Synthesis of the mono-*N*-alkylimine in a highly concentrated solvent solution.

Following this more promising result, we reasoned that given enough time or thermal encouragement, the bis-imine might also be formed under the reaction conditions. Fortunately, after 24 hours under the concentrated reaction conditions, we indeed isolated 1,5-bis-*N*-alkylnaphthylimine **202** (Eq. 5-6), although in low isolated yield (40%). All attempts to perform the imino Diels-Alder/Mannich-like cycloaddition in alcohol solvent failed.



**Equation 5-6.** Synthesis of (1*E*,1'*E*)-*N,N'*-(naphthalene-1,5-diyl)bis(5-(phenanthren-9-yl)pentan-1-imine).

These experiments were conducted prior to discovering two critical aspects of optimization. Important improvements were noted for anisole as solvent and the use of NaI/TBAI promoters. More recently, we applied this knowledge to the bidirectional MCR. However, under these “extensively optimized” conditions, the reaction produced only the bis-*N*-alkylimine, as indicated by TLC monitoring (Eq. 5-7). Our lack of success strongly suggested that a mechanistic alternative was required.

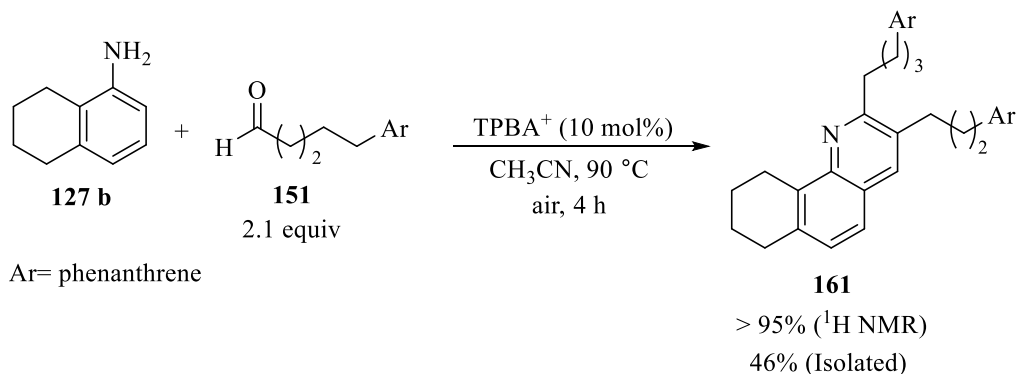


**Equation 5-7.** Bi-directional MCR using the semi-optimal/enhanced conditions identified in Chapter 3/4.

## 5.2. Further investigations. The radical cation MCR

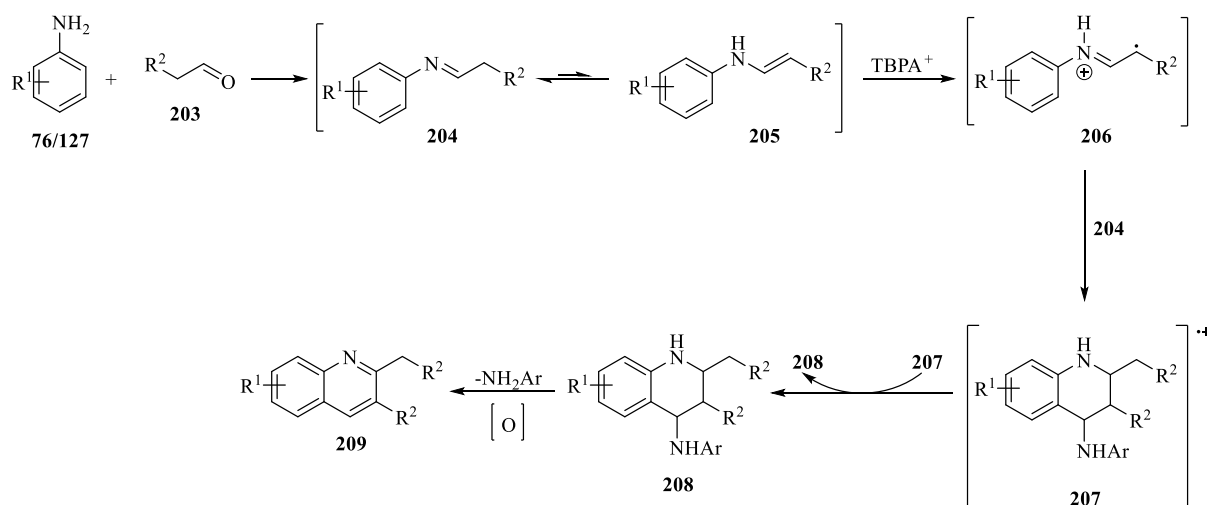
### Radical Cation Catalyst

The literature provides some precedent for using a radical cation catalyst to drive the cyclocondensation.<sup>[183]</sup> It is possible that these conditions will eliminate the need for elevated temperatures and pure oxygen. This investigation is being undertaken by Mark Aloisio; his preliminary efforts (Eq. 5-8) demonstrate that our standard MCR proceeds to completion at lower temperature (90 °C) using acetonitrile as solvent under air. The reaction was nearly quantitative by <sup>1</sup>H NMR spectroscopy, but the isolated yield of quinoline **161** was less than 50%. This represents a second great challenge for future research – how to deal with self-aggregating compounds that resist both crystallization and chromatography.



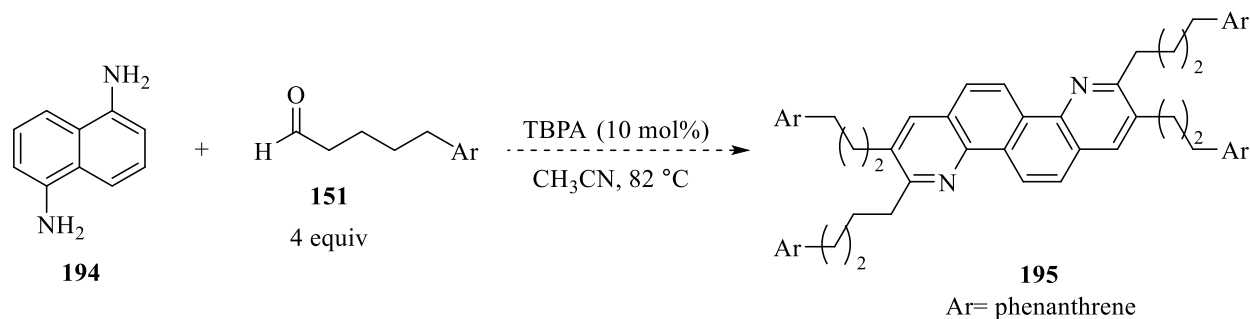
**Equation 5-8.** Catalytic radical cation MCR proof of principle.

The radical cation MCR is proposed to occur entirely in the odd electron manifold. Hereby, the aniline induces an intriguing alternative mechanism for the process, as alluded to in Chapter 4. For the radical cation Povarov reaction, only a catalytic amount of the tris(4-bromophenyl)aminium oxidant was required.<sup>[183,185,263]</sup> Although little evidence was provided, the proposed mechanism invokes an “imine/enamine” tautomerization prior to one-electron oxidation (Scheme 5-2).<sup>[183]</sup> The equilibrium presumably favors the more thermodynamically stable imine, but the more electron-rich enamine is more easily oxidized to the reactive radical cation. The enamine radical cation is presumed to react not with free aldehyde, but with the *N*-alkylimine present in solution (Scheme 5-2). The heterocyclic radical cation **207** is quenched by single electron transfer from the enamine, returning to the even-electron manifold and regenerating the enamine radical cation **206**. Acid-catalyzed elimination of aniline and subsequent air oxidation produces quinoline **209** (Scheme 5-2).



**Scheme 5-2.** Wang's proposed radical MCR mechanism.<sup>[183]</sup>

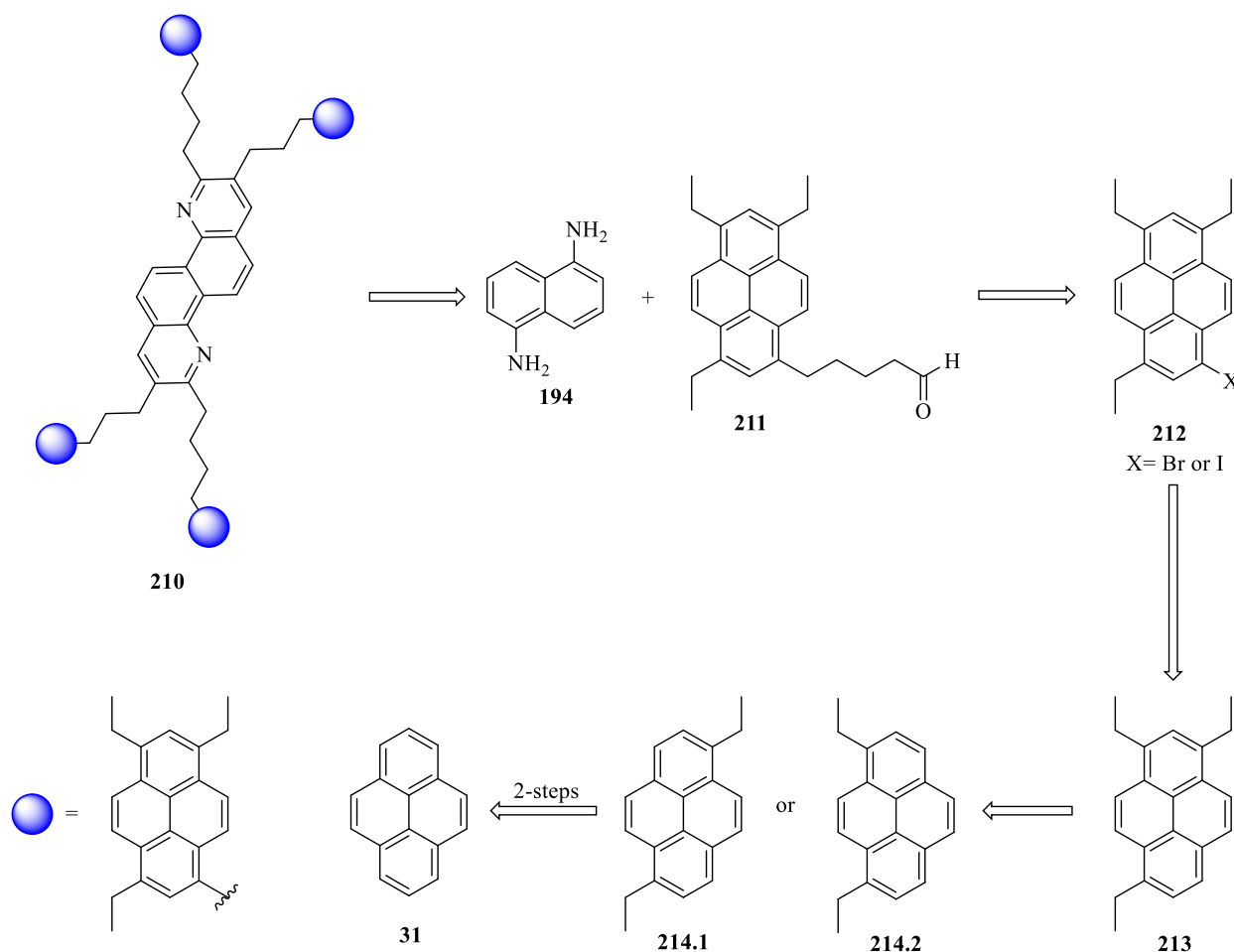
This mechanistic proposal deviates from traditional MCR proposals, as a consequence of an electrophilic, odd-electron manifold. Our intention is to exploit this process for bi-directional synthesis, increasing molecular weight, complexity, and heteroatom content in a single synthetic step (Eq. 5-9).



**Equation 5-9.** Prospective double-MCR model compound.

The combination of bi-directional synthesis with alkyl-substituted terminal islands, as discussed in Chapter 1, assures higher solubility in toluene despite self-aggregation (Scheme 5-3). Such

“mixed model” compounds bridge the gap between Yen-Mullins continental models and archipelago systems.

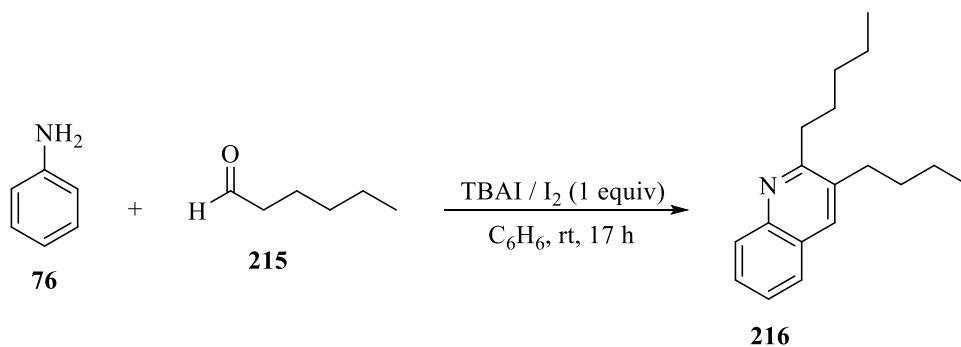


**Scheme 5-3.** Hypothetical synthesis which combines Gen 1 and MCR approaches.

### Generating Radical Cations Electrochemically

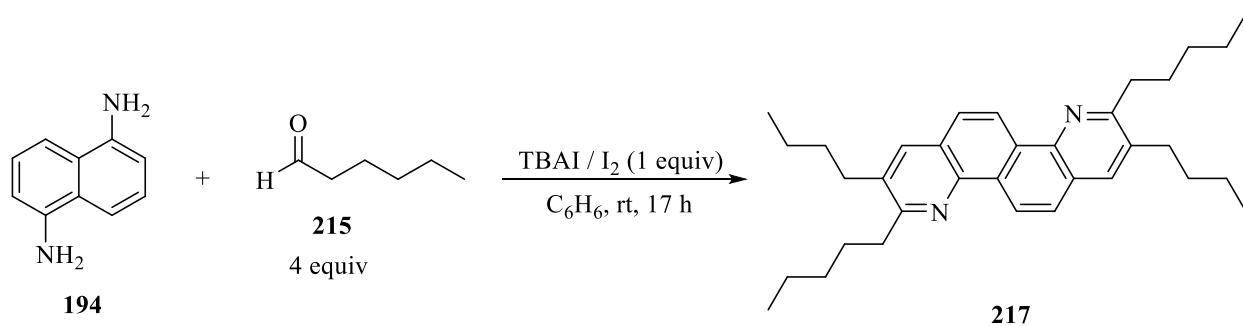
The electrochemical radical cation MCR is currently under development by Dr. Robin Hamilton in the group. The synthesis can be accomplished using a range of soluble redox modulators, including the tris(bromophenyl)amine. In one preliminary experiment, a stoichiometric amount of  $I_3^-$  oxidant was generated electrochemically, followed by the addition of aniline **76** (1 equiv) and

hexanal **215** (2 equivs). The reaction proceeded at room temperature overnight under constant current (0.1 mA). Generating radical cations electrochemically thus appears to be a viable MCR alternative; however, yields have yet to be quantified (Eq. 5-10).



**Equation 5-10.** Electrochemically generated stoichiometric I<sub>3</sub><sup>-</sup> for MCR application.

This procedure was then applied to a bi-directional reaction. Under the same conditions, the desired tetra-substituted 4,10-diazachrysene **222** was indeed observed, but not quantified (Eq. 5-11).



**Equation 5-11.** Electrochemical bi-directional MCR accomplished using stoichiometric I<sub>3</sub><sup>-</sup>.

### 5.3. Final thoughts

My research goal was to prepare new asphaltene model compounds using an MCR strategy. Synthesis of quinoline-core, three-island archipelago model compounds was accomplished by a one-step cyclocondensation reaction that is scalable, reproducible, and produces adducts in high purity. Though these compounds are simple to synthesize; purification and solution characterization remains challenging. The compounds were designed to study the drivers of aggregation. They apparently do.

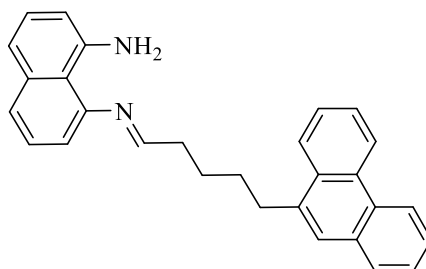
### Experimental Section

General experimental details are presented in Chapters 2, 3 and 4. Solvents and reagents were used without further purification. I was assisted in investigating the bidirectional MCR by (then) undergraduate co-worker Mark Aloisio. The following procedures include only preliminary characterization by  $^1\text{H}$  NMR analysis.

TLC analyses were performed using 0.5 mm analytical TLC plates from Macherey-Nagel (ALUGRAM<sup>®</sup> SIL G/UV<sub>254</sub>) and visualized by using UV-light of 254 nm and/or 366 nm. For flash column chromatography, silica gel 60 M (0.040–0.063 mm) from Macherey-Nagel was used.

NMR spectra were recorded on Agilent/Varian instruments (400 and 500 MHz for  $^1\text{H}$  NMR) at ambient temperature. Chemical shifts were referenced to residual solvent protium peaks ( $\delta$  in parts per million (ppm)  $\text{CHCl}_3$   $^1\text{H}$ : 7.26 ppm). Coupling constants were assigned as observed.  $^1\text{H}$  NMR coupling constants are rounded to nearest 1.0 Hz.

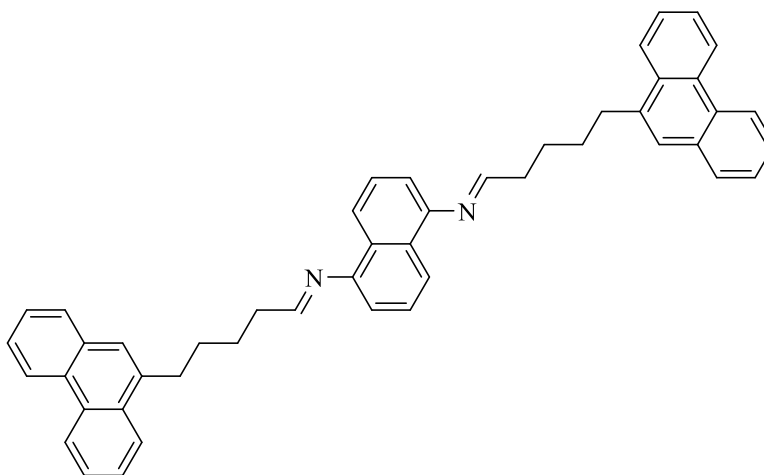
**(E)-8-((5-(phenanthren-9-yl)pentylidene)amino)naphthalen-1-amine (200).**



A mixture of 1,8-diaminonaphthalene (0.50 g, 0.0032 mol), 5-(phenanthren-9-yl) pentanal (0.82 g, 0.0032 mol) and ethanol (2 mL) was added to a three-neck RBF flask and stirred at rt for 15 min. The solvent was removed under reduced pressure. The crude material was purified by column chromatography (9 : 1 Hexane/EtOAc) to afford a light pink-purple solid 0.66 g (50%).

**<sup>1</sup>H NMR** (CDCl<sub>3</sub>, 500 MHz): δ 8.76 (d, *J* = 6.0 Hz, 1H), 8.69 (d, *J* = 2.0 Hz, 1H), 8.12 (d, *J* = 8.0 Hz, 1H), 7.85 (m, 1H), 7.65 (m, 5H), 7.25 (m, 4H), 6.50 (d, *J* = 7.0 Hz, 2H), 4.51 (t, *J* = 5.0 Hz, 1H), 4.32 (s, 2H), 3.19 (t, *J* = 7.0 Hz, 2H), 1.95 (q, *J* = 8.0 Hz, 2H), 1.85 (m, 2H), 1.7 (m, 2H).

**(1E,1'E)-N,N'-(naphthalene-1,5-diyl)bis(5-(phenanthren-9-yl)pentan-1-imine) (202).**



A mixture of 1,5-diaminonaphthalene (0.10 g 1.3 mmol), 5-(phenanthren-9-yl) pentanal (0.30 g, 2.5 mmol) and ethanol (2 mL) was added to a three-neck RBF flask and stirred at rt for 24 h. A white solid was collected by vacuum filtration 0.2 g (40%).

**<sup>1</sup>H NMR** (CDCl<sub>3</sub>, 400 MHz): δ 8.77 (d, *J* = 8.0 Hz, 2H), 8.68 (d, *J* = 8.0 Hz, 2H), 8.16 (d, *J* = 7.0 Hz, 2H), 7.86 (m, 4H), 7.84 (d, *J* = 8.0 Hz, 2H), 7.62 (m, 10H), 7.37 (t, *J* = 7.0 Hz, 2H), 6.85 (d, *J* = 7.0 Hz, 2H), 3.25 (t, *J* = 7.0 Hz, 4H), 2.70 (m, 4H), 2.01 (m, 8H)

## Bibliography

- (1) Judkins, R. R.; Fulkerson, W.; Sanghvi, M. K. *Energy Fuels* **1993**, *7*, 14–22.
- (2) Brandt, A. R.; Millard-Ball, A.; Ganser, M.; Gorelick, S. M. *Environ. Sci. Technol.* **2013**, *47*, 8031–8041.
- (3) Miller, R. G.; Sorrell, S. R. *Phil. Trans. R. Soc. A* **2014**, *372*, 20130179.
- (4) Teare, M.; Burrowes, A.; Baturin-Pollock, C.; Rokosh, D.; Evans, C.; Marsh, R.; Ashrafi, B.; Tamblyn, C.; Ito, S.; Willwerth, A.; Yemane, M.; Fong, J.; Kirsch, M.-A.; Crowfoot, C.; Board, E. R. C., Ed.; Energy Resources Conservation Board: Calgary, Alberta 2013. [http://www.baaqmd.gov/~media/files/planning-and-research/public-hearings/2015/121615/att-26\\_32-pdf.pdf](http://www.baaqmd.gov/~media/files/planning-and-research/public-hearings/2015/121615/att-26_32-pdf.pdf) (accessed July 5, 2018).
- (5) Santos, R. G.; Loh, W.; Bannwart, A. C.; Trevisan, O. V. *Brazilian J. Chem. Eng.* **2014**, *31*, 571–590.
- (6) Haji-Akbari, N.; Teeraphakul, P.; Fogler, H. S. *Energy Fuels* **2014**, *28*, 909–919.
- (7) Hauser, A.; Bahzad, D.; Stanislaus, A.; Behbahani, M. *Energy Fuels* **2008**, *22*, 449–454.
- (8) Xu, C. C.; Su, H.; Ghosh, M. *Energy Fuels* **2009**, *23*, 3645–3651.
- (9) Spiecker, P. M.; Gawrys, K. L.; Kilpatrick, P. K. *J. Colloid Interface Sci.* **2003**, *267*, 178–193.
- (10) Crittenden, J. C.; White, H. S. *J. Am. Chem. Soc.* **2010**, *132*, 4503–4505.
- (11) Gray, M. R.; Tykwinski, R. R.; Stryker, J. M.; Tan, X. *Energy Fuels* **2011**, *25*, 3125–3134.
- (12) Mullins, O. C.; Sabbah, H.; Eyssautier, J.; Pomerantz, A. E.; Barré, L.; Andrews, A. B.; Ruiz-Morales, Y.; Mostowfi, F.; McFarlane, R.; Goual, L.; Lepkowicz, R.; Copper, T.; Orbulescu, J.; Leblanc, R. M.; Edwards, J.; Zare, R. N. *Energy Fuels* **2012**, *26*, 3986–4003.
- (13) Adams, J. J. *Energy Fuels* **2014**, *28*, 2831–2856.
- (14) Akbarzadeh, K.; Dhillon, A.; Svrcek, W. Y.; Yarranton, H. W. *Energy Fuels* **2004**, *18*, 1434–1441.
- (15) Seifried, C. M.; Crawshaw, J.; Boek, E. S. *Energy Fuels* **2013**, *27*, 1865–1872.
- (16) Jaffe, S. B.; Freund, H.; Olmstead, W. N. *Ind. Eng. Chem. Res.* **2005**, *44*, 9840–9852.
- (17) Strausz, O. P.; Peng, P.; Murgich, J. *Energy Fuels* **2002**, *16*, 809–822.
- (18) Castañeda, L. C.; Muñoz, J. A. D.; Ancheyta, J. *Catal. Today* **2014**, *220–222*, 248–273.
- (19) Jewell, D. M.; Weber, J. H.; Bungler, J. W.; Plancher, H.; Latham, D. R. *Anal. Chem.* **1972**, *44*, 1391–1395.

- (20) Strausz, O. P.; Lown, E. M. *The Chemistry of Alberta Oil Sands, Bitumens and Heavy Oils*, Alberta Energy Research Institute, Calgary, Alberta, **2003**.
- (21) Pomerantz, A. E.; Hammond, M. R.; Morrow, A. L.; Mullins, O. C.; Zare, R. N. *Energy Fuels* **2009**, *23*, 1162–1168.
- (22) Hoepfner, M. P.; Vilas Bôas Fávero, C.; Haji-Akbari, N.; Fogler, H. S. *Langmuir* **2013**, *29*, 8799–8808.
- (23) Sabbah, H.; Morrow, A. L.; Pomerantz, A. E.; Zare, R. N. *Energy Fuels* **2011**, *25*, 1597–1604.
- (24) Marshall, A. G.; Rodgers, R. P. *Proc. Natl. Acad. Sci.* **2008**, *105*, 18090–18095.
- (25) Groenzin, H.; Mullins, O. C. *Energy Fuels* **2000**, *14*, 677–684.
- (26) Mullins, O. C. *Fuel* **2007**, *86*, 309–312.
- (27) Acevedo, S.; Escobar, G.; Gutiérrez, L. B.; D'Aquino, J. *Fuel* **1992**, *71*, 1077–1079.
- (28) Acevedo, S.; Gutierrez, L. B.; Negrin, G.; Pereira, J. C.; Mendez, B.; Delolme, F.; Dessalces, G.; Broseta, D. *Energy Fuels* **2005**, *19*, 1548–1560.
- (29) Hsu, C. S.; Hendrickson, C. L.; Rodgers, R. P.; McKenna, A. M.; Marshall, A. G. *J. Mass Spectrom.* **2011**, *46*, 337–343.
- (30) Qian, K.; Edwards, K. E.; Siskin, M.; Olmstead, W. N.; Mennito, A. S.; Dechert, G. J.; Hoosain, N. E. *Energy Fuels* **2007**, *21*, 1042–1047.
- (31) Barrera, D. M.; Ortiz, D. P.; Yarranton, H. W. *Energy Fuels* **2013**, *27*, 2474–2487.
- (32) Müller, H.; Andersson, J. T.; Schrader, W. *Anal. Chem.* **2005**, *77*, 2536–2543.
- (33) Panda, S. K.; Schrader, W.; al-Hajji, A.; Andersson, J. T. *Energy Fuels* **2007**, *21*, 1071–1077.
- (34) Mullins, O. C.; Martínez-Haya, B.; Marshall, A. G. **2008**, *22*, 1765–1773.
- (35) Pinkston, D. S.; Duan, P.; Gallardo, V. A.; Habicht, S. C.; Tan, X.; Qian, K.; Gray, M.; Mullen, K.; Kenttämä, H. I. *Energy Fuels* **2009**, *23*, 5564–5570.
- (36) Agrawala, M.; Yarranton, H. W. *Ind. Eng. Chem. Res.* **2001**, *40*, 4664–4672.
- (37) Smith, D. F.; McKenna, A. M.; Corilo, Y. E.; Rodgers, R. P.; Marshall, A. G.; Heeren, R. M. A. *Energy Fuels* **2014**, *28*, 6284–6288.
- (38) Ruddy, B. M.; Hendrickson, C. L.; Rodgers, R. P.; Marshall, A. G. *Energy Fuels* **2018**, *32*, 2901–2907.
- (39) Sheu, E. Y.; Liang, K. S.; Sinha, S. K.; Overfield, R. E. *J. Colloid Interface Sci.* **1992**, *153*, 399–410.
- (40) Groenzin, H.; Mullins, O. C.; Eser, S.; Mathews, J.; Yang, M. G.; Jones, D. *Energy Fuels* **2003**, *17*, 498–503.

- (41) Ruiz-Morales, Y.; Mullins, O. C. *Energy Fuels* **2007**, *21*, 256–265.
- (42) Moschopedis, S. E.; Speight, J. G. *Fuel* **1976**, *55*, 187–192.
- (43) Merino-Garcia, D.; Andersen, S. I. *Pet. Sci. Technol.* **2003**, *21*, 507–525.
- (44) Schuler, B.; Meyer, G.; Peña, D.; Mullins, O. C.; Gross, L. *J. Am. Chem. Soc.* **2015**, *137*, 9870–9876.
- (45) Schuler, B.; Zhang, Y.; Collazos, S.; Fatayer, S.; Meyer, G.; Pérez, D.; Guitián, E.; Harper, M. R.; Kushnerick, J. D.; Peña, D.; Gross, L. *Chem. Sci.* **2017**, *8*, 2315–2320.
- (46) Schuler, B.; Fatayer, S.; Meyer, G.; Rogel, E.; Moir, M.; Zhang, Y.; Harper, M. R.; Pomerantz, A. E.; Bake, K. D.; Witt, M.; Peña, D.; Kushnerick, J. D.; Mullins, O. C.; Ovalles, C.; van den Berg, F. G. A.; Gross L. *Energy Fuels* **2017**, *31*, 6856–6861.
- (47) Murgich, J.; Abanero, J. A.; Strausz, O. P. *Energy Fuels* **1999**, *13*, 278–286.
- (48) Mullins, O. C.; Sheu, E. Y.; Hammami, A.; Marshall, A. G. *Asphaltenes, Heavy Oils, and Petroleomics*; Springer: New York, **2007**.
- (49) Speight, J. G. *Oil Gas Sci. Technol.* **2004**, *59*, 467–477.
- (50) Dechaine, G. P.; Gray, M. R. *Energy Fuels* **2010**, *24*, 2795–2808.
- (51) Speight, J. G.; Moschopedis, S. E. *Chemistry of Asphaltenes: On the molecular nature of petroleum asphaltenes*; Bunger, J.W.; Li, N. C., Ed.; American Chemical Society, Washington, DC, **1982**.
- (52) Strausz, O. P.; Mojelsky, T. W.; Faraji, F.; Lown, E. M.; Peng, P. *Energy Fuels* **1999**, *13*, 207–227.
- (53) Koopmans, M. P.; De Leeuw, J. W.; Lewan, M. D.; Sinninghe Damste, J. S. *Org. Geochem.* **1996**, *25*, 391–426.
- (54) Snyder, L. R. *Acc. Chem. Res.* **1970**, *3*, 290–299.
- (55) Mitra-Kirtley, S.; Mullins, O. C.; van Elp, J.; George, S. J.; Chen, J.; Cramer, S. P. *J. Am. Chem. Soc.* **1993**, *115*, 252–258.
- (56) Shi, Q.; Hou, D.; Chung, K. H.; Xu, C.; Zhao, S.; Zhang, Y. *Energy Fuels* **2010**, *24*, 2545–2553.
- (57) Zuo, P.; Shen, W. *Int. J. Coal Sci. Technol.* **2017**, *4*, 281–299.
- (58) Ignasiak, T.; Bimer, J.; Samman, N.; Montgomery, D.S.; Strausz, O. P. *Chemistry of Asphaltenes: Lewis acids assisted degradation of Athabasca asphaltene*; Bunger, J.W.; Li, N. C., Ed.; American Chemical Society, Washington, DC, **1982**.
- (59) Sheremata, J. M.; Gray, M. R.; Dettman, H. D.; McCaffrey, W. C. *Energy Fuels* **2004**, *18*, 1377–1384.
- (60) Tan, X.; Fenniri, H.; Gray, M. R. *Energy Fuels* **2008**, *22*, 715–720.
- (61) De León, J.; Hoyos, B.; Cañas-Marín, W. *Dyna* **2015**, *82*, 39–44.

- (62) Andrews, A. B.; Edwards, J. C.; Pomerantz, A. E.; Mullins, O. C.; Nordlund, D.; Norinaga, K. *Energy Fuels* **2011**, *25*, 3068–3076.
- (63) Martínez-Haya, B.; Hortal, A. R.; Hurtado, P.; Lobato, M. D. . *P. J. Mass Spectrom.* **2007**, *42*, 701–703.
- (64) Freund, H.; Matturro, M. G.; Olmstead, W. N.; Reynolds, R. P.; Upton, T. H. *Energy Fuels* **1991**, *5*, 840–846.
- (65) Siddiquee, M. N.; de Klerk, A. *Energy Fuels* **2014**, *28*, 6848–6859.
- (66) Buckley, J. S.; Hirasaki, G. J.; Liu, Y.; Von Drasek, S.; Wang, J. X.; Gill, B. S. *Pet. Sci. Technol.* **1998**, *16*, 251–285.
- (67) Sabbah, H.; Pomerantz, A. E.; Wagner, M.; Müllen, K.; Zare, R. N. *Energy Fuels* **2012**, *26*, 3521–3526.
- (68) Jarrell, T. M.; Jin, C.; Riedeman, J. S.; Owen, B. C.; Tan, X.; Scherer, A.; Tykwinski, R. R.; Gray, M. R.; Slater, P.; Kenttämää, H. I. *Fuel* **2014**, *133*, 106–114.
- (69) Sharma, A.; Groenzin, H.; Tomita, A.; Mullins, O. C. *Energy Fuels* **2002**, *16*, 490–496.
- (70) Smith, C. M.; Savage, P. E. *Ind. Eng. Chem. Res.* **1991**, *30*, 331–339.
- (71) Smith, C. M.; Savage, P. E. *Energy Fuels* **1991**, *5*, 146–155.
- (72) Smith, C. M.; Savage, P. E. *AIChE J.* **1991**, *37*, 1613–1624.
- (73) Smith, C. M.; Savage, P. E. *Energy Fuels* **1994**, *8*, 545–551.
- (74) Savage, P. E.; Jacobs, G. E.; Javanmardian, M. *Ind. Eng. Chem. Res.* **1989**, *28*, 645–654.
- (75) Alvarez-Ramírez, F.; Ruiz-Morales, Y. *Energy Fuels* **2013**, *27*, 1791–1808.
- (76) Ruiz-Morales, Y.; Mullins, O. C. *Energy Fuels* **2009**, *23*, 1169–1177.
- (77) Oliveira, J. S. C.; da Costa, L. M.; Stoyanov, S. R.; Seidl, P. R. *Energy Fuels* **2015**, *29*, 2843–2852.
- (78) da Costa, L. M.; Stoyanov, S. R.; Gusarov, S.; Seidl, P. R.; de M. Carneiro, J. W.; Kovalenko, A. *J. Phys. Chem. A* **2014**, *118*, 896–908.
- (79) Lage, M. R.; Stoyanov, S. R.; de Mesquita Carneiro, J. W.; Dabros, T.; Kovalenko, A. *Energy Fuels* **2015**, *29*, 2853–2863.
- (80) George, G. N.; Gorbaty, M. L. *J. Am. Chem. Soc.* **1989**, *111*, 3182–3186.
- (81) Mitra-Kirtley, S.; Mullins, O. C.; van Elp, J.; George, S. J.; Chen, J.; Cramer, S. P. *J. Am. Chem. Soc.* **1993**, *115*, 252–258.
- (82) Waldo, G. S.; Mullins, O. C.; Penner-Hahn, J. E.; Cramer, S. P. *Fuel* **1992**, *71*, 53–57.
- (83) Akbarzadeh, K.; Bressler, D. C.; Wang, J.; Gawrys, K. L.; Gray, M. R.; Kilpatrick, P. K.; Yarranton, H. W. *Energy Fuels* **2005**, *19*, 1268–1271.
- (84) Sabbah, H.; Morrow, A. L.; Pomerantz, A. E.; Mullins, O. C.; Tan, X.; Gray, M. R.;

- Azyat, K.; Tykwinski, R. R.; Zare, R. N. *Energy Fuels* **2010**, *24*, 3589–3594.
- (85) Francisco, M. A.; Garcia, R.; Chawla, B.; Yung, C.; Qian, K.; Edwards, K. E.; Green, L. A. *Energy Fuels* **2011**, *25*, 4600–4605.
- (86) Rakotondradany, F.; Fenniri, H.; Rahimi, P.; Gawrys, K. L.; Kilpatrick, P. K.; Gray, M. R. *Energy Fuels* **2006**, *20*, 2439–2447.
- (87) Grzybowski, M.; Skonieczny, K.; Butenschön, H.; Gryko, D. T. *Angew. Chem. Int. Ed.* **2013**, *52*, 9900–9930.
- (88) Fechtenkötter, A.; Saalwächter, K.; Harbison, M. A.; Müllen, K.; Spiess, H. W. *Angew. Chem. Int. Ed.* **1999**, *38*, 3039–3042.
- (89) Stabel, A.; Herwig, P.; Müllen, K.; Rabe, J. P. *Angew. Chem. Int. Ed. Engl.* **1995**, *34*, 1609–1611.
- (90) Breure, B.; Subramanian, D.; Leys, J.; Peters, C. J.; Anisimov, M. A. *Energy Fuels* **2013**, *27*, 172–176.
- (91) Yin, C. X.; Tan, X.; Müllen, K.; Stryker, J. M.; Gray, M. R. *Energy Fuels* **2008**, *22*, 2465–2469.
- (92) Wiehe, I. A. *Energy Fuels* **1994**, *8*, 536–544.
- (93) Alshareef, A. H.; Tan, X.; Diner, C.; Zhao, J.; Scherer, A.; Azyat, K.; Stryker, J. M.; Tykwinski, R. R.; Gray, M. R. *Energy Fuels* **2014**, *28*, 1692–1700.
- (94) Alshareef, A. H.; Azyat, K.; Tykwinski, R. R.; Gray, M. R. *Energy Fuels* **2010**, *24*, 3998–4004.
- (95) Alshareef, A. H.; Scherer, A.; Tan, X.; Azyat, K.; Stryker, J. M.; Tykwinski, R. R.; Gray, M. R. *Energy Fuels* **2012**, *26*, 1828–1843.
- (96) Sripatha, K.; Andersson, J. T. *Anal. Bioanal. Chem.* **2005**, *382*, 735–741.
- (97) Hourani, N.; Andersson, J. T.; Möller, I.; Amad, M.; Witt, M.; Mani Sarathy, S. *Rapid Commun. Mass Spectrom.* **2013**, *27*, 2432–2438.
- (98) Andrews, A. B.; McClelland, A.; Korkeila, O.; Demidov, A.; Krummel, A.; Mullins, O. C.; Chen, Z. *Langmuir* **2011**, *27*, 6049–6058.
- (99) González, M. F.; Stull, C. S.; López-Linares, F.; Pereira-Almao, P. *Energy Fuels* **2007**, *21*, 234–241.
- (100) López-Linares, F.; Carbognani, L.; González, M. F.; Sosa-Stull, C.; Figueras, M.; Pereira-Almao, P. *Energy Fuels* **2006**, *20*, 2748–2750.
- (101) Juyal, P.; McKenna, A. M.; Yen, A.; Rodgers, R. P.; Reddy, C. M.; Nelson, R. K.; Andrews, A. B.; Atolia, E.; Allenson, S. J.; Mullins, O. C.; Marshall, A. G. *Energy Fuels* **2011**, *25*, 172–182.
- (102) Sjöblom, J.; Simon, S.; Xu, Z. *Adv. Colloid Interface Sci.* **2015**, *218*, 1–16.

- (103) Nordgård, E. L.; Landsem, E.; Sjöblom, J. *Langmuir* **2008**, *24*, 8742–8751.
- (104) Wang, J.; van der Tuuk Opedal, N.; Lu, Q.; Xu, Z.; Zeng, H.; Sjöblom, J. *Energy Fuels* **2012**, *26*, 2591–2599.
- (105) Nordgård, E. L.; Sjöblom, J. *J. Dispers. Sci. Technol.* **2008**, *29*, 1114–1122.
- (106) Nordgård, E. L.; Sørland, G.; Sjöblom, J. *Langmuir* **2010**, *26*, 2352–2360.
- (107) Wei, D.; Orlandi, E.; Barriet, M.; Simon, S.; Sjöblom, J. *J. Therm. Anal. Calorim.* **2015**, *122*, 463–471.
- (108) Knudsen, A.; Nordgård, E. L.; Diou, O.; Sjöblom, J. *J. Dispers. Sci. Technol.* **2012**, *33*, 1514–1524.
- (109) Langhals, H.; Jona, W. *Eur. J. Org. Chem.* **1998**, *5*, 847–851.
- (110) Holman, M. W.; Liu, R.; Adams, D. M. *J. Am. Chem. Soc.* **2003**, *125*, 12649–12654.
- (111) Lutnaes, B. F.; Brandal, Ø.; Sjöblom, J.; Krane, J. *Org. Biomol. Chem.* **2006**, *4*, 616–620.
- (112) Lutnaes, B. F.; Krane, J.; Smith, B. E.; Rowland, S. J. *Org. Biomol. Chem.* **2007**, *5*, 1873–1877.
- (113) Hanneseth, A. M. D.; Selsbak, C.; Sjöblom, J. *J. Dispers. Sci. Technol.* **2010**, *31*, 770–779.
- (114) Gore, P. H. *Chem. Rev.* **1955**, *55*, 229–281.
- (115) Tan, X.; Fenniri, H.; Gray, M. R. *Energy Fuels* **2009**, *23*, 3687–3693.
- (116) da Costa, L. M.; Stoyanov, S. R.; Gusarov, S.; Tan, X.; Gray, M. R.; Stryker, J. M.; Tykwinski, R.; de M. Carneiro, J. W.; Seidl, P. R.; Kovalenko, A. *Energy Fuels* **2012**, *26*, 2727–2735.
- (117) da Costa, L. M.; Hayaki, S.; Stoyanov, S. R.; Gusarov, S.; Tan, X.; Gray, M. R.; Stryker, J. M.; Tykwinski, R.; de M. Carneiro, J. W.; Sato, H.; Seidl, P. R.; Kovalenko, A. *Phys. Chem. Chem. Phys.* **2012**, *14*, 3922–3934.
- (118) Chinchilla, R.; Nájera, C. *Chem. Soc. Rev.* **2011**, *40*, 5084–5121.
- (119) Elangovan, A.; Wang, Y. H.; Ho, T. I. **2003**, *5*, 1841–1844.
- (120) Cahiez, G.; Chaboche, C.; Duplais, C.; Moyeux, A. *Org. Lett.* **2009**, *11*, 277–280.
- (121) Liu, N.; Wang, Z. X. *J. Org. Chem.* **2011**, *76*, 10031–10038.
- (122) Li, W. N.; Wang, Z. L. *RSC Adv.* **2013**, *3*, 25565–25575.
- (123) Diner, C.; Scott, D. E.; Tykwinski, R. R.; Gray, M. R.; Stryker, J. M. *J. Org. Chem.* **2015**, *80*, 1719–1726.
- (124) Wang, X. S.; Li, Q.; Yao, C. S.; Tu, S. J. *Eur. J. Org. Chem.* **2008**, *20*, 3513–3518.
- (125) Scherer, A.; Hampel, F.; Gray, M. R.; Stryker, J. M.; Tykwinski, R. R. *J. Phys. Org. Chem.* **2012**, *25*, 597–606.

- (126) Schulze, M.; Scott, D. E.; Scherer, A.; Hampel, F.; Hamilton, R. J.; Gray, M. R.; Tykwinski, R. R.; Stryker, J. M. *Org. Lett.* **2015**, *17*, 5930–5933.
- (127) Oldenburg, T. B. P.; Huang, H.; Donohoe, P.; Willsch, H.; Larter, S. R. *Org. Geochem.* **2004**, *35*, 665–678.
- (128) Gallegos, E. J.; Sundararaman, P. *Mass Spectrom. Rev.* **1985**, *4*, 55–85.
- (129) Philp, R. P. *Mass Spectrom. Rev.* **1985**, *4*, 1–54.
- (130) Ávila, B. M. F.; Pereira, R.; Gomes, A. O.; Azevedo, D. A. *J. Chromatogr. A* **2011**, *1218*, 3208–3216.
- (131) Wu, Y.; Xia, Y.; Wang, Y.; Lei, T.; Chang, J.; Wang, Y. *J. Pet. Sci. Eng.* **2013**, *103*, 97–105.
- (132) McKenna, A. M.; Williams, J. T.; Putman, J. C.; Aeppli, C.; Reddy, C. M.; Valentine, D. L.; Lemkau, K. L.; Kellermann, M. Y.; Savory, J. J.; Kaiser, N. K.; Marshall, A. G.; Rodgers, R. P. *Energy Fuels* **2014**, *28*, 2454–2464.
- (133) Peters, K.; Walters, C.; Moldowan, J. *The Biomarker Guide Volume 2*, 2nd ed.; Cambridge: Cambridge University Press., **2004**.
- (134) Schulze, M.; Scherer, A.; Hampel, F.; Stryker, J. M.; Tykwinski, R. R. *Chem. Eur. J.* **2016**, *22*, 3378–3386.
- (135) Littler, B. J.; Ciringh, Y.; Lindsey, J. S. *J. Org. Chem.* **1999**, *64*, 2864–2872.
- (136) Cardozo, S. D.; Schulze, M.; Tykwinski, R. R.; Gray, M. R. *Energy Fuels* **2015**, *29*, 1494–1502.
- (137) Diner, C. Scalable and Concise Approaches for the Synthesis of “Archipelago Model” Asphaltene Compounds, Ph. D. Dissertation, University of Alberta, Edmonton, AB, **2015**.
- (138) Eicher, T.; Hauptmann, S. *The Chemistry of Heterocycles*, 2nd ed.; Wiley-VCH Verlag GmbH & Co. KGaA, Weinheim, **2003**.
- (139) Alfa Aesar, *Heterocycles: The Chemical Compounds That Know No Bounds*, <https://www.alfa.com/en/organic-chemistry-blog/heterocycles-the-chemical-compounds-that-know-no-bounds/> (accessed July 20, 2018).
- (140) Eicher, T., Hauptmann, S., Speicher, A. *The Structure of Heterocyclic Compounds: Structure, Reactions, Synthesis, and Applications*, 3rd ed.; Wiley-VCH Verlag GmbH & Co. KGaA, **2012**.
- (141) Ranu, B. C.; Chatterjee, T.; Mukherjee, N.; Maity, P.; Majhi, B. Synthesis of Bioactive Five- and Six-Membered Heterocycles Catalyzed by Heterogeneous Supported Metals. *Green Synthetic Approaches for Biologically Relevant Heterocycles*, Brahmachari, G., Ed.; Elsevier Inc., **2015**.
- (142) Shukla, P. K.; Verma, A., Mishra, P. Significance of Nitrogen Heterocyclic Nuclei in the Search of Pharmacological Active Compounds. *New Perspective in Agriculture and Human Health* Shukla, R. P.; Mishra, R. S.; , Tripathi, A. D.; Yadav, A. K.; Tiwari, M.;

- Mishra, R. R., Ed.; Bharti Publication, New Dehli, **2017**.
- (143) Thakkar, A. *Int. J. Theor. Appl. Sci.* **2016**, *8*, 53–54.
- (144) Bentzinger, G.; De Souza, W.; Mullié, C.; Agnamey, P.; Dassonville-Klimpt, A.; Sonnet, P. *Tetrahedron: Asymmetry* **2016**, *27*, 1–11.
- (145) Kumar, T. O. S.; Mahadevan, K. M.; Sujanganapathy, P. S.; Kumara, M. N. *Lett. Drug Des. Discov.* **2016**, *13*, 982–991.
- (146) Boonyasuppayakorn, S.; Reichert, E. D.; Manzano, M.; Nagarajan, K.; Padmanabhan, R. *Antiviral Res.* **2014**, *106*, 125–134.
- (147) Al-mulla, A. *Der Pharma Chemica* **2017**, *9*, 141–147.
- (148) Manjunath, G.; Mahesh, M.; Bheemaraju, G.; Reddy, P. V. B.; Ramana, P. V. *Heterocycl. Lett.* **2016**, *6*, 42–51.
- (149) Gohil, J. D.; Patel, H. B.; Patel, M. P. *RSC Adv.* **2016**, *6*, 74726–74733.
- (150) Selvi, G.; Rajendran, S. P. *Asian J. Chem.* **2004**, *16*, 1017–1022.
- (151) Kharb, R.; Kaur, H. *Int. Res. J. Pharm.* **2013**, *4*, 63–69.
- (152) Powell, W. H. *Pure & Appl. Chem.* **1985**, *55*, 409–416.
- (153) Joule, J. A.; Mills, K. *Heterocyclic Chemistry at a Glance*, 2nd Ed.; John Wiley & Sons, Ltd., **2013**.
- (154) Skraup, Z. H. *Chem. Ber.* **1880**, *13*, 2086–2087.
- (155) Mansake, R. H.; Kulka, M. *Org. React.* **1953**, *7*, 59–61.
- (156) Doebner, O.; Miller, V. W. *Chem. Ber.* **1881**, *14*, 2812–2813.
- (157) Conrad, M.; Limpach, L. M. *Chem. Ber.* **1887**, *20*, 944–948.
- (158) Combes, A. *Compt. Rend.* **1888**, *106*, 142–143.
- (159) Pfitzinger, W. *J. Prakt. Chem.* **1886**, *33*, 100.
- (160) Povarov, L. S. *Russ. Chem. Rev.* **1967**, *36*, 656–670.
- (161) Kouznetsov, V. V. *Tetrahedron* **2009**, *65*, 2721–2750.
- (162) Cohn, E. W. *J. Am. Chem. Soc.* **1930**, *52*, 3685–3688.
- (163) Manske, R. H. *Chem. Rev.* **1942**, *30*, 113–144.
- (164) Yamashkin, S. A.; Oreshkina, E. A. *Chem. Heterocycl Compd.* **2006**, *42*, 701–718.
- (165) Reitsema, R. H. *Chem. Rev.* **1948**, *43*, 43–68.
- (166) Brouet, J. C.; Gu, S.; Peet, N. P.; Williams, J. D. *Synth Commun.* **2009**, *39*, 5193–5196.
- (167) Li, J. J. *Combes Quinoline Synthesis; Name Reactions: A Collection of Detailed Mechanisms and Synthetic Applications*, Springer, Berlin, Heidelberg, **2009**.

- (168) Shvekhgeimer, M. G. *Chem. Heterocycl. Compd.* **2004**, *40*, 257–294.
- (169) Buu-Hoi, N. P.; Royer, R.; Xuong, N. D.; Jacquignon, P. *J. Org. Chem* **1953**, *18*, 1209–1224.
- (170) Li, J. J. *Name Reactions: A Collection of Detailed Mechanisms and Synthetic Applications*; Springer International Publishing, Switzerland, **2014**.
- (171) Ugi, I.; Domling, A.; Horl, W. *Endeavor* **1994**, *18*, 115–122.
- (172) Haji, M. *Beilstein J. Org. Chem.* **2016**, *12*, 1269–1301.
- (173) Strecker, A. *Liebigs Ann. Chem.* **1850**, *75*, 27–45.
- (174) Kouznetsov, V. V.; Galvis, C. E. P. *Tetrahedron* **2018**, *74*, 773–810.
- (175) Ugi, I.; Meyr, R.; Fetzer, U.; Steinbrückner, C. *Angew. Chem.* **1959**, *71*, 386.
- (176) Fogg, D. E.; dos Santos, E. N. *Coordin. Chem. Rev.* **2004**, *248*, 2365–2379.
- (177) Herrera, R. P., Marqués-López, E. *Multicomponent Reactions Concepts and Applications for Design and Synthesis*; John Wiley & Sons, Inc., New Jersey, **2015**.
- (178) Galván, A.; Fañanás, F. J.; Rodríguez, F. *Eur. J. Inorg. Chem.* **2016**, *2016*, 1306–1313.
- (179) Togo, H.; Iida, S. *Synlett* **2006**, *14*, 2159–2175.
- (180) Parvatkar, P. T.; Parameswaran, P. S.; Tilve, S. G. *Chem. Eur. J.* **2012**, *18*, 5460–5489.
- (181) Ren, Y. M.; Cai, C.; Yang, R. C. *RSC Adv.* **2013**, *3*, 7182–7204.
- (182) Nammalwar, B.; Bunce, R. A. *Molecules* **2014**, *19*, 204–232.
- (183) Jia, X.; Peng, F.; Qing, C.; Huo, C.; Wang, Y.; Wang, X. *Tetrahedron Lett.* **2013**, *54*, 4950–4952.
- (184) Kouznetsov, V. V.; Meléndez Gómez, C. M.; Rojas Ruíz, F. A.; Del Olmo, E. *Tetrahedron Lett.* **2012**, *53*, 3115–3118.
- (185) Jia, X.; Ren, Y.; Huo, C.; Wang, W.J.; Chen, X.N.; Xu, X.L.; Wang, X. *Tetrahedron Lett.* **2010**, *51*, 6779–6782.
- (186) Lin, X. F.; Cui, S. L.; Wang, Y. G. *Tetrahedron Lett.* **2006**, *47*, 4509–4512.
- (187) Li, Y. C.; Zhang, J. M.; Dong, L. T.; Yan, M. *Chinese J. Chem.* **2006**, *24*, 929–932.
- (188) Jin, G.; Zhao, J.; Han, J.; Zhu, S.; Zhang, J. *Tetrahedron* **2010**, *66*, 913–917.
- (189) Rai, N. P.; Shashikanth, S.; Arunachalam, P. N. *Synth. Commun.* **2009**, *39*, 2125–2136.
- (190) Wang, X. S.; Zhou, J.; Yin, M. Y.; Yang, K.; Tu, S. J. *J. Comb. Chem.* **2010**, *12*, 266–269.
- (191) Wang, X. S.; Zhou, J.; Yin, M. Y.; Yang, K.; Tu, S. J. *J. Heterocycl. Chem.* **2010**, *47*, 873–877.
- (192) Wang, W.; Jiang, H.; Zhang, M. M.; Wang, X. S. *J. Heterocycl. Chem.* **2014**, *51*, 830–834.

- (193) Kaiho, T. *Iodine Chemistry and Applications*; John Wiley & Sons, Inc., New Jersey, **2015**.
- (194) Zhang, M.; Ding, Y. Q.; Xiong, B.; Wang, T.; Wang, L. *Heterocycles* **2011**, *83*, 2289–2298.
- (195) Guo, Q.; Liao, L.; Teng, W.; Ren, S.; Wang, X.; Lin, Y.; Meng, F. *Catal. Today* **2016**, *263*, 117–122.
- (196) Guo, Q.; Wang, W.; Teng, W.; Chen, L.; Wang, Y.; Shen, B. *Synth. Commun.* **2012**, *42*, 2574–2584.
- (197) Schulze, M. Synthesis and Investigation of Asphaltene Model Compounds, Ph. D. Dissertation, Friedrich-Alexander-University of Erlangen-Nürnberg, Erlangen-Nürnberg, Germany, **2016**.
- (198) Finger, H.; Spitz, C. *J. für Prakt. Chemie* **1908**, 445–449.
- (199) Lin, X. F.; Cui, S. L.; Wang, Y. G. *Tetrahedron Lett.* **2006**, *47*, 3127–3130.
- (200) Larock, R. C.; Leung, W. Y.; Stolz-Dunn, S. *Tetrahedron Lett.* **1989**, *30*, 6629–6632.
- (201) Colbon, P.; Ruan, J.; Purdie, M.; Mulholland, K.; Xiao, J. *Org. Lett.* **2011**, *13*, 5456–5459.
- (202) Schulze, M.; Scherer, A.; Diner, C.; Tykwinski, R. R. *Org. Synth.* **2016**, *93*, 100–114.
- (203) Klapars, A.; Buchwald, S. L. *J. Am. Chem. Soc.* **2002**, *124*, 14844–14845.
- (204) Spencer, J. N.; Holmboe, E.; Kirshenbaum, M.; Firth, D.; Pinto, P. *Can. J. Chem.* **1982**, *60*, 1178–1182.
- (205) Matwiczuk, A.; Karcz, D.; Walkowiak, R.; Furso, J.; Gładyszewska, B.; Wybraniec, S.; Niewiadomy, A.; Karwasz, G. P.; Gagoś, M. *J. Phys. Chem. A* **2017**, *121*, 1402–1411.
- (206) Ruysbergh, E.; Stevens, C. V.; De Kimpe, N.; Mangelinckx, S. *RSC Adv.* **2016**, *6*, 73717–73730.
- (207) Hegarty, A. F.; Dowling, J. P.; Eustace, S. J.; McGarraghy, M. *J. Am. Chem. Soc.* **1998**, *120*, 2290–2296.
- (208) Guardia, L. Della; King Jr., A. D. *J. Colloid Interface Sci.* **1982**, *88*, 8–16.
- (209) Sato, T.; Hamada, Y.; Sumikawa, M.; Araki, S.; Yamamoto, H. *Ind. Eng. Chem. Res.* **2014**, *53*, 19331–19337.
- (210) Monroe, B. M. *Photochem. Photobiol.* **1982**, *35*, 863–865.
- (211) Hansen, C. M. *Hansen Solubility Parameters: A User's Handbook, 2nd Ed.*; CRC Press: Boca Raton, FL, **2007**.
- (212) Acevedo, S.; Castro, A.; Vásquez, E.; Marcano, F.; Ranaudo, M. A. *Energy Fuels* **2010**, *24*, 5921–5933.
- (213) Morimoto, M.; Imamura, H.; Shibuta, S.; Morita, T.; Nishikawa, K.; Yamamoto, H.; Tanaka, R.; Takanohashi, T. *Energy Fuels* **2015**, *29*, 5737–5743.

- (214) Redelius, P. *Energy Fuels* **2004**, *18*, 1087–1092.
- (215) Sato, T.; Araki, S.; Morimoto, M.; Tanaka, R.; Yamamoto, H. *Energy Fuels* **2014**, *28*, 891–897.
- (216) Morimoto, M.; Fukatsu, N.; Tanaka, R.; Takanohashi, T.; Kumagai, H.; Morita, T.; Tykwinski, R. R.; Scott, D. E.; Stryker, J. M.; Gray, M. R.; Sato, T.; Yamamoto, H. *Energy Fuels* **2018**, *32*, 11296–11303.
- (217) Huggins, M. L. *J. Phys. Chem.* **1951**, *55*, 619–620.
- (218) Kauffman, G. B.; Fang, L. Y. Chapter Two: Transition Metal Complexes and Compounds; *Inorganic Syntheses*, Vol. 22, Holt Jr., S. L., Inorganic Syntheses, Inc., **1983**.
- (219) Marcó, A.; Compañó, R.; Rubio, R.; Casals, I. *Mikrochim. Acta* **2003**, *142*, 13–19.
- (220) Phillips, S. C.; Johnson, J. E.; Miranda, E.; Disenhof, C. *Limnol. Oceanogr. Methods* **2011**, *9*, 194–203.
- (221) Sternglanz, P. D.; Kollig, H. *Anal. Chem.* **1962**, *34*, 544–547.
- (222) Culmo, R. *The Elemental Analysis of Various Classes of Chemical Compounds Using CHN*; PerkinElmer, Inc., **2013**.
- (223) Stevenson, P. J. *Org. Biomol. Chem.* **2011**, *9*, 2078–2084.
- (224) Stark, T.; Suhartono, M.; Göbel, M. W.; Lautens, M. *Synlett* **2013**, *24*, 2730–2734.
- (225) Godoy-Alcántar, C.; Yatsimirsky, A. K.; Lehn, J. M. *J. Phys. Org. Chem.* **2005**, *18*, 979–985.
- (226) Wang, X. S.; Li, Q.; Wu, J. R.; Li, Y. L.; Yao, C. S.; Tu, S. J. *Synthesis* **2008**, *12*, 1902–1910.
- (227) Wang, X. S.; Li, Q.; Zhang, M. M.; Yao, C. S.; Tu, S. J. *J. Heterocycl. Chem.* **2008**, *45*, 1027–1031.
- (228) Foxley, G. H. *Analyst* **1961**, *86*, 348–349.
- (229) Hebden, J. *Chem 13 News*. **1984**, *3*.
- (230) Jackson, H. L.; McCormack, W. B.; Rondestvedt, C. S.; Smeltz, K. C.; Viele, I. E. *J. Chem. Educ.* **1970**, *47*, A175-A188.
- (231) Jeong, S. Y.; Kim, N.; Lee, J. C. *Bull. Korean Chem. Soc.* **2014**, *35*, 3366–3368.
- (232) Eigen, M.; Kustin, K. *J. Am. Chem. Soc.* **1962**, *84*, 1355–1361.
- (233) Palmer, D. A.; van Eldik, R. *Inorg. Chem.* **1986**, *25*, 928–931.
- (234) Karimi, B.; Zareyee, D. *J. Iran. Chem. Soc.*, **2008**, *5*, 1–5.
- (235) Coeey, E. J.; Erickson, B. W. *J. Org. Chem.* **1971**, *36*, 3553–3560.
- (236) Harville, R.; Reed, S. F. *J. Org. Chem.* **1968**, *33*, 3976–3977.

- (237) Schulek, E.; Burger, K. *Talanta* **1960**, *7*, 41–45.
- (238) Faull, J. H. *J. Am. Chem. Soc.* **1934**, *56*, 522–526.
- (239) Huwiler, M.; Bürg, U.; Kohler, H. *Eur. J. Biochem.* **1985**, *147*, 469–476.
- (240) Garrett, R. A.; Gillespie, R. J.; Senior, J. B. *Inorg. Chem.* **1965**, *4*, 563–566.
- (241) Gillespie, R. J.; Milne, J. B. *Inorg. Chem.* **1966**, *5*, 1577–1582.
- (242) Gillespie, R. J.; Senior, J. B. *Inorg. Chem.* **1964**, *3*, 440–444.
- (243) Cantrel, L.; Chopin, J. *PSI-Bericht* **1996**, 187–211.
- (244) Liebhafsky, H. A. *J. Am. Chem. Soc.* **1932**, *54*, 3499–3508.
- (245) Bao, W.; Renganathan, V. *FEBS Lett.* **1991**, *279*, 30–32.
- (246) Bray, W. C.; Liebhafsky, H. A. *J. Am. Chem. Soc.* **1931**, *53*, 38–44.
- (247) Schmitz, G. *Russ. J. Phys. Chem. A* **2009**, *83*, 1447–1451.
- (248) Maity, A.; Hyun, S. M.; Powers, D. C. *Nat. Chem.* **2018**, *10*, 200–204.
- (249) Lopalco, A.; Dalwadi, G.; Niu, S.; Schowen, R. L.; Douglas, J.; Stella, V. J. *J. Pharm Sci.* **2016**, *105*, 705–713.
- (250) Ajdačić, V.; Nikolić, A.; Kerner, M.; Wipf, P.; Opsenica, I. M. *Synlett* **2018**, *29*, 1781–1785.
- (251) Dawes, G. J. S.; Scott, E. L.; Le Nôtre, J.; Sanders, J. P. M.; Bitter, J. H. *Green Chem.* **2015**, *17*, 3231–3250.
- (252) Domingo, L. R.; Aurell, M. J.; Sáez, J. A.; Mekelleche, S. M. *RSC Adv.* **2014**, *4*, 25268–25278.
- (253) Haghdadí, M.; Mousavi, S. S.; Ghasemnejad, H. *J. Serbian Chem. Soc.* **2016**, *81*, 67–80.
- (254) Andersson, J. T. *Int. J. Environ. Anal. Chem.* **1992**, *48*, 1–15.
- (255) Soto-Cantu, E.; Cueto, R.; Koch, J.; Russo, P. S. *Langmuir* **2012**, *28*, 5562–5569.
- (256) Haynes, J. P.; Miller, K. E.; Majestic, B. J. *Environ. Sci. Technol.* **2019**, *53*, 682–691.
- (257) Mcconkey, B. J.; Hewitt, L. M.; Dixon, D. G.; Greenberg, B. M. *Water, Air, & Soil Pollution* **2002**, *136*, 347–359.
- (258) Sakuragi, H.; Furusawa, G.; Ueno, K.; Tokumaru, K. *Chem. Lett.* **1982**, *72*, 1213–1216.
- (259) Poss, C. S.; Schreiber, S. L. *Acc. Chem. Res.* **1994**, *27*, 9–17.
- (260) Mortensen, K. T.; Osberger, T. J.; King, T. A.; Sore, H. F.; Spring, D. R. *Chem. Rev.* **2019**, DOI: 10.1021/acs.chemrev.9b00084.
- (261) Vrettou, M.; Gray, A. A.; Brewer, A. R. E.; Barrett, A. G. M. *Tetrahedron* **2007**, *63*, 1487–1536.

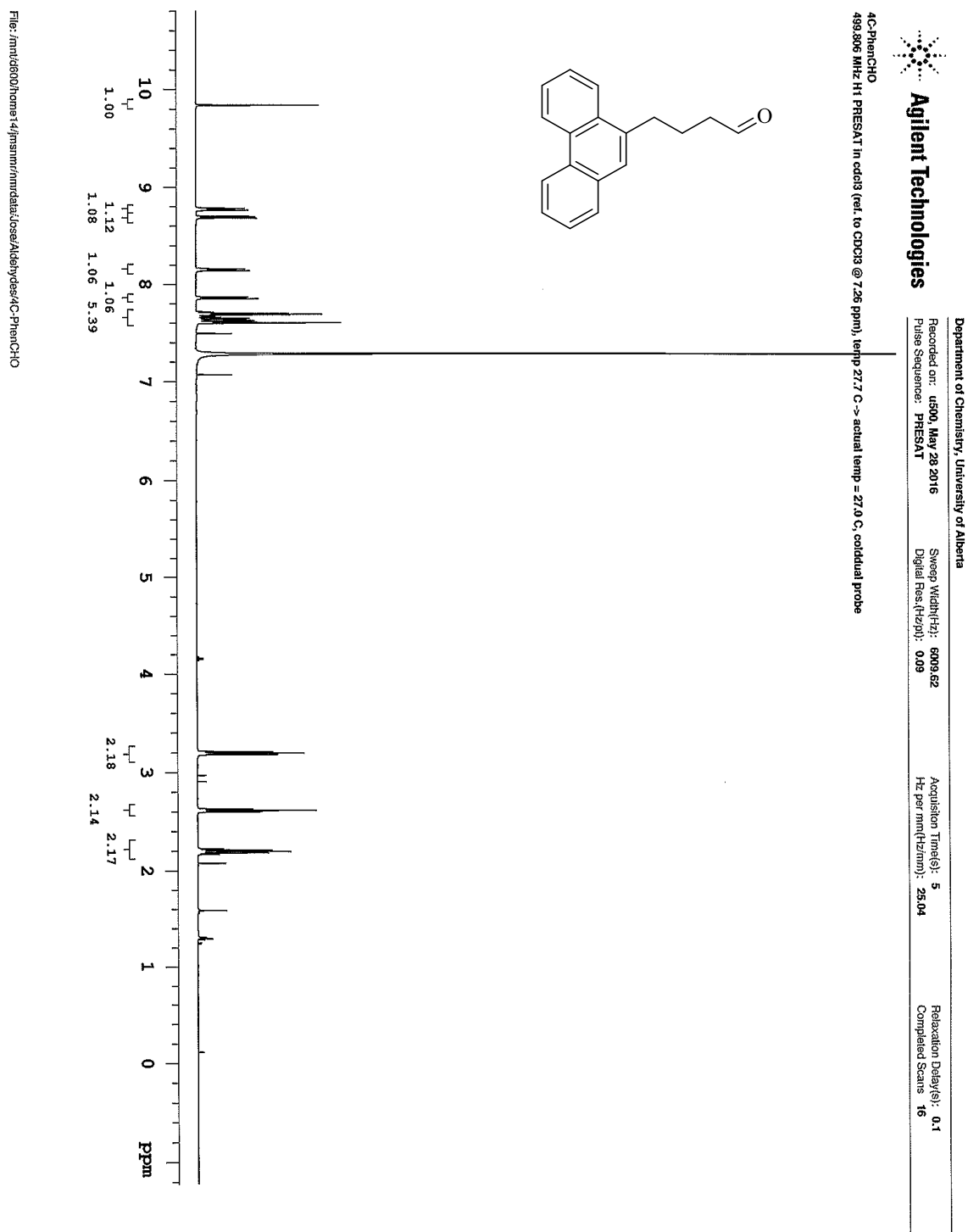
(262) Magnuson, S. R. *Tetrahedron* **1995**, *51*, 2167–2213.

(263) Liu, J.; Liu, F.; Zhu, Y.; Ma, X.; Jia, X. *Org. Lett.* **2015**, *17*, 1409–1412.

# Appendix I: $^1\text{H}$ and $^{13}\text{C}$ NMR Spectra

Due to the nature of the compounds, not all the  $^{13}\text{C}$  NMR signals for tertiary carbons have been assigned.

## 4-(phenanthren-9-yl) butanal (157).





Agilent Technologies

Department of Chemistry, University of Alberta

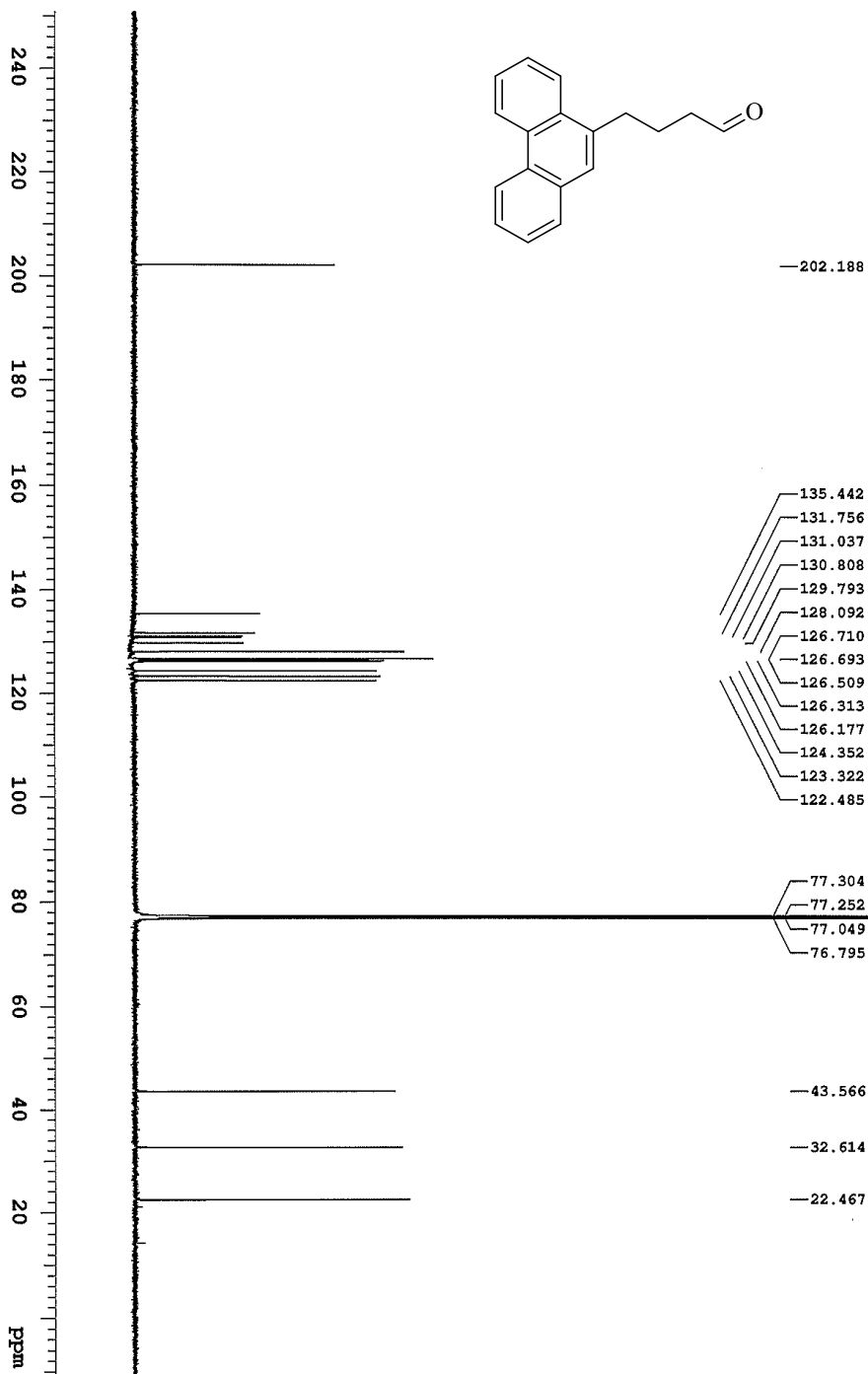
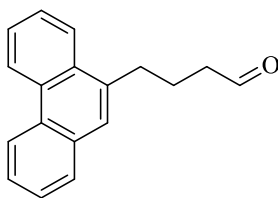
Recorded on: **us00, May 28 2016**  
Pulse Sequence: **szpul**

Sweep Width(Hz): **22994.7**  
Digital Res.(Hz): **0.23**

Acquisition Time(s): **2.5**  
Hz per mHz: **137.06**

Relaxation Delay(s): **0.1**  
Completed Scans: **128**

4C-PhenCHO  
125.691 MHz C13[1H] 1D In cdCl3 (ref. to CDCl3 @ 77.06 ppm), temp 27.7 C -> actual temp = 27.0 C, solidstate probe



File: mm165007hcmr1 47msmmrmmdata\cse\Aldhydes\4C-PhenCHO\_13C\_

# 5-(phenanthren-9-yl) pentanal (151).



Agilent Technologies

Department of Chemistry, University of Alberta

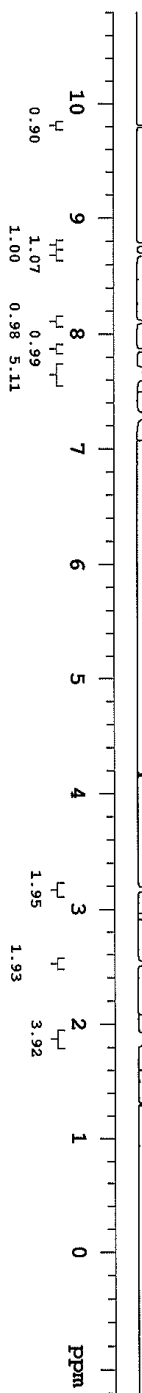
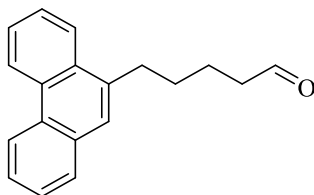
Recorded on: **u500\_May 27 2016**  
Pulse Sequence: **PHESAT1**

Sweep Width(Hz): **6009.62**  
Digital Res.(Hz/ppm): **0.09**

Acquisition Time(s): **5**  
Hz per point(Hz/min): **25.04**

Relaxation Delay(s): **0.1**  
Completed Scans: **16**

5C-PhenCHO  
499.806 MHz H1 PRESAT in cdcl3 (ref. to CDCl3 @ 7.26 ppm), temp 27.7 C -> actual temp = 27.0 C, cold dual probe



File: fmr1626001homo141jmsm/nmrdata/lose/Aldehyde/5C-PhenCHO



Agilent Technologies

Department of Chemistry, University of Alberta

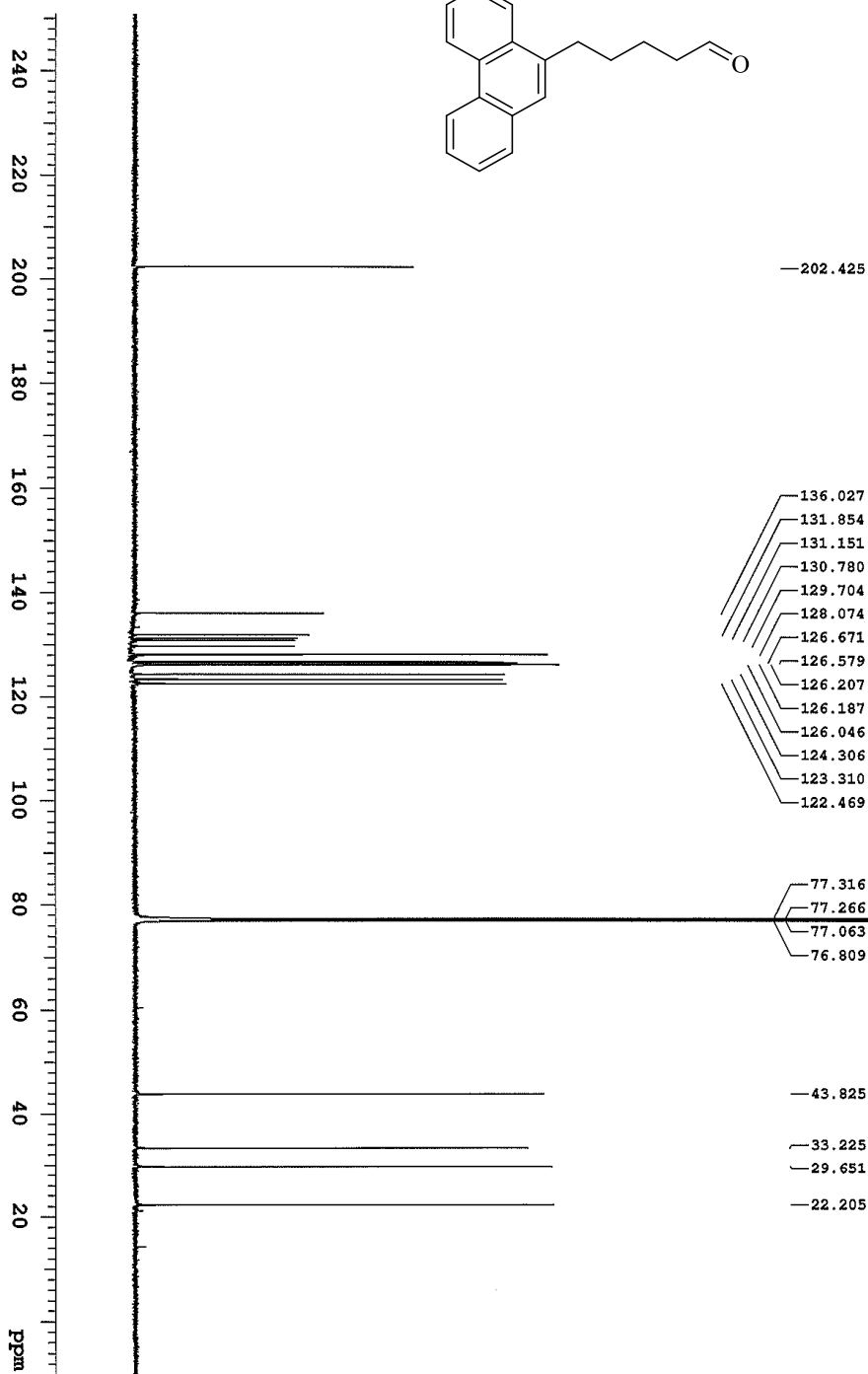
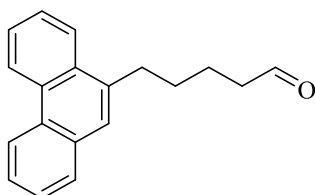
Recorded on: **4500, May 27 2016**

Sample Width(Hz): **32894.7**  
Digital Res.(Hz/pt): **0.25**

Acquisition Time(s): **2.5**  
Hz per ppm(Hz/ppm): **137.06**

Relaxation Delay(s): **0.1**  
Completed Scans: **128**

5C-PhenCHO  
125.691 MHz C13{H1} 1D In odd3 (ref. to CDCl3 @ 77.06 ppm), temp 27.7 C -> actual temp = 27.0 C, coldstart probe



File: amtk6600home14\jmsm\rm\data\loss\Aldelydes\5C-PhenCHO\_13C

# 6-(phenanthren-9-yl) hexanal (153).



Agilent Technologies

Department of Chemistry, University of Alberta

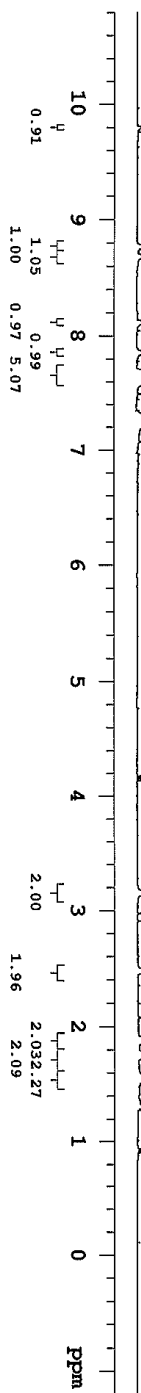
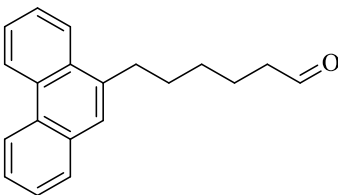
Recorded on: **us90**, **May 31 2016**  
Pulse Sequence: **PRESAT**

Sweep Width(Hz): **6009.62**  
Digital Res.(Hz): **0.09**

Acquisition Time(s): **5**  
Hz per mm(Hz/mm): **25.04**

Relaxation Delay(s): **0.1**  
Completed Scans: **16**

6C-PhenCH0  
499.806 MHz H1 PRESAT in cdcl3 (ref. to CDCl3 @ 7.26 ppm), temp 27.7 C -> actual temp = 27.0 C, coldstart probe



File: /mnt/d80/home/14jennan/rnmr/data/loose/Aldehyde/6C-PhenCH0



Agilent Technologies

Department of Chemistry, University of Alberta

Recorded on: us00, May 31 2016

Sheep Vial#(Hz): 32984.7

Acquisition Time(s): 2.5

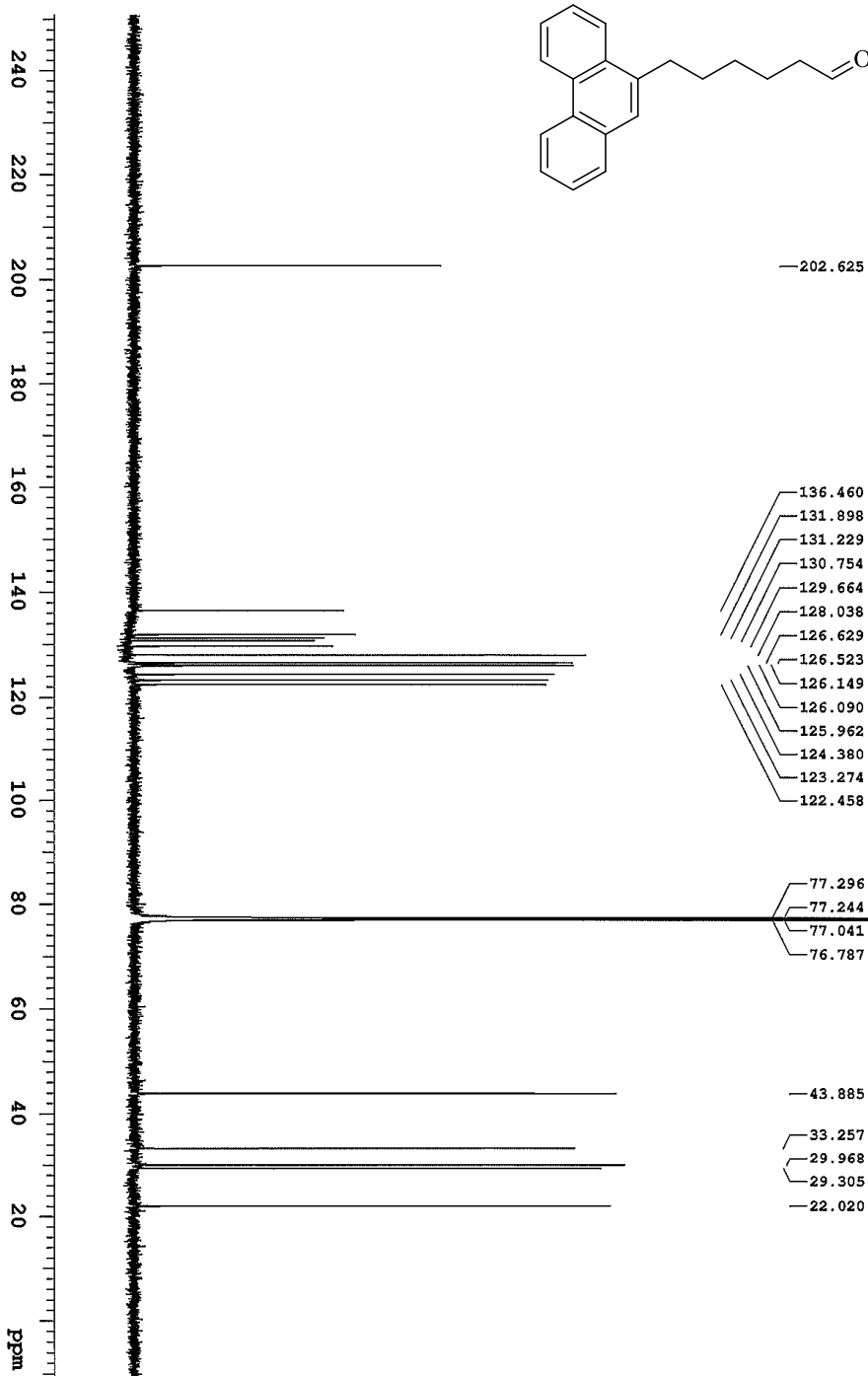
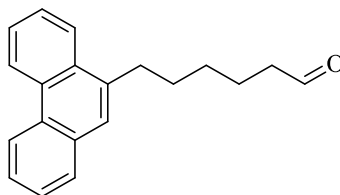
Relaxation Delay(s): 0.1

Completed Scans: 128

Digital Res. (Hz/ppm): 0.25

Fz. per mm(Hz/mm): 137.06

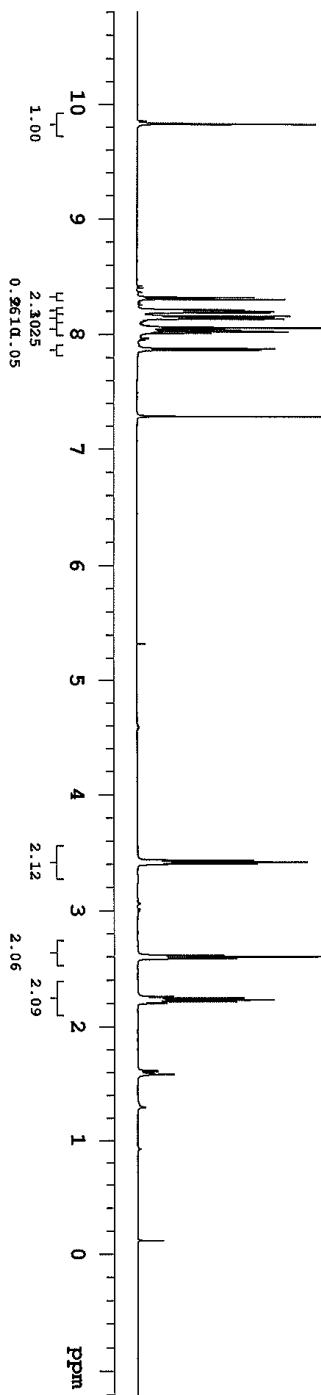
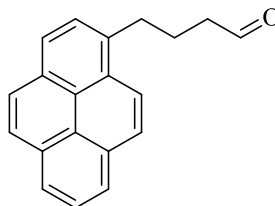
6C-PhenCHO  
125.691 MHz C13[1H] 1D in cdcl3 (ref. to CDCl3 @ 77.06 ppm), temp 27.7 C -> actual temp = 27.0 C, coldstart probe



File: /mnt/600/home14/jmsmm/mtdat/lose/Aldehydes/6C-PhenCHO\_13C

**Agilent Technologies**

Department of Chemistry, University of Alberta

Recorded on: **us00**, May 18 2016  
Pulse Sequence: **PRESAT**Sweep Width(Hz): **6009.62**  
Digital Res.(Hz): **0.09**Acquisition Time(s): **5**  
Hz per mHz(mn): **25.04**Relaxation Delay(s): **0.1**  
Completed Scans: **16****4C-PyCHO**  
499.806 MHz H1 PRESAT in cdcl3 (ref. to CDCl3 @ 7.26 ppm), temp 27.7 C -> actual temp = 27.0 C, coldstart probe

File: /mnt/d/0/home1/4/jnsnmr/mrdata/JoseAldehyd4C-PyCHO

**4-(Pyren-1-yl) butanal (158).**



Agilent Technologies

Department of Chemistry, University of Alberta

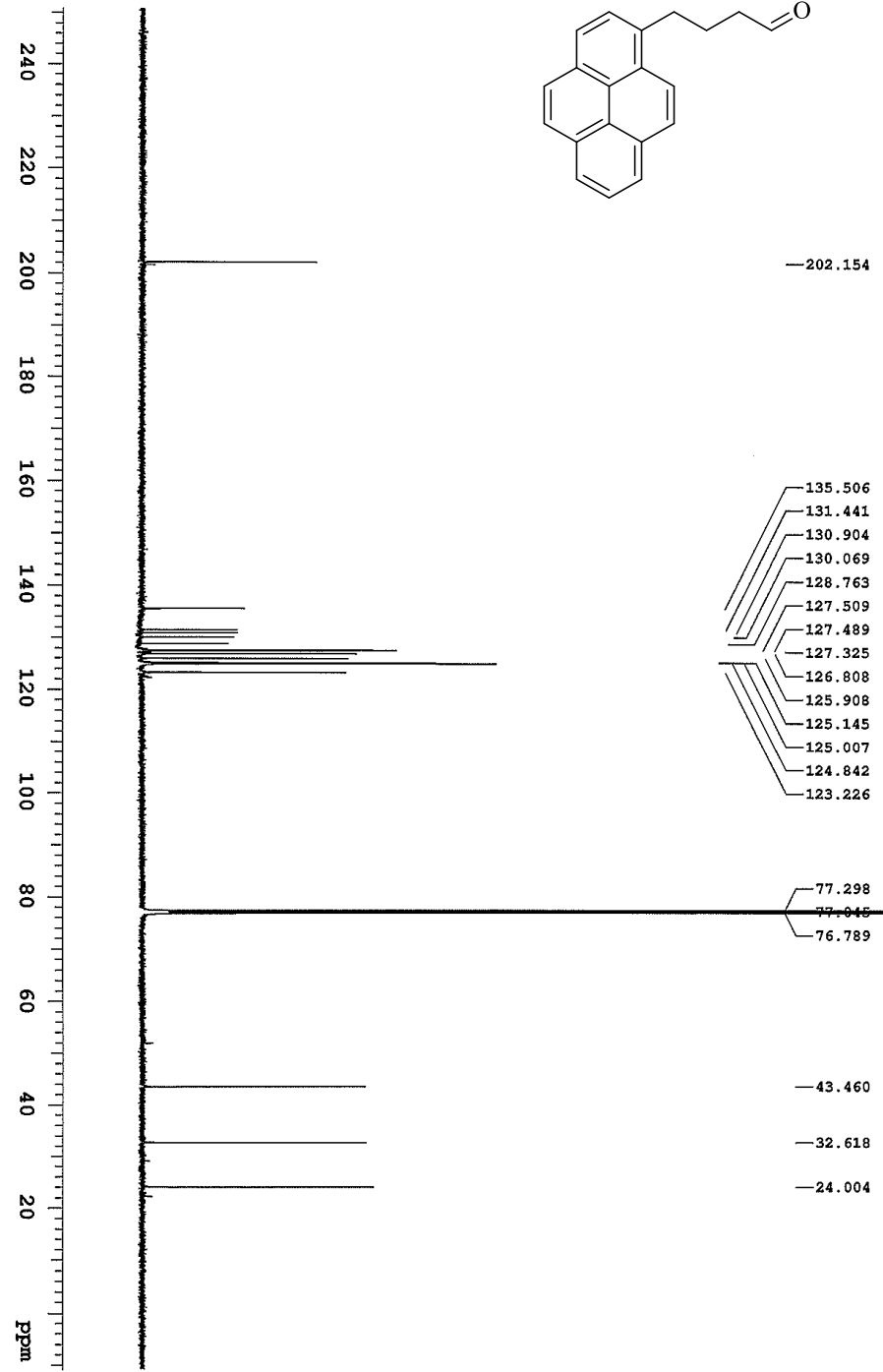
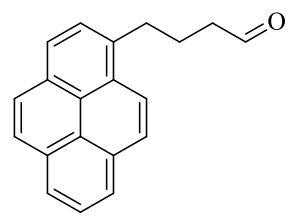
Recorded on: **u500, May 18 2016**  
Pulse Sequence: **zgpg30**

Sweep Width(Hz): **32894.7**  
Digital Res.(Hz/pp): **0.25**

Acquisition Time(s): **2.5**  
Hz per mm(Hz/mm): **137.06**

Relaxation Delay(s): **0.1**  
Completed Scans: **128**

4C-PyCHO  
125.691 MHz C13[1H] 1D in cdcl3 (ref. to CDCl3 @ 77.06 ppm), temp 27.7 C -> actual temp = 27.0 C, coldchill probe



File: /mnt/ds0/home14/msm/mrmdat/Losev/Aldehydes/4C-PyCHO\_13C\_

# 5-(Pyren-1-yl) pentanal (159).



Department of Chemistry, University of Alberta

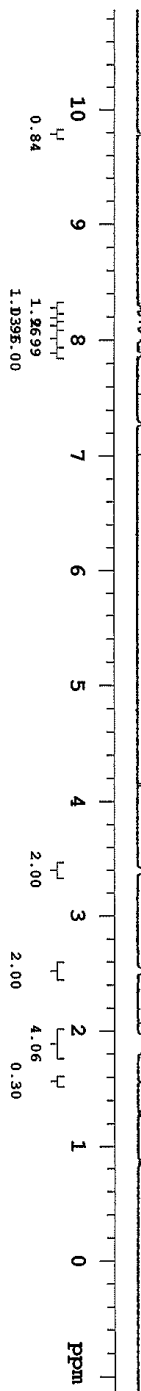
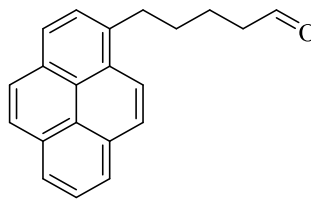
Recorded on: 1400, Nov 10 2015  
Pulse Sequence: s2pul

Sweep Width(Hz): 4901.92  
Digital Res.(Hz/pp): 0.07

Acquisition Time(s): 4.998  
Hz per nm(Hz/nm): 20.01

Relaxation Delay(s): 0.1  
Completed Scans: 16

<sup>5</sup>C-PyCHO  
399,794 MHz H1 1D in cdcl3 (ref. to CDCl3 @ 7.26 ppm), temp 26.5 C -> actual temp = 27.0 C; autoxdo probe



File: /mkl600/home14/jmsnm/nmrdata/ase/Aldehydes/5C-PyCHO



Agilent Technologies

Department of Chemistry, University of Alberta

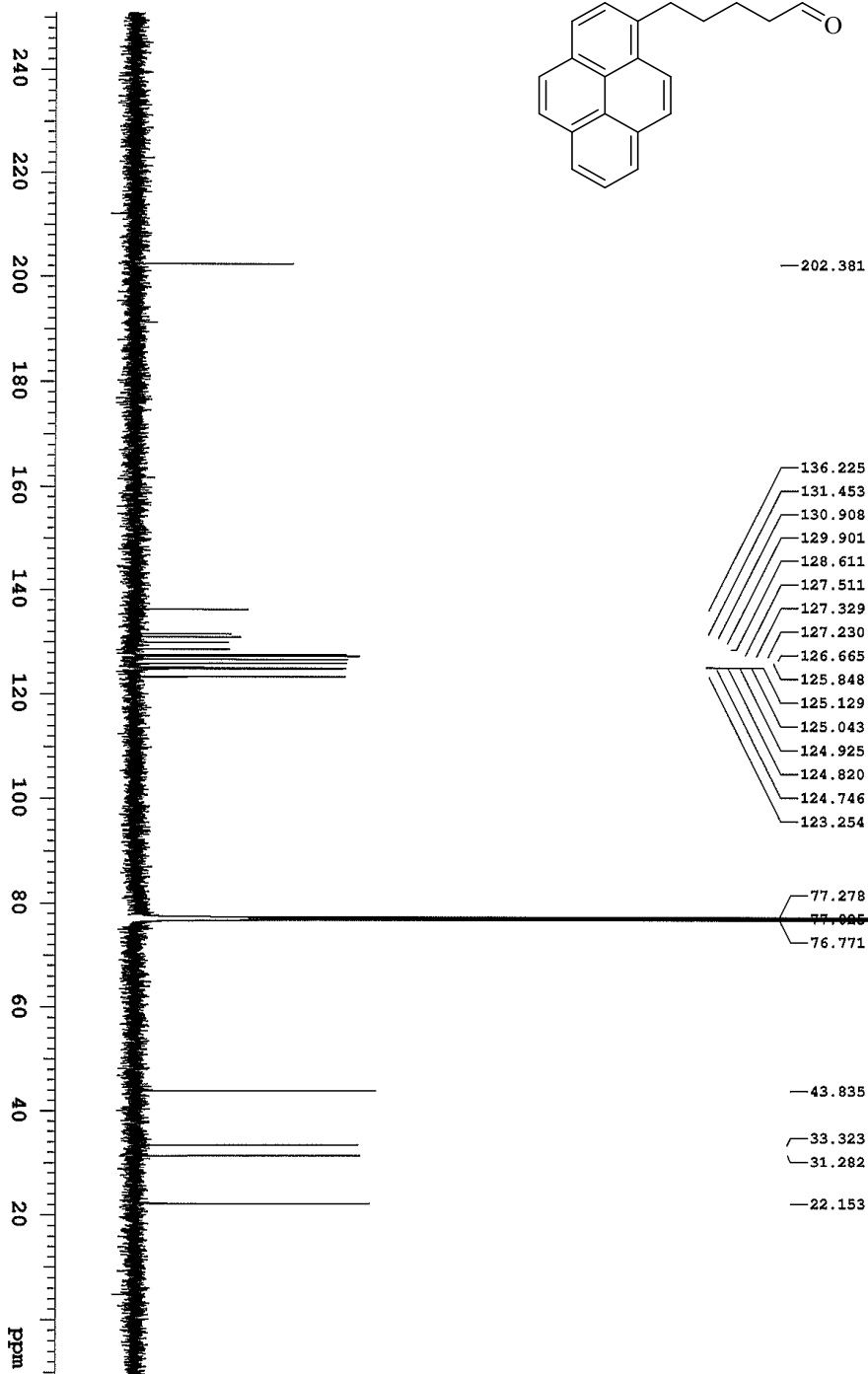
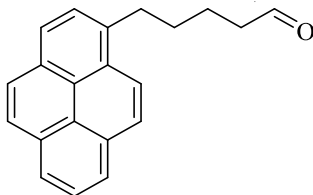
Recorded on: **u500, May 18 2016**  
Pulse Sequence: **zgpg30**

Sweep Width(Hz): **32994.7**  
Digital Res.(Hz/pt): **0.25**

Acquisition Time(s): **2.5**  
Hz per mm(Hz/mm): **137.06**

Relaxation Delay(S): **0.1**  
Completed Scans: **128**

5C-PyCHO  
125.691 MHz C13{H1} 1D in cdcls (ref: to CDCl3 @ 77.06 ppm), temp 27.7 C -> actual temp = 27.0 C, coldstart probe



File: /mnt/d60/home14/jmsm/mr/data/5c/Aldehydes/5C-PyCHO\_13C\_



Department of Chemistry, University of Alberta

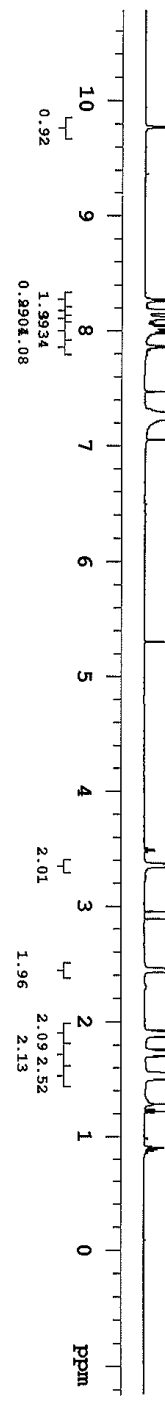
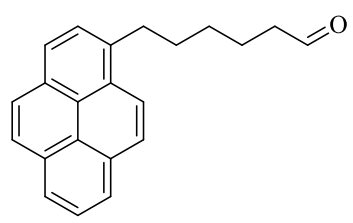
Recorded on: 0500, May 25 2016  
Pulse Sequence: PRESAT

Sweep Width(Hz): 6009.62  
Digital Res.(Hz/pt): 0.09

Acquisition Time(s): 5  
Hz per ppm(Hz/ppm): 25.04

Relaxation Delay(s): 0.1  
Completed Scans: 16

6C-PyCHO  
499.806 MHz <sup>1</sup>H PRESAT in cdcl3 (ref. to CDCl3 @ 7.26 ppm), temp 27.7 C -> actual temp = 27.0 C, cond:atd probe



### 6-(Pyren-1-yl) hexanal (160).

File: /mnt/c600/home14/jmsnmr/mntdata/losses/Aldehydes/6C-PyCHO



Agilent Technologies

Department of Chemistry, University of Alberta

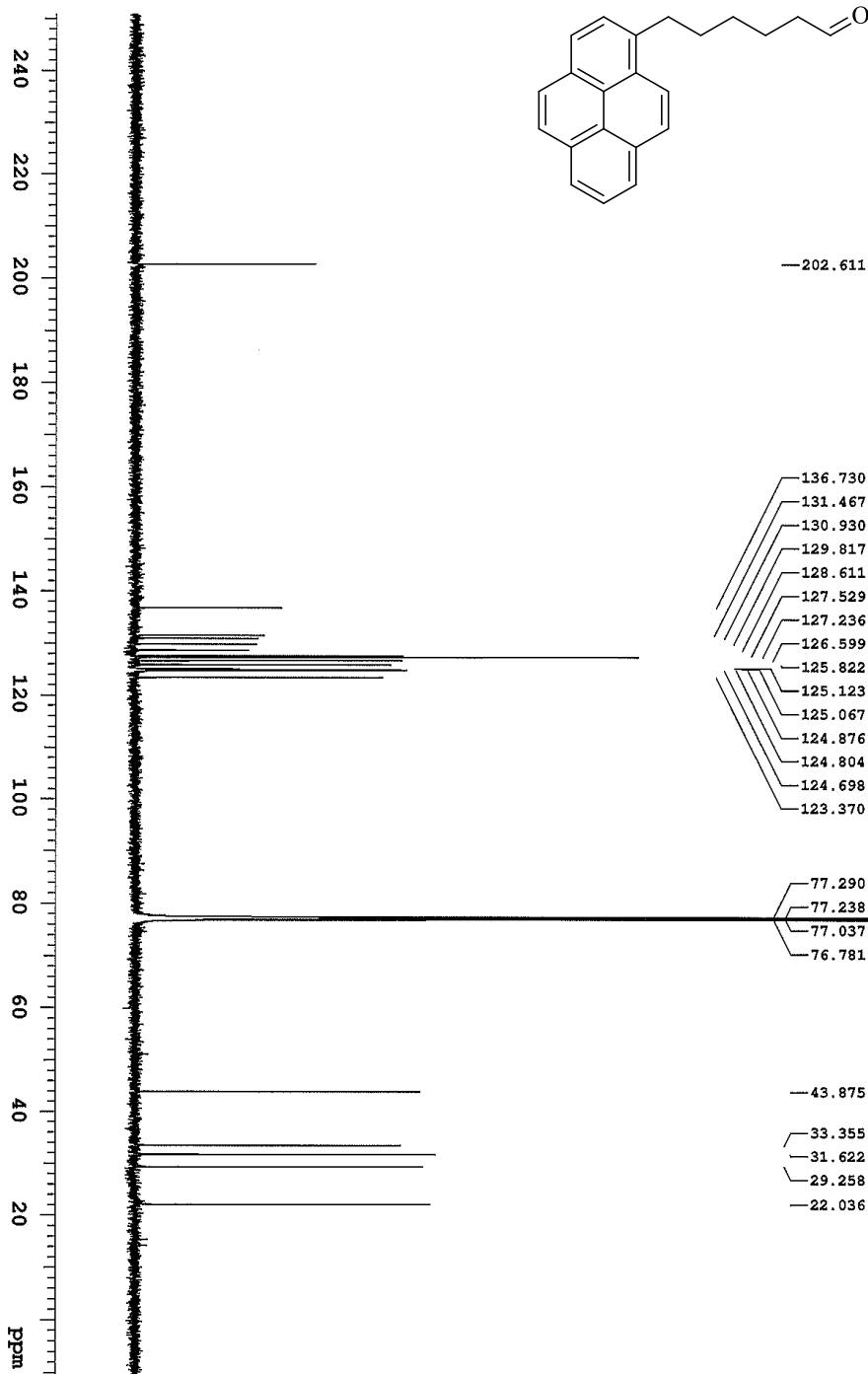
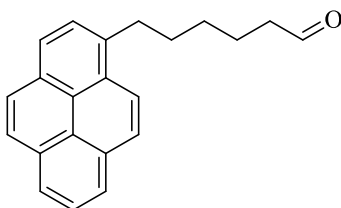
Recorded on: **u500, May 25 2016**

Sweep Width(Hz): **32884.7**  
Digital Res.(Hz): **0.25**

Acquisition Time(s): **2.5**  
Hz per mm(Hz/mm): **137.06**

Relaxation Delay(s): **0.1**  
Completed Scans: **128**

6C-PyCHO  
125.691 MHz C13{H1} 1D in cdcl3 (ref. to CDCl3 @ 77.06 ppm), temp 27.7 C -> actual temp = 27.0 C, condual probe



File: /mnt/600/home14/jms/mr/mrdata/Lose/Aldehyde/6C-PyCHO\_13C\_

2-(4-(phenanthren-9-yl)butyl)-3-(3-(phenanthren-9-yl)propyl)-7,8,9,10-tetrahydrobenzo[*h*]quinoline (161).



Agilent Technologies

Department of Chemistry, University of Alberta

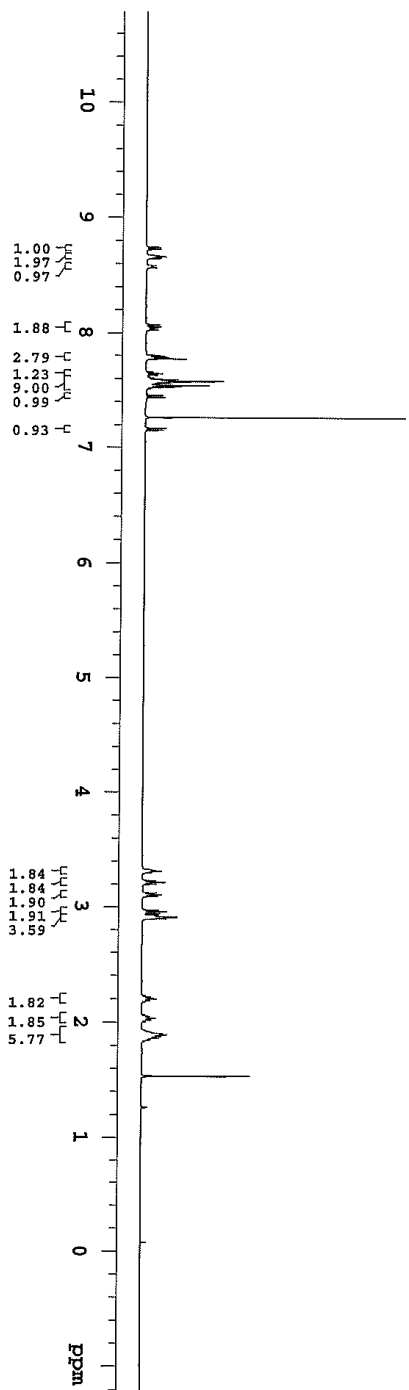
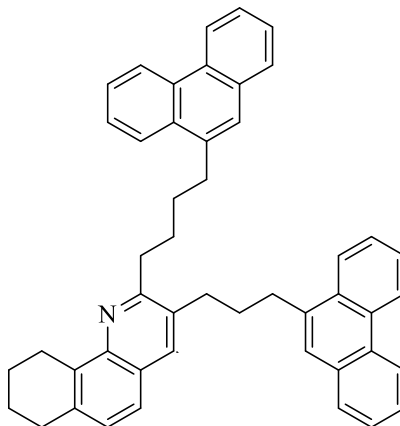
Recorded on: **us00, Jul 14 2018**  
Pulse Sequence: **PRESAT**

Sweep Width(Hz): **6009.62**  
Digital Res.(Hz/p): **0.09**

Acquisition Time(s): **5**  
Hz per mm(Hz/mm): **25.04**

Relaxation Delay(s): **0.1**  
Completed Scans: **8**

499.797 MHz H<sup>1</sup> 1D in cdcl3 (ref to CDCl<sub>3</sub> @ 7.26 ppm)  
temp 27.7 C -> actual temp = 27.0 C, coldstart probe



File: nmr16001home14\fnmr\mrdata\DATA\_FROM\_NMRSERVICE\CD\18.07\2018.07.14.us\_B9-P177\_loc12\_13.16\_H1\_1D



**Agilent Technologies**

Department of Chemistry, University of Alberta

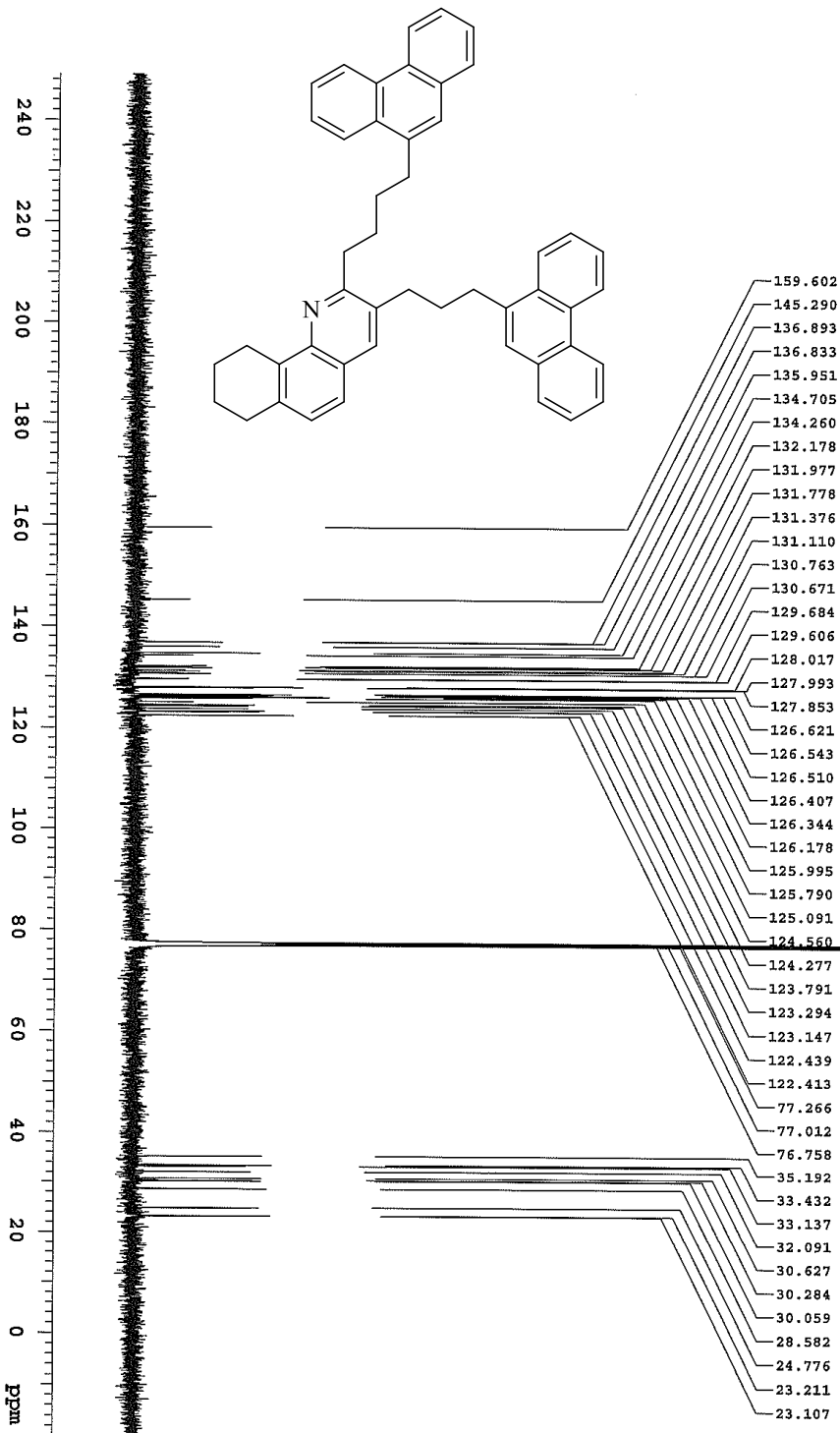
Recorded on: **us00, Jul 14 2018**  
Pulse Sequence: **s2pul**

Sweep Width(Hz): **33793.8**  
Digital Res.(Hz): **0.26**

Acquisition Time(s): **1**  
Hz per unit(Hz/ppm): **140.76**

Relaxation Delay(s): **1**  
Completed Scans: **256**

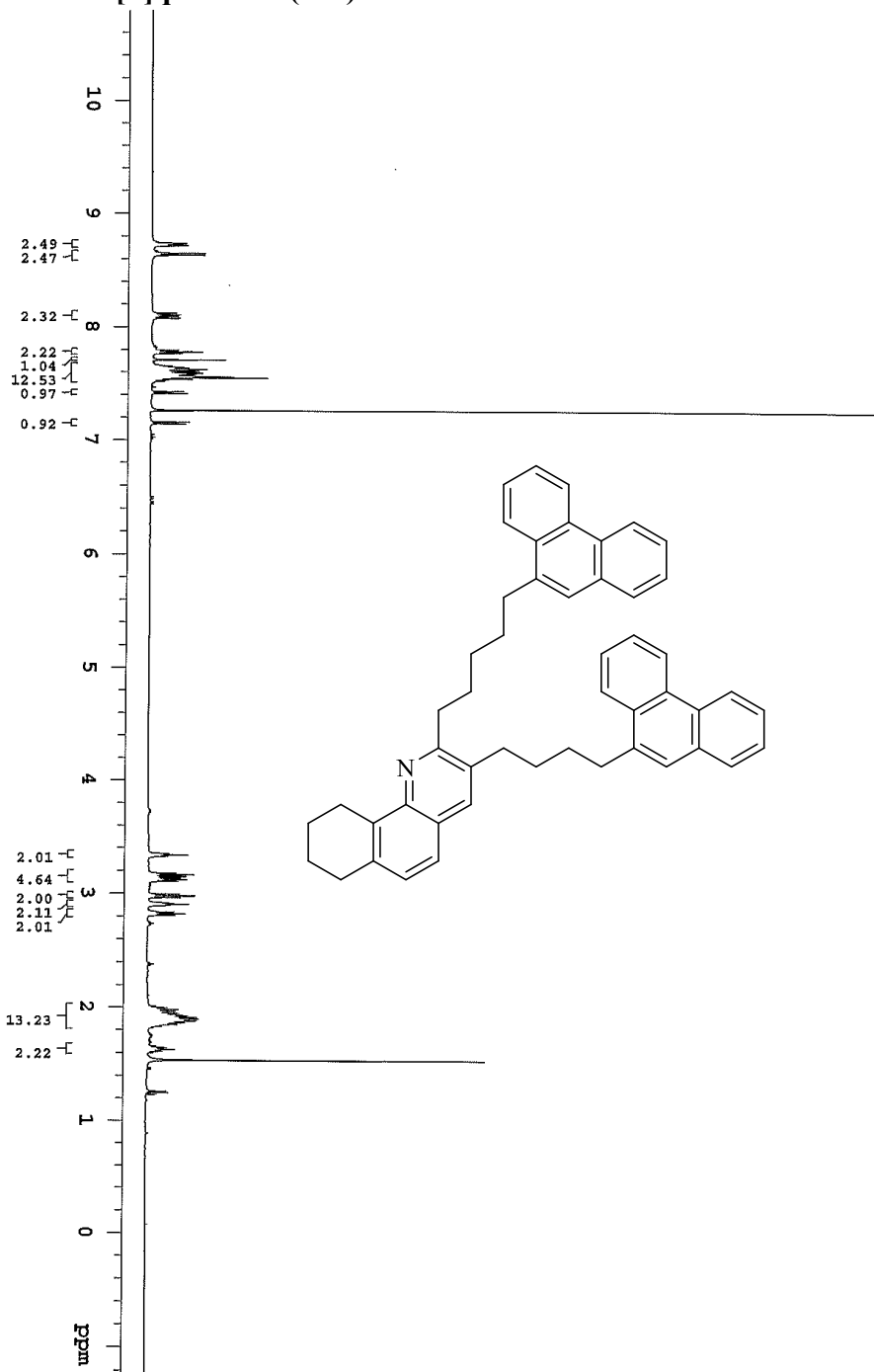
125.688 MHz C13{H1} 1D in cdcl3 (ref. to CDCl3 @ 77.06 ppm)  
temp 27.7 C -> actual temp = 27.0 C, coldstart probe



File: /mnt/600/home1/4/fmsrnmr/data/DA1A\_FROM\_NMRSERVICE/Dawd2018.072018.07.14.us\_B3-P177\_1oc12\_13.17\_C13.1D

3-(4-(phenanthren-9-yl)butyl)-2-(5-(phenanthren-9-yl)pentyl)-7,8,9,10-tetrahydrobenzo[h]quinoline (165).

File: /mnt/660/0/home1/4/jmsnmrnmr/data/DA\_TAFROM\_JMMSERVICE/David/2018.07/2018.07.03.US\_B3-P173\_loct1\_15.16.H1\_1D



B3-P173  
499.797 MHz H1 1D in cdcl3 (ref. to CDCl3 @ 7.26 ppm)  
temp 27.7 C -> actual temp = 27.0 C, coldlual probe



Department of Chemistry, University of Alberta

Recorded on: **u500, Jul 3 2018**  
Pulse Sequence: **PRESAT**

Sweep Width(Hz): **6009.62**  
Digital Res.(Hz): **0.09**

Acquisition Time(s): **5**  
Hz per mm(Hz/mm): **25.04**

Relaxation Delay(s): **0.1**  
Completed Scans: **8**



Agilent Technologies

Department of Chemistry, University of Alberta

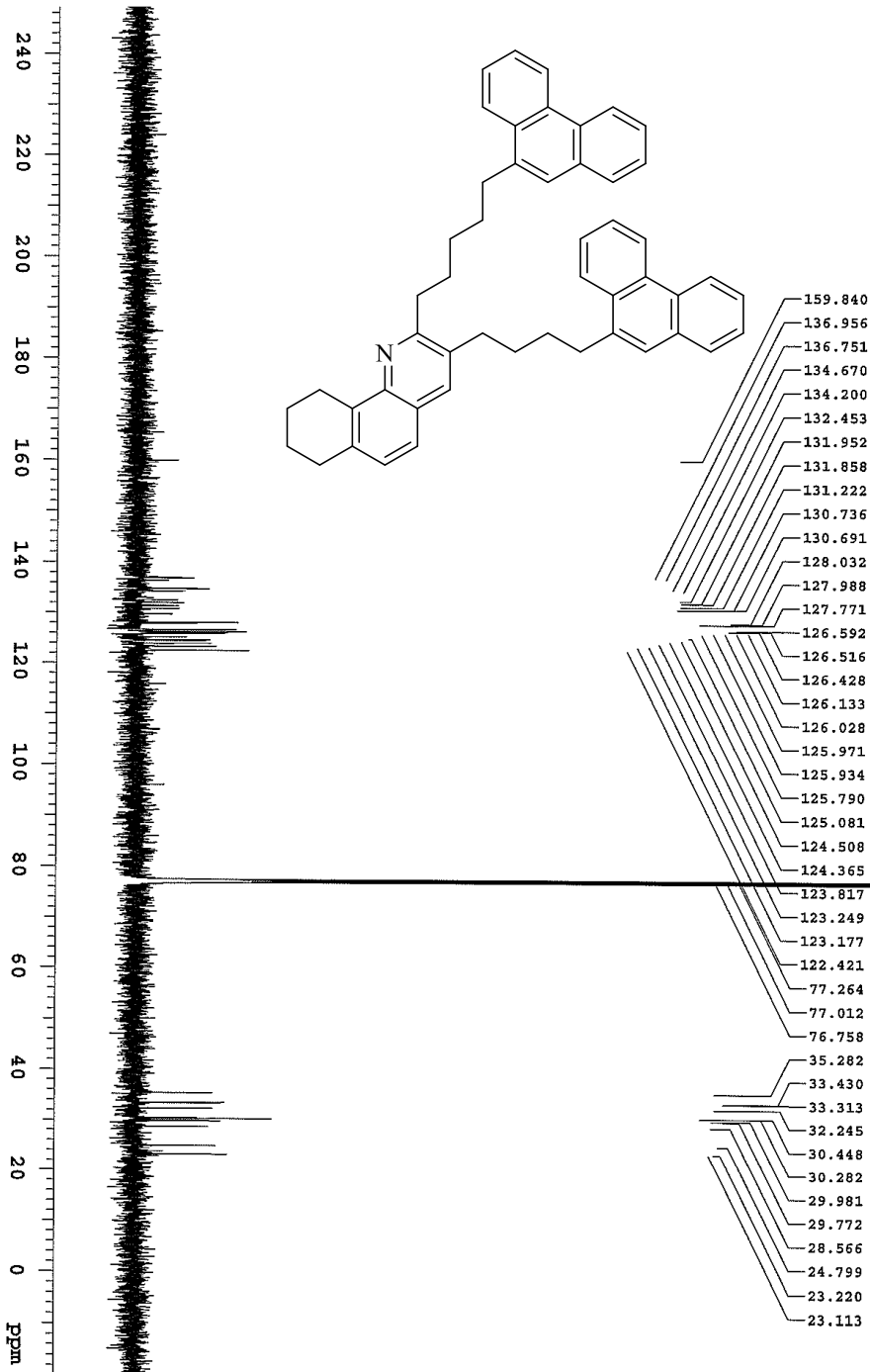
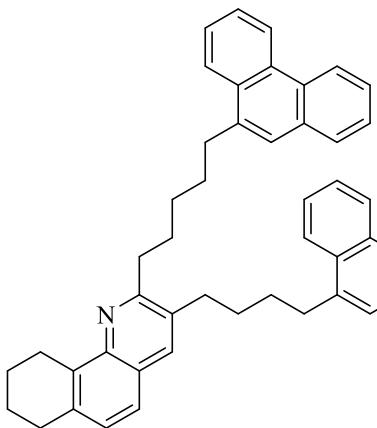
Recorded on: **us00, Jul 3 2018**  
Pulse Sequence: **szpul**

Sweep Width(Hz): **33783.8**  
Digital Res.(Hz/pt): **0.28**

Acquisition Time(s): **1**  
Hz per mm(Hz/mm): **140.76**

Relaxation Delay(s): **1**  
Completed Scans **128**

David, B3-P173  
125.688 MHz C13(H1) 1D in cdcl3 (ref. to CDC13 @ 77.06 ppm)  
temp 27.7 C -> actual temp = 27.0 C, coldlual probe



File: /mnt/d600/home14/jmsnmr/mrdata/DATA\_FROM\_NMRSERVICE/David/2018.07.2018.07.03.us\_B3-P173\_loc1\_15.17\_C13\_1D

3-(2-(phenanthren-9-yl)ethyl)-2-(3-(phenanthren-9-yl)propyl)-7,8,9,10-tetrahydrobenzo[h]quinoline (166).



Agilent Technologies

Department of Chemistry, University of Alberta

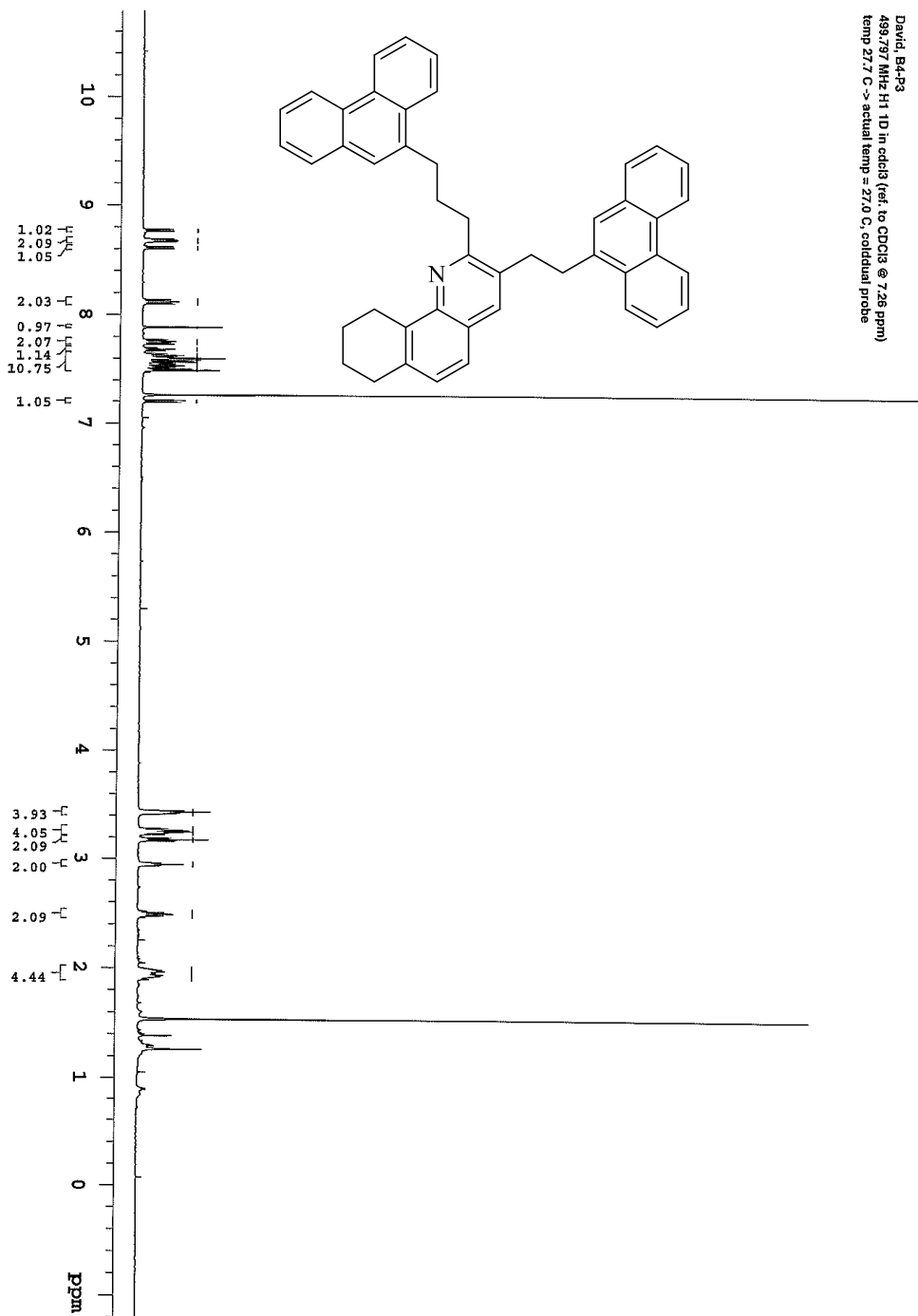
David, B4-P3  
499.797 MHz H1 1D in cdd13 (ref. to CDCl3 @ 726 ppm)  
temp 27.7 C -> actual temp = 27.0 C, coldstart probe

Recorded on: **us00, Jul 3 2018**  
Pulse Sequence: **PRESAT**

Sweep Width(Hz): **6009.62**  
Digital Res.(Hz/pp): **0.09**

Acquisition Time(s): **5**  
Hz per min(Hz/min): **25.04**

Relaxation Delay(s): **0.1**  
Completed Scans: **8**



File: /mnt/660/home14/jfmsnmr/mrtdatg/DA1A\_FROM\_NMRSERVER/CE/David/2018.07/2018.07.03.us\_05\_B4-P3\_10e2\_115.06\_H1\_1D



**Agilent Technologies**

Department of Chemistry, University of Alberta

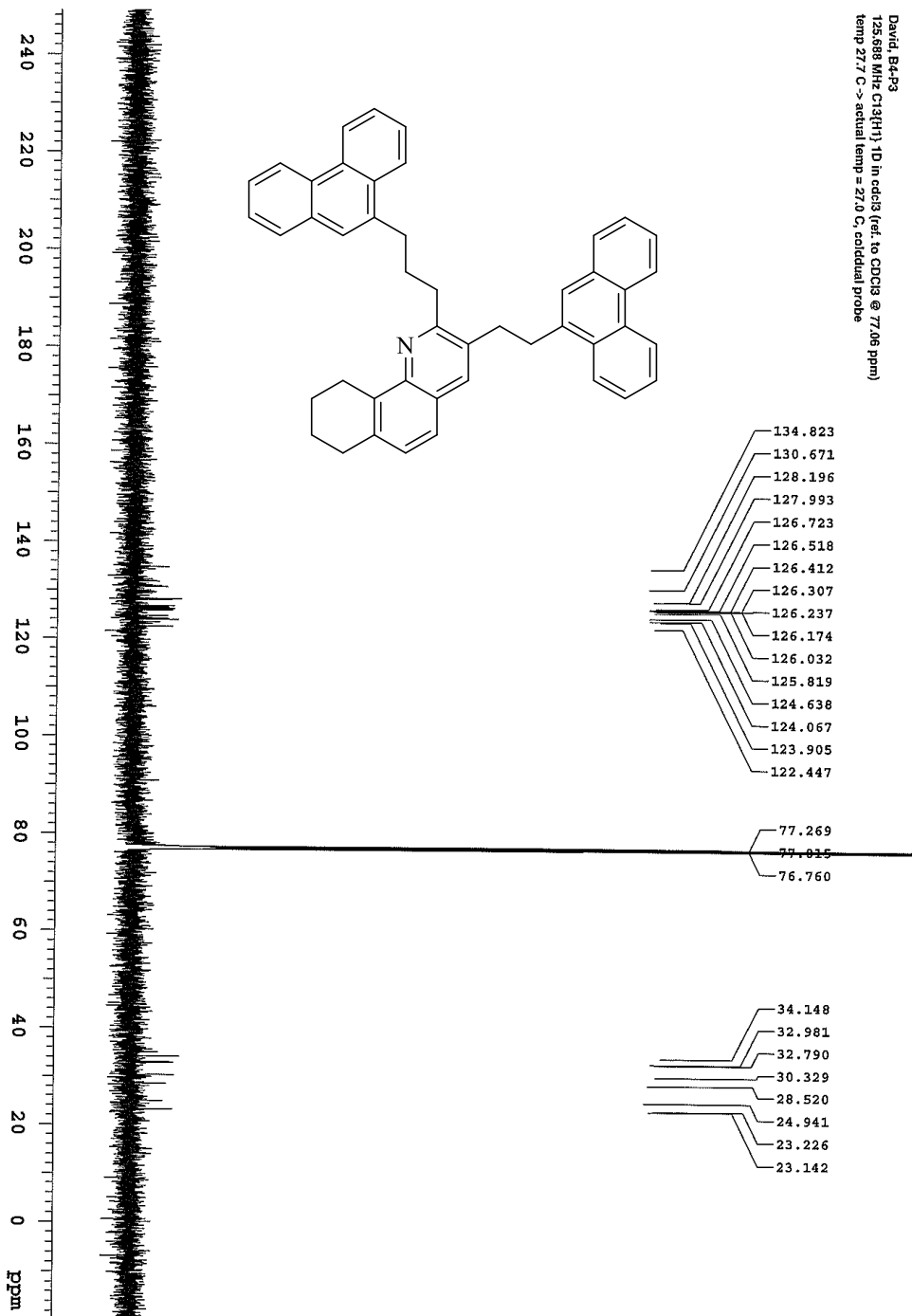
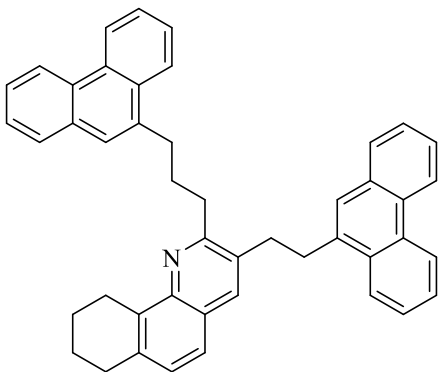
Recorded on: **us00, Jul 3 2018**  
 Pulse Sequence: **szpul**

Sweep Width(Hz): **33783.3**  
 Digital Res.(Hz/p): **0.26**

Acquisition Time(s): **1**  
 Hz per mm(Hz/mm): **140.76**

Relaxation Delay(s): **1**  
 Completed Scans: **56**

David, B4-P3  
 125.688 MHz C13(HT) 1D in cdcl3 (ref. to CDCl3 @ 77.06 ppm)  
 temp 27.7 C -> actual temp = 27.0 C, coldlial probe



File: /mnt/600/home14/jnsmv/rmtdat/DA1A\_FROM\_NMRSERVICE/David2018\_072018/07\_03.us\_B4-P3\_loc2\_15.27\_C13\_1D

6-ethyl-2-[4-(phenanthren-9-yl)butyl]-3-[3-(phenanthren-9-yl)propyl]quinoline (168).



Agilent Technologies

Department of Chemistry, University of Alberta

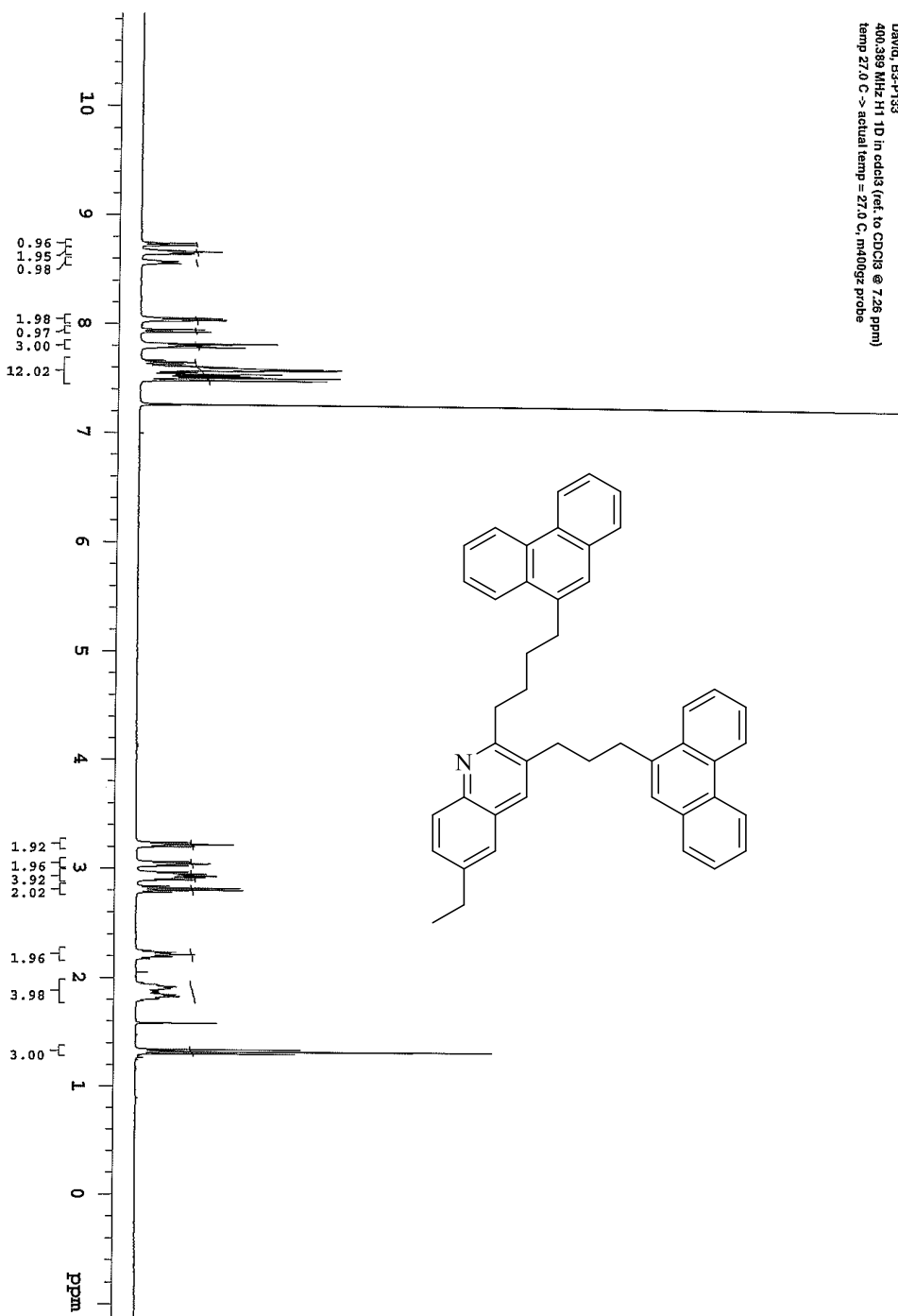
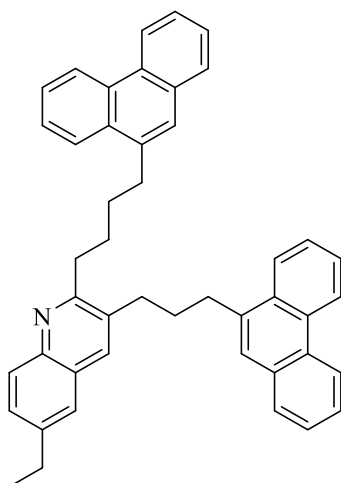
Recorded on: **m400, Jun 29 2018**  
Pulse Sequence: **PRESAT**

Sweep Width(Hz): **4603.07**  
Digital Res.(Hz/pp): **0.07**

Acquisition Time(s): **4.997**  
Hz per mm(ftz/mm): **20.01**

Relaxation Delay(s): **0.1**  
Completed Scans: **32**

David, B3-P133  
400.389 MHz H1 ID in cdcl3 (ref to CDCl3 @ 7.26 ppm)  
temp 27.0 C -> actual temp = 27.0 C; m400gc probe



File: /mnt/6600/home14/greiner/mrdata/DATA\_FROM\_MMRSERVICE/awd/2018.06/2018.06.29.m4\_B3-P133\_joc8\_14.23\_H1\_ID



Agilent Technologies

Department of Chemistry, University of Alberta

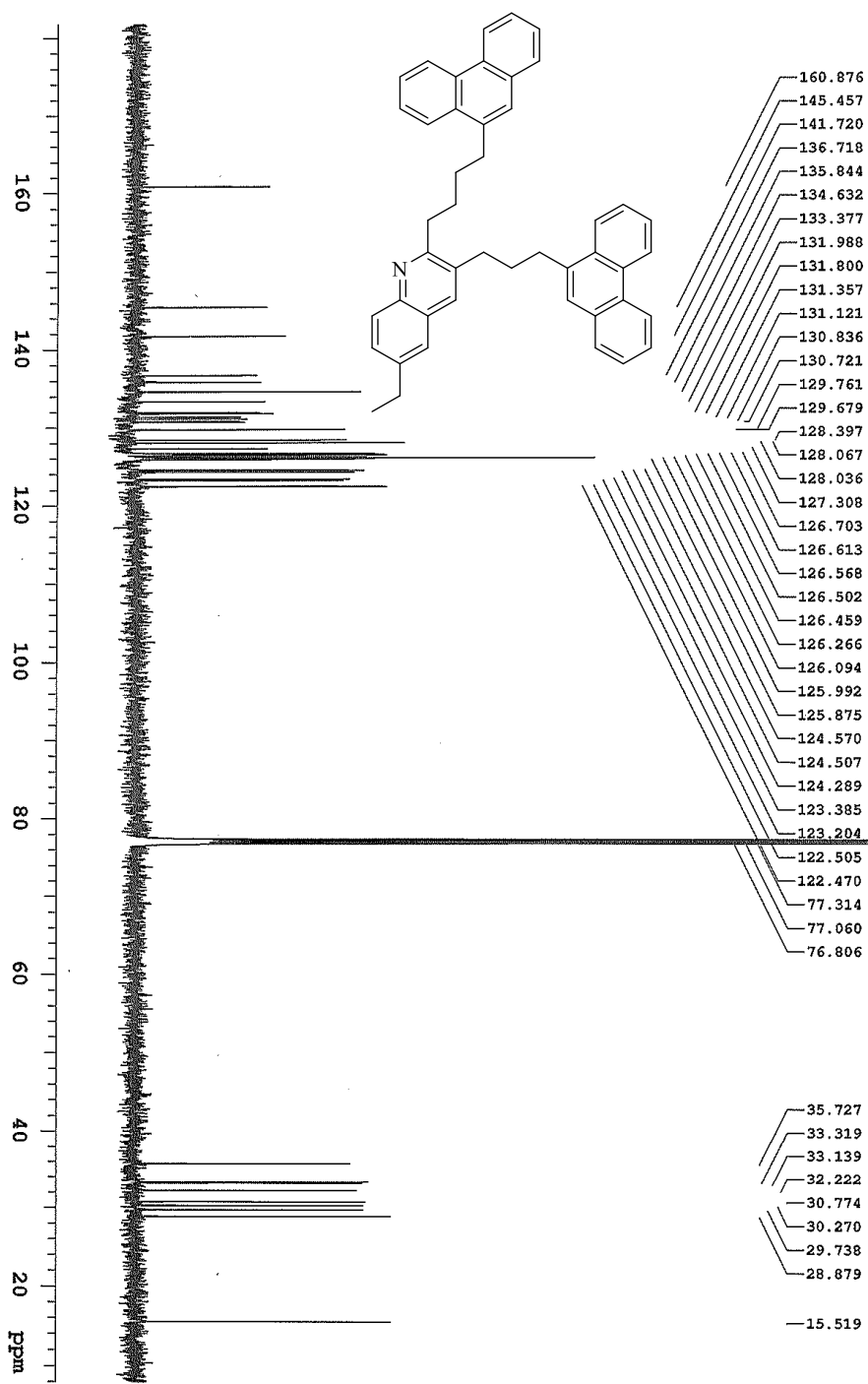
Recorded on: 1500, Jun 29 2018  
Pulse Sequence: szpul

Sweep Width(Hz): 33733.8  
Digital Res.(Hz): 0.26

Acquisition Time(s): 1  
Hz per mm(Hz/mm): 91.03

Relaxation Delay(s): 1  
Completed Scans: 92

125.668 MHz CDCl<sub>3</sub>(H<sub>2</sub>O) In cdcl3 (ref. In CDCl<sub>3</sub> @ 77.06 ppm)  
temp 27.7 C -> actual temp = 27.0 C, cooled via probe



File: h:\msd1\work\p\msmsys\Automation\auto\_20180627\_01\entireQ.mnactrf\acq1\_0114current



Agilent Technologies

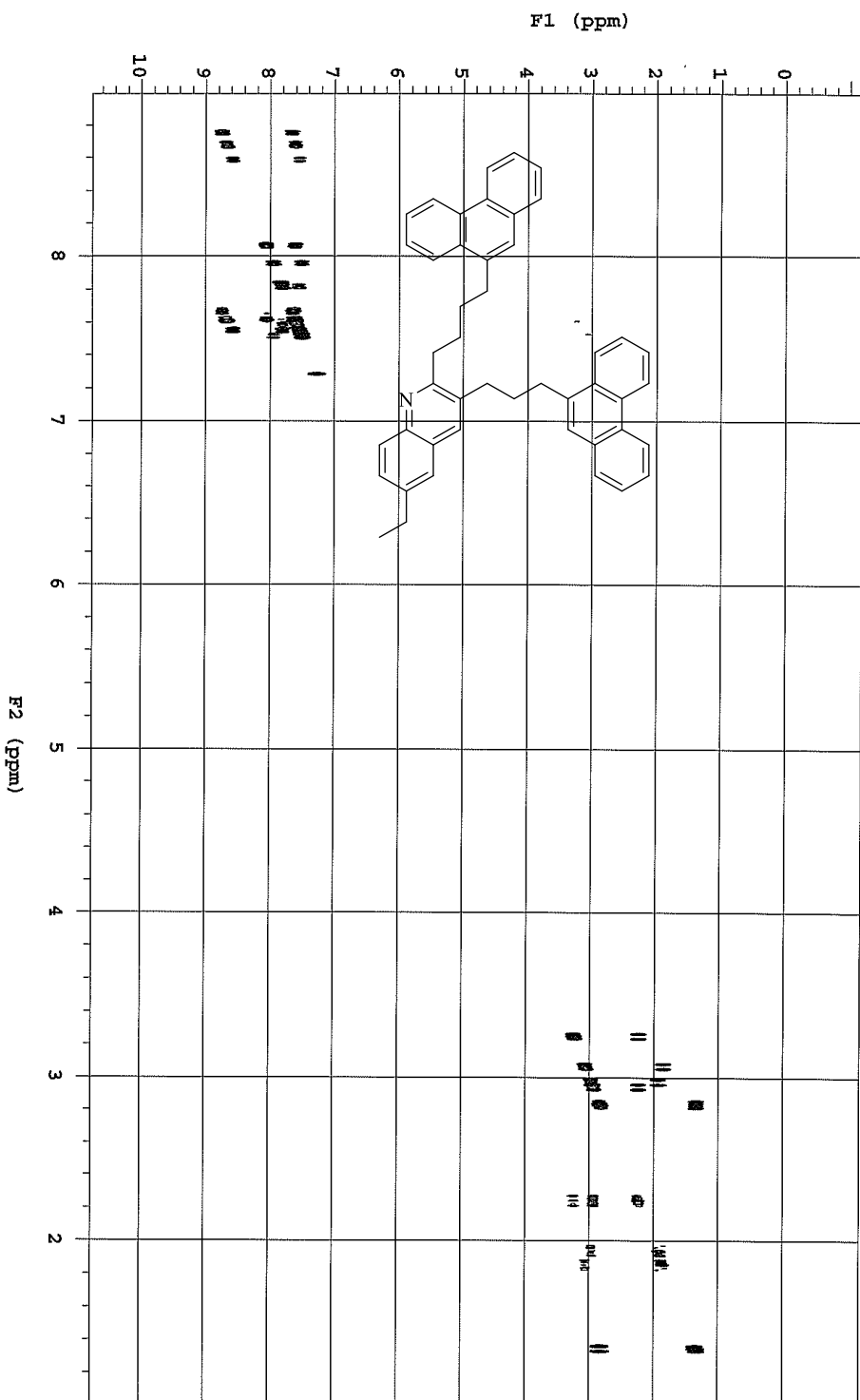
Department of Chemistry, University of Alberta

Recorded on: **us00\_Mar 6 2019**  
Pulse Sequence: **gCOSY**

Sweep Width F2(F1Hz): **6009.62 | 6009.62** Acquisition Time(s): **1**  
Digital Res. F2(F1Hz): **1.47 | 11.74** Hz per ppm F2(F1Hz): **16.66 | 42.59**

Relaxation Delay(s): **1**  
No. of Scans/Increments: **1 | 170**

499.787 MHz <sup>1</sup>H gCOSY in cdcl3 (ref. to CDCl<sub>3</sub> @ 7.26 ppm)  
temp: 27.7 C -> actual temp = 27.0 C, coldstart probe



File: /msd/060/noname1/4/nmr/nmr\data\DATA\_FROM\_MMRSERVICE/Dwd/2019.03/2019.03.06.us\_p-BIQ\_lo5\_14.16.LH\_gCOSY



2-(4-(phenanthren-9-yl) butyl)-3-(3-(phenanthren-9-yl) propyl) quinoline (170).



Agilent Technologies

David, B4-P5  
499.797 MHz H1 1D in cdcl3 (ref. to CDCl3 @ 7.26 ppm)  
temp 27.7 C -> actual temp = 27.0 C, coldlual probe

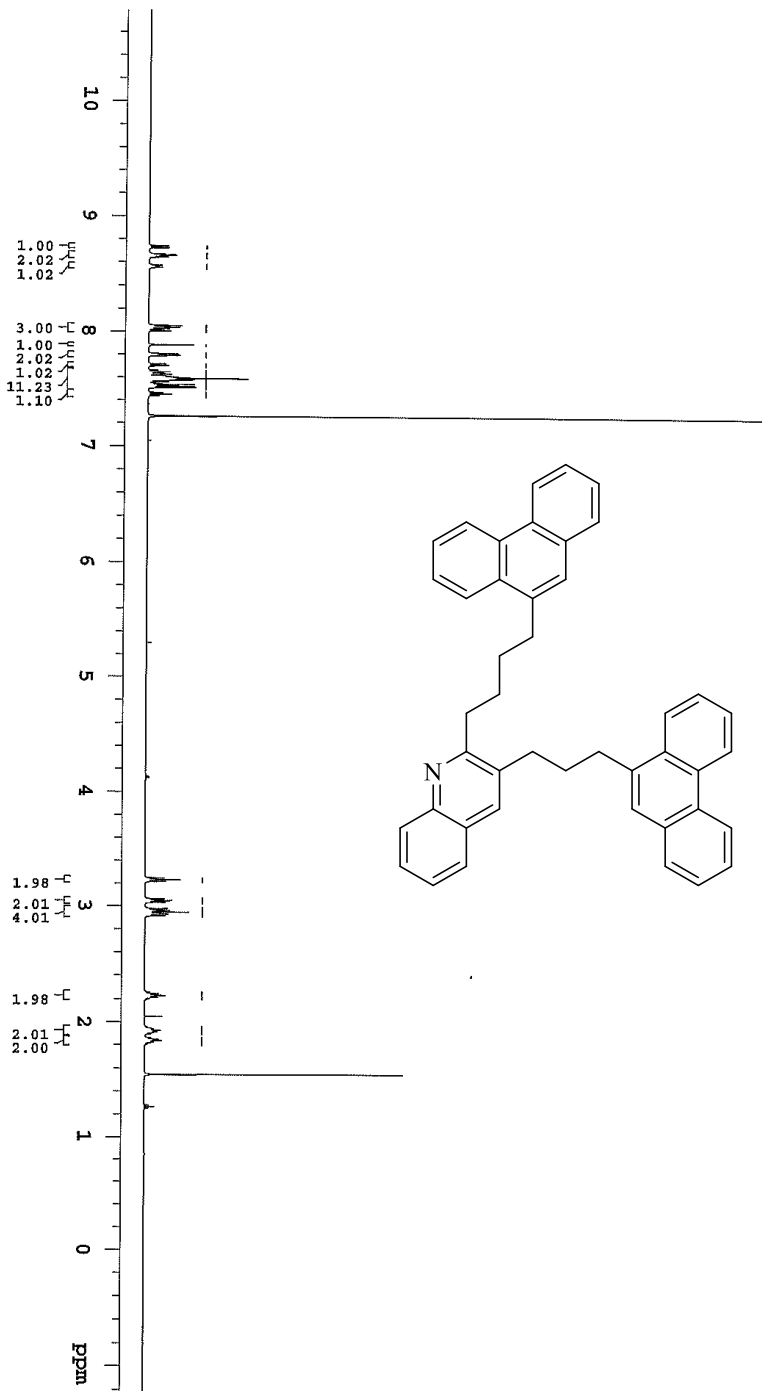
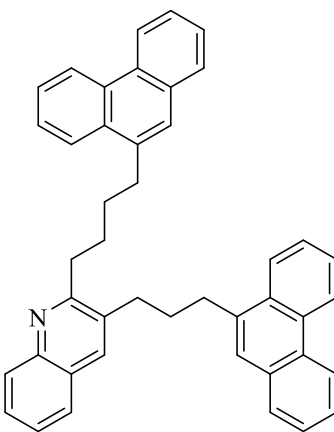
Department of Chemistry, University of Alberta

Recorded on: **u500, Aug 10 2018**  
Pulse Sequence: **PRESAT**

Sweep Width(Hz): **6009.62**  
Digital Res.(Hz/pt): **0.09**

Acquisition Time(s): **5**  
Hz per mm(Hz/mm): **25.04**

Relaxation Delay(s): **0.1**  
Completed Scans: **8**



File: /mnt/600/home14/jmnmr/mrdata/DA\_T4\_FROM\_NMRSERVICE/David/2018\_09/2018\_08\_10.u5\_B4-P5\_loc5\_14.57\_H1\_1D



Agilent Technologies

Department of Chemistry, University of Alberta

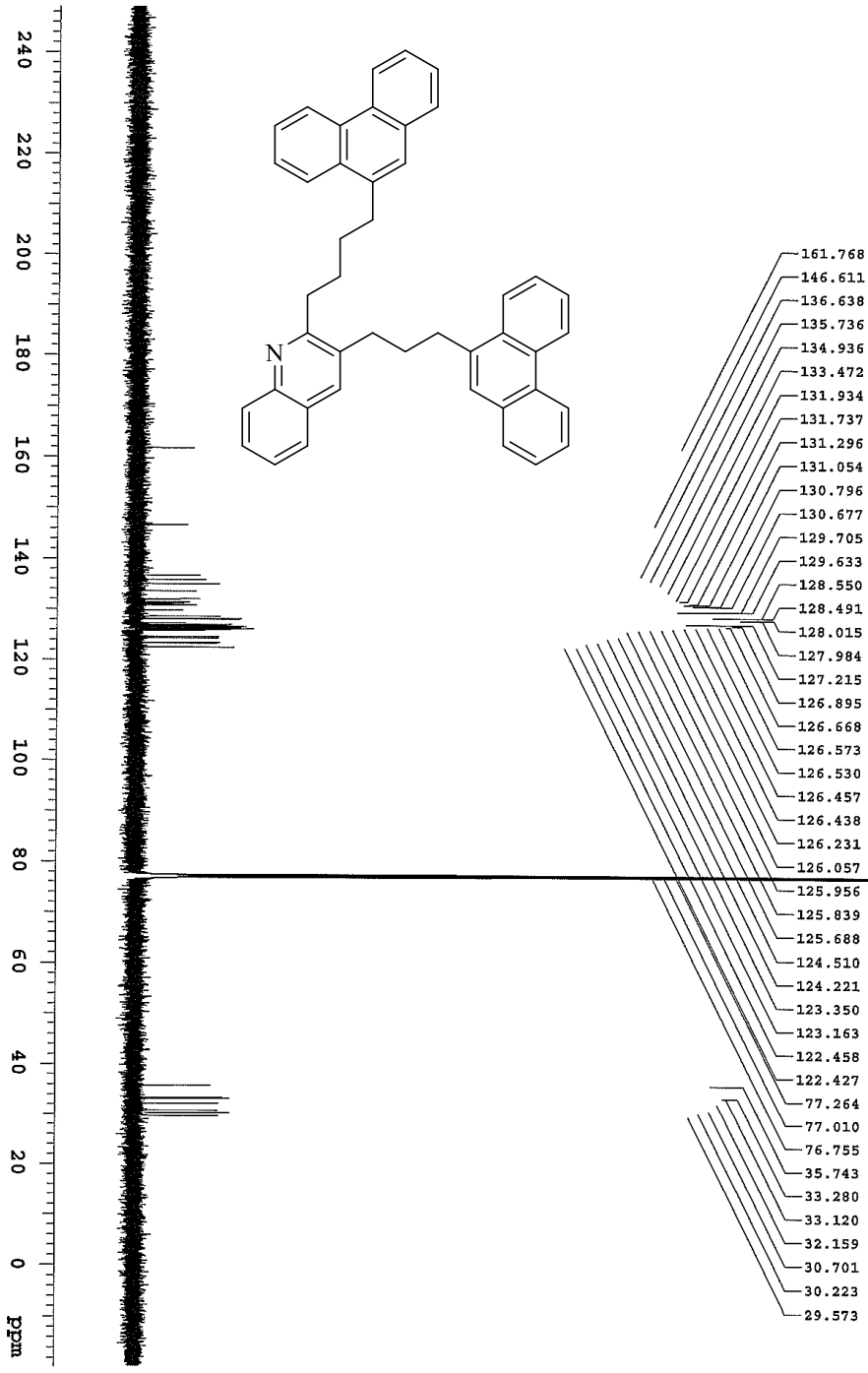
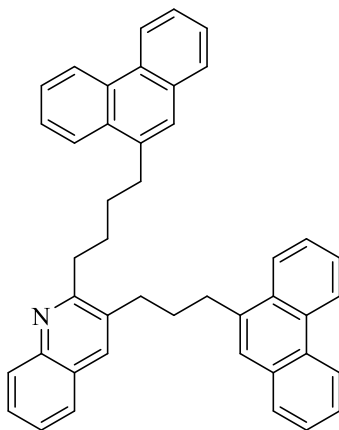
Recorded on: **us00, Aug 10 2018**  
Pulse Sequence: **szpul**

Sweep Width(Hz): **33723.3**  
Digital Res.(Hz/gt): **0.28**

Acquisition Time(s): **1**  
Hz per mnt(Hz/mt): **140.76**

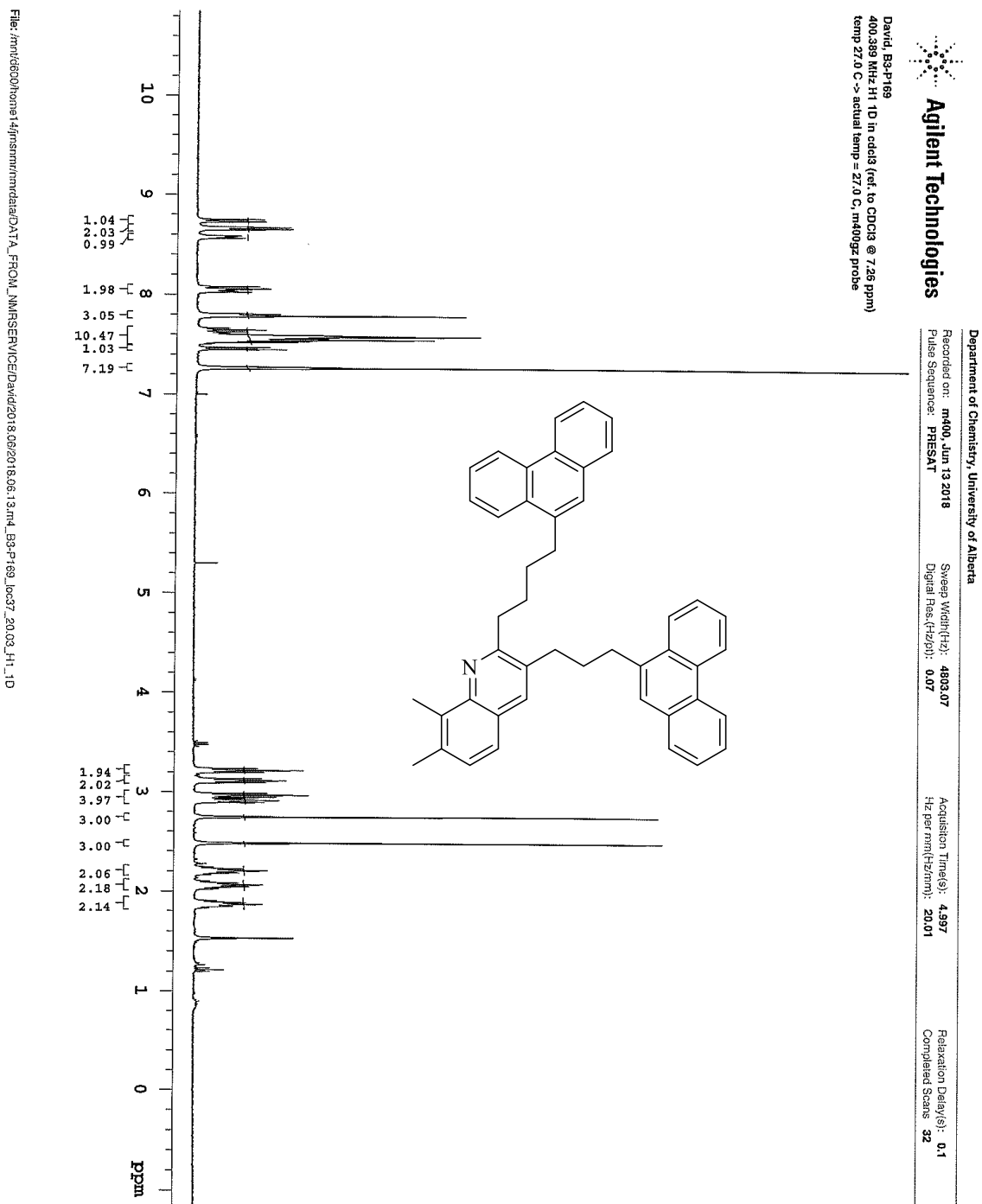
Relaxation Delay(s): **1**  
Completed Scans: **258**

David, B4-P5  
125.688 MHz C13(1H) 1D In cdcl3 (ref. to CDCl3 @ 77.06 ppm)  
temp 27.7 C -> actual temp = 27.8 C, coldlual probe



File: /mnt/d800/home14/jmsnmr/mrdata/DATA\_FROM\_NMRSERVICE/David/2018\_08/2018.08.10.us\_B4-P5\_loc5\_14.58\_C13\_1D

# 7,8-dimethyl-2-[4-(phenanthren-9-yl)butyl]-3-[3-(phenanthren-9-yl)propyl]quinoline (171).





Agilent Technologies

Department of Chemistry, University of Alberta

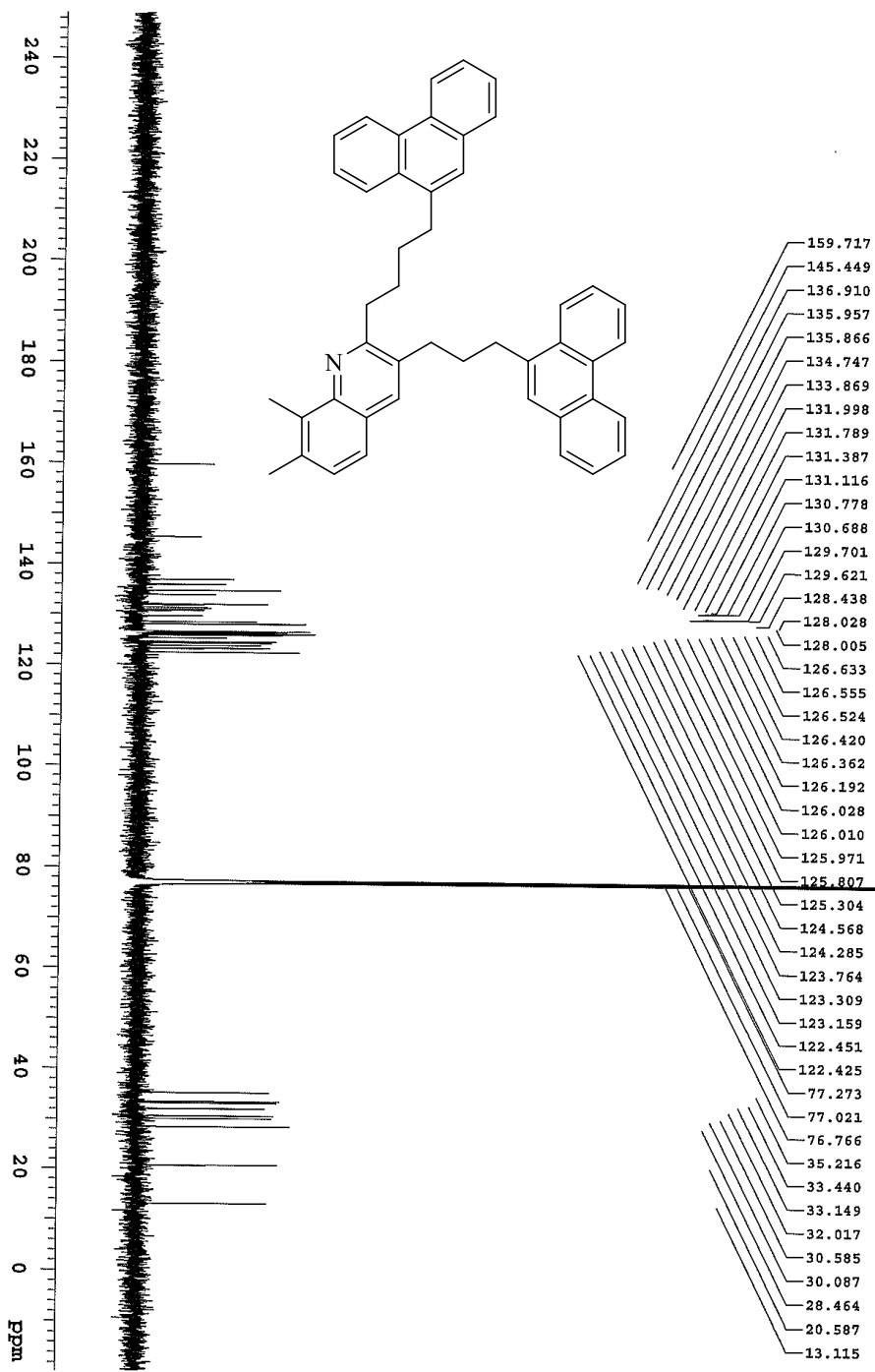
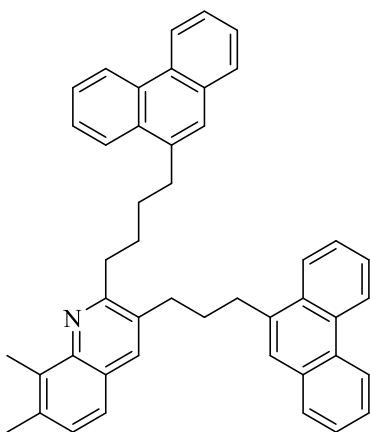
Recorded on: **us00, Jun 29 2018**  
Pulse Sequence: **szpul**

Swap Width(Hz): **33783.8**  
Digital Res.(Hz/g): **0.26**

Acquisition Time(s): **1**  
Hz per mm(Tz/mm): **140.76**

Relaxation Delay(s): **1**  
Completed Scans: **120**

David\_B3-P169A  
125.688 MHz C13(HT) 1D In cdcl3 (ref. to CDCl3 @ 77.06 ppm)  
temp 27.7 C -> actual temp = 27.0 C, coldstart probe



File: /mnt/d60/home14/jmsrnmr/irmdata/DA\_T\_FROM\_JMRSERVICE/David/2018.06.29.us\_05\_B3-P169A\_1oc11\_17.24\_C13\_1D

6,8-dimethyl-2-[4-(phenanthren-9-yl)butyl]-3-[3-(phenanthren-9-yl)propyl]quinoline (172).



Agilent Technologies

499.787 MHz, H<sup>1</sup> 1D in cdcl<sub>3</sub> (ref. to CDCl<sub>3</sub> @ 7.26 ppm)  
Temp 27.7 C -> actual temp = 27.0 C, coldlual probe

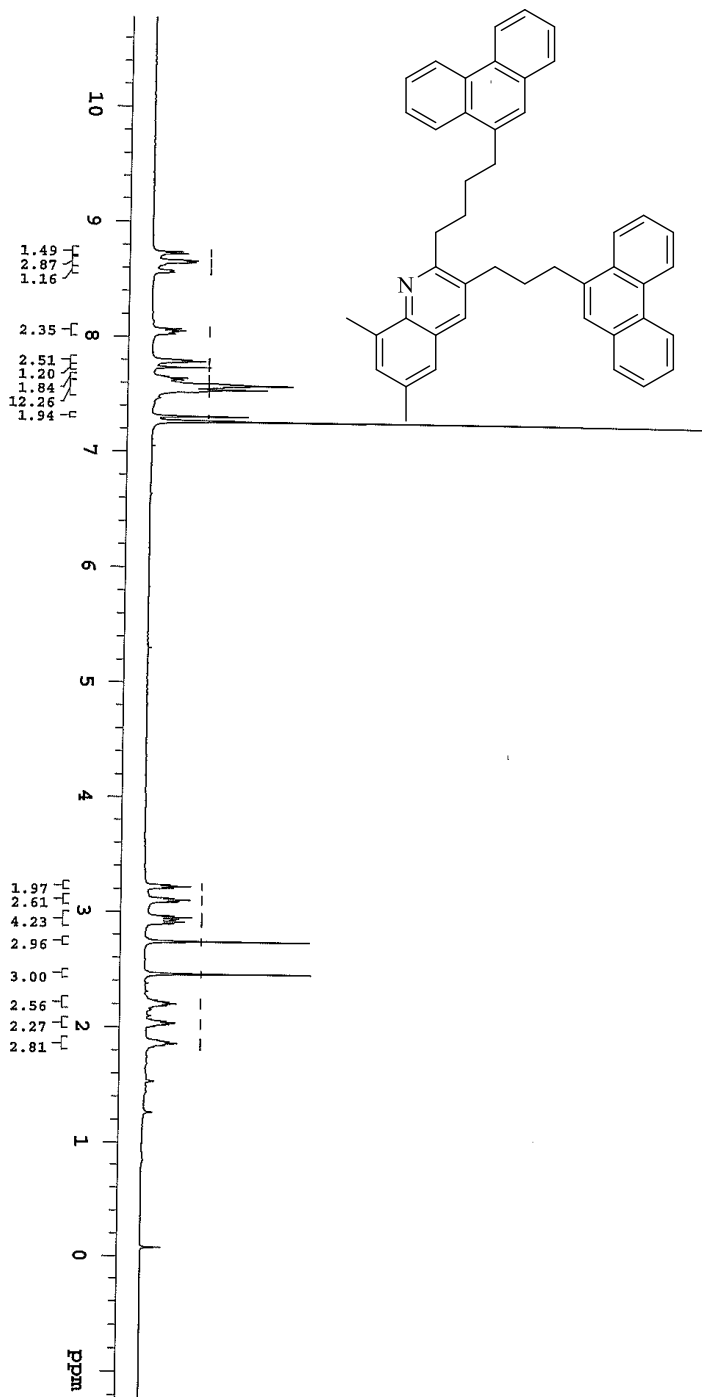
Department of Chemistry, University of Alberta

Recorded on: us60, Mar 5 2019  
Pulse Sequence: PRESAT

Sweep Width(Hz): 6009.62  
Digital Res.(Hz/pt): 0.09

Acquisition Time(s): 5  
Hz per mm(Hz/mm): 25.04

Relaxation Delay(s): 0.1  
Completed Scans: 8



File: /mnt/600/home14/jnanni/mrdata/DA1A\_FRQM\_NMRSERVICE/DA1A/2019.03.20/19.05.06.us\_1\_5Mhz2\_10ed\_14.00\_H1\_1D



Agilent Technologies

Department of Chemistry, University of Alberta

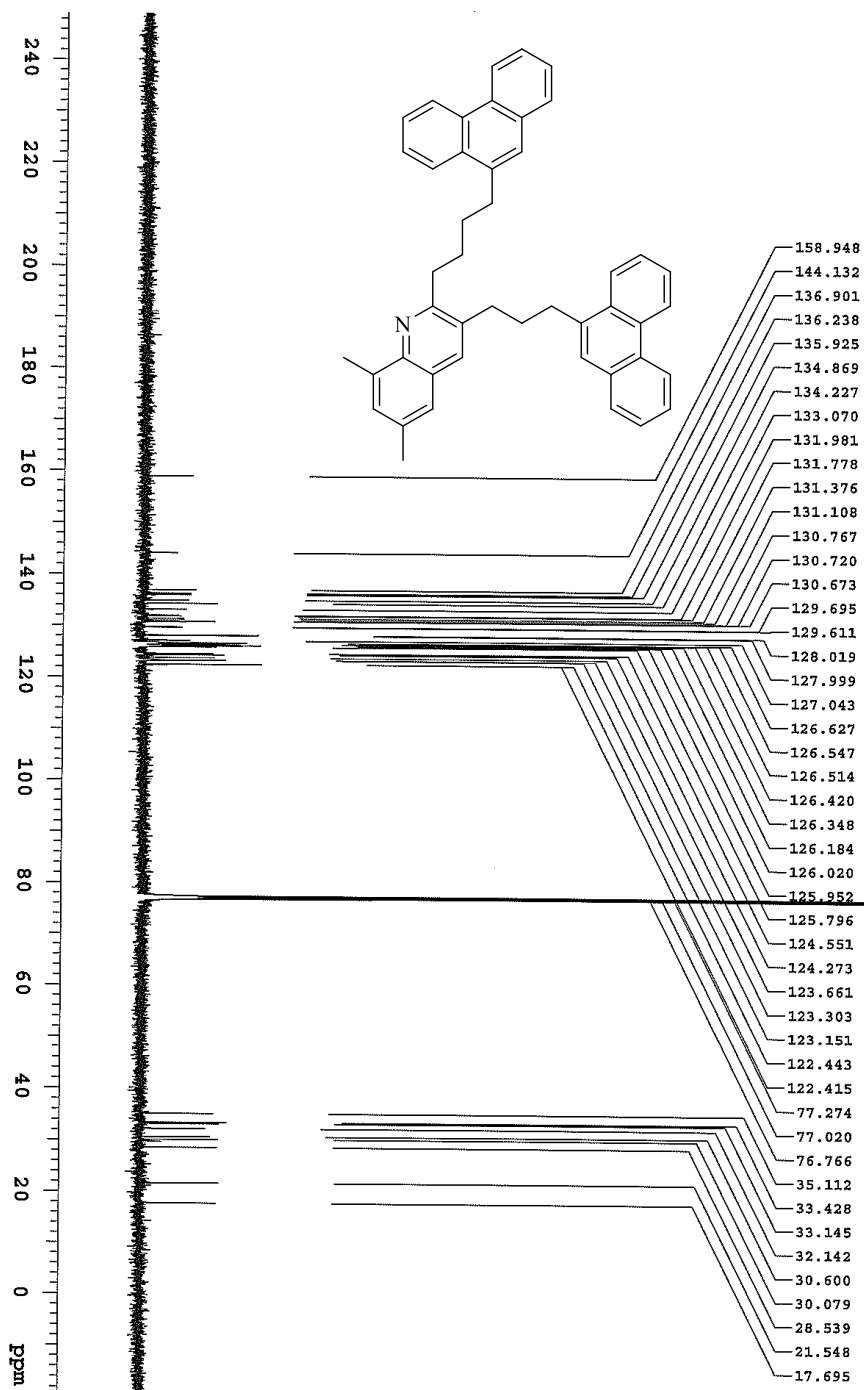
Recorded on: **us00, Jun 29 2018**  
Pulse Sequence: **szpul**

Sweep Width(Hz): **33783.8**  
Digital Res.(Hz/pt): **0.26**

Acquisition Time(s): **1**  
Hz per mm(Hz/mm): **140.76**

Relaxation Delay(s): **1**  
Completed Scans: **128**

125.688 MHz C13{H1} 1D in cdcl3 (ref. to CDCl3 @ 77.06 ppm)  
temp 27.7 C -> actual temp = 27.0 C, solidstate probe



File: /mnt/650/home14/pnsnmr/mrdata/2018.06/2018.06.29.us\_B3-p179A\_J002\_17.44\_C13\_1D

5,8-dimethyl-2-[4-(phenanthren-9-yl)butyl]-3-[3-(phenanthren-9-yl)propyl]quinoline (173).



Agilent Technologies

Department of Chemistry, University of Alberta

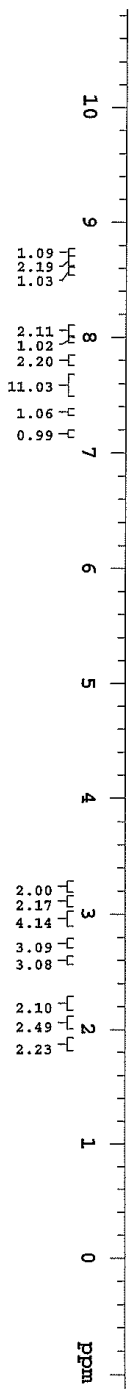
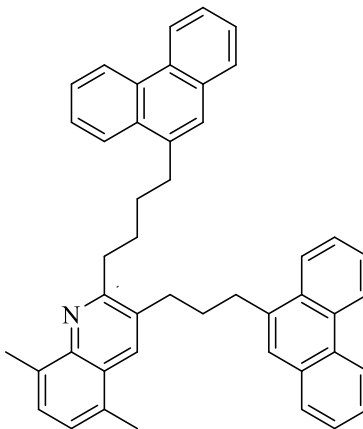
David\_B3-P181  
400.389 MHz H1 1D in ccd18 (ref. to CDCl3 @ 7.26 ppm)  
temp 27.0 C -> actual temp = 27.0 C; m4dlogz probe

Recorded on: m400, Jun 27 2018  
Pulse Sequence: PRESAT

Sweep Width(Hz): 4803.07  
Digital Res.(Hz/pt): 0.07

Acquisition Time(s): 4.998  
Hz per mm(Hz/mm): 20.01

Relaxation Delay(s): 0.1  
Completed Scans: 32



File: /mnt/d60/chem14/mgsmr/mrdata/DA\_T\_A\_FRQW\_NMHSERVICE/David/2018.06/2018.06.27.m4\_B3-P181\_loc35\_21.56\_H1\_1D



**Agilent Technologies**

Department of Chemistry, University of Alberta

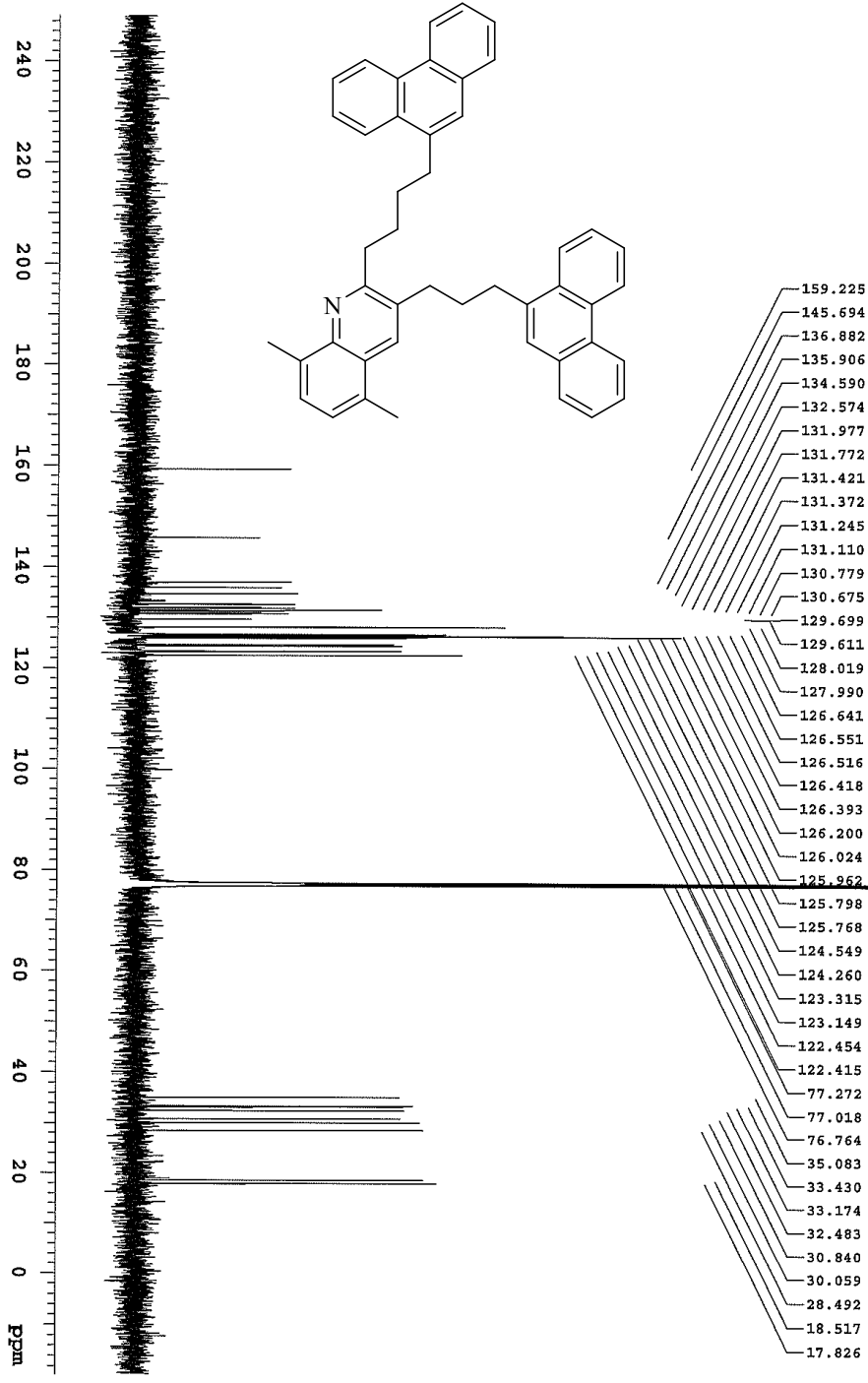
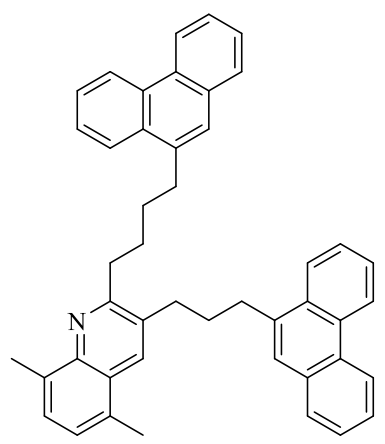
Recorded on: **us00, Jun 29 2018**  
 Pulse Sequence: **szpul**

Sweep Width(Hz): **33783.8**  
 Digital Res.(Hz/pt): **0.26**

Acquisition Time(s): **1**  
 Hz Per mm(Hz/mm): **140.76**

Relaxation Delay(s): **1**  
 Completed Scans: **128**

David\_B3-P181A  
 125.688 MHz C13(HT) 1D in cdcl3 (ref. to CDCl3 @ 77.06 ppm)  
 temp 27.7 C -> actual temp = 27.0 C, coldltdl probe



File: /mnt/d800/hcrce14/jynsmnmrdata/ATA\_FROM\_NMRSERVICE/David/2018\_06/2018\_06\_29/us\_B3-P181A\_loc3\_17\_S2\_C13\_1D

2-(4-(phenanthren-9-yl)butyl)-3-(3-(phenanthren-9-yl)propyl)benzo[h]quinoline (174).



David\_B4-P7  
499.797 MHz H1 1D in cdcl3 (ref. to CDCl3 @ 7.26 ppm)  
temp 27.7 C -> actual temp = 27.0 C, coldlual probe

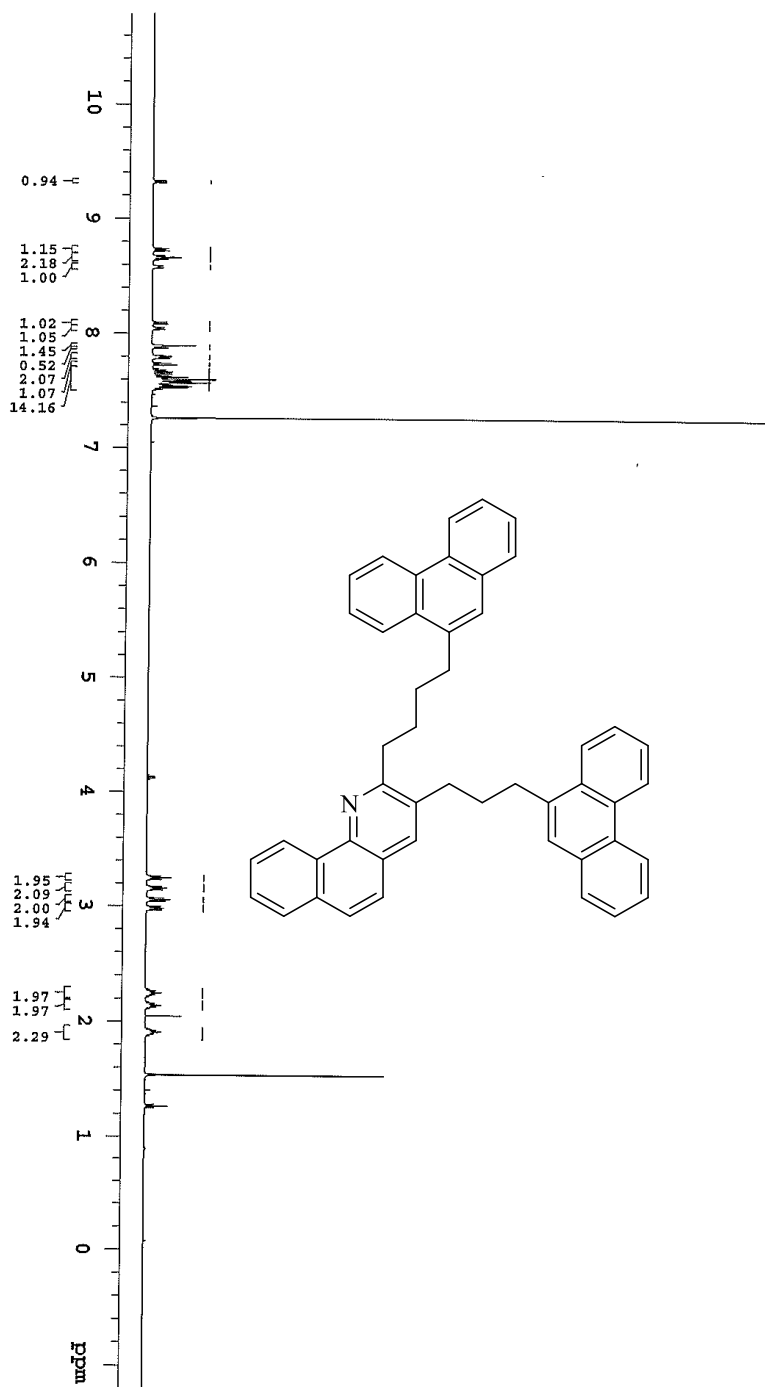
Department of Chemistry, University of Alberta

Recorded on: 0500, Sep 8 2018  
Pulse Sequence: PRESAT

Sweep Width (Hz): 6009.62  
Digital Res. (Hz/p): 0.09

Acquisition Time(s): 5  
Hz per mm (Hz/mm): 25.04

Relaxation Delay(s): 0.1  
Completed Scans: 16



File: /mnt/660/0/home14/jgmsm/mrmdatal/DAVA\_FROM\_MMRSERVICE/David2018.09.2018.09.08.us\_B4-P7\_loc11\_12.16.H1\_1D



**Agilent Technologies**

Department of Chemistry, University of Alberta

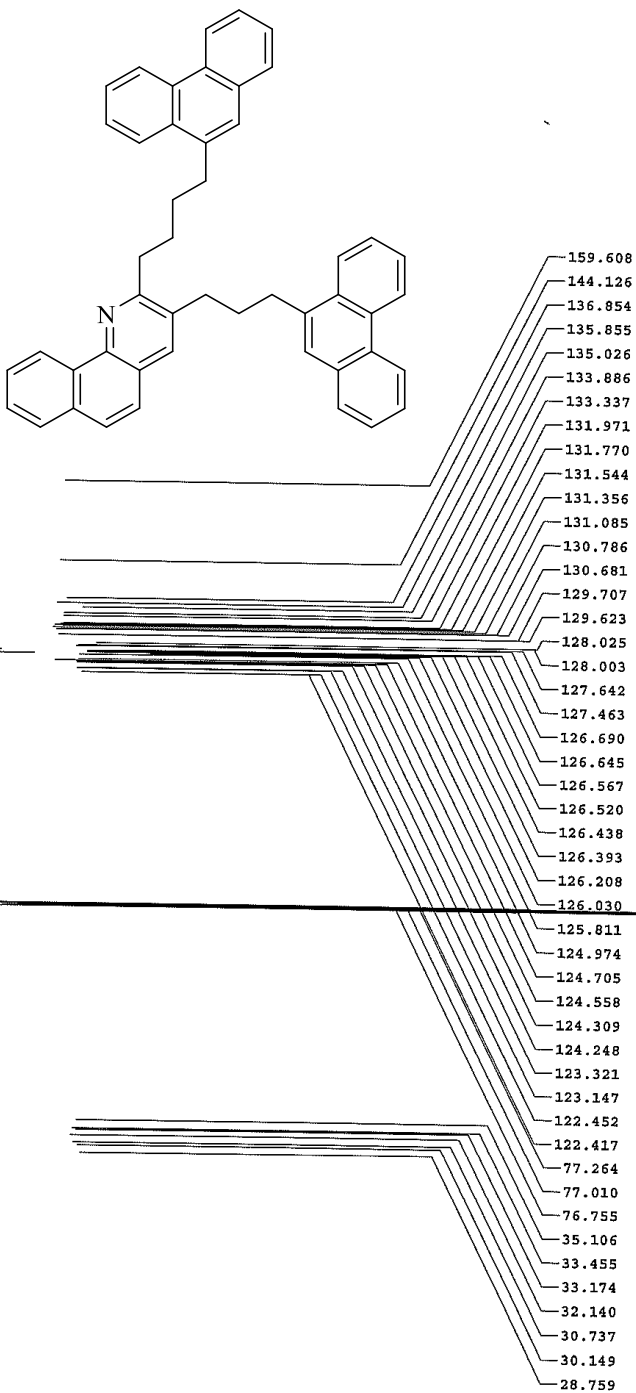
Recorded on: **us00, Sep 8 2018**  
 Pulse Sequence: **s2pul**

Sweep Width(Hz): **33763.8**  
 Digital Res.(Hz/ppm): **0.26**

Acquisition Time(s): **1**  
 Hz per mm(Hz/cm): **140.76**

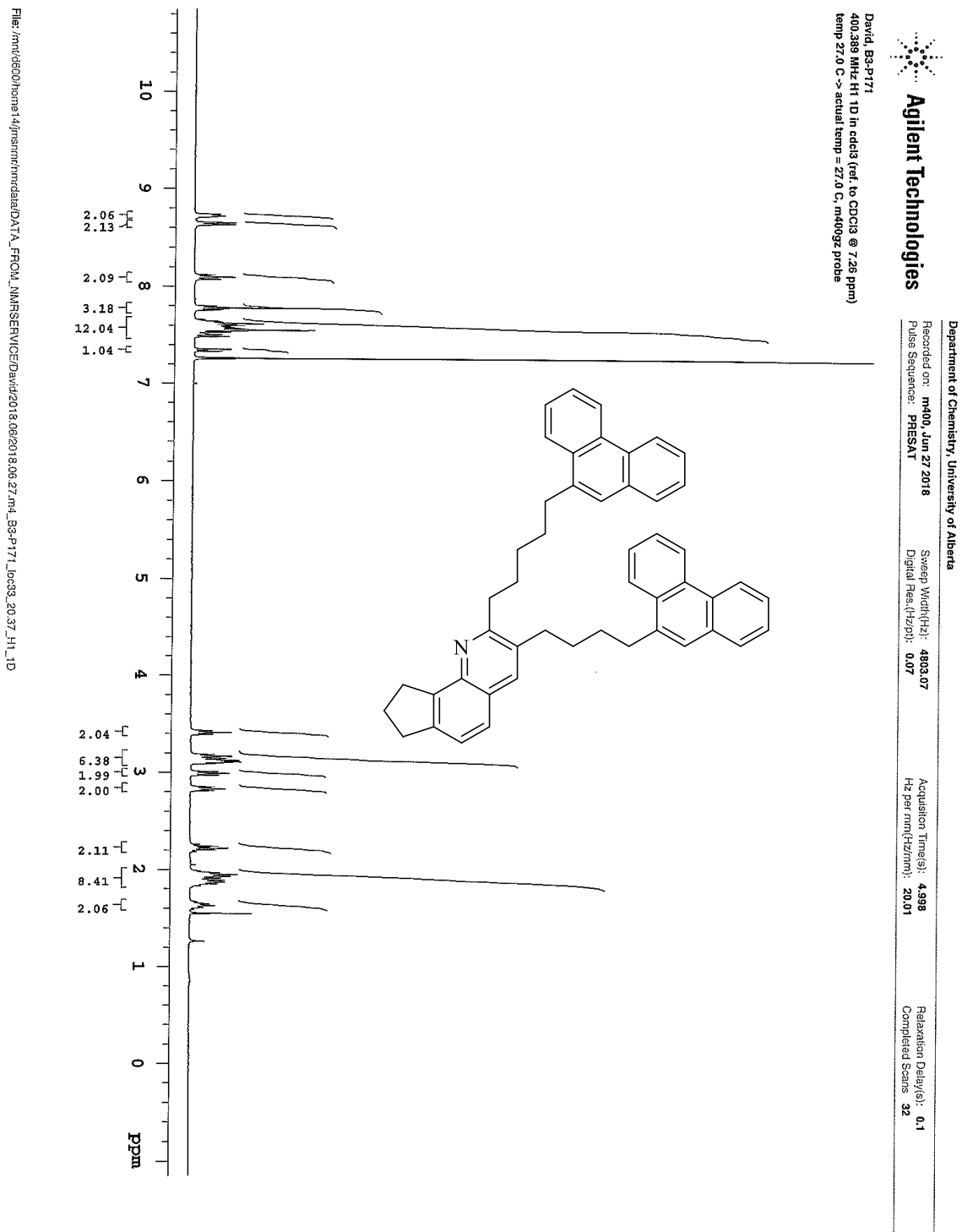
Relaxation Delay(s): **1**  
 Completed Scans: **512**

David, B4-P7  
 125.688 MHz C13(H1) 1D in cdcl3 (ref. to CDCl3 @ 77.06 ppm)  
 Temp 27.7 C -> actual temp = 27.0 C, coldlual probe



File: /mnt/c600/home14/mrnmr/rimdata/ATA\_FROM\_NMRSERVICE/David2018.09.20/18.09.08.us\_B4-P7\_1oct11\_11.58\_C13\_1D

3-[4-(phenanthren-9-yl) butyl]-2-[5-(phenanthren-9-yl) pentyl]-7,8,9-cyclopenta[*h*]quinoline (175).





**Agilent Technologies**

Department of Chemistry, University of Alberta

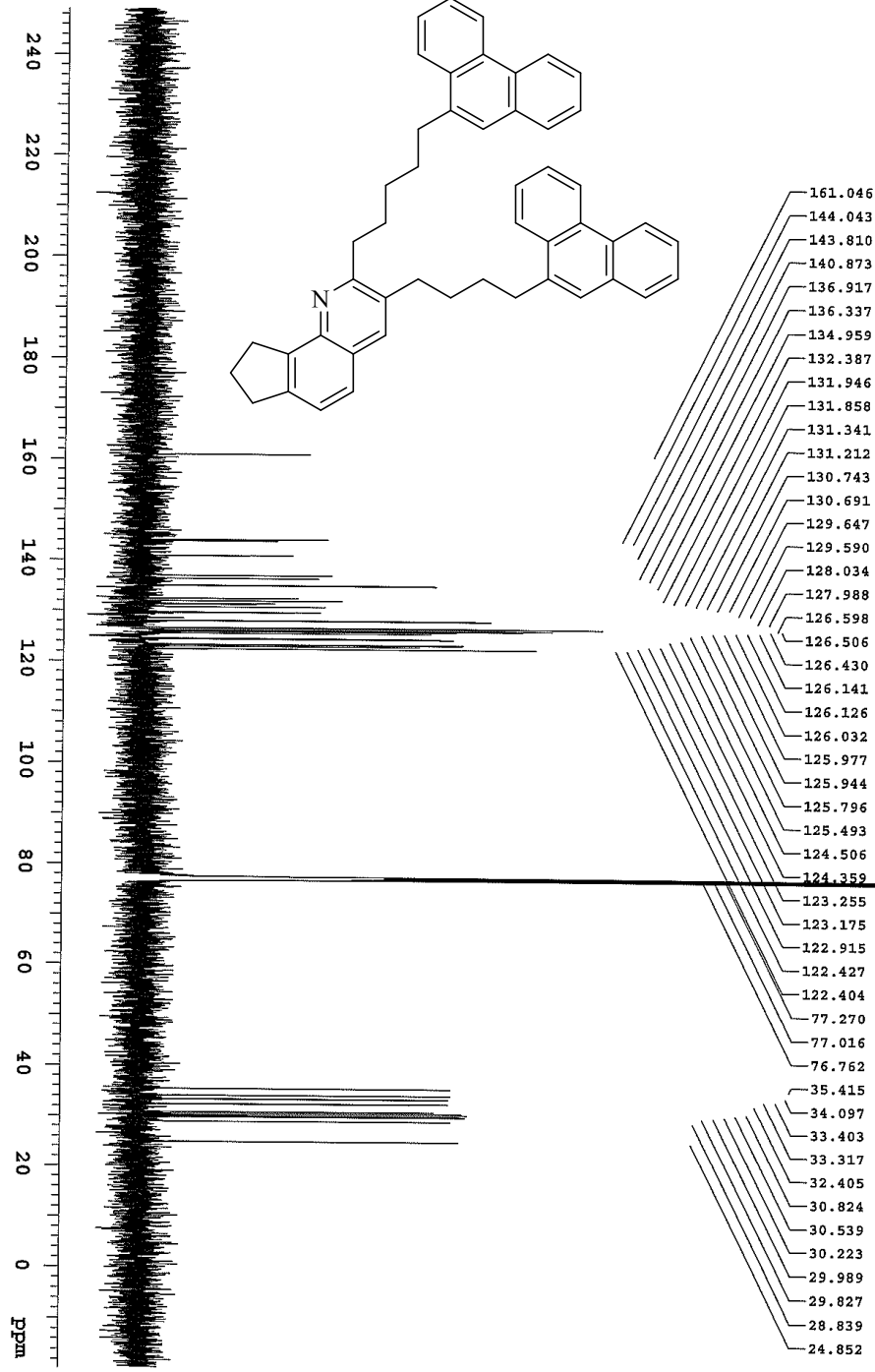
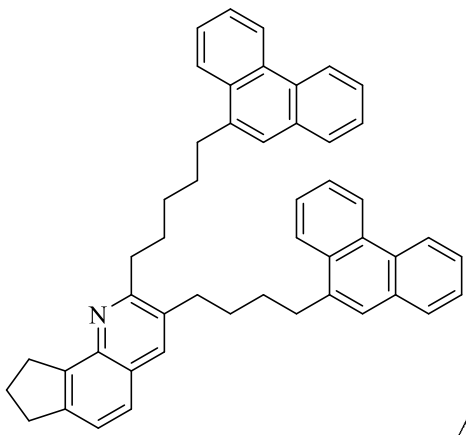
Recorded on: **us00**, Jun 29 2018  
 Pulse Sequence: **szpul**

Sweep Width(Hz): **33723.8**  
 Digital Res.(Hz/pp): **0.26**

Acquisition Time(s): **1**  
 Hz per mm(fz/mm): **140.79**

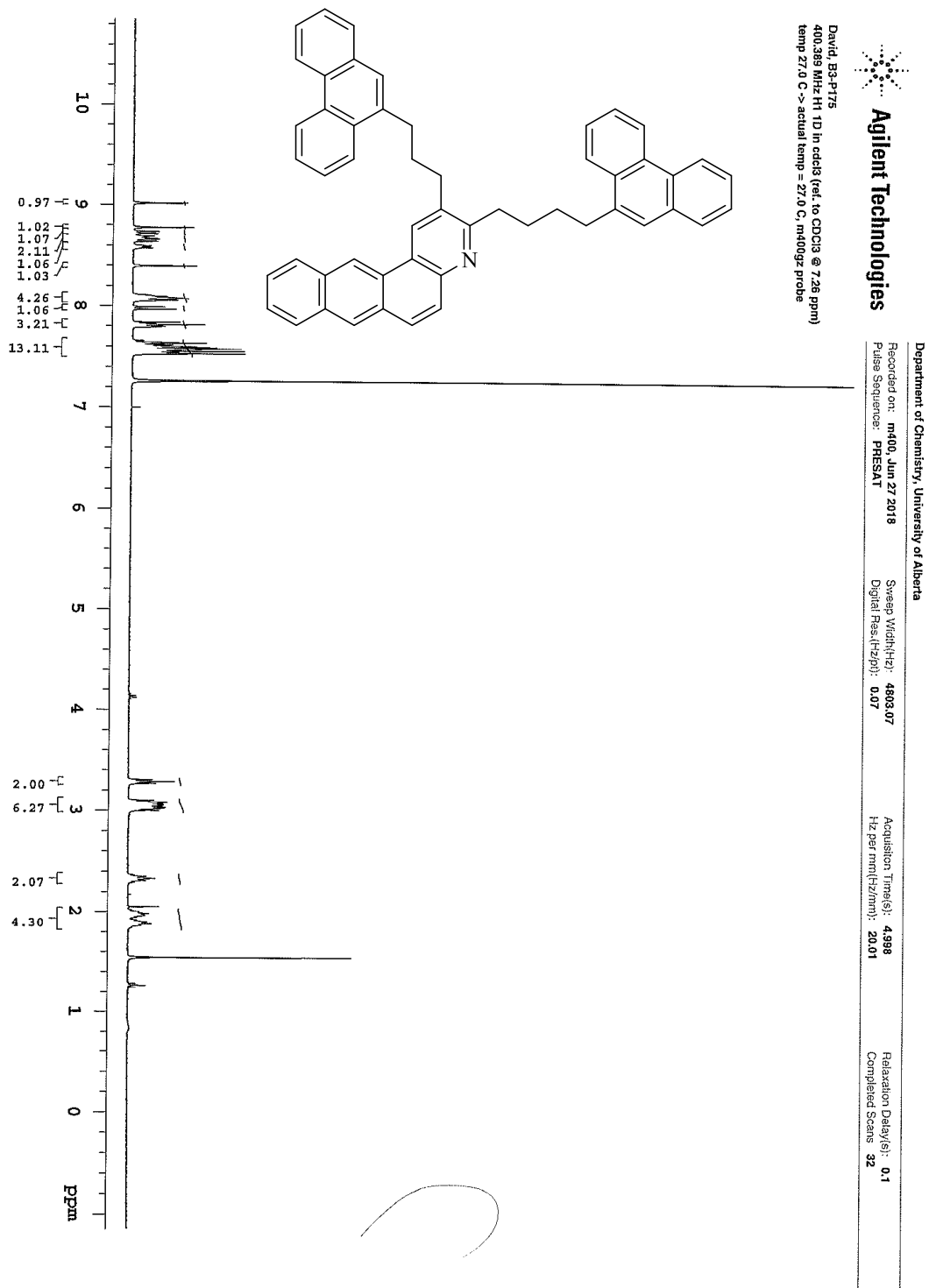
Relaxation Delay(s): **1**  
 Completed Scans: **128**

David\_B3-P171-A1  
 125.688 MHz C13(1H) 1D in cdcl3 (ref. to CDCl3 @ 77.06 ppm)  
 temp 27.7 C -> actual temp = 27.0 C, coldlual probe



File: \\mvl660\home\14\jmsam\m\m\data\DATA\_FROM\_MMRSERVICE\David\2018.06.29\us\_B3-P171-A1\_1003\_17.11\_C13\_1D

2-[4-(phenanthren-9-yl)butyl]-3-[3-(phenanthren-9-yl) propyl]-1-azatetraphene (176).





**Agilent Technologies**

Department of Chemistry, University of Alberta

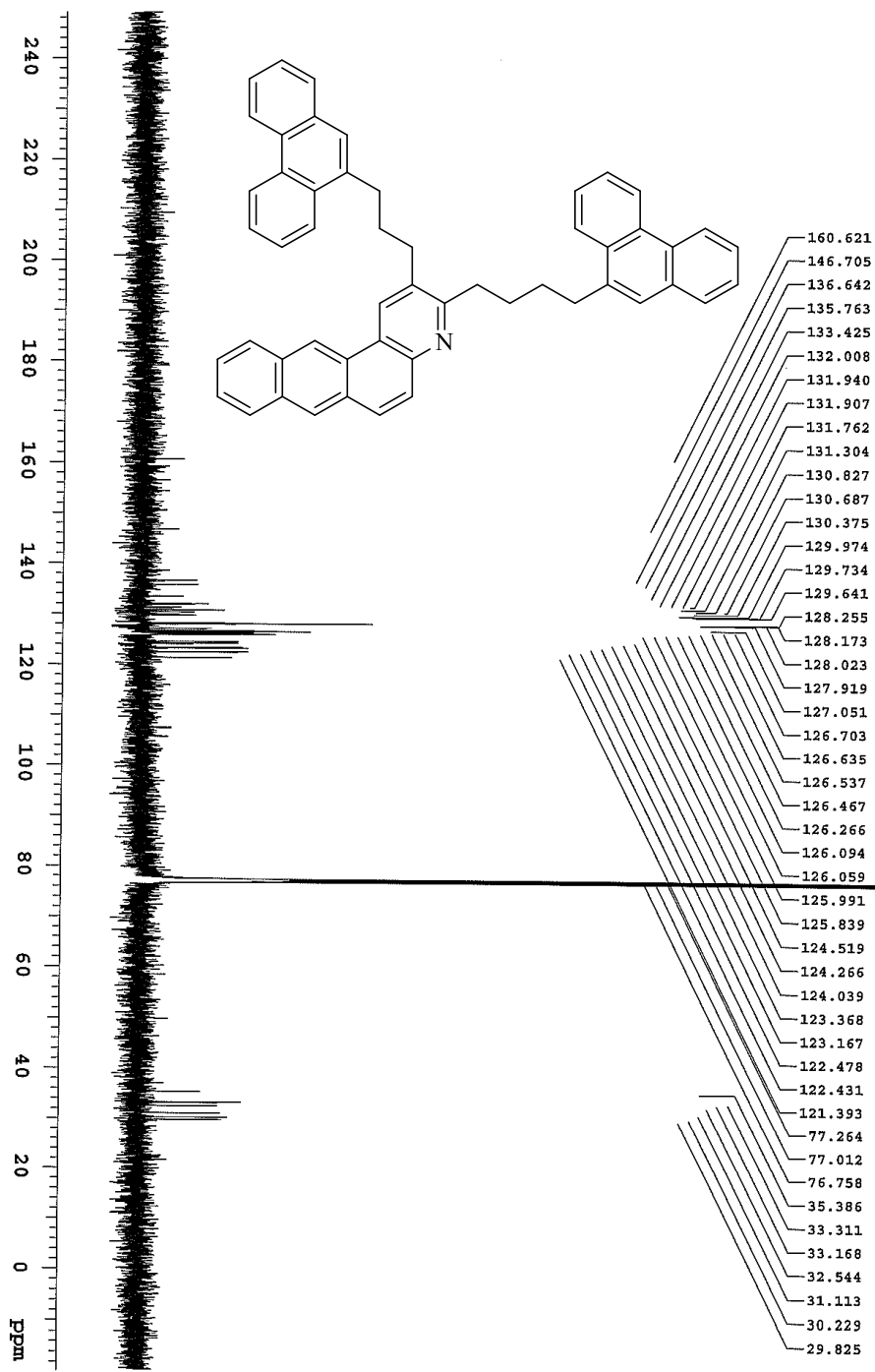
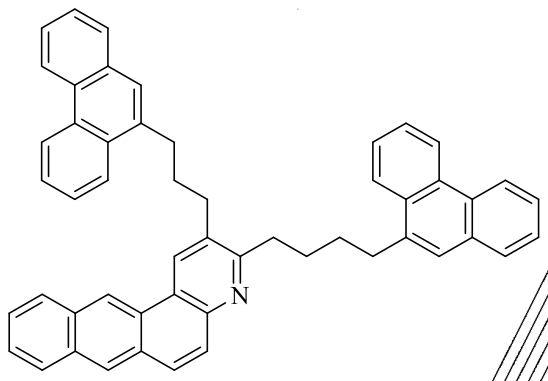
Recorded on: **us506**, Jun 29 2018  
 Pulse Sequence: **szpul**

Sweep Width(Hz): **33783.8**  
 Digital Res.(Hz/g): **0.26**

Acquisition Time(s): **1**  
 Hz per mm(Hz/mm): **140.76**

Relaxation Delay(s): **1**  
 Completed Scans: **128**

David\_B3-P175A  
 125.688 MHz C13(H1) 1D in cdd13 (ref. to CDCl3 @ 77.06 ppm)  
 temp 27.7 C -> actual temp = 27.0 C; cold/dial probe



File: /mnt/660/home14/jrns/mr/ncr/data/ATA\_FROM\_NMRSERVICE/David/2018\_06/2018\_06\_29\_us\_B3-P175A\_loc3\_16\_48\_C13\_1D

6-methoxy-3-[2-(phenanthren-9-yl)ethyl]-2-[3-(phenanthren-9-yl)propyl]quinoline (177).



David, B3-P207  
400,389 MHz H1 1D in odd13 (ref. to CDCl3 @ 7.26 ppm)  
temp 27.0 C -> actual temp = 27.0 C, m400qz probe

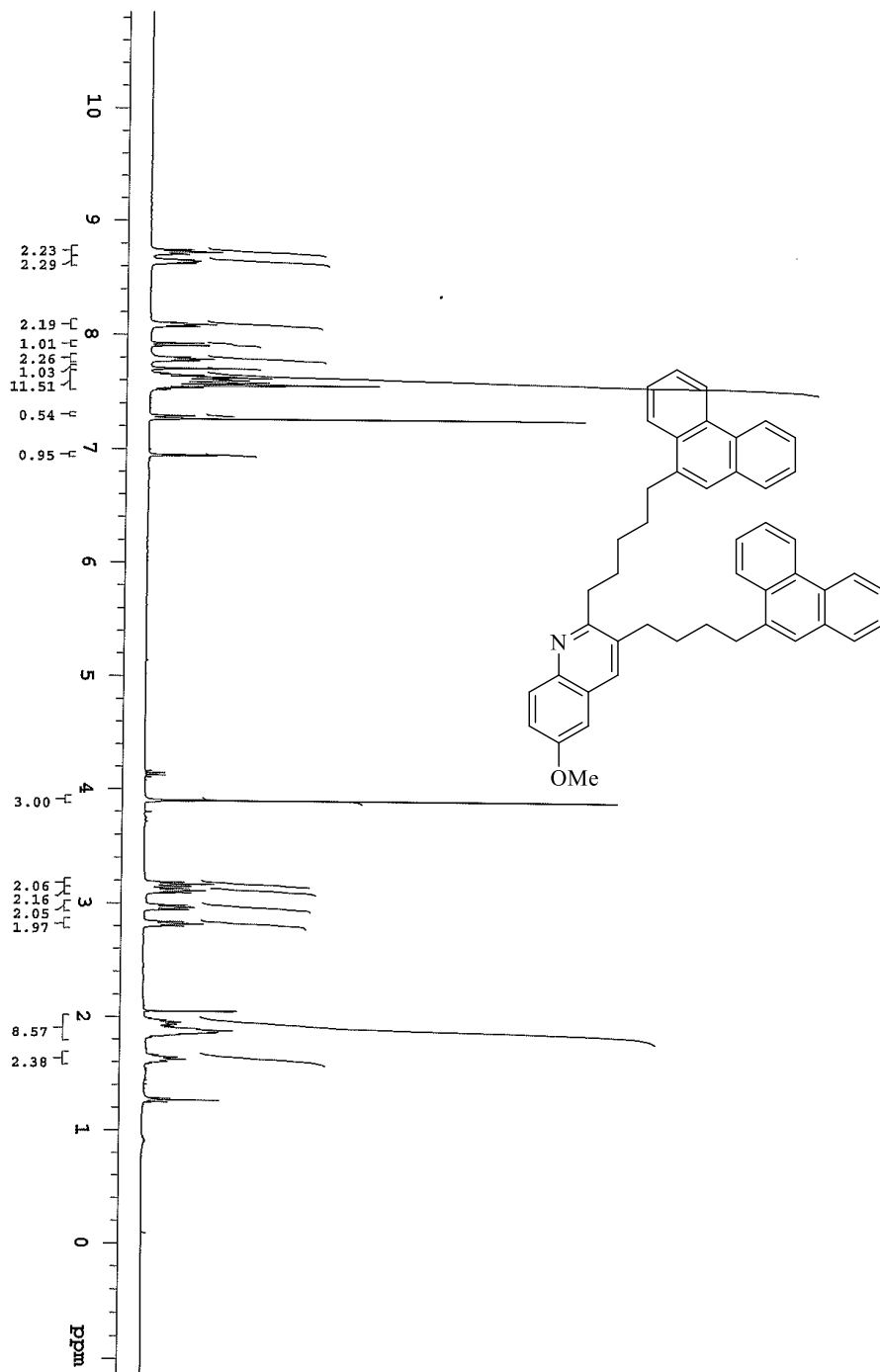
Department of Chemistry, University of Alberta

Recorded on: m400, Jun 27 2018  
Pulse Sequence: PRESAT

Sweep Width(Hz): 4803.07  
Digital Res.(Hz/p1): 0.07

Acquisition Time(s): 4.998  
Hz per mm(Hz/mm): 20.01

Relaxation Delay(s): 0.1  
Completed Scans: 32



File: /mnt/d600/home14/jfsmrnmrdata/DA1A\_FROM\_NMRSEVICED/DA1A/2018\_06/27/m4\_B3-P207\_loc38\_22\_26\_H1\_1D



**Agilent Technologies**

Department of Chemistry, University of Alberta

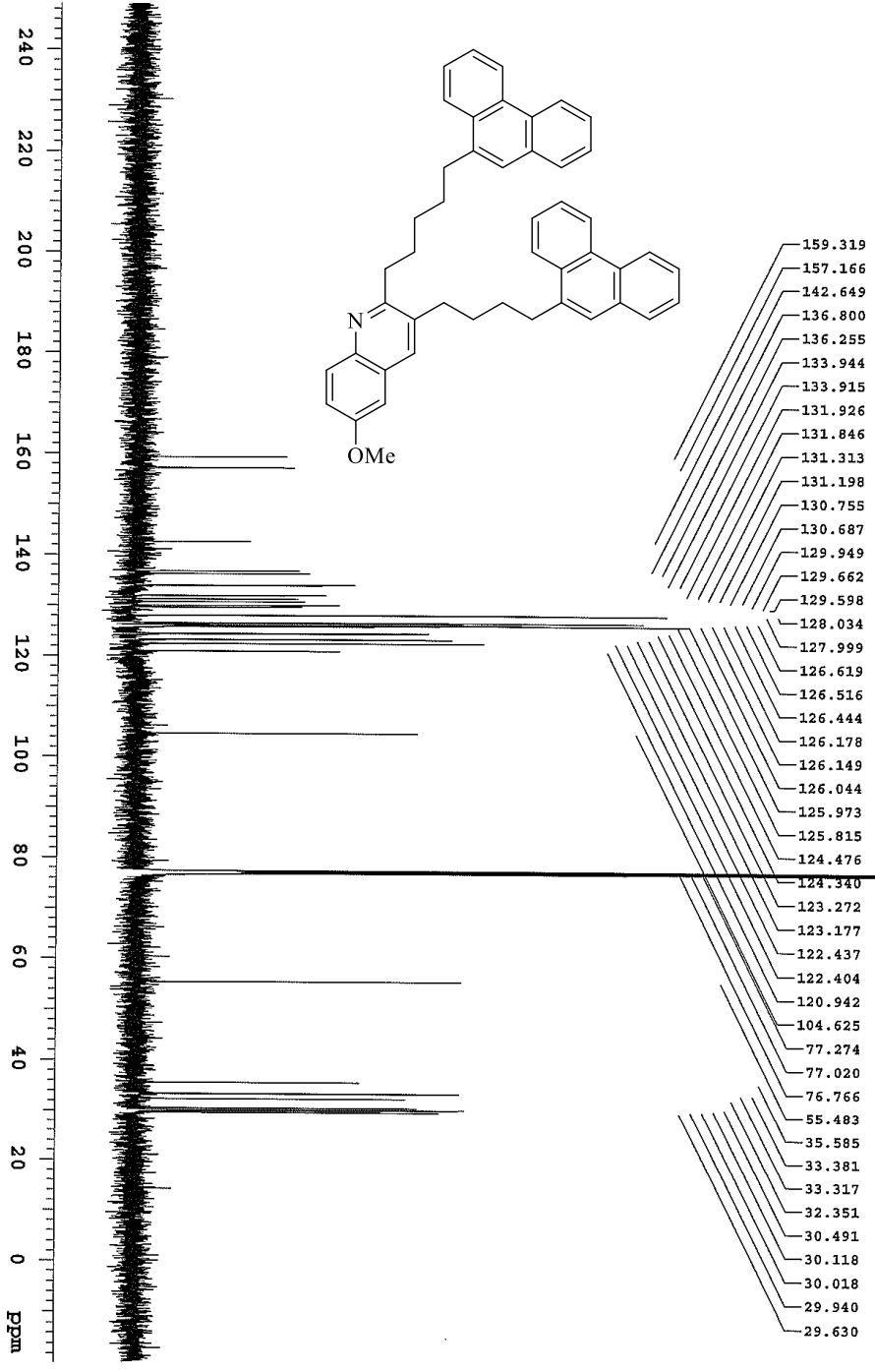
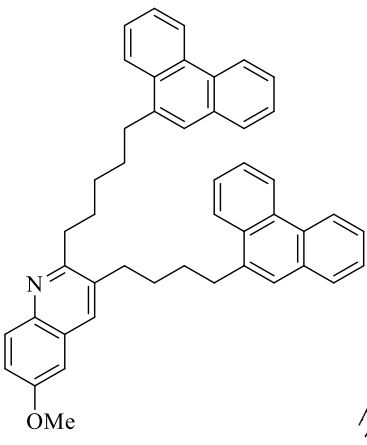
Recorded on: **us00, Jun 29 2018**  
 Pulse Sequence: **szpul**

Sweep Width(Hz): **33783.8**  
 Digital Res.(Hz): **0.26**

Acquisition Time(s): **1**  
 Hz per mnt(Hz/mn): **140.76**

Relaxation Delay(s): **1**  
 Completed Scans: **128**

David, B3-P207A  
 125.688 MHz C13(1H) 1D in edc13 (ref. to CDCl3 @ 77.05 ppm)  
 temp 27.7 C -> actual temp = 27.0 C, coldstart probe



File: /mnt/d600/home14/jmsrnu/rntdata/DA1A\_FROM\_NMRSERVICE/David/2018\_06/29/us\_01/B3-P207A\_loc1\_17\_36\_C13\_1D

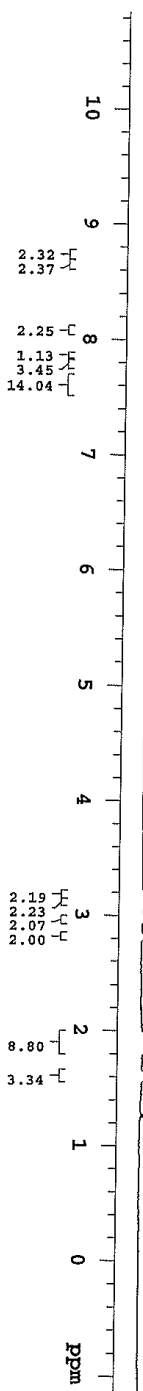
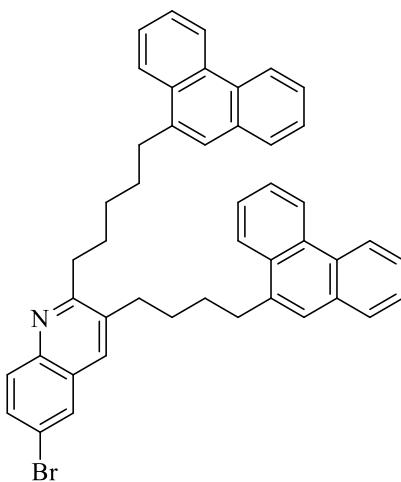
6-bromo-3-[2-(phenanthren-9-yl)ethyl]-2-[3-(phenanthren-9-yl)propyl]quinoline (178).



400.389 MHz <sup>1</sup>H 1D in cdcls (ref. to CDCl<sub>3</sub> @ 7.26 ppm)  
temp 27.0 C -> actual temp = 27.0 C, m400qz probe

Department of Chemistry, University of Alberta

Recorded on: m400, Jun 13 2018 Sweep Width(Hz): 4803.07 Acquisition Time(s): 4.997 Relaxation Delay(s): 0.1  
Pulse Sequence: PRESAT Digital Res.(Hz/pt): 0.07 Hz per mm(Hz/mm): 20.01 Completed Scans: 32



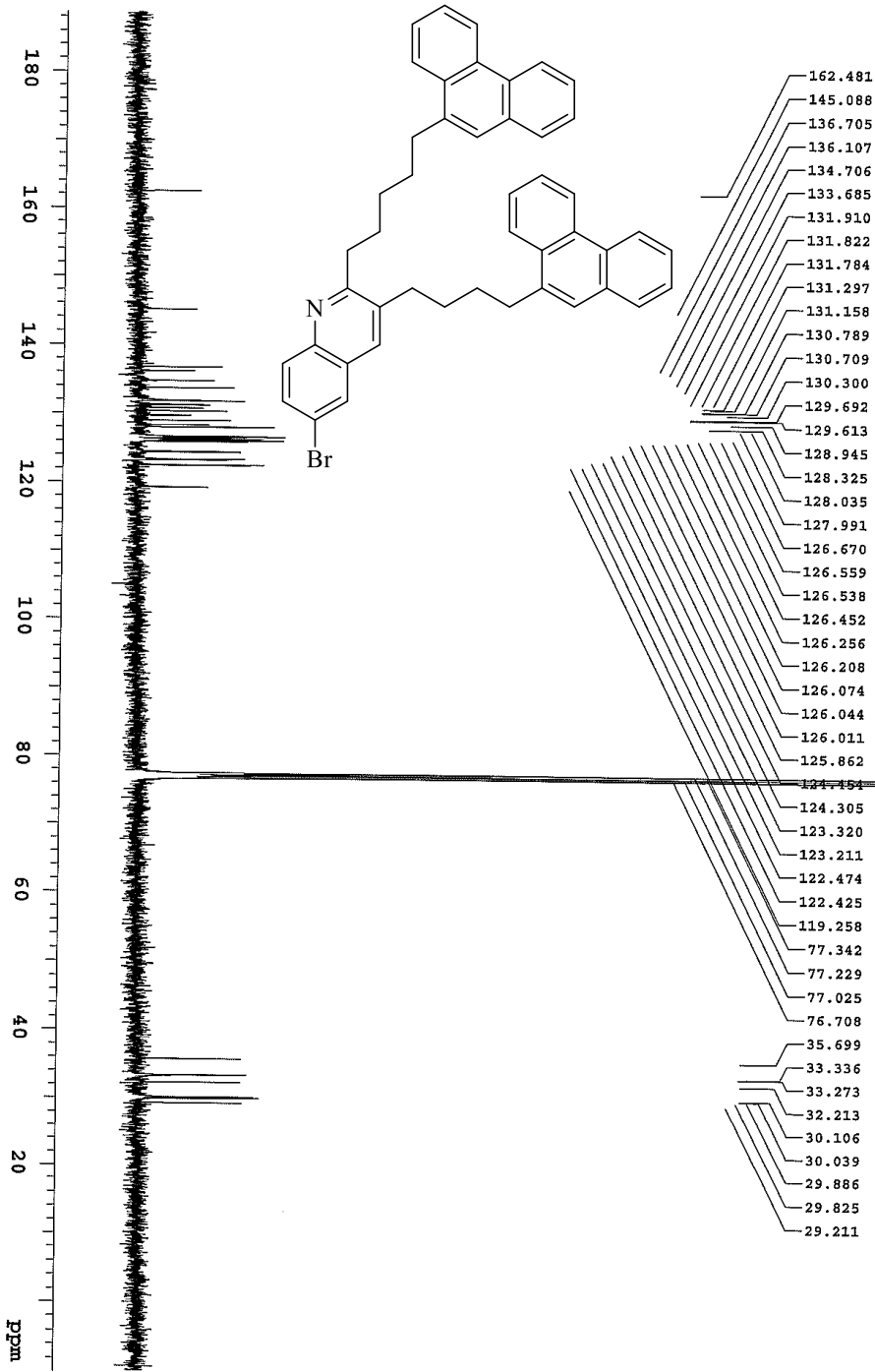
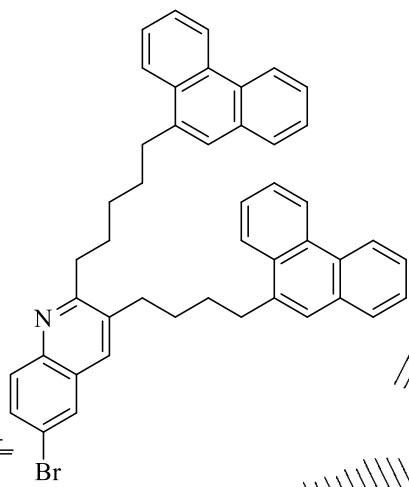
File: /m400/home14/jmsm/rmdata/ATA\_FROM\_NMRSERVICE/DAVID/2018.06.20/18.06.13.m400\_B4-P1-3.10c39\_21.23\_H1\_1D



Department of Chemistry, University of Alberta

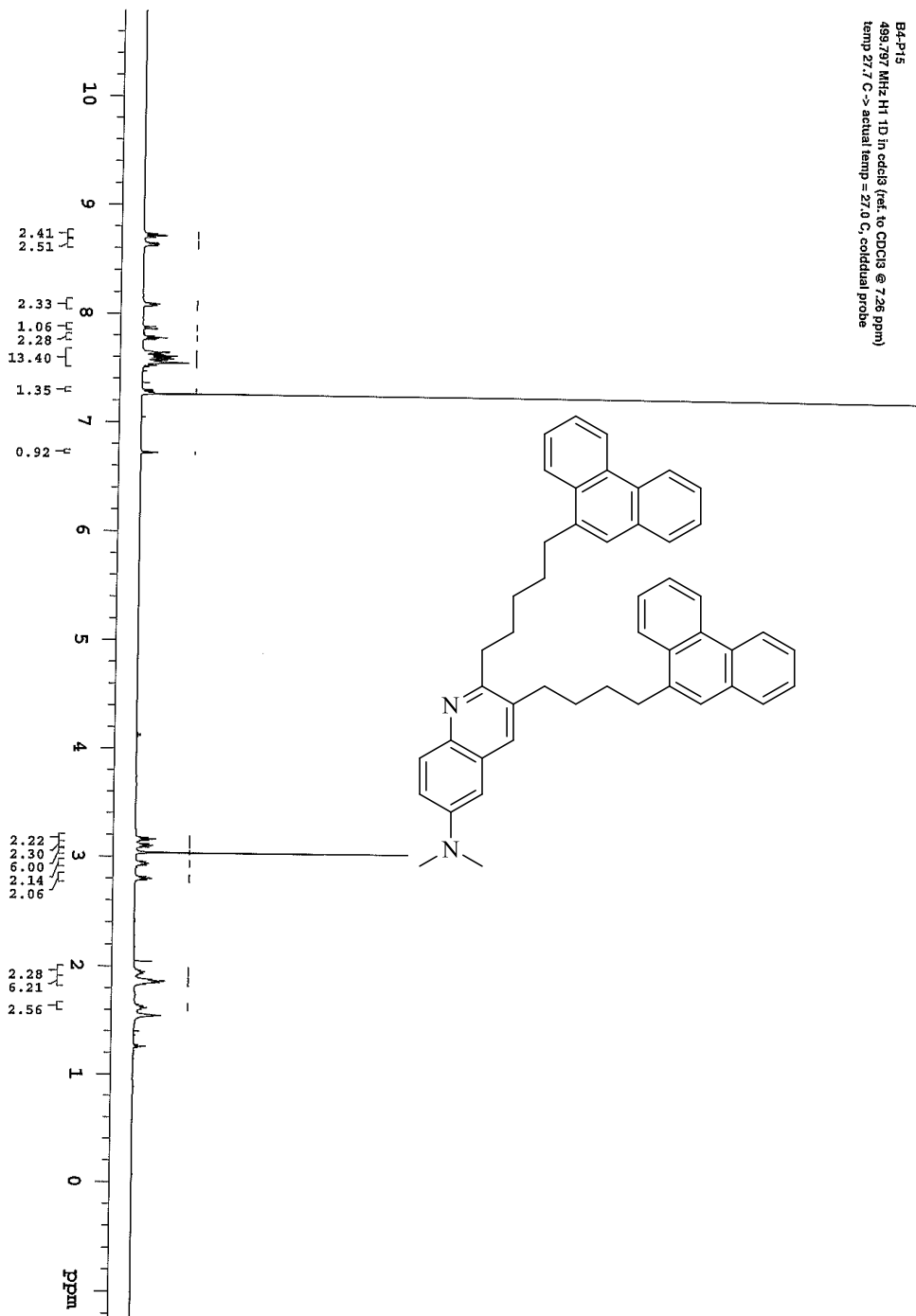
Recorded on: m400, Jun 29 2018      Sweep Width(Hz): 29188.9      Acquisition Time(s): 1      Relaxation Delay(s): 2  
 Pulse Sequence: s2pul      Digital Res.(Hz/pt): 0.19      Hz per ppm(Hz/ppm): 83.33      Completed Scans: 1536

David\_B4-P1A  
 100.628 MHz C13(H) 1D In edis3 (ref. to CDCl3 @ 77.06 ppm)  
 temp 27.0 C -> actual temp = 27.0 C, m400gz probe



File: /mnt/6600/home14/jmsm/mrmdata/ATA\_FROM\_NMRSERVICE/David/2018.06.29/m4\_B4-P1A\_loc7\_12.40\_C13.1D

***N,N*-dimethyl-3-(4-(phenanthren-9-yl)butyl)-2-(5-(phenanthren-9-yl)pentyl)quinolin-6-amine (179).**



B4-P15  
499.797 MHz H1 1D in cdcl3 (ref. to CDCl3 @ 726 ppm)  
temp 27.7 C -> actual temp = 27.0 C, coldlial probe



Department of Chemistry, University of Alberta

Recorded on: **0506\_Sep 8 2018**  
Pulse Sequence: **PRESAT**

Sweep Width(Hz): **6009.82**  
Digital Res.(Hz/ppt): **0.09**

Acquisition Time(s): **5**  
Hz per mm.(Hz/mm): **25.04**

Relaxation Delay(s): **0.1**  
Completed Scans: **16**

File: /nrv/c60/home14/jmsnmr/mrdata/DATA\_FROM\_MMRSERVICE/Datw/2018.09/2018.09.08.us\_B4-P15\_fc08\_13.02\_H1\_1D



**Agilent Technologies**

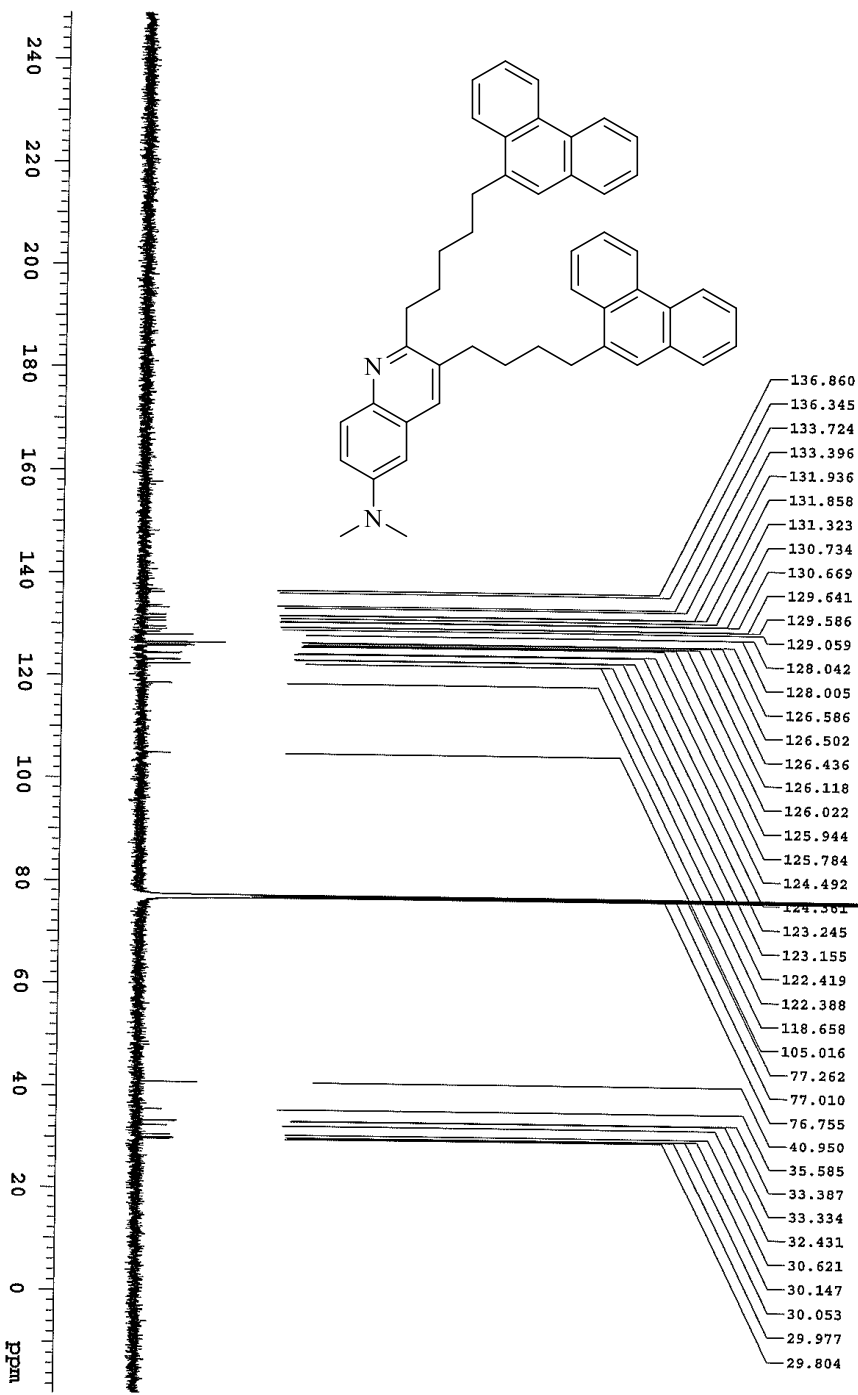
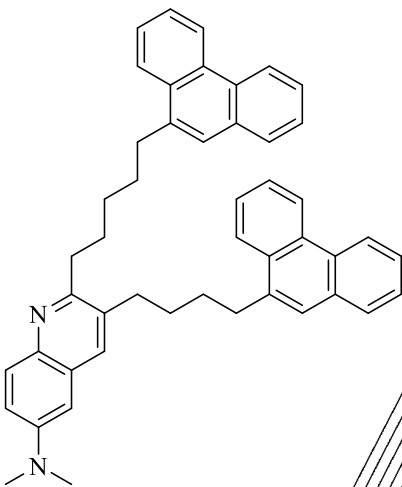
Department of Chemistry, University of Alberta

Recorded on: **u500\_Sep 8 2018**  
 Pulse Sequence: **szpul**  
 Sweep Width(Hz): **33783.8**  
 Digital Res.(Hz/pp): **0.26**

Acquisition Time(s): **1**  
 Hz per mm(Hz/mm): **140.76**

Relaxation Delay(s): **1**  
 Completed Scans: **512**

David, B4-P15  
 125.588 MHz C13(H1) 1D in cdcl3 (ref. to CDC13 @ 77.06 ppm)  
 temp 27.7 C -> actual temp = 27.0 C, coldlual probe



File: /mnt/6600/home14/frsmrnmr/data/DA\_1\_FROM\_NMRSERVICE/Dav682018.09.08.us\_B4-P15\_1e98\_12.44\_C13\_1D

6-ethyl-2-[4-(pyren-1-yl) butyl]-3-[3-(pyren-1-yl) propyl] quinoline (180).



Agilent Technologies

Department of Chemistry, University of Alberta

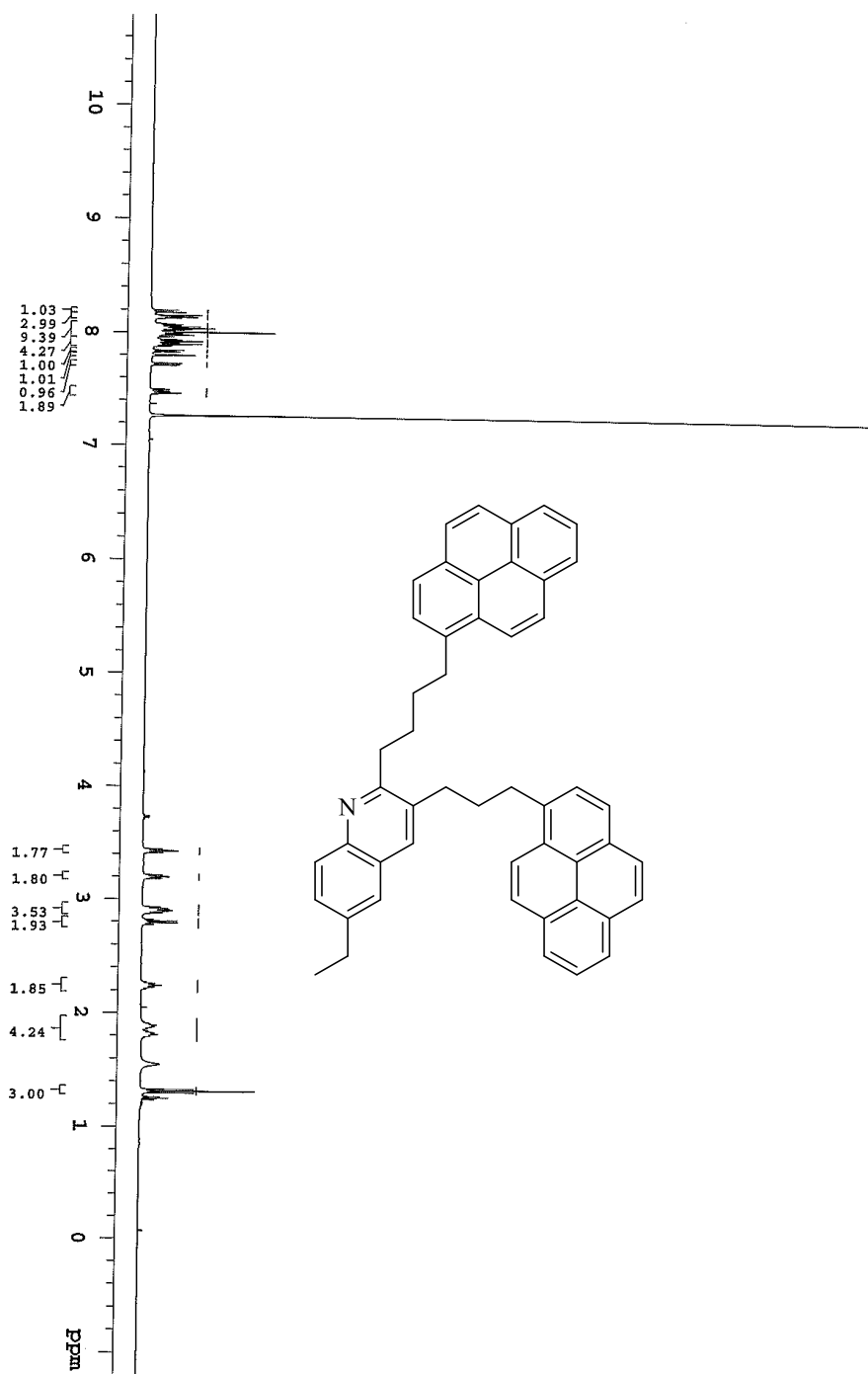
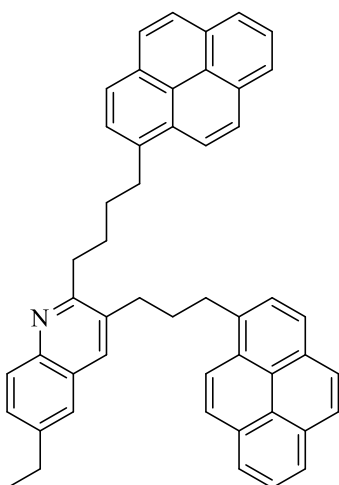
B3-P167  
499.797 MHz H1 1D in cdcl3 (ref. to CDCl3 @ 7.26 ppm)  
temp 27.7 C -> actual temp = 27.0 C, coldlual probe

Recorded on: **u500, Sep 8 2018**  
Pulse Sequence: **PRESAT**

Sweep Width(Hz): **6009.62**  
Digital Res.(Hz): **0.09**

Acquisition Time(s): **5**  
Hz per mm(Hz/mm): **25.04**

Relaxation Delay(s): **0.1**  
Completed Scans: **16**



File: /mnt/d60/home14/jmasm/mrdata/DA1A\_FROM\_MMRSERVICE/David/2018.09.20/18.09.08.us\_B3-P167\_loc10\_11\_S4\_H1\_1D



**Agilent Technologies**

Department of Chemistry, University of Alberta

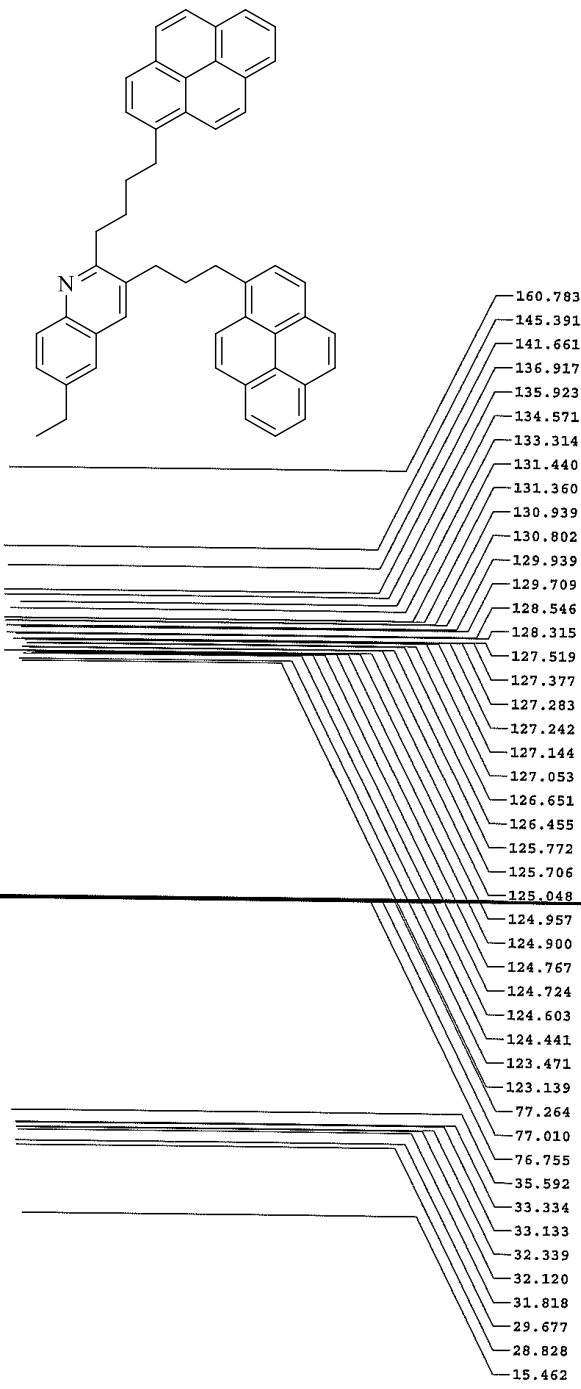
Recorded on: **us00, Sep 8 2018**  
 Pulse Sequence: **sgpr1**

Sweep Width(Hz): **33783.8**  
 Digital Res.(Hz/pp): **0.26**

Acquisition Time(s): **1**  
 Hz per mm(Hz/cm): **140.76**

Relaxation Delay(s): **1**  
 Completed Scans: **312**

David\_B3-P167  
 125.698 MHz C13{H1} 1D in cdcl3 (ref. to CDCl3 @ 77.06 ppm)  
 temp 27.7 C -> actual temp = 27.0 C, coldlial probe



File: /mnt/60/Volume1/4/gmsnm/mrdata/DA\_TVA\_FRCK\_MMSERVICE/David/2018.09/2018.09.08.us\_B3-P167\_1ct10\_1136\_C13\_1D

3-(2-(pyren-1-yl)-2-(3-(pyren-1-yl)propyl)-7,8,9,10-tetrahydrobenzo[h]quinoline (181).



Agilent Technologies

699.762 MHz H1 1D in ecds (ref. to CDCl3 @ 7.26 ppm)  
temp 27.5 C -> actual temp = 27.0 C, coldid probe

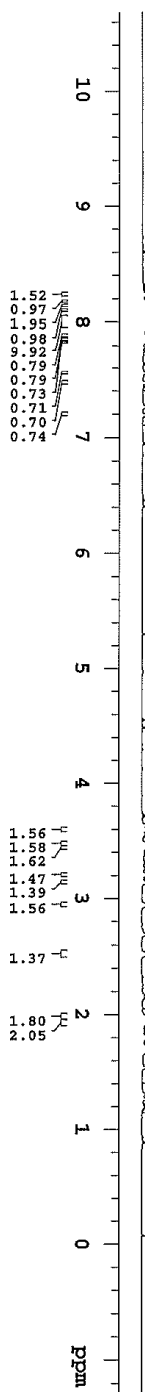
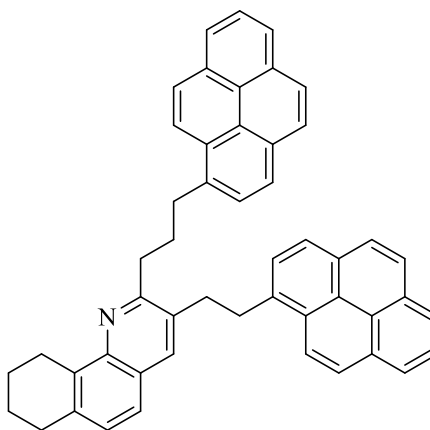
Department of Chemistry, University of Alberta

Recorded on: V700, Jul 30 2019  
Pulse Sequence: PRESAT1

Sweep Width(Hz): 6399.26  
Digital Res.(Hz/p): 0.13

Acquisition Time(s): 5  
Hz per mm(Hz/mm): 34.95

Relaxation Delay(s): 0.1  
Completed Scans: 8



File: /mnt/6s0/home14/fmsnmr/mrdata/DA1A\_FROM\_MMSERVICE/David2019.07.2019.07.30.V7\_MCF-4C5-pyrene\_loc31\_08.22\_H1\_1D







Agilent Technologies

Department of Chemistry, University of Alberta

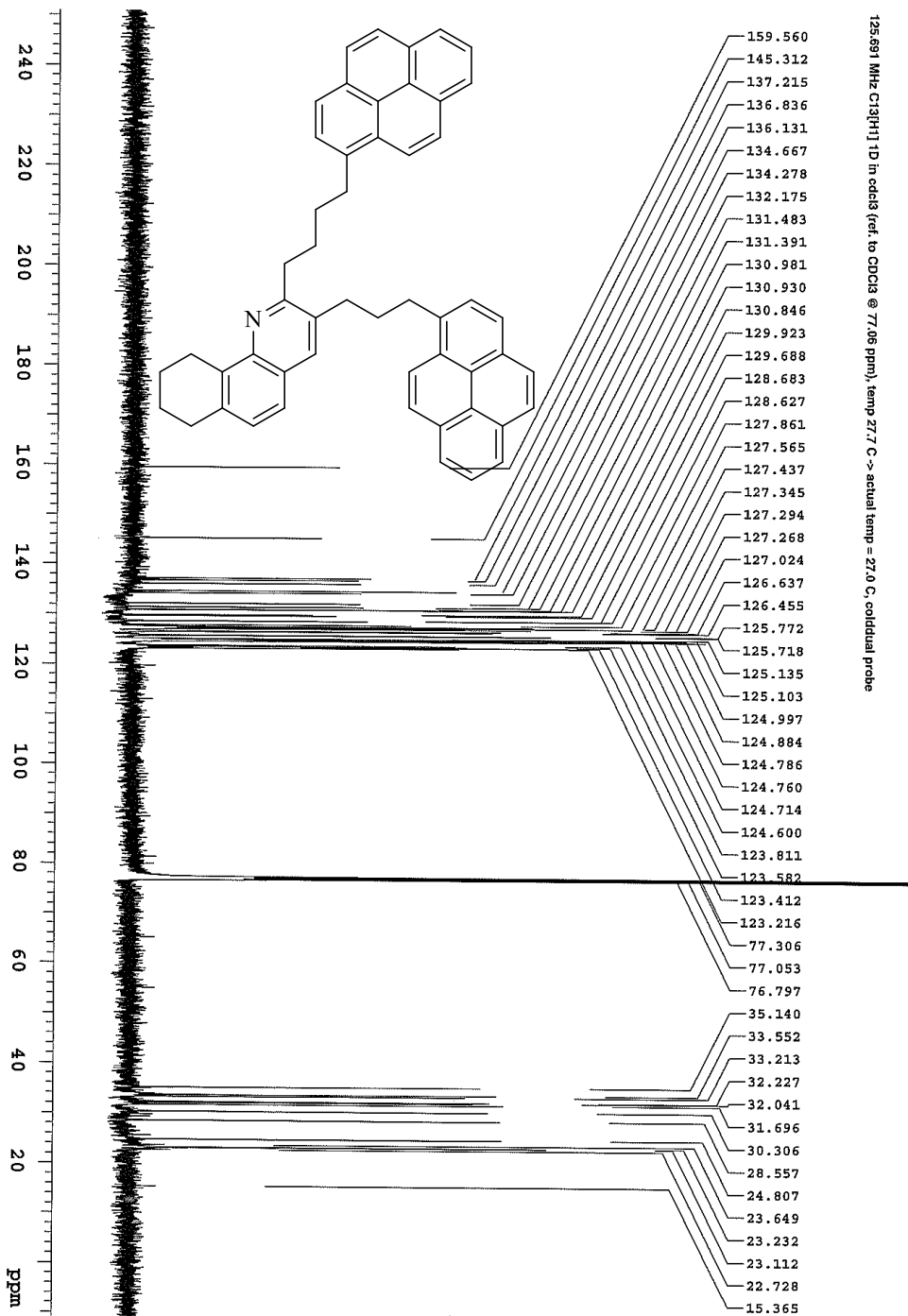
Recorded on: us00, Jun 29 2016  
Pulse Sequence: szpul

Sweep Width(kHz): 32894.7  
Digital Res.(Hz/p1): 0.25

Acquisition Time(s): 1  
Hz per mm(Hz/mm): 137.06

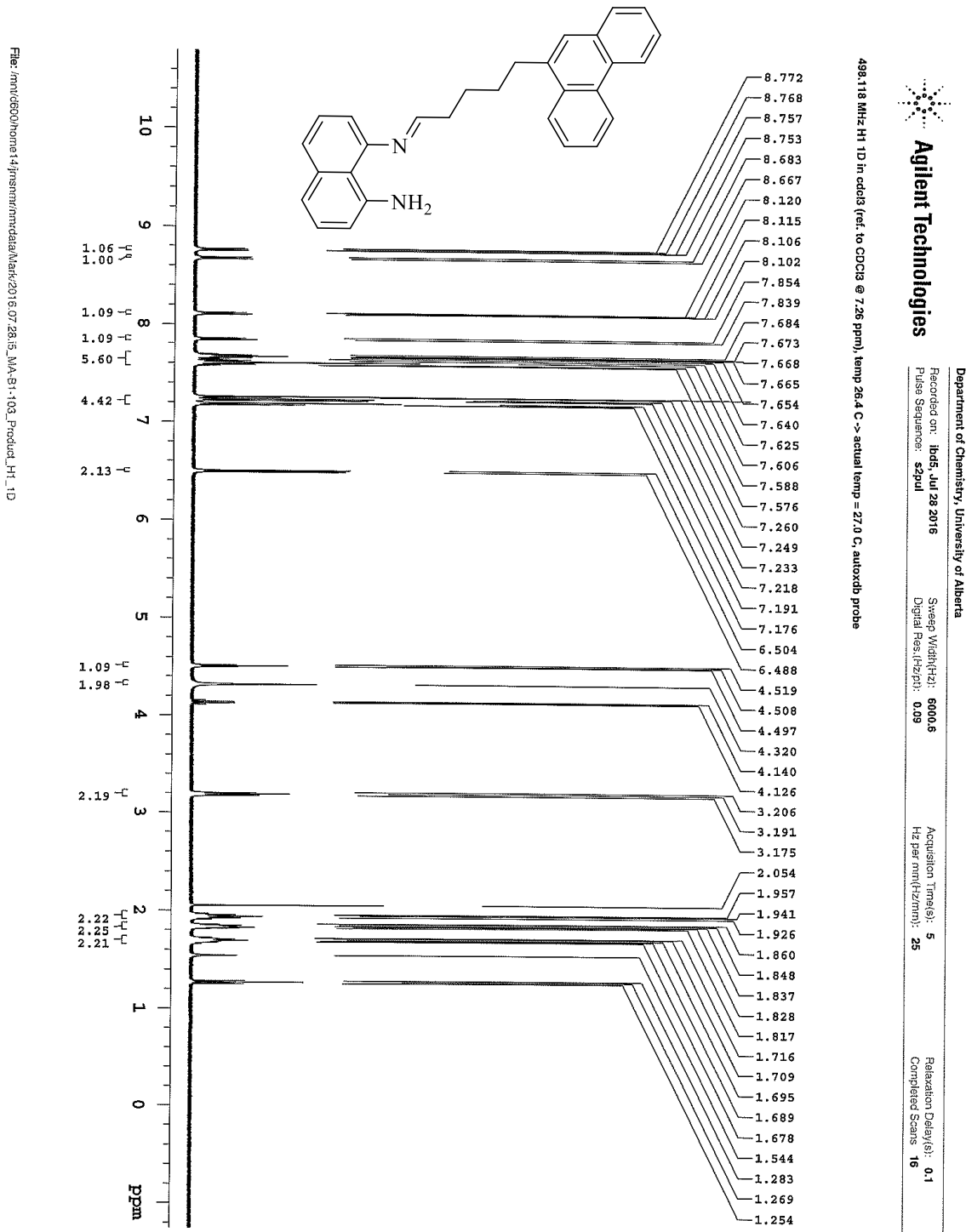
Relaxation Delay(s): 1  
Completed Scans: 128

125.691 MHz C13[MH] 1D in cdcl3 (ref. to CDCl3 @ 77.06 ppm), temp 27.7 C -> actual temp = 27.0 C, solid dual probe



File: /mnt/c800/home14/jmsnmr/mrntdata/DA1A\_FROM\_NMRSERVICE/Case/2016.06/2016.06.29.us\_JR-73\_10s\_10.11\_C13\_1D

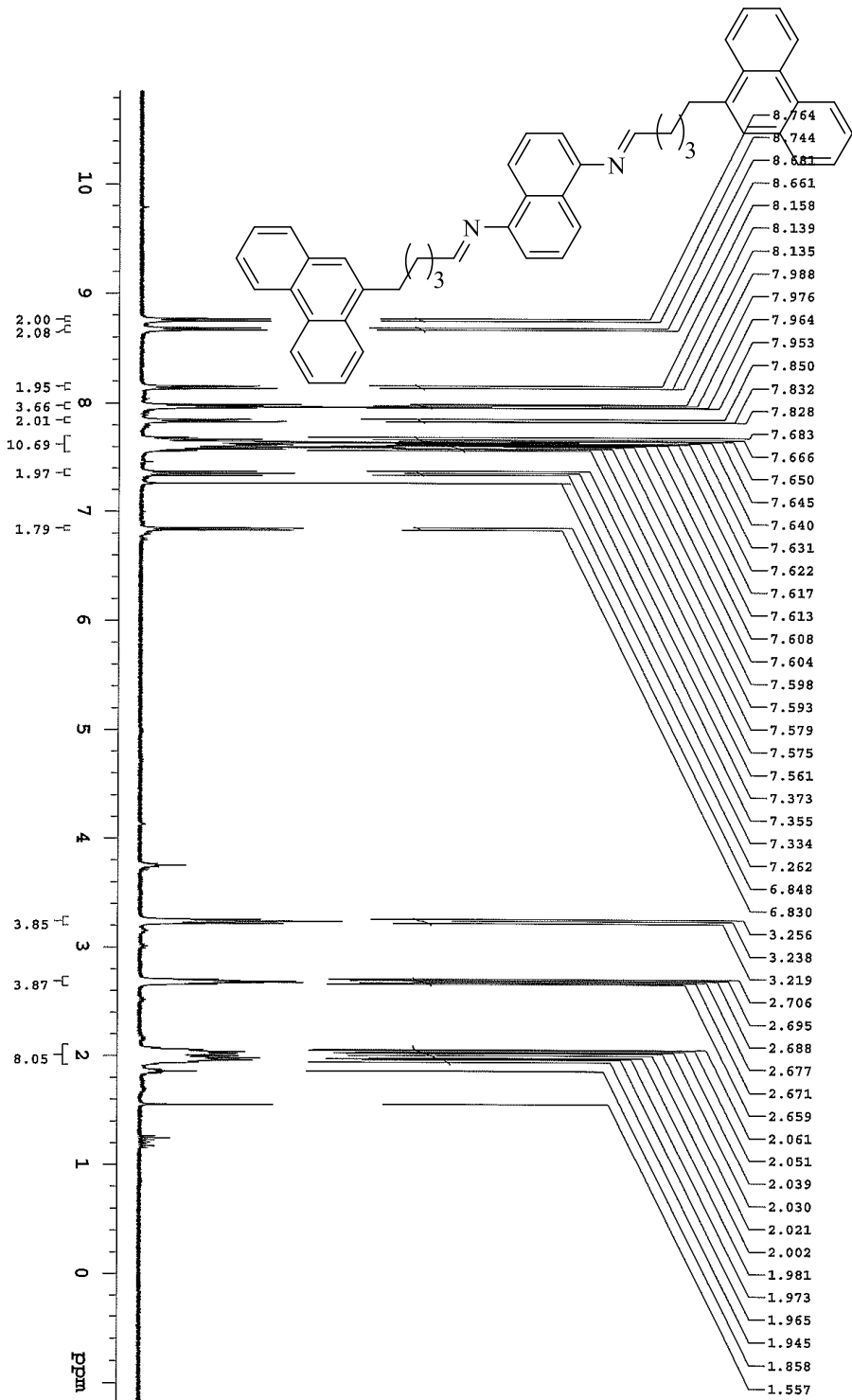
**(E)-8-((5-(phenanthren-9-yl)pentylidene)amino)naphthalen-1-amine (200).**



499.118 MHz <sup>1</sup>H 1D in cdcl3 (ref. to CDCl<sub>3</sub> @ 7.26 ppm), temp 26.4 C -> actual temp = 27.0 C, autoxchb probe

Department of Chemistry, University of Alberta  
 Recorded on: 18:55, Jul 28 2016  
 Pulse Sequence: szpul  
 Digital Res. (Hz/pt): 0.09  
 Sweep Width (Hz): 6000.6  
 Acquisition Time(s): 5  
 Hz per mm (Hz/mm): 25  
 Relaxation Delay(s): 0.1  
 Completed Scans: 16

**(1E,1'E)-N,N'-(naphthalene-1,5-diyl)bis(5-(phenanthren-9-yl)pentan-1-imine) (202).**



File: /mnt/d800/home14/jnsnmr/mrdata/Mark/2016\_11\_10/mr4\_MAA-B1-159\_Solid\_1H\_1.D

399.978 MHz <sup>1</sup>H 1D in cdcl3 (ref. to CDCl3 @ 7.26 ppm), temp 25.9 C -> actual temp = 27.0 C, onemmr probe



Department of Chemistry, University of Alberta  
 Recorded on: **mr400, Nov 10 2016** Sweep Width(Hz): **4807.69** Acquisition Time(s): **5** Relaxation Delay(s): **0.1**  
 Pulse Sequence: **sppul** Digital Res.(Hz/pt): **0.07** Hz per mn(Hz/mn): **20.03** Completed Scans: **16**